frontiers | Research Topics

Insights in terrestrial microbiology 2023/2024

Edited by
Jeanette M. Norton, Paola Grenni and Ruibo Sun

Published in
Frontiers in Microbiology

ISSN 1664-8714
ISBN 978-2-8325-6195-9
DOI 10.3389/978-2-8325-6195-9

About Frontiers

Frontiers is more than just an open access publisher of scholarly articles: it is a pioneering approach to the world of academia, radically improving the way scholarly research is managed. The grand vision of Frontiers is a world where all people have an equal opportunity to seek, share and generate knowledge. Frontiers provides immediate and permanent online open access to all its publications, but this alone is not enough to realize our grand goals.

Frontiers journal series

The Frontiers journal series is a multi-tier and interdisciplinary set of open-access, online journals, promising a paradigm shift from the current review, selection and dissemination processes in academic publishing. All Frontiers journals are driven by researchers for researchers; therefore, they constitute a service to the scholarly community. At the same time, the *Frontiers journal series* operates on a revolutionary invention, the tiered publishing system, initially addressing specific communities of scholars, and gradually climbing up to broader public understanding, thus serving the interests of the lay society, too.

Dedication to quality

Each Frontiers article is a landmark of the highest quality, thanks to genuinely collaborative interactions between authors and review editors, who include some of the world's best academicians. Research must be certified by peers before entering a stream of knowledge that may eventually reach the public - and shape society; therefore, Frontiers only applies the most rigorous and unbiased reviews. Frontiers revolutionizes research publishing by freely delivering the most outstanding research, evaluated with no bias from both the academic and social point of view. By applying the most advanced information technologies, Frontiers is catapulting scholarly publishing into a new generation.

What are Frontiers Research Topics?

Frontiers Research Topics are very popular trademarks of the *Frontiers journals series*: they are collections of at least ten articles, all centered on a particular subject. With their unique mix of varied contributions from Original Research to Review Articles, Frontiers Research Topics unify the most influential researchers, the latest key findings and historical advances in a hot research area.

Find out more on how to host your own Frontiers Research Topic or contribute to one as an author by contacting the Frontiers editorial office: frontiersin.org/about/contact

Insights in terrestrial microbiology: 2023/2024

Topic editors

Jeanette M. Norton — Utah State University, United States

Paola Grenni — Water Research Institute, National Research Council, Italy

Ruibo Sun — Anhui Agricultural University, China

Citation

Norton, J. M., Grenni, P., Sun, R., eds. (2025). *Insights in terrestrial microbiology: 2023/2024*. Lausanne: Frontiers Media SA. doi: 10.3389/978-2-8325-6195-9

Table of contents

04 Editorial: Insights in terrestrial microbiology: 2023/2024
Paola Grenni, Ruibo Sun and Jeanette M. Norton

07 Toward an intensive understanding of sewer sediment prokaryotic community assembly and function
Jingjing Xia, Kai Yu, Zhiyuan Yao, Huafeng Sheng, Lijuan Mao, Dingnan Lu, HuiHui Gan, Shulin Zhang and David Z. Zhu

20 Continuous cropping of potato changed the metabolic pathway of root exudates to drive rhizosphere microflora
Yanhong Xing, Pingliang Zhang, Wenming Zhang, Chenxu Yu and Zhuzhu Luo

38 Dynamics of soil microbial communities involved in carbon cycling along three successional forests in southern China
Minghui Hu, Shuyidan Zhou, Xin Xiong, Xuan Wang, Yu Sun, Ze Meng, Dafeng Hui, Jianling Li, Deqiang Zhang and Qi Deng

51 Enhancing insights: exploring the information content of calorespirometric ratio in dynamic soil microbial growth processes through calorimetry
Shiyue Yang, Eliana Di Lodovico, Alina Rupp, Hauke Harms, Christian Fricke, Anja Miltner, Matthias Kästner and Thomas Maskow

68 The combined application of salt-alkali tolerant phosphate solubilizing microorganisms and phosphogypsum is an excellent measure for the future improvement of saline-alkali soils
Lingli Li, Shiqi Yang, Xin Hu, Zhen Li and Haoming Chen

73 Understanding and exploring the diversity of soil microorganisms in tea (*Camellia sinensis*) gardens: toward sustainable tea production
Motunrayo Y. Jibola-Shittu, Zhiang Heng, Nemat O. Keyhani, Yuxiao Dang, Ruiya Chen, Sen Liu, Yongsheng Lin, Pengyu Lai, Jinhui Chen, Chenjie Yang, Weibin Zhang, Huajun Lv, Ziyi Wu, Shuaishuai Huang, Pengxi Cao, Lin Tian, Zhenxing Qiu, Xiaoyan Zhang, Xiayu Guan and Junzhi Qiu

89 Microbial hydrogen sinks in the sand-bentonite backfill material for the deep geological disposal of radioactive waste
Camille Rolland, Niels Burzan, Olivier X. Leupin, Aislinn A. Boylan, Manon Frutschi, Simiao Wang, Nicolas Jacquemin and Rizlan Bernier-Latmani

104 Rare microbial taxa as the major drivers of nutrient acquisition under moss biocrusts in karst area
Xintong Dong, Man Chen, Qi Chen, Kangfei Liu, Jie Long, Yunzhou Li, Yinuo Ren, Tao Yang, Jinxing Zhou, Saman Herath and Xiawei Peng

117 Synergy and competition during the anaerobic degradation of N-acetylglucosamine in a methane-emitting, subarctic, pH-neutral fen
Katharina Kujala, Oliver Schmidt and Marcus A. Horn

frontiers | Frontiers in Microbiology

TYPE Editorial
PUBLISHED 18 March 2025
DOI 10.3389/fmicb.2025.1583425

OPEN ACCESS

EDITED AND REVIEWED BY
Paul David Cotter,
Seqbiome Ltd, Ireland

*CORRESPONDENCE
Paola Grenni
paola.grenni@cnr.it

RECEIVED 25 February 2025
ACCEPTED 03 March 2025
PUBLISHED 18 March 2025

CITATION
Grenni P, Sun R and Norton JM (2025) Editorial: Insights in terrestrial microbiology: 2023/2024. *Front. Microbiol.* 16:1583425. doi: 10.3389/fmicb.2025.1583425

Editorial: Insights in terrestrial microbiology: 2023/2024

Paola Grenni[1,2]*, Ruibo Sun[3] and Jeanette M. Norton[4]

[1]Water Research Institute, National Research Council (IRSA-CNR), Rome, Italy, [2]NBFC, National Biodiversity Future Center, Università degli Studi di Palermo, Palermo, Italy, [3]College of Resources and Environment, Anhui Agricultural University, Hefei, China, [4]Department of Plants, Soils and Climate, Utah State University, Logan, UT, United States

KEYWORDS

peatlands, biogeochemistry, methane, hydrogen, saline soil, biocrust, soil reclamation

Editorial on the Research Topic
Insights in terrestrial microbiology: 2023/2024

The role of microorganisms in terrestrial ecosystems is crucial for several functions, including recycling nutrients and restoring soils after contamination (Grenni et al., 2023; Kotschik et al., 2023; Onet et al., 2025) (Figure 1). The Terrestrial Microbiology section of Frontiers (https://www.frontiersin.org/journals/microbiology/sections/terrestrial-microbiology) aims to highlight these key roles, addressing the study and comprehension of the various microbial functions in terrestrial ecosystems. In 2025, this section has a new mission statement that emphasizes the importance of the United Nations Sustainable Development Goals (SDGs), to advance knowledge and promote innovation for contributing to global sustainability and address major environmental challenges. In fact, the section brings together contributions on microbial functions in terrestrial ecosystems, the adaptation and evolution of microbial communities, biogeochemical cycles, the structure and functioning of the soil food web, and the interactions between microorganisms and their environment, contributing insights to various United Nations Sustainable Development Goals: SDG 13 (Climate Action), SDG 14 (Life Under Water), and SDG 15 (Life on Earth).

According to these aims, the Research Topic "*Insights in terrestrial microbiology: 2023/2024*" collected nine articles that address several important aspects of the microbial community of soil ecosystems.

Soil has an essential role in maintaining carbon balance on Earth and the soil microbiome mediates carbon pools and therefore climate regulation by affecting the balance of CO_2 emissions. This equilibrium strongly depends on the catalytic functions performed by microbial communities on soil organic matter (Yang et al.). The latter can be used by microorganisms (for their growth by anabolic reactions) or dissipated as CO_2 to the environment by catabolic reactions. The kinetics of the organic matter and energy fluxes were studied by Yang et al. through calorimetry, and specific data processing, gaining an improved understanding of the relations between matter and energy fluxes in tightly controlled soil systems.

Kujala et al. unraveled the crucial role of the soil microbiome in the trophic interactions between fermenters and methanogens in peatlands, ecosystems which are, despite their importance, currently poorly understood. Peatlands are considered invaluable but vulnerable ecosystems where huge amounts of organic carbon are stored, with the carbon in the deep peat remaining stable due to limited thermodynamic energy and transport (Rajakaruna et al., 2024). However, peatlands emit greenhouse gases such as carbon dioxide

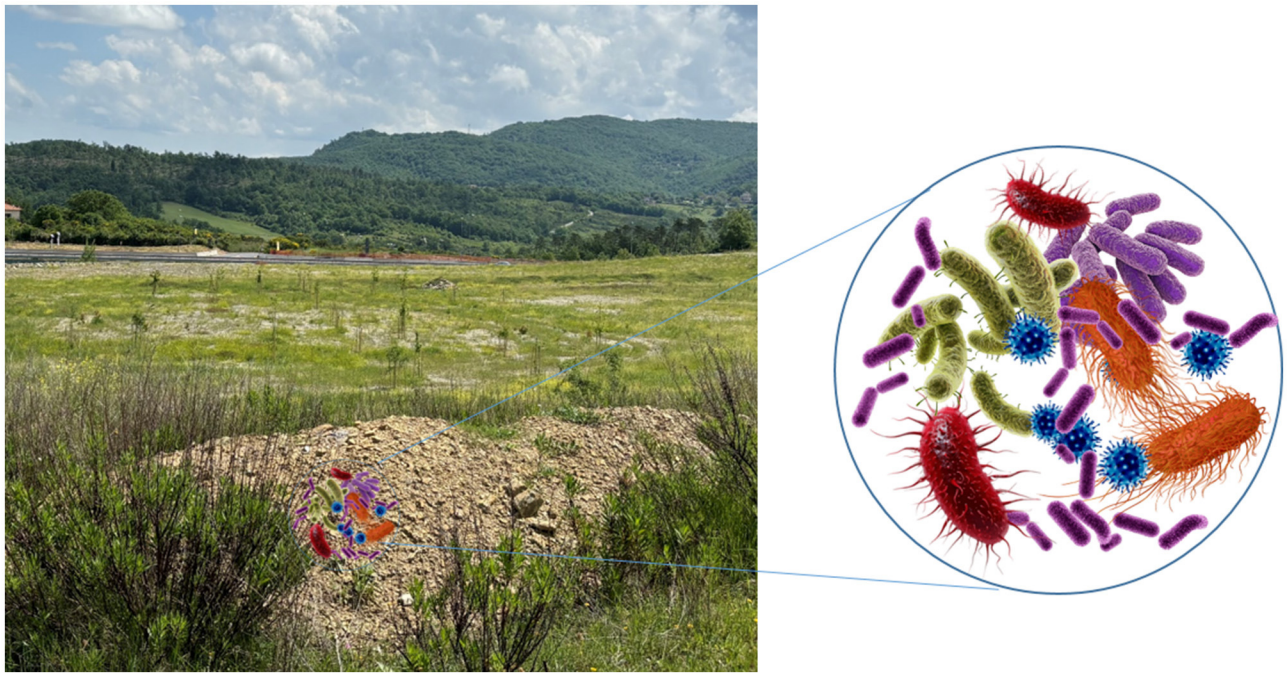

FIGURE 1
Microbial communities of soil have key roles such as: recycling nutrients, restoring soils after contamination, and climate regulation affecting the balance of CO_2 emissions.

(CO_2) and methane (CH_4). Methanogenesis is an anaerobic respiration that produces CH_4 as the final product of metabolism, and it is performed by methanogens, which are strictly anaerobic Archaea (Lyu et al., 2018). The CH_4-emitting peatland microbial community showed a pronounced response to additional substrates for fermentation and hydrogenotrophic methanogenesis, indicating high potential activity of both processes. These results indicate that the identification of active primary and secondary fermenters, the role of acetogens, the pathways for anaerobic conversion of acetate to methane, and the taxa involved are key challenges to be considered in future studies. Rolland et al. also examined the role of hydrogen consumers and methanogens in environments of long-term radioactive waste disposal. Microbial systems were observed to consume H_2 and demonstrating the potential to contribute positively to the long-term safety of a radioactive waste repository.

The impact of continuous cropping in terms of autotoxicity, due to accumulation and imbalance of microorganisms in soil, which can lead to crop failure, and this was the focus of the study by Xing et al.. The research focuses on a long (more than 4 years) cultivation of potato, analyzing the potato root exudates and the bacterial and fungal communities around potato plants. The communities were significantly changed, with a substantial reduction of beneficial bacteria and accumulation of harmful fungi. Moreover, differentially expressed metabolites were significantly correlated with microflora biomarkers, suggesting that the continuous cultivation of potato changed the microorganism's metabolism in response to root exudates and pushed the rhizosphere microflora in a less favorable direction for crop growth. These microbial community aspects must be considered in effective crop management to guarantee potato productivity, as it is an important global staple used for food, feed, and raw materials in the industry due to its high yield, tolerance to wet environments, and great adaptability. Tea agricultural systems were investigated for their bacterial and fungal communities and potential for biocontrol of pathogens by Jibola-Shittu et al.. Further characterization of the roles and functions of the microbiomes will be required to create more sustainable tea systems.

Microbial communities in forest soils drive a variety of functions, including forest soil carbon turnover, with a key role in ecosystem services that promote forest health (Onet et al., 2025). Plant community dynamics in forest succession have been the subject of considerable attention in recent decades, but information on soil microbial communities involved in the carbon cycle is still limited. This was the main focus of Hu et al. investigating the soil microbial community composition and carbohydrate degradation potential in subtropical forests in China. Interestingly, although bacteria and fungi abundances in soil increased with forest succession in relation to both soil and litter characteristics, the diversity remained unchanged (for bacteria) or decreased (for fungi). Some important microbial functional genes related to carbohydrate degradation (e.g., cellulase, hemicellulase, and pectinase) were correlated with specific soil abiotic factors (organic carbon, total nitrogen, and moisture) and increased with forest succession, while amylase was mainly affected by soil total phosphorus and litterfall. The role of the rare biosphere was emphasized by the results of Dong et al. on the biocrust communities in karst systems. The biogeochemical transformations and enzymatic functions described are crucial to

these wildland sites but also may be influential in the restoration of disturbed ecosystems.

The microbial community in sediments of sewer systems from distinct urban areas (multifunctional, commercial, and residential) was examined by Xia et al.. The overall microbial communities were related to physicochemical properties (pH and nutrients), together with the type of sewer sediment, although in-depth investigations of prokaryotic communities in sediments on a larger scale and with greater depth have to be performed to confirm these findings. The role of microbial transformations may also be instrumental in the restoration of saline alkali soils (Li et al.). Large land areas under irrigation are degraded by severe accumulation of salts, their poor physical conditions, and nutrient imbalances, including decreased available phosphorus. Technologies for improving these degraded soils require combinations of amendments, selective leaching, and biological improvements. The authors contend that combinations of phosphogypsum and phosphate solubilizing microorganisms can work toward improvements in these degraded salt-alkali soils.

The role of microbial communities in elemental cycling, soil remediation, and intensive agriculture highlights how microbial management is an important tool for progress toward achieving the UN Sustainable Development Goals for healthy soils.

Author contributions

PG: Writing – original draft, Writing – review & editing. RS: Writing – review & editing. JN: Writing – original draft, Writing – review & editing.

Funding

The author(s) declare that no financial support was received for the research and/or publication of this article. This research was partially funded by the Ministry University and Research, "Next Generation EU–Piano Nazionale Resistenza e Resilienza (PNRR)—Missione 4 Componente 2 Investimento 1.4—Notice No. 3138 16 December 2021 rectified by D.D. n. 3175 18 December 2021". Award Number: CN_00000033, Decree MUR n. 1034 17 June 2022, CUP B83C22002930006, Project title "National Biodiversity Future Center—NBFC, Microbial diversity and functioning of freshwater and terrestrial ecosystems".

Conflict of interest

The authors declare that the research was conducted in the absence of any commercial or financial relationships that could be construed as a potential conflict of interest.

The author(s) declared that they were an editorial board member of Frontiers, at the time of submission. This had no impact on the peer review process and the final decision.

Publisher's note

References

Grenni, P., Kujala, K., and Barra Caracciolo, A. (2023). Editorial: Women in terrestrial microbiology: 2022. *Front. Microbiol.* 14:1326145. doi: 10.3389/fmicb.2023.1326145

Kotschik, P., Princz, J., Silva, C. L. E., Renaud, M., Marti-Roura, M., Brooks, B., et al. (2023). The upcoming european soil monitoring law: an effective instrument for the protection of terrestrial ecosystems? *Integr. Environ. Assess. Manag.* 20, 316–321. doi: 10.1002/ieam.4834

Lyu, Z., Shao, N., Akinyemi, T., and Whitman, W. B. (2018). Methanogenesis. *Curr. Biol.* 28, R727–R732. doi: 10.1016/j.cub.2018.05.021

Onet, A., Grenni, P., Onet, C., Stoian, V., and Crisan, V. (2025). Forest soil microbiomes: a review of key research from 2003 to 2023. *Forests* 16:148. doi: 10.3390/f16010148

Rajakaruna, S., Makke, G., Grachet, N. G., Ayala-Ortiz, C., Bouranis, J., Hoyt, D. W., et al. (2024). Adding labile carbon to peatland soils triggers deep carbon breakdown. *Commun. Earth Environ.* 5:792. doi: 10.1038/s43247-024-01954-y

frontiers | Frontiers in Microbiology

TYPE Original Research
PUBLISHED 20 December 2023
DOI 10.3389/fmicb.2023.1327523

OPEN ACCESS

EDITED BY
Ruibo Sun,
Anhui Agricultural University, China

REVIEWED BY
Huan Li,
Lanzhou University, China
Cheng Zhang,
Jiangnan University, China

*CORRESPONDENCE
Zhiyuan Yao
✉ yaozhiyuan@nbu.edu.cn

RECEIVED 25 October 2023
ACCEPTED 20 November 2023
PUBLISHED 20 December 2023

CITATION
Xia J, Yu K, Yao Z, Sheng H, Mao L, Lu D, Gan H, Zhang S and Zhu DZ (2023) Toward an intensive understanding of sewer sediment prokaryotic community assembly and function.
Front. Microbiol. 14:1327523.
doi: 10.3389/fmicb.2023.1327523

Toward an intensive understanding of sewer sediment prokaryotic community assembly and function

Jingjing Xia[1,2], Kai Yu[1,2], Zhiyuan Yao[1,2]*, Huafeng Sheng[3], Lijuan Mao[4], Dingnan Lu[1,2], HuiHui Gan[1,2], Shulin Zhang[4] and David Z. Zhu[1,2,5]

[1]School of Civil & Environmental Engineering and Geography Science, Ningbo University, Ningbo, China, [2]Institute of Ocean Engineering, Ningbo University, Ningbo, China, [3]School of Marine Sciences, Ningbo University, Ningbo, China, [4]Zhenhai Urban Planning and Survey Research Institute of Ningbo, Ningbo, China, [5]Department of Civil and Environmental Engineering, University of Alberta, Edmonton, AB, Canada

Prokaryotic communities play important roles in sewer sediment ecosystems, but the community composition, functional potential, and assembly mechanisms of sewer sediment prokaryotic communities are still poorly understood. Here, we studied the sediment prokaryotic communities in different urban functional areas (multifunctional, commercial, and residential areas) through 16S rRNA gene amplicon sequencing. Our results suggested that the compositions of prokaryotic communities varied significantly among functional areas. *Desulfomicrobium*, *Desulfovibrio*, and *Desulfobacter* involved in the sulfur cycle and some hydrolytic fermentation bacteria were enriched in multifunctional area, while *Methanospirillum* and *Methanoregulaceae*, which were related to methane metabolism were significantly discriminant taxa in the commercial area. Physicochemical properties were closely related to overall community changes ($p < 0.001$), especially the nutrient levels of sediments (i.e., total nitrogen and total phosphorus) and sediment pH. Network analysis revealed that the prokaryotic community network of the residential area sediment was more complex than the other functional areas, suggesting higher stability of the prokaryotic community in the residential area. Stochastic processes dominated the construction of the prokaryotic community. These results expand our understanding of the characteristics of prokaryotic communities in sewer sediment, providing a new perspective for studying sewer sediment prokaryotic community structure.

KEYWORDS

sewer sediment, prokaryotic community function, sulfur cycle, co-occurrence pattern, assembly mechanism

1 Introduction

Urban sewer system, commonly known as "the blood vessel of a city", serves sewage collection and transportation functions, but also is a "biochemical reactor" that can change the form of pollutants, responsible for many important ecological functions (Mathioudakis and Aivasidis, 2009), serving as a reflection of urban ecology. Different from natural

environments such as soil/water which have been around for millions of years, the sewer system is an artificial environment and is a comparatively new habitat for microorganisms (McLellan and Roguet, 2019). The feature of the prokaryotic community in sediment has caught the attention of environmental microbiologists.

Most previous studies have used different types of molecular tools to study specific sediment microorganisms (e.g., sulfur-oxidizing, sulfate-reducing, and methanogenic bacteria) in sewer systems (Dong et al., 2017; Shi X. et al., 2020). There are fewer comprehensive studies on the composition and functional characteristics of prokaryotic communities in sewer sediments. In recent years, high-throughput sequencing technologies have dramatically deepened our insights into prokaryotic communities in diverse ecosystems (Song et al., 2023; Yang et al., 2023). Jin et al. (2018) preliminarily explored the prokaryotic succession patterns in biofilms along urban sewage networks and explored the relationship between sewage quality and prokaryotic communities. However, most sewer sediment studies were conducted using lab-scale reactors (Ren et al., 2022; Sharma et al., 2023), which failed to accurately replicate the intricate environmental conditions in actual sewer systems. In different urban functional areas, the sediment physicochemical properties showed regular change due to the various sources of sewage which likely led to prokaryotic community change. The sewage and sewer sediment properties are highly related to land use patterns (Ekklesia et al., 2015; Maritz et al., 2019). As a result, we assume that functional area could be an important factor that shapes the prokaryotic community distribution and functions in sewer sediment. Since various sewer systems demand different management strategies, understanding the prokaryotic variance across different functional areas could contribute to precision management, improving sewer quality and health.

Microbes do not exist in isolation and often establish an intricate inter-species web that regulates the function and structure of ecosystems (Freilich et al., 2010). Analyzing the co-occurrence patterns could offer fresh perspectives on the sediment habitat and enhance our comprehension of the sediment prokaryotic community, going beyond considerations of diversity and composition (Barberán et al., 2012; Faust and Raes, 2012). Although a wide array of studies revealed the prokaryotic community co-occurrence pattern in complex sediment environments ranging from river to ocean (Djurhuus et al., 2020; Zhang et al., 2021), there is still a knowledge gap remains regarding the sewer sediment, a special artificial habitat for prokaryotic co-occurrence. Intense debates and discussions have surrounded this enduring issue concerning community assembly mechanisms. Both stochastic processes (including homogenizing dispersal, dispersal limitation, and drift) and deterministic processes (including homogeneous selection and heterogeneous selection) facilitate the assembly of prokaryotic communities in diverse habitats. However, it is not yet clear how the sediment prokaryotic community assemblies vary with the functional areas.

Here we hypothesized that functional area could be a significant factor that shapes the prokaryotic community distribution and functions in sewer sediment. Physicochemical properties may impose different stresses that drive community assembly processes, thereby shifting the prokaryotic community structure in the sediment. To address the research needs discussed above and to provide an improved basis for future sewer sediment monitoring efforts, we profiled prokaryotic communities in sewer sediments from typical urban functional areas, including multifunctional, commercial, and residential areas. This study aims to (1) characterize the prokaryotic diversity and composition of sewer sediment; (2) elucidate the relationship between prokaryotic community structure and physicochemical properties; (3) uncover the prokaryotic co-occurrence and assembly patterns in the sewer sediment in different functional areas. This study aims to comprehensively provide insights into prokaryotic communities in different functional areas, and provide new insights for the analysis of urban sewer sediment prokaryotic communities.

2 Materials and methods

2.1 Sample collection

Typical multifunctional, commercial, and residential areas were selected in Ningbo, China. In each functional area, two separate main sewer systems were randomly selected. Under the expert guidance of the Zhenhai Urban Planning and Survey Research Institute of Ningbo, we selected an area in the city where residential buildings were relatively concentrated as a residential area, a district where retail businesses were clustered and transactions were frequent as a commercial area, and a district with multiple functions, such as residential, commercial, service, and administrative areas, as a multifunctional area. A total of 15 sampling sites were strategically designated, spanning three distinct functional areas. The specific information on sewer is detailed in **Supplementary Table 1**. The in-field criteria are as described by Crabtree (1989). There was a two-week drying period before sampling. Determination of temperature, dissolved oxygen, and pH of sewage at different sampling sites using the Multiparameter Instrument (Pro-Plus, Xylem, America). Additionally, the hydrogen sulfide concentrations in the manhole were measured using the Hydrogen sulfide gas recorder (H_2S Gas Monitor (PPM) gas monitor, Acrulog^{TM}, Australia). Sediments were collected in quadruplicate using a shovel. The 60 collected samples (fifteen sites by four replicates) were carefully placed into sterile plastic bags with airtight seals. These bags were stored in ice packs at controlled low temperatures to maintain sample integrity. After transportation, sediments were preserved at 4°C for sedimentary physicochemical property analysis and at −80°C for DNA isolation, respectively.

2.2 Physicochemical analysis

The sediment metrics including sediment pH, total organic carbon (TOC), total phosphorus (TP), total nitrogen (TN), nitrate-nitrogen (NO_3^--N), ammonium-nitrogen (NH_4^+-N), and available sulfur (AS) contents, total solid (TS), volatile solid (VS), and physical texture (sand, silt, and clay contents) were measured. Determination of pH in sediments using a pH meter: water (1:5) extract. Sediment TOC and TN were assessed with TOC

analyzer (multi-N/C3100, analytic jena, Germany). Sediment TP was measured using a digestion method. Sediment NH_4^+-N and NO_3^--N were determined by the method described in the Chinese Committee of Agricultural Chemistry (1983). Sediment AS was determined by the $BaSO_4$ turbidimetric method. Sediment TS was measured by high-temperature burning weighing method and sediment VS was measured by the Gravimetric method. Sediment physical texture was measured by a laser diffraction particle size analyzer (2000LD, Bettersize, China). The physicochemical properties of each sediment sample were obtained from four independent replicate samples. The temperature, pH, and dissolved oxygen of sewage are detailed in **Supplementary Table 2**.

2.3 DNA extraction, PCR amplification and sequencing

The PowerSoil® DNA kit (MoBio Laboratories, Carlsbad, CA, USA) was used to isolate prokaryotic DNA from each sample. For the prokaryotic community, we used the universal primers 515F (5′-GTGCCAGCMGCCGCGGTAA-3′) and 806R (5′-GGACTACNVGGGTWTCTAAT-3′) to amplify the V4 region of the 16S rRNA gene. Next, the amplified and cleaned DNA samples were sequenced using the pairwise end-to-end (2 × 300 bp) method by an Illumina MiSeq platform (Illumina, Inc., San Diego, CA, USA). The raw sequences were submitted to the NCBI BioProject database. The accession number was PRJNA1015661.

2.4 Illumina data processing

Use Usearch fastq_mergepairs command with default parameters in USEARCH v.11 software to combine paired-end reads (Edgar, 2010). In brief, redundant sequences and chimeras are filtered using the USEARCH unoise3 algorithm. USEARCH fastx_uniques was used to sort the retained clean markers in non-redundant abundance order. We classified sequences with ≥97% similarity as zero-radius operational taxonomic units (ZOTUs) (Edgar, 2010). The sequences with the highest abundance and coverage in each ZOTU were selected as representative sequences and compared with the Greengenes Database (release 13.8) using PyNAST to get taxonomic information of each ZOTU (DeSantis et al., 2006; Caporaso et al., 2010).

2.5 Statistical analysis

Calculation of alpha diversity indices of the sediment prokaryotic communities used the "vegan" package (Dixon, 2003). Differences in prokaryotic community samples between functional areas were analyzed by principal coordinate analysis (PCoA). The significance of differences was tested by Permutational multivariate analysis of variance (PERMANOVA). Linear discriminant analysis effect size (LEfSE) was used to identify the taxa with significant differences across functional areas (Chen H. et al., 2021). The program "functional annotation of prokaryotic taxa" (FAPROTAX) was used to predict the environmental biochemical functions of the prokaryotic communities in sediment. The effect of physicochemical properties on prokaryotic community composition was investigated using redundancy analysis (RDA). The two-way correlation network analysis was conducted using the 200 most abundant genera in terms of taxonomic abundance and physicochemical properties (performed using Network and Gephi). The correlation matrix was constructed by performing the Spearman's rank correlation coefficient for each pairwise comparison (with a threshold of Spearman coefficient ≥ 0.6 and $p < 0.05$).

2.6 Co-occurrence network and community assembly analysis

Co-occurrence network analysis was based on Spear correlation (Spearman $|R| > 0.9$, $p < 0.01$), occurring in more than 80% of the samples. Subsequently, the prokaryotic co-occurrence network was established in Gephi (0.9.7). The role of each node in the network is identified by the inter-module connectivity (Pi) and intra-module connectivity (Zi) of the module attributes (Guimerà and Nunes Amaral, 2005). The "keystone species" refers to nodes determined to be network hub and module hub based on intra-module connectivity (Zi) and inter-module connectivity (Pi) values. The neutral community model was predicted by the "Hmisc" package. The iCAMP method was used to determine the assembly process (Ning et al., 2020).

3 Results

3.1 Sediment physicochemical properties and prokaryotic community diversity

Sewer sediment physicochemical properties fluctuated dramatically across functional areas (**Supplementary Figure 1**). The hydrogen sulfide (H_2S) concentration in the multifunctional area (7.69 ppm) was found to be significantly higher compared to the commercial area (3.06 ppm) and the residential area (3.2 ppm) ($p < 0.05$). Moreover, the multifunctional area exhibited the highest content of available sulfur (AS), total nitrogen (TN), total phosphorus (TP), and total organic carbon (TOC) while the residential area had the highest level of nitrate-nitrogen (NO_3^--N) (**Supplementary Figure 1**). The pH was higher in the commercial area compared to the multifunctional area and residential area (**Supplementary Figure 1**). At the ZOTU level, the functional area significantly affected the diversity of sediment prokaryotic communities (**Figure 1A**). The Shannon and Richness indices were significantly different among functional areas ($p < 0.05$). Shannon index was the highest in multifunctional area, followed by residential area and commercial area. Similarly, the Richness index showed the same phenomena. Additionally, the random forest (RF) analysis identified TS (total solid), TOC (total organic carbon), and TP (total phosphorus) as relatively important variables in regulating the diversity of sediment prokaryotic communities (**Supplementary Figure 2**). Differences in prokaryotic communities in sewer sediments from three functional areas were analyzed using the principal coordinate analysis (PCoA) (**Figure 1B**). Prokaryotic community

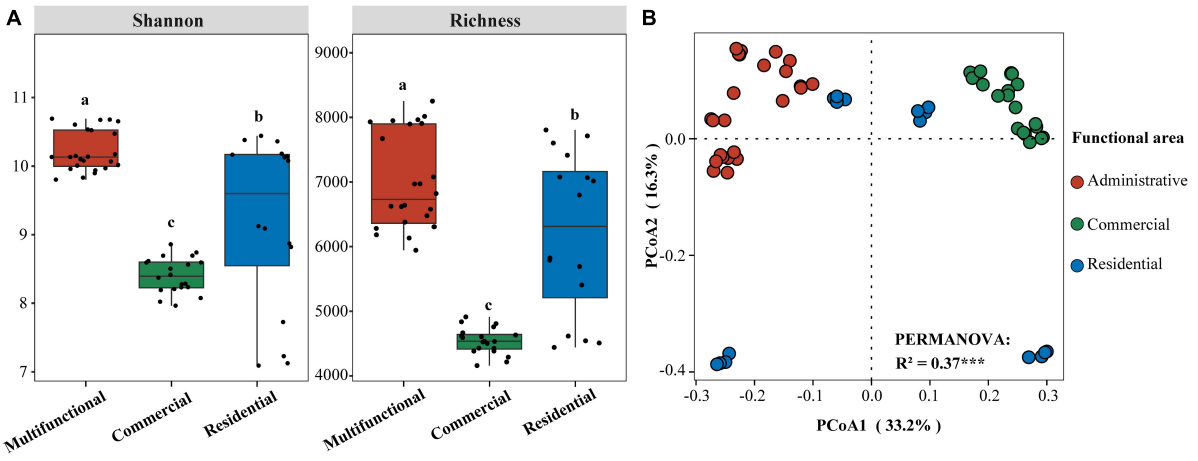

FIGURE 1
(A) Differences of Shannon and Richness indices in sediment from different functional areas. Significance of differences is indicated by "a, b, c" ($p < 0.05$; multiple comparison with ANOVA tests); **(B)** Principal coordinate analysis (PCoA) based on Bray-Curtis dissimilarity and PERMANOVA tests showing the variation of sediment prokaryotic communities from different functional areas. ***$p < 0.001$.

composition differed significantly among functional areas ($p < 0.001$) (Figure 1B).

3.2 Variation of sediment prokaryotic community composition and function

Circos plot uncovered the distribution of sewer sediment prokaryotic community composition in different functional areas at the phylum level (Figure 2). *Proteobacteria* and *Bacteroidetes* were the most abundant phyla in the sediment. *Proteobacteria* exhibited significantly higher abundance in the multifunctional sediment ($p < 0.05$), whereas the relative abundance of *Aminicenantes* was found to be the highest in the commercial area. Linear discriminant analysis (LDA) was used to identify the differentially abundant taxa among different functional areas (Supplementary Figure 3). Interestingly, various functional taxa were identified as significantly discriminant taxa in different functional areas. *Desulfomicrobium*, *Desulfovibrio*, and *Desulfobacter* (Wang et al., 2023) are involved in the sulfur cycle, and some hydrolytic fermentation bacteria, such as *Trichococcus*, *Ornatilinea*, and *Anaerolinea* (Jin et al., 2018), were enriched within the prokaryotic communities in the multifunctional area. In addition, *Methanospirillum* and *Methanoregulaceae* (Qian et al., 2023), which were related to methane metabolism were significantly discriminant in the commercial area.

We conducted further analysis to investigate the distribution of methanogenic archaea (MA) and sulfate-reducing bacteria (SRB) in sediments across various functional areas. The relative abundances of SRB in the multifunctional, commercial, and residential areas were quantified as 1.96, 1.05, and 0.91%, respectively. Remarkably, the multifunctional area exhibited a comparatively higher relative abundance of SRB. Furthermore, we identified four primary genera, namely *Methanothrix*, *Methanobacterium*, *Methanospirillum*, and *Methanomassiliicoccus*, as the predominant members of the accumulated MA community. The relative abundances of MA were determined to be 3.58% in the multifunctional area, 4.73% in the commercial area, and 3.44% in the residential area. These findings indicated that the commercial area has the highest relative abundance of MA.

The ecological functions of prokaryotic communities present in the sewer sediment were characterized by annotating them into 76 functional groups and categorized into 5 major groups including carbon cycle, nitrogen cycle, sulfur cycle, energy source, and other predicted functions using "functional annotation of prokaryotic taxa" (FAPROTAX) (Figure 3). Based on principal coordinate analysis (PCoA), there was an obvious separation among functional areas (Supplementary Figure 4). Permutational multivariate analysis of variance (PERMANOVA) further revealed that significant differences were observed in the prokaryotic community functions among functional areas ($p < 0.05$). The top 30 most abundant functions were identified and presented as a heatmap (Figure 3). According to the results, chemoheterotrophy, methanogenesis, and fermentation were the most common functions, and multiple sulfur metabolism-related function genes, including dark oxidation of sulfur compounds, respiration of sulfur compounds, and sulfate respiration were also observed. Interestingly, we observed distinct patterns in the functional group relative abundance associated with different ecological functions (Figure 3). Specifically, the multifunctional area exhibited the highest relative abundance of functions related to the sulfur cycle. On the other hand, functional groups associated with methanogenesis, the process involved in methane production, were concentrated in the commercial area.

3.3 Physicochemical properties affecting the prokaryotic community

Redundancy analysis (RDA) revealed that the prokaryotic community structure was tightly related to physicochemical properties (Figure 4). The first axis (RDA1) and second axis (RDA2) explained 49.4% of differences in the community structure.

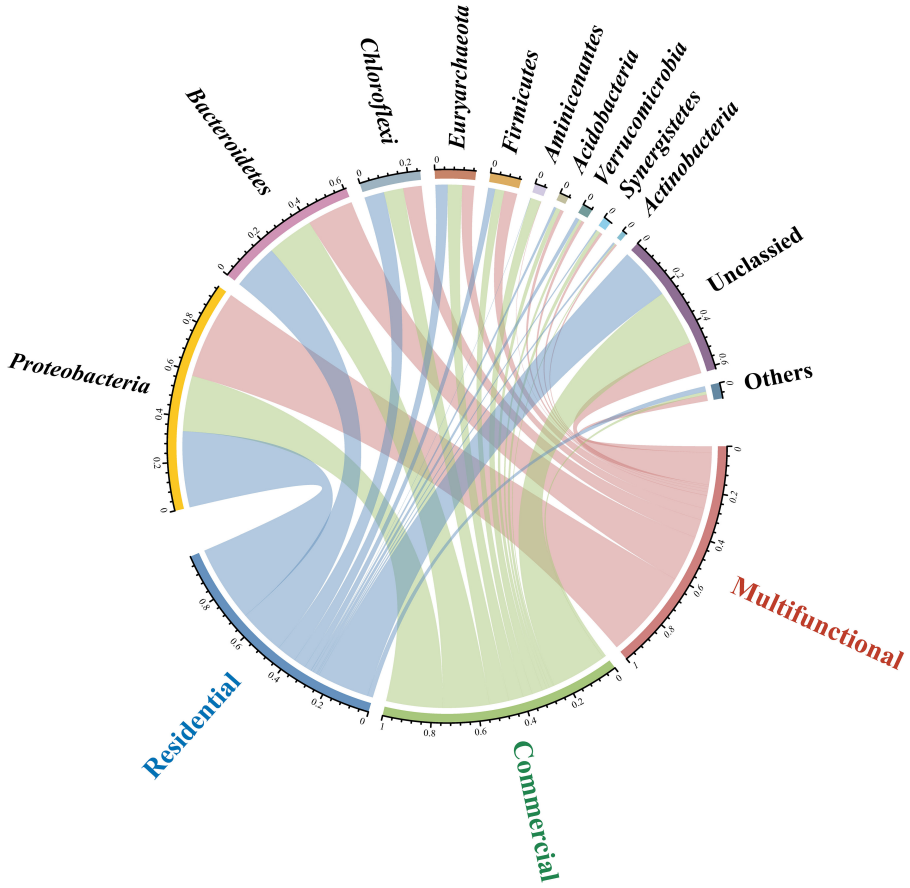

FIGURE 2
Circos plot showing the distribution of sewer sediment prokaryotic community composition at phylum level in different functional areas.

TP (R^2 = 0.51, p < 0.01), TN (R^2 = 0.36, p < 0.01), and pH (R^2 = 0.41, p < 0.01), were significantly related to the sediment prokaryotic community (Supplementary Table 3). Two-way correlation network analysis was conducted to further demonstrate the correlation between sediment physicochemical properties and genus-level prokaryotic communities (Figure 5). TOC, pH, and TN stood for the key hub nodes in the network, showing complex connections with prokaryotes. TOC and TN were positively correlated with most prokaryotes. On the contrary, pH and TS showed negative correlations with most prokaryotes.

Given the disparities in the distribution of methanogenic archaea (MA) and sulfate-reducing bacteria (SRB) in various functional areas, we further investigated their correlation with physicochemical properties. Spearman correlation analysis revealed that the response sensitivity of MA and SRB to physicochemical properties in sewer sediments was different (Supplementary Figure 5). Most SRB was positively correlated with total nitrogen (TN), total phosphorus (TP), total organic carbon (TOC), nitrate-nitrogen (NO_3^--N), ammonium-nitrogen (NH_4^+-N), available sulfur (AS), and volatile solid (VS), while negatively correlated with pH and total solid (TS). *Methanothrix*, which was the most abundant genus of MA, was positively correlated with total organic carbon (TOC), total phosphorus (TP), and volatile solid (VS). In contrast, it was negatively correlated with nitrate-nitrogen (NO_3^--N) and total solid (TS).

3.4 Co-occurrence pattern and keystone species in sediment prokaryotic communities

The co-occurrence patterns of prokaryotic ZOTUs (at least 80%) were visualized by network analysis (Figure 6A). More positive edges were detected in all networks, implying that prokaryotic ZOTUs tended to cooperate and coexist rather than compete in the sewer sediment. The topological parameters were summarized as shown in Table 1. The node numbers, edge numbers, and average degree which can assess sediment prokaryotic network complexity were the highest in the residential sediment, whereas the lowest in the commercial area sediment. On the contrary, modularity and positive proportion were the highest in the commercial sediment. The potential topological roles of taxa in the networks were assessed according to within-module connectivity (Zi) and among-module connectivity (Pi) values:(1) network hub (Zi > 2.5 and Pi > 0.62); (2) module hub (Zi > 2.5 and Pi ≤ 0.62); (3) connector (Zi ≤ 2.5 and Pi > 0.62); and (4) peripheral (Zi ≤ 2.5 and Pi ≤ 0.62) (Zhang et al., 2023; Figure 6B). *Thiobacillus*, *Methanospirillum,* and *Geobacter* were keystone species with the highest frequency of occurrence in multifunctional, commercial, and residential areas, respectively. In the multifunctional area, 1 network hub (ZOTU275, belonging to *Anaerolineaceae*) was recognized. More specifically, 152

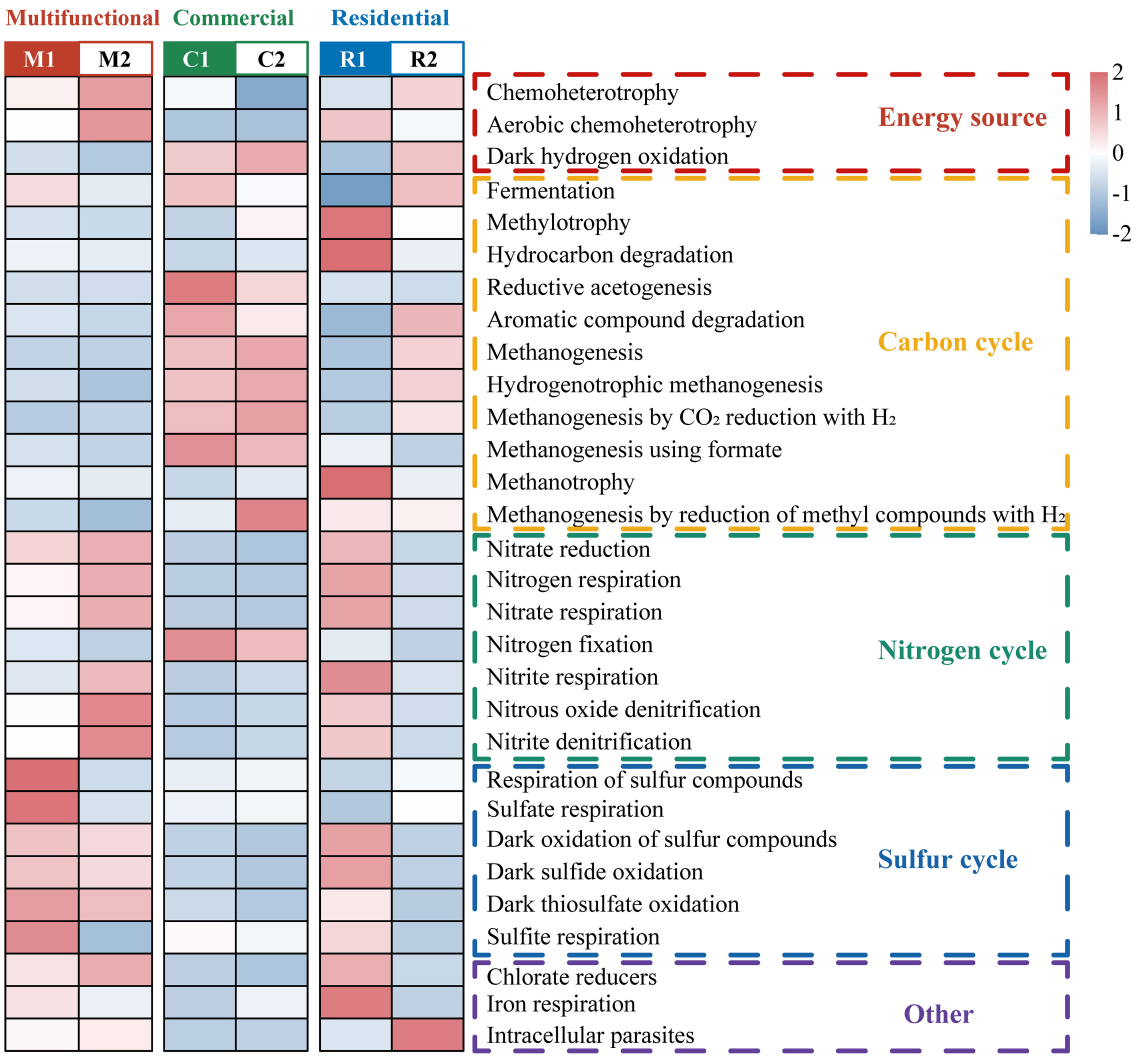

FIGURE 3
Heatmap representing major differences in predicted functions among sewer sediments from different functional areas based on Functional annotation of prokaryotic taxa (FAPROTAX).

keystone species including 140 connectors, 11 module hubs, and 1 network hub were identified in the multifunctional sewer network, which mainly belongs to *Thiobacillus*, *Desulfovibrio*, and *Methanobacterium*. In the commercial area, we identified a total of 63 connectors and 6 module hubs, which mainly belonged to *Methanospirillum*, *Holophaga*, and *Methanothrix*. In the residential area, keystone species mainly belonged to *Geobacter*, *Syntrophorhabdus*, and *Candidatus_Cloacamonas*.

3.5 Assembly mechanisms across sewer sediment in different functional areas

Considering that the composition and diversity of sewer sediment prokaryotes were spatially dynamic, we investigated the community assembly mechanisms driving forces that shaped the community structure, which could provide the theoretical basis for sediment prokaryotic community regulation. The neutral model fitted the data of all three functional areas, producing the lowest R^2 (0.65) in residential area and the highest R^2 (0.86) in commercial area (Figure 7A). The majority of dots were in the neutral range (86.2% ~ 91.2%), suggesting that stochastic processes dominated the prokaryotic community assembly in sewer sediments. Mitigation rates were higher in the multifunctional area (m = 0.82) and the commercial area (m = 0.82) than in the residential (m = 0.49) area, suggesting that the multifunctional area and commercial area were less limited by dispersal (Figure 7A). Among the three functional areas, the neutral part was consistently dominant. In general, the result of the neutral model suggested that the processes of random dispersal and ecological drift were more significant than selection in assembling the prokaryotic community in different functional areas.

In addition, we quantified the relative contribution of major ecological processes that structure the prokaryotic community in the sediments. The ecological processes mainly include stochastic and deterministic processes. The stochastic processes included homogenizing dispersal, dispersal limitation, and drift, while the deterministic processes were divided into heterogeneous selection

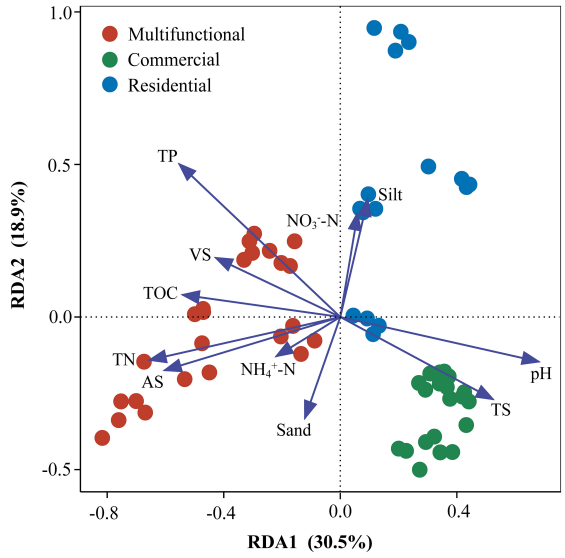

FIGURE 4
Redundancy analysis (RDA) of sewer sediment prokaryotic communities with physicochemical properties. TP, total phosphorus; TN, total nitrogen; AS, available sulfur; TS, total solid; TOC, total organic carbon; VS, volatile solid; NO_3^--N, nitrate-nitrogen; NH_4^+-N, ammonium-nitrogen; pH, sediment pH; physical texture (sand, and silt contents).

and homogeneous selection. Generally, our findings reveal that stochastic processes significantly dominate the assembly of the prokaryotic community, as shown in Figure 7B. Homogeneous selection was the highest in the residential area sediments (39.2%) (Figure 7B). Conversely, the importance of dispersal limitation was lowest in residential sediments (9.1 and 0.2%, respectively) (Figure 7B).

4 Discussion

4.1 Sediment prokaryotic diversity varies with functional area

Our research revealed that, compared to various natural sediment ecosystems, the Shannon index of the sewer sediment was notably higher (Zhang et al., 2021; Wang et al., 2022). This might be attributed to the varying environmental conditions between artificial pipes and natural ecosystems. The organic matter from sewage might be decomposed into numerous compounds (Shi et al., 2018; McLellan and Roguet, 2019), leading to the increased species richness and diversity of the sewer sediment prokaryotic community. In addition, the existence of foreign matter such as fibers and plastics can create extra microhabitats and ecological niches that afford diverse microorganisms the chance to establish and flourish (Wright et al., 2020), thereby contributing to overall diversity. Furthermore, the rapid flow velocity of sewage creates a distinct physical environment compared to natural ecosystems. The constant movement and turbulent flow of wastewater could influence the distribution of microorganisms and nutrient availability within the sediment (Gudjonsson et al., 2002), further contributing to the increased diversity observed in sewer sediment compared to natural ecosystems.

Moreover, the prokaryotic diversity values (Shannon and Richness indices) were significantly higher in the multifunctional area sediments (Figure 1A), while they were significantly correlated with total solid (TS), total organic carbon (TOC), total phosphorus (TP), and volatile solid (VS) (Figure 4). In the multifunctional area, higher levels of total phosphorus (TP) and total organic carbon (TOC) were observed compared to the commercial and residential areas (Supplementary Figure 1). These carbon and phosphorus components are essential nutrients for the growth and reproduction of prokaryotic communities (Wang et al., 2020; Yi et al., 2021), which leads to a higher α-diversity of prokaryotic communities in multifunctional areas. In addition, the β-diversity analysis yielded a distinct clustering of the samples (Figure 1B). This finding is consistent with a previous study on urban river sediments, which also showed similar clustering patterns based on functional area types (Wang et al., 2021). In urban sewer system, sewage is an important source for the sediment community, so the various sources of sewage might contribute to the different sediment prokaryotic structures of each functional area (Figure 1B). Indicating that the sewer sediment of each functional area owned its unique microbiome.

4.2 Dominant prokaryotic assemblages and functions are altered with distinct sewer habitats

Consistent with observations from previous studies, the prokaryotic communities in sewer sediment were dominated by *Proteobacteria* and *Bacteroidetes* (Figure 2). However, this is different from natural habitats, which were mainly dominated by *Actinobacteria* and *Proteobacteria* (Zhang et al., 2021). The sewerage contains a high concentration of pollutants, such as organic matter, nutrients, and heavy metals. The physicochemical properties of the sewerage, including low pH value and dissolved oxygen levels, were significantly different from natural environments (McLellan and Roguet, 2019). These differences may result in changes in sewer sediment prokaryotic composition. Additionally, distinct sewer sediment prokaryotic community compositions were observed among functional areas. *Desulfomicrobium*, *Desulfovibrio,* and *Desulfobacter*, typical sulfate-reducing bacteria (SRB), were more abundant in the multifunctional area sediment (Supplementary Figure 3). Some significantly discriminant taxa remain in the multifunctional area sediment, including fermentation bacteria (FB) and hydrogen-producing acetogen (HPA) (Supplementary Figure 3). The hydrolysis and fermentation processes produce volatile fatty acids and macromolecular acids, which provide appropriate conditions for the SRB (Jin et al., 2015), which may lead to a higher relative abundance of SRB, ultimately leading to relatively high hydrogen sulfide concentrations in multifunctional areas. Functional annotation of prokaryotic taxa (FAPROTAX) further demonstrated that functions associated with sulfur cycling were particularly notable in the multifunctional areas (Figure 3). Combined with in-field measurements of hydrogen sulfide concentrations, we should pay attention to the hydrogen sulfide

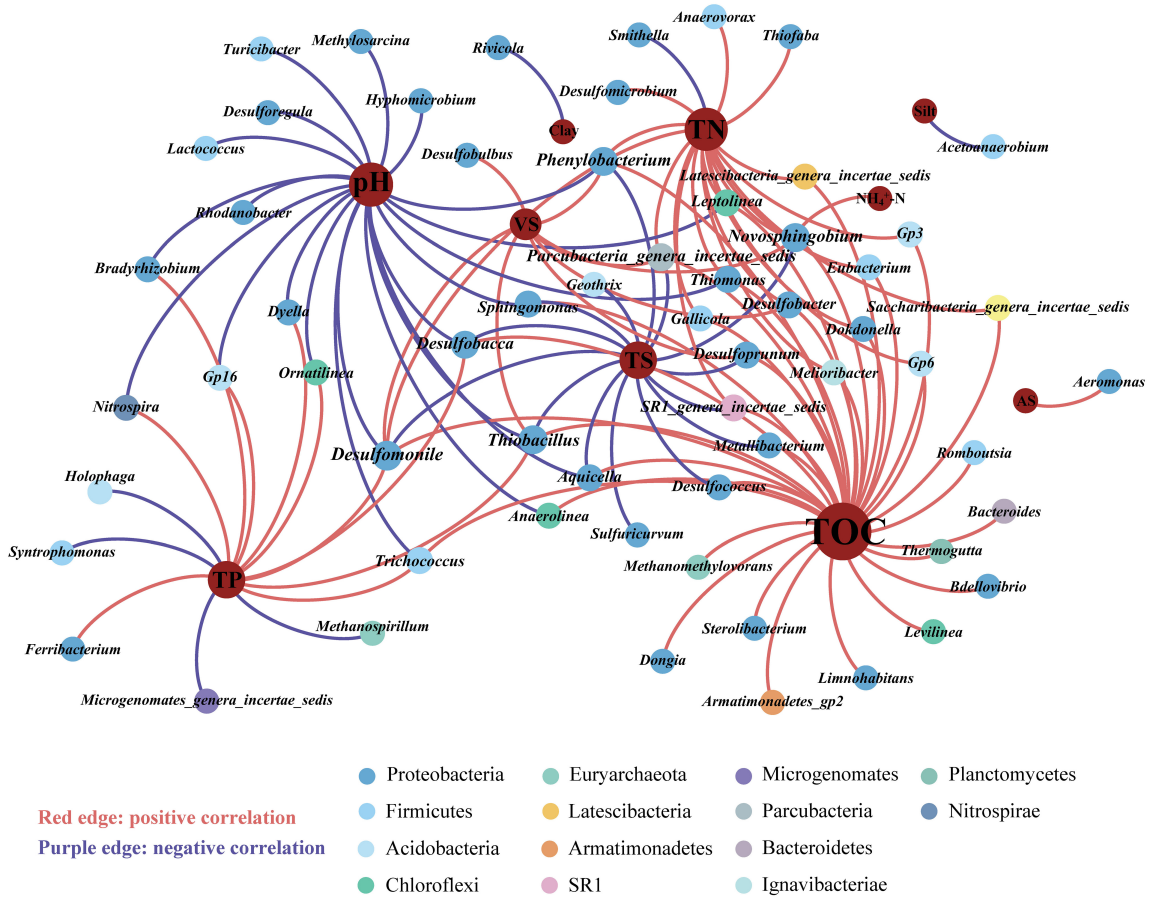

FIGURE 5
Two-way correlation network analysis between prokaryotic genera and sediment physicochemical properties. Different colors of nodes were classified into various phyla. TOC, total organic carbon; pH, sediment pH; TP, total phosphorus; TN, total nitrogen; TS, total solid; VS, volatile solid; AS, available sulfur; NH_4^+-N, ammonium-nitrogen; physical texture (sand, and silt contents).

risk in multifunctional area sewers. Recently, amounts of studies have reported methane production from freshwater sewerage systems, implying that sewer sediment is an important greenhouse gas contributor to the environment (Chen et al., 2020; Chen S. et al., 2023). Our work revealed that *Methanospirillum, and Methanoregulaceae*, associated with methane production, were more abundant in the commercial area sediments (**Supplementary Figure 3**). Moreover, *Syntrophomonas* and *Smithella* also had a higher relative abundance in commercial area ($p < 0.05$). It was reported that they can form powerful symbiotic interactions with methanogens (McInerney et al., 1981; Embree et al., 2013). Meanwhile, the functional capacity for methane metabolism was also predominantly concentrated in the commercial area (**Figure 3**). Thus, we speculated that sewer sediments in commercial areas may obtain higher potential in methanogenesis.

4.3 Local physicochemical properties shape the prokaryotic distribution

Environmental factors play a crucial role in the formation of microbial community composition and functional characteristics (Nelson et al., 2016; Gibbons, 2017; Louca et al., 2017). It has been demonstrated that the structure of natural sediment prokaryotic communities is correlated with TN, TOC pH, etc., (Bao et al., 2023; Feng et al., 2023). Our results revealed that sediment TN, TP, TOC, and pH were the major elements strongly related to the structure of the prokaryotic community (**Figures 4**, **5**). Nutrient levels affect the growth of prokaryotic communities in sediments. In most sediment ecosystems, TN and TP serve as the main limiting nutrients and play an essential role in regulating prokaryotic community structure (Cai et al., 2022; Chen Y. et al., 2023). Similarly, TOC, as a source of energy and carbon for microbial metabolism, also influences the composition, diversity, and function of microbial communities (Hu et al., 2022). The significance of pH in forming microbial communities has been widely documented across a variety of ecosystems (Fierer and Jackson, 2006; Jones et al., 2019; Naz et al., 2022). It affects the various life processes of aquatic organisms by influencing cellular osmotic pressure, enzyme synthesis, and nutrient uptake (Santini et al., 2022). A large number of studies have revealed that pH could change nutrient effectiveness and organic carbon content, thus directly or indirectly affecting the diversity, composition, and abundance of microbial communities (Colman et al., 2016; Dong et al., 2022). In total, these physicochemical properties were demonstrated to a crucial role in forming prokaryotic communities.

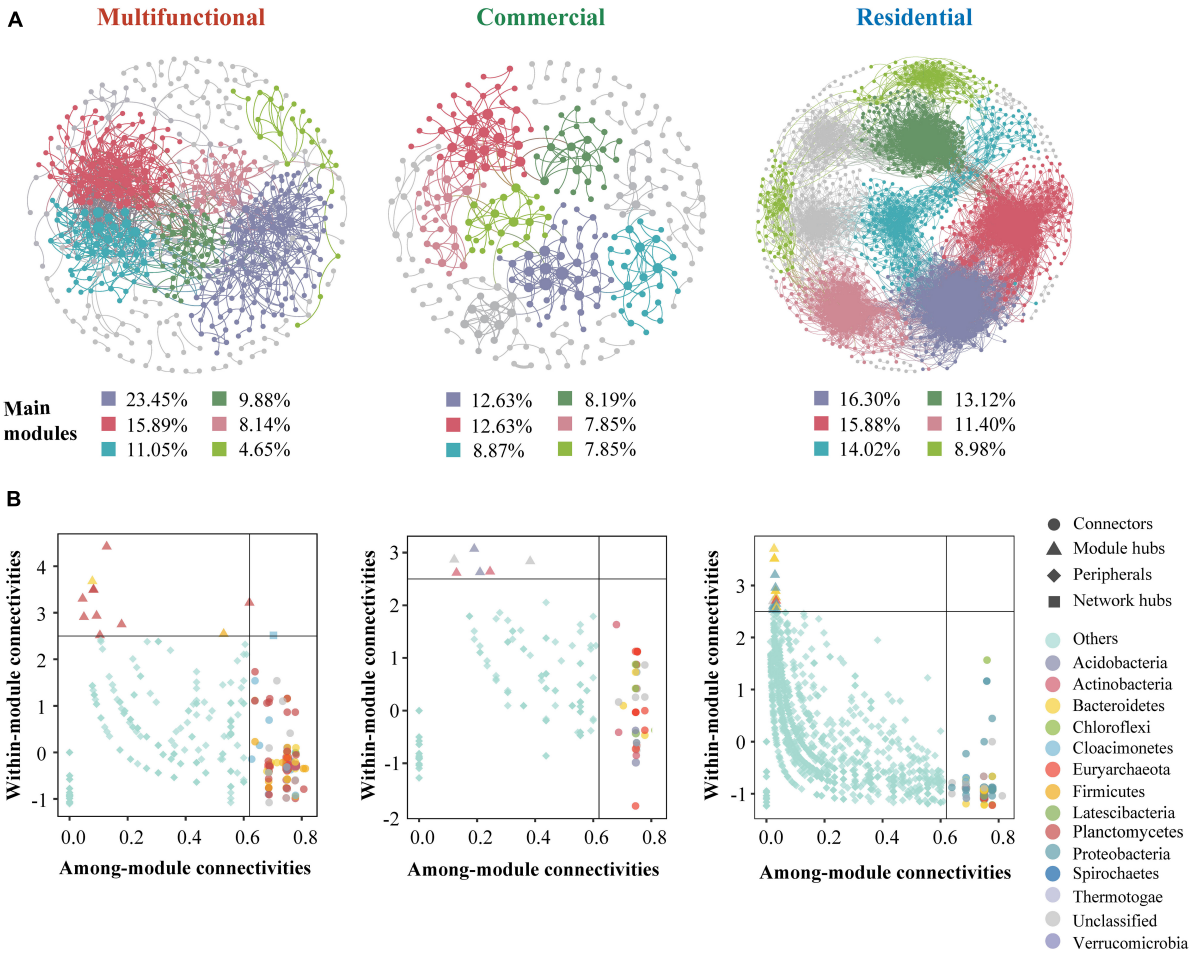

FIGURE 6
Co-occurrence network analysis of the sewer sediment prokaryotic communities from different functional areas. **(A)** Co-occurrence networks in different functional areas. **(B)** keystone species analysis.

Nonetheless, this study may not provide a complete explanation for all the observed changes. Therefore, more comprehensive investigations are needed to explore the potential influence of other factors.

4.4 The co-occurrence networks revealed a more complex co-occurrence network in sewer sediment from residential area

Microbial networks have been proven to be an efficient method for revealing microbial co-occurrence patterns (Qiu et al., 2021). In terms of global network topology, the findings indicated that the residential area network was characterized by a higher level of complexity and a lower proportion of positive correlations (**Figure 6A** and **Table 1**). Conversely, the commercial area characterized by the simplest network exhibited the highest level of positive correlations (**Figure 6A** and **Table 1**). Previous studies indicated that an increase in complexity is generally accompanied by a decrease in positive correlation proportion (Li and Xiao, 2023), which is consistent with our study. Complexity leads to stability, suggesting a robust correlation between ecological stability and the complexity of microbial networks (Okuyama and Holland, 2008). Higher network complexity increases inter-specific interaction, providing microbial communities with favorable characteristics for effective resistance to environmental interference (Konopka et al., 2015; Jiao et al., 2020), which leads to a significant increase in the stability of microbial ecosystems. We speculated the possible reason was that the sources and characteristics of the sediment in residential area were relatively homogeneous. Generally, in more homogeneous environments, the composition of prokaryotic communities tends to be more stable, which favors the formation of a complex and stable network. In contrast, commercial area sewage was always characterized by a large sewage flow rate, complex water quality, and significant water quality fluctuations. These implied that the composition of prokaryotes in commercial areas sediment might be variable, leading to an unstable network. Previous studies indicated that positive correlations represent cooperative relationships and can enhance or maintain community stability and diversity through ecological niche complementation or synergism (Coyte et al., 2015). Therefore, prokaryotic communities in commercial area

TABLE 1 Topological properties of the sewer sediment co-occurrence network from different functional areas.

Functional areas	Multifunctional	Commercial	Residential
Nodes	516	293	1448
Edge	1385	459	19530
Average degree	5.368	3.133	26.975
Modularity	0.6	0.817	0.72
Percentage of negative correlations	29.24	24.18	32.7
Percentage of positive correlations	70.76	75.82	67.3
Graph density	0.01	0.011	0.019
Clustering coefficient	0.342	0.376	0.511
Average path length	5.058	6.897	5.435

tend to cluster forming a more cooperative network to transfer information and share resources, to enhance the stability of the network.

The key module hubs or nodes may be important members of the prokaryotic community in a network, playing a vital role in sustaining community stability (Shi Y. et al., 2020). It has been demonstrated that keystone species have more significant roles in sustaining network structure than the other microbes, and the deprivation of these key taxa may contribute to the dissolution or even disintegration of the network (Shi Y. et al., 2020; Liu et al., 2022). *Anaerolineaceae*, which as the representative group of the *Chloroflexi*, could degrade carbohydrates (e.g., amino acids) (Zhang et al., 2017), was the network hub in the multifunctional area network. The highest occurrence of keystone species in multifunctional area network is *Thiobacillus* and *Desulfovibrio*, which are involved in nitrogen metabolism and sulfur biogeochemical cycling (Chen et al., 2018; Li et al., 2023). *Desulfovibrio*, a typical sulfate-reducing bacterium, was found to be a keystone species in the multifunctional area network, indicating that this network has specific ecological and geochemical functions related to sulfate cycling, such as sulfide generation. *Geobacter* was the keystone species of the residential area networks. *Geobacter* is an oligotrophic bacterium that can transfer electrons to facilitate the degradation of the chemical compound (Fan et al., 2019). In addition, the keystone species of the commercial area such as *Methanospirillum* were reported to be involved in methanogenesis, which could convert certain compounds from organic waste and

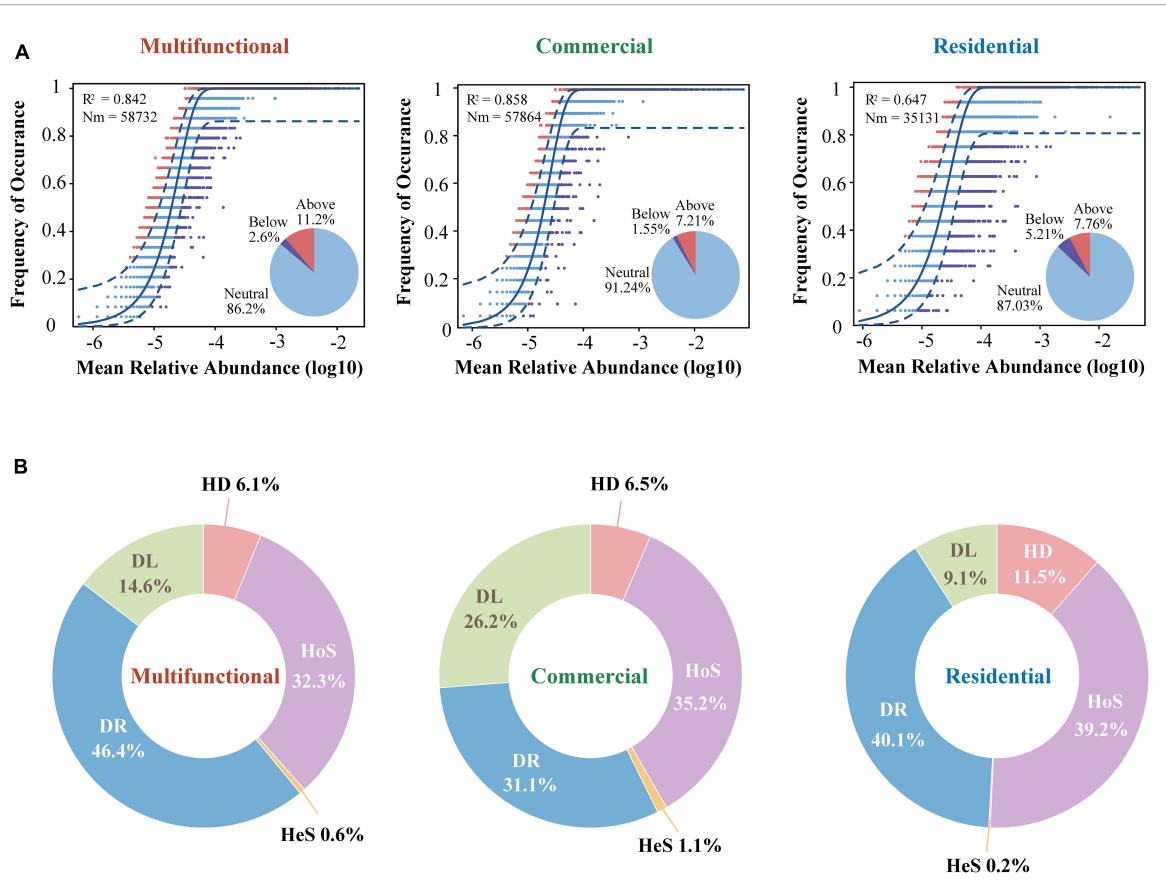

FIGURE 7
The assembly process of sewer sediment prokaryotic communities from different functional area. **(A)** The neutral community model. The Blue dashed line indicates 95% confidence intervals for the prediction of neutral model. R^2 values indicate the goodness of fit. The Nm parameter reflects immigration times metacommunity size. **(B)** The contributions of different ecological processes in assembling the prokaryotic community. HeS, heterogeneous selection; HoS, homogeneous selection; HD, homogenizing dispersal; DL, dispersal limitation; DR, drift.

wastewater into methane. This implied that the emission of greenhouse gases from commercial areas ought to be given greater consideration.

4.5 Stochastic processes dominate prokaryotic community assembly in sewer sediment

A key target in microbial ecology is quantifying the relative contribution of deterministic and stochastic processes in microbiome assembly (Weigel et al., 2023). In different ecosystems, the relative importance of deterministic and stochastic processes seems to be different (Matar et al., 2017; Huo et al., 2023; Lin et al., 2023). Considering that microbial diversity and community composition vary across functional areas, we further investigated the microbial assembly mechanisms. In this study, the stochasticity process dominated the prokaryotic community assembly across the three functional areas. Previous studies showed that stochastic processes largely dominate the assembly of microbial communities in some urban wastewater infrastructure (Wu et al., 2019), while deterministic processes were relatively more important in some natural ecosystems (Chen Q. et al., 2021; Lu et al., 2023). Natural ecosystems are typically relatively stable and undisturbed systems, while engineered ecosystems are typically dynamic and constantly changing systems that require adaptation to changing environmental conditions. In a constantly perturbed environment, microbial inhabitants may have been able to adapt to such dynamics and be less responsive to deterministic factors (Santillan et al., 2019). This may explain why stochastic processes dominate the assembly of sediment prokaryotic communities in this study.

Additionally, the specific contributions of subcategories of stochastic and deterministic processes to the prokaryotic community assembly differed across distinct functional areas. Drift, a subcategory of stochastic processes, was 46.4, 31.1, and 40.1% in the multifunctional, commercial, and residential sediments, respectively, (**Figure 7B**). This could be explained by the alpha diversity variation of sediment communities across the three functional areas. The stochastic process regulates the assembly of a high-diversity prokaryotic community, whereas the deterministic process exhibits a more pronounced prominence when bacterial diversity is lower (Xun et al., 2019). In this study, the highest alpha diversity was found in multifunctional sediments, followed by residential area and commercial area. As a result, the proportion of drift process was the highest in the multifunctional area, while lowest in the commercial area. The neutral model fit well with the prokaryotic communities in all areas, with R^2 values ranging between 0.647 and 0.858 (**Figure 7A**). These results confirmed that stochastic (neutral) processes played prominent roles in the prokaryotic community assembly of sewer sediment. Comparative analyses among functional areas provide the first informative insights into the patterns in the sewer sediments community assembly. These findings contribute to a better comprehension of the formation and evolution mechanisms of sewer sediment prokaryotic communities, providing significant reference value for future ecological restoration and control strategies.

5 Conclusion

In the study, we analyzed the dynamics of prokaryotic communities in the urban sewer in different functional areas using 16S rRNA gene amplicon sequencing. Significant prokaryotic community diversity and composition differences were observed among sediment from typical urban functional areas (multifunctional, commercial, and residential areas), which were mainly correlated with changes in sediment nutrient level and pH. Prokaryotic microorganisms with different functions were gathered in different functional areas. The residential area network has the highest complexity and stability. Potential keystone taxa identified by co-occurrence network analysis also differed among functional areas. The stochasticity process dominated the prokaryotic community assembly. The results of this study will help improve the understanding of the prokaryotic ecology in sewer sediment, providing a foundation for screening of functional microorganisms and supporting a genomic basis for the precise administration of sewer systems in different functional areas. For urban sewer system ecosystems, functional areas may be a new perspective for in-depth analysis of the characteristics of communities. In future work, time-series sampling should be conducted to confirm the observed pattern. In addition, in-depth investigations on sediment prokaryotic communities on a larger scale with greater depth are hoped to further improve our insight into prokaryotic community assembly in sewer sediment.

Data availability statement

The datasets presented in this study can be found in online repositories. The names of the repository/repositories and accession number(s) can be found below: NCBI - PRJNA1015661.

Author contributions

JX: Data curation, Formal analysis, Investigation, Methodology, Writing – original draft. KY: Data curation, Formal analysis, Investigation, Writing – review & editing. ZY: Funding acquisition, Investigation, Resources, Supervision, Writing – review & editing. HS: Data curation, Investigation, Software, Supervision, Writing – review & editing. LM: Investigation, Resources, Supervision, Writing – review & editing. DL: Investigation, Project administration, Supervision, Writing – review & editing. HG: Investigation, Supervision, Writing – review & editing. SZ: Investigation, Supervision, Writing – review & editing. DZ: Formal analysis, Investigation, Resources, Supervision, Writing – review & editing.

Funding

The author(s) declare financial support was received for the research, authorship, and/or publication of this article. The work was supported by the Zhejiang Provincial Natural Science

Foundation of China (LY22C030005), National Natural Science Foundation of China (grant number 41977348), National Key Research and Development Program of China (2022YFC3203200), Key Research and Development Program of Zhejiang Province (2020C03082), Ningbo YouthScience and Technology Innovation Leading Project (2023QL032), the Fundamental Research Funds for the Provincial Universities of Zhejiang (SJLY2021006 and SJLZ2021004), and K.C. Wong Magna Fund in Ningbo University.

Conflict of interest

The authors declare that the research was conducted in the absence of any commercial or financial relationships that could be construed as a potential conflict of interest.

Publisher's note

Supplementary material

The Supplementary Material for this article can be found online at: https://www.frontiersin.org/articles/10.3389/fmicb.2023.1327523/full#supplementary-material

References

Bao, Q., Liu, Z., Zhao, M., Sun, H., Hu, Y., and Li, D. (2023). Response of OC, TN, and TP deposition mediated by aquatic photosynthetic community structures in shallow karst surface waters under different land uses. *Environ. Res.* 223:115488. doi: 10.1016/j.envres.2023.115488

Barberán, A., Bates, S. T., Casamayor, E. O., and Fierer, N. (2012). Using network analysis to explore co-occurrence patterns in soil microbial communities. *ISME J.* 6, 343–351. doi: 10.1038/ismej.2011.119

Cai, W., Huang, Q., Li, H., Cheng, H., Li, Y., and Hu, J. (2022). Longitudinal patterns of microbial communities in the water diversion rivers of South-to-North water diversion project. *Clean* 50:2100303. doi: 10.1002/clen.202100303

Caporaso, J. G., Bittinger, K., Bushman, F. D., DeSantis, T. Z., Andersen, G. L., and Knight, R. (2010). PyNAST: A flexible tool for aligning sequences to a template alignment. *Bioinformatics* 26, 266–267. doi: 10.1093/bioinformatics/btp636

Chen, H., Wang, Z., Liu, H., Nie, Y., Zhu, Y., Jia, Q., et al. (2021). Variable sediment methane production in response to different source-associated sewer sediment types and hydrological patterns: Role of the sediment microbiome. *Water Res.* 190:116670. doi: 10.1016/j.watres.2020.116670

Chen, H., Ye, J., Zhou, Y., Wang, Z., Jia, Q., Nie, Y., et al. (2020). Variations in CH_4 and CO_2 productions and emissions driven by pollution sources in municipal sewers: An assessment of the role of dissolved organic matter components and microbiota. *Environ. Pollut.* 263:114489. doi: 10.1016/j.envpol.2020.114489

Chen, Q., Hu, H., Yan, Z., Li, C., Nguyen, B. T., Sun, A., et al. (2021). Deterministic selection dominates microbial community assembly in termite mounds. *Soil Biol. Biochem.* 152:108073. doi: 10.1016/j.soilbio.2020.108073

Chen, S., Zhang, L., Liu, B., Yi, H., Su, H., Kharrazi, A., et al. (2023). Decoupling wastewater-related greenhouse gas emissions and water stress alleviation across 300 cities in China is challenging yet plausible by 2030. *Nat. Water* 1, 534–546. doi: 10.1038/s44221-023-00087-4

Chen, Y., Chen, J., Xia, R., Li, W., Zhang, Y., Zhang, K., et al. (2023). Phosphorus – The main limiting factor in riverine ecosystems in China. *Sci. Total Environ.* 870:161613. doi: 10.1016/j.scitotenv.2023.161613

Chen, Z., Lu, J., Gao, S., Jin, M., Bond, P. L., Yang, P., et al. (2018). Silver nanoparticles stimulate the proliferation of sulfate reducing bacterium *Desulfovibrio vulgaris*. *Water Res.* 129, 163–171. doi: 10.1016/j.watres.2017.11.021

Colman, D. R., Feyhl-Buska, J., Fecteau, K. M., Xu, H., Shock, E. L., Boyd, E. S., et al. (2016). Ecological differentiation in planktonic and sediment-associated chemotrophic microbial populations in Yellowstone hot springs. *Fems Microbiol. Ecol.* 92:fiw137. doi: 10.1093/femsec/fiw137

Coyte, K. Z., Schluter, J., and Foster, K. R. (2015). The ecology of the microbiome: Networks, competition, and stability. *Science* 350, 663–666. doi: 10.1126/science.aad2602

Crabtree, R. W. (1989). sediments in sewers. *Water Environ. J.* 3, 569–578. doi: 10.1111/j.1747-6593.1989.tb01437.x

DeSantis, T. Z., Hugenholtz, P., Larsen, N., Rojas, M., Brodie, E. L., Keller, K., et al. (2006). Greengenes, a chimera-checked 16S rRNA gene database and workbench compatible with ARB. *Appl. Environ. Microb.* 72, 5069–5072. doi: 10.1128/AEM.03006-05

Dixon, P. (2003). VEGAN, a package of R functions for community ecology. *J. Veg. Sci.* 14, 927–930. doi: 10.1111/j.1654-1103.2003.tb02228.x

Djurhuus, A., Closek, C. J., Kelly, R. P., Pitz, K. J., Michisaki, R. P., Starks, H. A., et al. (2020). Environmental DNA reveals seasonal shifts and potential interactions in a marine community. *Nat. Commun.* 11, 254–259. doi: 10.1038/s41467-019-14105-1

Dong, Q., Shi, H., and Liu, Y. (2017). Microbial character related sulfur cycle under dynamic environmental factors based on the microbial population analysis in Sewerage system. *Front. Microbiol.* 8:64. doi: 10.3389/fmicb.2017.00064

Dong, Z., Li, H., Xiao, J., Sun, J., Liu, R., and Zhang, A. (2022). Soil multifunctionality of paddy field is explained by soil pH rather than microbial diversity after 8-years of repeated applications of biochar and nitrogen fertilizer. *Sci. Total Environ.* 853:158620. doi: 10.1016/j.scitotenv.2022.158620

Edgar, R. (2010). Search and clustering orders of magnitude faster than BLAST. *Bioinformatics* 26, 2460–2461. doi: 10.1093/bioinformatics/btq461

Ekklesia, E., Shanahan, P., Chua, L. H. C., and Eikaas, H. S. (2015). Associations of chemical tracers and faecal indicator bacteria in a tropical urban catchment. *Water Res.* 75, 270–281. doi: 10.1016/j.watres.2015.02.037

Embree, M., Nagarajan, H., Movahedi, N., Chitsaz, H., and Zengler, K. (2013). Single-cell genome and metatranscriptome sequencing reveal metabolic interactions of an alkane-degrading methanogenic community. *ISME J.* 8, 757–767. doi: 10.1038/ismej.2013.187

Fan, K., Delgado-Baquerizo, M., Guo, X., Wang, D., Wu, Y., Zhu, M., et al. (2019). Suppressed N fixation and diazotrophs after four decades of fertilization. *Microbiome* 7, 110–143. doi: 10.1186/s40168-019-0757-8

Faust, K., and Raes, J. (2012). Microbial interactions: From networks to models. *Nat. Rev. Microbiol.* 10, 538–550. doi: 10.1038/nrmicro2832

Feng, L., Zhang, Z., Yang, G., Wu, G., Yang, Q., and Chen, Q. (2023). Microbial communities and sediment nitrogen cycle in a coastal eutrophic lake with salinity and nutrients shifted by seawater intrusion. *Environ. Res.* 225:115590. doi: 10.1016/j.envres.2023.115590

Fierer, N., and Jackson, R. B. (2006). The diversity and biogeography of soil bacterial communities. *Proc. Natl. Acad. Sci. U. S. A.* 103, 623–631. doi: 10.1073/pnas.0507535103

Freilich, S., Kreimer, A., Meilijson, I., Gophna, U., Sharan, R., and Ruppin, E. (2010). large-scale organization of the bacterial network of ecological co-occurrence interactions. *Nucleic Acids Res.* 38, 3857–3868. doi: 10.1093/nar/gkq118

Gibbons, S. M. (2017). Microbial community ecology: Function over phylogeny. *Nat. Ecol. Evol.* 1:32. doi: 10.1038/s41559-016-0032

Gudjonsson, G., Vollertsen, J., and Hvitved-Jacobsen, T. (2002). Dissolved oxygen in gravity sewers – measurement and simulation. *Water Sci. Technol.* 2002, 35–44. doi: 10.2166/wst.2002.0049

Guimerà, R., and Nunes Amaral, L. A. (2005). Functional cartography of complex metabolic networks. *Nature* 433, 895–900. doi: 10.1038/nature03288

Hu, A., Choi, M., Tanentzap, A. J., Liu, J. F., Jang, K. S., Lennon, J. T., et al. (2022). Ecological networks of dissolved organic matter and microorganisms under global change. *Nat. Commun.* 13:3600. doi: 10.1038/s41467-022-31251-1

Huo, X., Ren, C., Wang, D., Wu, R., Wang, Y., Li, Z., et al. (2023). Microbial community assembly and its influencing factors of secondary forests in Qinling Mountains. *Soil Biol. Biochem.* 184:109075. doi: 10.1016/j.soilbio.2023.109075

Jiao, S., Yang, Y., Xu, Y., Zhang, J., and Lu, Y. (2020). Balance between community assembly processes mediates species coexistence in agricultural soil microbiomes across eastern China. *ISME J.* 14, 202–216. doi: 10.1038/s41396-019-0522-9

Jin, P., Shi, X., Sun, G., Yang, L., Cai, Y., and Wang, X. C. (2018). Co-Variation between distribution of microbial communities and biological metabolization of organics in urban sewer systems. *Environ. Sci. Technol.* 52, 1270–1279. doi: 10.1021/acs.est.7b05121

Jin, P., Wang, B., Jiao, D., Sun, G., Wang, B., and Wang, X. C. (2015). Characterization of microflora and transformation of organic matters in urban sewer system. *Water Res.* 84, 112–119. doi: 10.1016/j.watres.2015.07.008

Jones, D. L., Cooledge, E. C., Hoyle, F. C., Griffiths, R. I., and Murphy, D. V. (2019). PH and exchangeable aluminum are major regulators of microbial energy flow and carbon use efficiency in soil microbial communities. *Soil Biol. Biochem.* 138:107584. doi: 10.1016/j.soilbio.2019.107584

Konopka, A., Lindemann, S., and Fredrickson, J. (2015). Dynamics in microbial communities: Unraveling mechanisms to identify principles. *ISME J.* 9, 1488–1495. doi: 10.1038/ismej.2014.251

Li, W., and Xiao, Y. (2023). Microplastics increase soil microbial network complexity and trigger diversity-driven community assembly. *Environ. Pollut.* 333:122095. doi: 10.1016/j.envpol.2023.122095

Li, Y., Guo, L., Yang, R., Yang, Z., Zhang, H., Li, Q., et al. (2023). Thiobacillus spp. and Anaeromyxobacter spp. mediate arsenite oxidation-dependent biological nitrogen fixation in two contrasting types of arsenic-contaminated soils. *J. Hazard. Mater.* 443(Pt A):130220. doi: 10.1016/j.jhazmat.2022.130220

Lin, W., Fan, F., Xu, G., Gong, K., Cheng, X., Yuan, X., et al. (2023). Microbial community assembly responses to polycyclic aromatic hydrocarbon contamination across water and sediment habitats in the Pearl River Estuary. *J. Hazard. Mater.* 457:131762. doi: 10.1016/j.jhazmat.2023.131762

Liu, S., Yu, H., Yu, Y., Huang, J., Zhou, Z., Zeng, J., et al. (2022). Ecological stability of microbial communities in Lake Donghu regulated by keystone taxa. *Ecol. Indic.* 136:108695. doi: 10.1016/j.ecolind.2022.108695

Louca, S., Jacques, S. M. S., Pires, A. P. F., Leal, J. S., González, A. L., Doebeli, M., et al. (2017). Functional structure of the bromeliad tank microbiome is strongly shaped by local geochemical conditions. *Environ. Microbiol.* 19, 3132–3151. doi: 10.1111/1462-2920.13788

Lu, X., Yu, X., Burkovsky, I., Esaulov, A., Li, X., Jiang, Y., et al. (2023). Community assembly and co-occurrence network complexity of interstitial microbial communities in the Arctic (investigation of ciliates in the White Sea intertidal zone). *Mar. Pollut. Bull.* 188:114656. doi: 10.1016/j.marpolbul.2023.114656

Maritz, J. M., Ten Eyck, T. A., Elizabeth Alter, S., and Carlton, J. M. (2019). Patterns of protist diversity associated with raw sewage in New York City. *ISME J.* 13, 2750–2763. doi: 10.1038/s41396-019-0467-z

Matar, G. K., Bagchi, S., Zhang, K., Oerther, D. B., and Saikaly, P. E. (2017). Membrane biofilm communities in full-scale membrane bioreactors are not randomly assembled and consist of a core microbiome. *Water Res.* 123, 124–133. doi: 10.1016/j.watres.2017.06.052

Mathioudakis, V. L., and Aivasidis, A. (2009). Heterotrophic denitrification kinetics in a pressurized sewer biofilm reactor. *Desalination* 248, 696–704. doi: 10.1016/j.desal.2009.01.008

McInerney, M. J., Bryant, M. P., Hespell, R. B., and Costerton, J. W. (1981). Syntrophomonas wolfei gen. nov. sp. nov., an anaerobic, syntrophic, fatty acid-oxidizing bacterium. *Appl. Environ. Microb.* 41, 1029–1039. doi: 10.1128/aem.41.4.1029-1039.1981

McLellan, S. L., and Roguet, A. (2019). The unexpected habitat in sewer pipes for the propagation of microbial communities and their imprint on urban waters. *Curr. Opin. Biotech.* 57, 34–41. doi: 10.1016/j.copbio.2018.12.010

Naz, M., Dai, Z., Hussain, S., Tariq, M., Danish, S., Khan, I. U., et al. (2022). The soil pH and heavy metals revealed their impact on soil microbial community. *J. Environ. Manage.* 321:115770. doi: 10.1016/j.jenvman.2022.115770

Nelson, M. B., Martiny, A. C., and Martiny, J. B. H. (2016). Global biogeography of microbial nitrogen-cycling traits in soil. *Proc. Natl. Acad. Sci. U. S. A.* 113, 8033–8040. doi: 10.1073/pnas.1601070113

Ning, D., Yuan, M., Wu, L., Zhang, Y., Guo, X., Zhou, X., et al. (2020). A quantitative framework reveals ecological drivers of grassland microbial community assembly in response to warming. *Nat. Commun.* 11:4717. doi: 10.1038/s41467-020-18560-z

Okuyama, T., and Holland, J. N. (2008). Network structural properties mediate the stability of mutualistic communities. *Ecol. Lett.* 11, 208–216. doi: 10.1111/J.1461-0248.2007.01137.x

Qian, L., Yu, X. L., Gu, H., Liu, F., Fan, Y. J., Wang, C., et al. (2023). Vertically stratified methane, nitrogen and sulphur cycling and coupling mechanisms in mangrove sediment microbiomes. *Microbiome* 11:71. doi: 10.1186/s40168-023-01501-5

Qiu, L., Zhang, Q., Zhu, H., Reich, P. B., Banerjee, S., van der Heijden, M. G. A., et al. (2021). Erosion reduces soil microbial diversity, network complexity and multifunctionality. *ISME J.* 15, 2474–2489. doi: 10.1038/s41396-021-00913-1

Ren, D., Zuo, Z., Xing, Y., Ji, P., Yu, T., Zhu, D., et al. (2022). Simultaneous control of sulfide and methane in sewers achieved by a physical approach targeting dominant active zone in sediments. *Water Res.* 211:118010. doi: 10.1016/j.watres.2021.118010

Santillan, E., Seshan, H., Constancias, F., Drautz-Moses, D. I., and Wuertz, S. (2019). Frequency of disturbance alters diversity, function, and underlying assembly mechanisms of complex bacterial communities. *NPJ Biofilms Microbiomes.* 5:8. doi: 10.1038/s41522-019-0079-4

Santini, T. C., Gramenz, L., Southam, G., and Zammit, C. (2022). Microbial community structure is most strongly associated with geographical distance and PH in salt lake sediments. *Front. Microbiol.* 13:920056. doi: 10.3389/fmicb.2022.920056

Sharma, E., Sivakumar, M., Kelso, C., Zhang, S., Shi, J., Gao, J., et al. (2023). Effects of sewer biofilms on the degradability of carbapenems in wastewater using laboratory scale bioreactors. *Water Res.* 233:119796. doi: 10.1016/j.watres.2023.119796

Shi, X., Gao, G., Tian, J., Wang, X. C., Jin, X., and Jin, P. (2020). Symbiosis of sulfate-reducing bacteria and methanogenic archaea in sewer systems. *Environ. Int.* 143:105923. doi: 10.1016/j.envint.2020.105923

Shi, X., Sang, L., Wang, X. C., and Jin, P. K. (2018). Pollutant exchange between sewage and sediment in urban sewer systems. *Chem. Eng. J.* 351, 240–247. doi: 10.1016/j.cej.2018.06.096

Shi, Y., Delgado-Baquerizo, M., Li, Y., Yang, Y., Zhu, Y., Peñuelas, J., et al. (2020). Abundance of kinless hubs within soil microbial networks are associated with high functional potential in agricultural ecosystems. *Environ. Int.* 142:105869. doi: 10.1016/j.envint.2020.105869

Song, Y., Zhang, S., Lu, J., Duan, R., Chen, H., Ma, Y., et al. (2023). Reed restoration decreased nutrients in wetlands with dredged sediments: Microbial community assembly and function in rhizosphere. *J. Environ. Manage.* 344:118700. doi: 10.1016/j.jenvman.2023.118700

Wang, F., Dong, W., Zhao, Z., Wang, H., Li, W., Chen, G., et al. (2021). Heavy metal pollution in urban river sediment of different urban functional areas and its influence on microbial community structure. *Sci. Total Environ.* 778:146383. doi: 10.1016/j.scitotenv.2021.146383

Wang, H. L., Yang, Q., Li, D., Wu, S. H., Yang, S., Deng, Y. R., et al. (2023). Stable isotopic and metagenomic analyses reveal microbial-mediated effects of microplastics on sulfur cycling in coastal sediments. *Environ. Sci. Technol.* 57, 1167–1176. doi: 10.1021/acs.est.2c06546

Wang, X., Ren, Y., Yu, Z., Shen, G., Cheng, H., and Tao, S. (2022). Effects of environmental factors on the distribution of microbial communities across soils and lake sediments in the Hoh Xil Nature Reserve of the Qinghai-Tibetan Plateau. *Sci. Total Environ.* 838(Pt 2):156148. doi: 10.1016/j.scitotenv.2022.156148

Wang, X., Zhang, Z., Yu, Z., Shen, G., Cheng, H., and Tao, S. (2020). Composition and diversity of soil microbial communities in the alpine wetland and alpine forest ecosystems on the Tibetan Plateau. *Sci. Total Environ.* 747:141358. doi: 10.1016/j.scitotenv.2020.141358

Weigel, B., Graco-Roza, C., Hultman, J., Pajunen, V., Teittinen, A., Kuzmina, M., et al. (2023). Local eukaryotic and bacterial stream community assembly is shaped by regional land use effects. *ISME Commun.* 3:65. doi: 10.1038/s43705-023-00272-2

Wright, R. J., Erni-Cassola, G., Zadjelovic, V., Latva, M., and Christie-Oleza, J. A. (2020). Marine plastic debris: A new surface for microbial colonization. *Environ. Sci. Technol.* 54, 11657–11672. doi: 10.1021/acs.est.0c02305

Wu, L., Ning, D., Zhang, B., Li, Y., Zhang, P., Shan, X., et al. (2019). Global diversity and biogeography of bacterial communities in wastewater treatment plants. *Nat. Microbiol.* 4, 1183–1195. doi: 10.1038/s41564-019-0426-5

Xun, W., Li, W., Xiong, W., Ren, Y., Liu, Y., Miao, Y., et al. (2019). Diversity-triggered deterministic bacterial assembly constrains community functions. *Nat. Commun.* 10, 3810–3833. doi: 10.1038/s41467-019-11787-5

Yang, Q., Zhang, P., Li, X., Yang, S., Chao, X., Liu, H., et al. (2023). Distribution patterns and community assembly processes of eukaryotic microorganisms along an altitudinal gradient in the middle reaches of the Yarlung Zangbo River. *Water Res.* 239:120047. doi: 10.1016/j.watres.2023.120047

Yi, Y., Lin, C., Wang, W., and Song, J. (2021). Habitat and seasonal variations in bacterial community structure and diversity in sediments of a Shallow lake. *Ecol. Indic.* 120:106959. doi: 10.1016/j.ecolind.2020.106959

Zhang, B., Xu, X., and Zhu, L. (2017). Structure and function of the microbial consortia of activated sludge in typical municipal wastewater treatment plants in winter. *Sci. Rep.* 7:17930. doi: 10.1038/s41598-017-17743-x

Zhang, J., Xu, Z., Chu, W., Ju, F., Jin, W., Li, P., et al. (2023). Residual chlorine persistently changes antibiotic resistance gene composition and increases the risk of antibiotic resistance in sewer systems. *Water Res.* 15:120635. doi: 10.1016/j.watres.2023.120635

Zhang, L., Yin, W., Wang, C., Zhang, A., Zhang, H., Zhang, T., et al. (2021). Untangling microbiota diversity and assembly patterns in the World's largest water diversion canal. *Water Res.* 204:117617. doi: 10.1016/j.watres.2021.117617

frontiers | Frontiers in Microbiology

TYPE Original Research
PUBLISHED 05 January 2024
DOI 10.3389/fmicb.2023.1318586

OPEN ACCESS

EDITED BY
Jeanette M. Norton,
Utah State University, United States

REVIEWED BY
Wei Zhang,
Nanjing Normal University, China
Madjid Morsli,
Centre Hospitalier Universitaire de Nîmes, France

*CORRESPONDENCE
Wenming Zhang
✉ zhangwm@gsau.edu.cn
Chenxu Yu
✉ chenxuyu@iastate.edu
Zhuzhu Luo
✉ luozz@gsau.edu.cn

RECEIVED 11 October 2023
ACCEPTED 04 December 2023
PUBLISHED 05 January 2024

CITATION
Xing Y, Zhang P, Zhang W, Yu C and Luo Z (2024) Continuous cropping of potato changed the metabolic pathway of root exudates to drive rhizosphere microflora. *Front. Microbiol.* 14:1318586. doi: 10.3389/fmicb.2023.1318586

Continuous cropping of potato changed the metabolic pathway of root exudates to drive rhizosphere microflora

Yanhong Xing[1], Pingliang Zhang[2], Wenming Zhang[1]*, Chenxu Yu[3]* and Zhuzhu Luo[1]*

[1]College of Resources and Environmental Sciences, Gansu Agricultural University, Lanzhou, China, [2]Dryland Agriculture Institute, Gansu Academy of Agricultural Sciences, Lanzhou, China, [3]Department of Agriculture and Biosystem Engineering, Iowa State University, Ames, IA, United States

For potato production, continuous cropping (CC) could lead to autotoxicity buildup and microflora imbalance in the field soil, which may result in failure of crops and reduction in yield. In this study, non-targeted metabolomics (via liquid chromatography with tandem mass spectrometry (LC–MS/MS)) combined with metagenomic profiling (via high-throughput amplicon sequencing) were used to evaluate correlations between metabolomics of potato root exudates and communities of bacteria and fungi around potato plants to illustrate the impacts of CC. Potato plants were grown in soil collected from fields with various CC years (0, 1, 4, and 7 years). Metabolomic analysis showed that the contents and types of potential autotoxins in potato root exudates increased significantly in CC4 and CC7 plants (i.e., grown in soils with 4 and 7 years of CC). The differentially expressed metabolites were mainly produced via alpha-linolenic acid metabolism in plant groups CC0 and CC1 (i.e., no CC or 1 year CC). The metabolomics of the groups CC4 and CC7 became dominated by styrene degradation, biosynthesis of siderophore group non-ribosomal peptides, phenylpropanoid biosynthesis, and biosynthesis of various plant secondary metabolites. Continuous cropping beyond 4 years significantly changed the bacterial and fungal communities in the soil around the potato crops, with significant reduction of beneficial bacteria and accumulation of harmful fungi. Correlations between DEMs and microflora biomarkers were established with strong significances. These results suggested that continuous cropping of potato crops changed their metabolism as reflected in the plant root exudates and drove rhizosphere microflora to directions less favorable to plant growth, and it needs to be well managed to assure potato yield.

KEYWORDS

potato, continuous cropping obstacle, metabolomics, bacterial community, fungal community

1 Introduction

Potato (*Solanum tuberosum* L.) is an important commodity crop globally as food, feed, and industrial raw material due to its high-yield, strong tolerance against hash environment, and excellent adaptability (Camire et al., 2009). Potato is a good source of proteins, amino acids, minerals, vitamins, and dietary fiber (Camire et al., 2009). Worldwide, acreage of potato planting is increasing every year. High demands of potato create strong motivation for continuous cropping (CC), especially in China where the arable land is limited (Qin et al., 2017a). However, studies showed that the yield of potato from CC fields decreased gradually, by as much as 27, 75, and 85% in years 2, 3, and 4, respectively (Qin et al., 2017a). Such drop in yield calls into question the benefit of continuous cropping for potato.

The deterioration of crop yield during CC is defined as continuous cropping obstacle (CCO), which is most likely resulted from changes in root exudates and soil microflora (Gao et al., 2019, 2021; Han et al., 2022). Although most of root exuded metabolites have beneficial effects to the plant, for example, organic acids are known to increase nutrient mobilization (thus absorption by the roots; Khademi et al., 2010), sugars and amino acids feed the microbiota that could play beneficial roles in plant growth (Kang et al., 2015; Topalovic et al., 2020), and as CC continues, root exudates could increase allelopathic autotoxicity that are detrimental to plant growth and recruit harmful microbes to the plants (Han et al., 2022). Accumulation of autotoxic allelochemicals in soil as a mechanism of CCO has been identified in many plants (Qin et al., 2017b; Wu et al., 2018; Huang et al., 2020), which could affect the health of the plants, and the complex interactions between plants and soil microbes (Gao et al., 2019, 2021). Changes in types and amounts of allelochemicals secreted by plant roots can have impact on the growth and reproduction of soil microbes and change the ratio of pathogenic to beneficial microorganisms in the soil, leading to soil microflora imbalance (Xia et al., 2015; Bonanomi et al., 2016; Jin et al., 2019). Plant autotoxicity was also reported to cause CCO (Xiang et al., 2022). For instance, autotoxicity has been reported to cause replant failure in the continuous cropping of *Angelica sinensis* (Xin et al., 2019), *Lilium davidii* var. *unicolor* (Wu Z. J. et al., 2015), *Nicotiana tabacum* L. (Deng et al., 2017), *Panax quinquefolium* (He et al., 2009), and *Panax notoginseng* (Yang et al., 2015). Many compounds from different root exudates were shown to be autotoxins. Imperatorin, α-spinasterol, vanillin, dibutyl phthalate, and ferulic acid were discovered to be potential autotoxic allelochemicals in *Angelica sinensis* (Xin et al., 2019); the accumulation of phthalic acid was reported to be one of the main CCO factors for *Lilium davidii* var. *unicolor* replantation (Wu Z. J. et al., 2015); dibutyl phthalate, diisobutyl phthalate, and diisooctyl phthalate in root exudates were shown to play important roles in autotoxicity of *Nicotiana tabacum* L. (Deng et al., 2017); some phenolic acids in root exudate of *Panax quinquefolium* and rhizosphere soil have been identified as potential allelochemicals (He et al., 2009); ferulic acid and saponin were shown to inhibit the growth of *P. notoginseng* (Yang et al., 2015). Studies on potato CCO revealed that high concentrations of allelopathic substances secreted by potato roots could produce allelopathy effects on the plants (Soltys-Kalina et al., 2019; Xin et al., 2022; Szajko et al., 2023), and soil microflora around the roots were changed in response to potato CC (Qin et al., 2017a). However, key questions remain to be answered: What are the main autotoxins secreted by potato roots under continuous cropping? Are they changing over time, and how? What are the relationships between soil microflora changes and allelochemical accumulation around potato plants? Answers to these questions are needed for better understanding CCO for potato and for finding ways to overcome the CCO to promote potato production.

This study aimed to understand how potato CC can alter root exudates and induce changes in rhizosphere microorganisms. Potato plants were grown in pot groups with soil collected from fields with different continuous cropping years (0, 1, 4, and 7, namely, CC0, CC1, CC4, and CC7 groups). Rhizosphere and bulk soil from each pot were collected and analyzed to assess changes of bacterial and fungal communities around the plants. Meanwhile, root exudates from the plants were collected and analyzed for changes and metabolic pathways by non-targeted metabolomics. By identifying biomarkers of root exudates and microbes (i.e., rhizosphere and bulk soil) in samples from different CC groups, the relationships between microbes and root exudates were established to clarify the chemotaxis or avoidance tendencies of microbes toward the root exudates and reveal the mechanisms of CCO for potato.

2 Materials and methods

2.1 Pot experiment design

Soil for the potato pot experiments was collected in 2021 from the positioning testing site located in the National Soil Quality Stability Observation and Experiment Station of Gansu Academy of Agricultural Sciences, Gansu Province, North-west China (104 ° 36′E, 35 ° 35′N). The average altitude of the site is 1970 m, the average annual temperature is 6.2°C, the average annual precipitation is 415 mm, the average annual evaporation is 1,531 mm, and the frost-free period is 146–149 day/year. The physical and chemical properties of the soil in 2015 were organic carbon 10.62 g·kg^{-1}, total nitrogen 0.78 g·kg^{-1}, available phosphorus 10.12 mg·kg^{-1}, available potassium 163.8 mg·kg^{-1}, and pH 8.32. The characteristics of the soil changed over 7 years of CC, as shown in Table 1.

TABLE 1 Soil physical and chemical properties under different treatments (2021).

Factors	CCO	CC1	CC4	CC7
Total nitrogen (g·kg^{-1})	0.80 ± 0.02b	0.76 ± 0.01b	0.78 ± 0.02b	1.33 ± 0.09a
Total phosphorus (g·kg^{-1})	0.88 ± 0.01a	0.68 ± 0.01c	0.67 ± 0.003c	0.70 ± 0.01b
Available phosphorus (mg·kg^{-1})	15.52 ± 0.02a	5.37 ± 0.02d	7.87 ± 0.02c	14.31 ± 0.02b
Available potassium (mg·kg^{-1})	81.63 ± 0.18d	98.83 ± 0.07c	128.57 ± 0.12b	168.50 ± 0.21a
pH	8.22 ± 0.01d	8.59 ± 0.03b	8.71 ± 0.01a	8.35 ± 0.02c

Values are mean ± SE in triplicate replicates. Different lowercase letters indicate significant differences with a $p < 0.05$ based on the analysis of variance.

Topsoil (0–20 cm) from fields of rotation (maize/potato, with maize planted the previous season) and continuous cropping of 1, 4, and 7 years (potato alone) were collected in 2021 and sieved through a 10.0 mm sieve to remove large root chips and stones after air-drying, four groups were set up and denoted by CC0 (rotation control), CC1 (continuous cropping for 1 year), CC4 (continuous cropping for 4 years), and CC7 (continuous cropping for 7 years), and each group included six pots for replication. Each pot had 2.0 kg air-dried soil, with fertilizers applied at 0.1 gN/kg soil, N/P = 2:1 (urea for N, and potassium dihydrogen phosphate for P). In each pot, two plants (Longshu no.3) were seeded at 9 cm apart and 4 cm from the surface. Pots were placed in the greenhouse on campus of Gansu Agricultural University from 10 May to 14 July of 2021.

2.2 Sample collection

Potato plants in the pot were taken out as a whole at the blossoming stage, 65 days after seeding, and paired rhizosphere soils (R) and bulk soils (B) were collected with the "soil adhering to fine roots after shaking" method (Huo et al., 2022); in brief, soil was first collected by shaking the roots gently till dropping of large soil aggregates ceased, and the soil was defined as bulk soil (BS); then, soil adhering to the fine roots was collected by brushing the roots with sterile brushes, which was defined as rhizosphere soil (RS). Soil samples were then split into two parts: One part was air-dried, and another was frozen at −80°C. After RS collection, the plants were put into a 250 mL conical flask, and ultrapure water was added until the roots were completely submerged. After 24 h (16 h under light and 8 h in the dark), the solution was collected and centrifuged at 1200 rpm, at 4°C for 15 min; then, the supernatant was filtrated by a 0.22 μm microfilter, and the filtrate was freeze-dried to get the root exudates, which was frozen-stored at −80°C. The root exudates alongside with soil samples from three pots (randomly selected) of each group were sent to Biomarker Technologies Co., Ltd. (Beijing, China) for metabolomics analysis and gene sequencing.

2.3 Non-targeted metabolomic analysis

Untargeted metabolites in the root exudates were determined using a liquid chromatography with tandem mass spectrometry (LC–MS/MS) platform (Biomarker Technologies Co., Ltd.). In brief,1 mL extraction liquid (methanol: acetonitrile: water = 2:2:1) was added into 50 mg of the samples and vortexed for 30 s, and steel balls were added and ground in a 45 Hz grinder for 10 min and ultrasonicated in an ice water bath for 10 min (Dunn et al., 2011). The sample was then sat at 20°C for 1 h to precipitate the proteins and then centrifugated at 4°C, 12000 rpm for 15 min. 500 μL of supernatant were then moved into an EP tube and dried in a vacuum concentrator; then, 160 μL of an extraction liquid (acetonitrile: water = 1:1) was added to redissolve the sample. It was then vortexed for 30 s, ultrasonicated for 10 min (in ice water bath), and centrifugated for 15 min (4°C, 12,000 rpm). Finally, 120 μL of the supernatant were used for Ultra-High Performance Liquid Chromatography-Q Exactive (UHPLC-QE) orbital trap/mass spectrometry analysis. The LC/MS system for metabolomics analysis is composed of Waters Acquity I-Class PLUS ultra-high performance liquid tandem Waters Xevo G2-XS QT of high-resolution mass spectrometer, and the column used was from Waters Acquity UPLC HSS T3 column (Waters Corp., Milford, CT, United States).

2.4 DNA extraction and sequencing

The total genomic DNA from 0.5 g of both BS and RS samples of each group was extracted with the TGuide S96 Magnetic Soil/Stool DNA Kit (Tiangen Biotech (Beijing) Co., Ltd.) according to manufacturer instructions, and the DNA concentration of the samples was measured with the Qubit dsDNA HS Assay Kit and Qubit 4.0 Fluorometer (Invitrogen, Thermo Fisher Scientific, Oregon, United States). PCR amplification was performed for each soil DNA extract in triplicate and combined into a single composite sample. Fungal ITS region was amplified using the primer pair ITS1F (5'-CTTGGTCATTTAGAGGAAGTAA-3′) and ITS2 (5'-GCTGCGTTCTTCATCGATGC-3′) (Yang et al., 2017), and the thermal cycling conditions were 95°C for 5 min, 15 cycles of 95°C for 1 min, 50°C for 1 min, and 72°C for 1 min, followed by 72°C for 7 min. Bacterial 16S rRNA gene V3-V4 region of 16S rRNA was amplified using the primer pair 338F (5'-ACTCCTACGGGAGGCAGCA-3′) and 806R (5'-GGACTACHVGGGTWTCTAAT-3′) (Wang et al., 2020), and the thermal cycling conditions were pre-denaturation at 98°C for 2 min, denaturation at 98°C for 15 s, annealing at 55°C for 30 s, extension at 72°C for 30 s, and final extension at 72°C for 5 min (30 cycles). The PCR amplicons were gel-purified with Agencourt AMPure XP Beads (Beckman Coulter, Indianapolis, IN). The resultant PCR products were combined at equimolar concentrations and use Illumina NovaSeq 6000 (Illumina, Santiago CA, United States) for sequencing (250 × 250 bp) in Beijing Biomarker Technologies Co., Ltd. (Beijing, China).

Paired-end (PE) reads obtained from previous steps were assembled by USEARCH (version 10) (Segata et al., 2011) and followed by chimera removal using UCHIME (version 8.1) (Quast et al., 2013). The high-quality reads generated by the above steps will be used for subsequent analysis.

2.5 Data processing and analysis

The MS raw data were collected using MassLynx software (version 4.2, Waters Corp., Milford, CT, United States) and processed by the Progenesis QI software (Waters Corp., Milford, CT, United States). The METLIN database (Waters Corp., Milford, CT, United States) and an in-house database (Biomarker Technologies Co., LTD.) were used for peak annotation and identification of various compounds (Zhang et al., 2022). The projection (VIP > 1), Student's *t*-test ($p < 0.05$), and $|\log_2 FC| \geq 0.58$ were used as criteria to screen for differentially expressed metabolites (DEMs), and the threshold (VIP > 1, $p < 0.05$, $|\log2FC| \geq 2.32$) was used to screen the DEMS that varied greatly, defined as greatly differentially expressed metabolites (GDEMs).

The orthogonal partial least-squares discrimination analysis (OPLS-DA; R, 3.3.2, ropls packages) and the principal component analysis (PCA; R, 3.1.1, "scales," "ggplot2," "ggrepel," "scatterplot3d" packages) were used to distinguish different groups of overall differences in metabolic profile, the volcano map (R, 3.1.1, "ggplot2" packages) was used for visualization of the differential substance, and

the KEGG pathway of the DEMs was mapped in R (version 3.1.1, "clusterprofiler," "enrichplot" packages; Wu et al., 2022).

Operational taxonomic units (OTUs) were clustered with 97% similarity using Usearch (version 10.0) software. Beta diversity analysis of samples was evaluated by QIIME2 software (version 2020.6), and non-metric multidimensional scaling (NMDS) analysis of Gower distance and sperman-approx distance was used to show the divergence of the rhizosphere microbial communities for bacterial and fungal, respectively. NMDS analysis of Hellinger distance and binary-chord distance was used to show the divergence of bacterial and fungal communities in both rhizosphere and bulk soil, respectively. The linear discriminant analysis (LDA) effect size (LEfSe) was used to identify biomarker with statistical difference using R (version3.1.1, stats package) and python (version1.0.0, scipy package; Segata et al., 2011). Correlation network analysis was used to identify key species using Cytoscape (version 3.7.1) and R (version3.1.1, igraph package; Shannon et al., 2003; Zheng et al., 2018), genera with average relative abundances higher than 0.1% were subject to Spearman's correlation analysis, and bacterial and fungal genera with Spearman's correlation >0.8 or < −0.8 and significance $p < 0.01$ were used to establish microbial networks.

The related network between metabolites and genus was established with Pearson's correlation coefficient (PCC) > |0.8| and a $p < 0.05$ and visualized with Cytoscape (version 3.7.1; Pyo et al., 2022). The high-level correlation network analysis (Spearman's correlation ($r > 0.8$ and $p < 0.05$)) between top 20 microbe and DEMs was involved in metabolic pathways, the correlation heatmap between DEMs, and the significantly differentiated microbes from rhizosphere and bulk soil with *t*-test ($p < 0.05$).

3 Results

3.1 Physiological indicators of plants grown in soils with different CC years

Dry weight, stem thickness, and height of plants all decreased in groups of increasing CC years (Table 2), while the amount of root secretion increased significantly, indicating CC depressed the potato growth, while promoted root secretion, which consumed large amount of photosynthates. Biomass of the plant (i.e., dry weight) and physiological indicators (stem thickness and height) suggested that plants grown with soil under the growing impact of CCO were getting less healthy. Meanwhile, the plants were producing more root secretion, especially in soil with longer CC, which were signs of plants responding to the changing soil environment. These signs were further clarified by the metabolomic analysis of the root exudates.

3.2 Metabolomic analysis of root exudates of potato with CCO

A total of 27,975 peaks were detected in 12 samples by metabolome characterization and quantitative analysis, of which 1,722 metabolites were annotated (Supplementary Table S1), and these compounds mainly included fatty acyls, prenol lipids, carboxylic acids and derivatives, and organooxygen compounds (Supplementary Figure S1). PCA analysis and OPLS-DA model showed that metabolite data from different groups (CC0, CC1, CC4, and CC7) formed clusters that are completely separated (Figures 1A,C), indicating that the metabolites from root exudates of potato grown in pots with soil from different CC fields (0, 1, 4, and 7 years, respectively) were significantly different. Analysis of the root exudates showed that CC significantly changed the chemical composition of the root exudates, and longer the continuous cropping years, greater the differences shown in the differentially expressed metabolites (DEMs). Upregulated DEMs in CC1, CC4, and CC7 were 54, 142, and 184, and downregulated DEMs were 169, 114, and 149 (Figures 1B,D), respectively, and the entire lists are given in Supplementary Tables S2–S4. It is worth noting that more upregulated DEMs are produced with the increase of CC years.

Notably the upregulated DEMs are autotoxins reported for various plants. Eight potential autotoxins including phenols, flavonoids, coumarins, and alkaloids were found in group CC1, 18 potential autotoxins including phenols, flavonoids, coumarins, alkaloids, and terpenoids were found in group CC4, and 30 potential autotoxins including phenols, coumarins, flavonoids, alkaloids, terpenoids, and fatty acids were found in group CC7 (Supplementary Table S5). Both the types and the quantities of phenolic compounds increased significantly with CC years; in addition, the GDEMs (Supplementary Table S6) may play important roles in CCO for potato, for example, 1-(4-hydroxyphenyl) ethanol (phenols) in CC4, and 1,2-naphthoquinone, 4-methylumbelliferone (coumarins), 1-(4-hydroxyphenyl) ethanol, phloretin (flavonoids), and psoralen (coumarins) in CC7 appeared to be the key autotoxins that could negatively impact the potato yields in these groups.

3.3 Enrichment of differentially expressed metabolites as affected by CC

Analysis of metabolic pathways can reveal the metabolic process leading to the production of the DEMs among groups. KEGG map of metabolic pathways (Figure 2) showed that DEMs were mainly enriched via alpha-linolenic acid metabolism, biosynthesis of plant secondary metabolites, benzoate degradation,

TABLE 2 Plant physiological indicators under different CC years.

Factors	CC0	CC1	CC4	CC7
Dry weight (g.pot^{-1})	3.79 ± 0.09a	2.68 ± 0.06b	2.69 ± 0.06b	2.54 ± 0.09b
Stem thick (mm)	5.55 ± 0.15a	5.39 ± 0.09ab	4.91 ± 0.26b	4.88 ± 0.22b
Plant height (cm)	25.95 ± 0.45a	25.63 ± 0.39a	25.62 ± 0.17a	25.37 ± 0.20a
Mass of root secretion (g. plant^{-1})	0.0408 ± 0.01b	0.0469 ± 0.01ab	0.0706 ± 0.01ab	0.0728 ± 0.01a

Values are mean ± SE in triplicate replicates. Different lowercase letters indicate significant differences with a $p < 0.05$ based on the analysis of variance.

10.3389/fmicb.2023.1318586

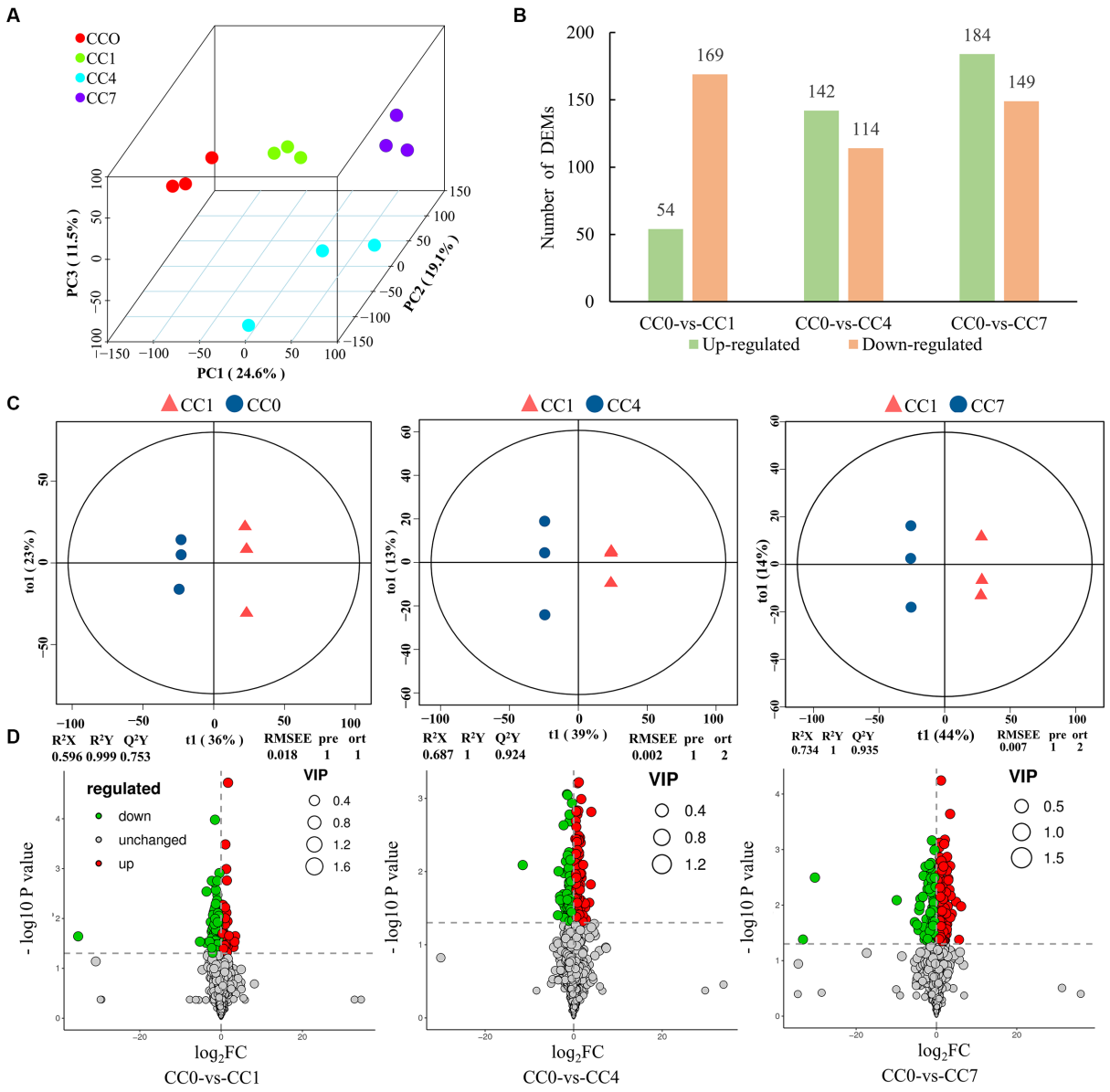

FIGURE 1
Metabolomic analysis of root exudates. **(A)** Principal component analysis (PCA) of root exudates, where the x-axis represents the first principal component, the Y-axis represents the second principal component, and the Z-axis represents the third principal component. **(B)** Number of upregulated and downregulated differentially expressed metabolites (DEMs). **(C)** Orthogonal partial least-squares discrimination analysis (OPLS-DA) scores plot of metabolites in soil between control and treatments, the parameters of the model, including R^2X, R^2Y, Q^2Y, RMSEE (root mean squared error), pre (predict the number of components), and ort (the number of orthogonal components), where R^2X and R^2Y denote the percentage of X and Y matrix information that can be interpreted by the OPLS-DA classification model, respectively, and Q^2Y is calculated by cross-validation to evaluate the predictive power of the OPLS-DA model, and the closer these metrics are to 1, the better the OPLS-DA model fits the data. **(D)** Volcano map of differential metabolites, green dots represent downregulated metabolites, red dots represent upregulated metabolites, and gray dots represent no-differential metabolites.

and biosynthesis of plant hormones in group CC1; pyruvate metabolism, styrene degradation, biosynthesis of siderophore group non-ribosomal peptides, alanine, aspartate, and glutamate metabolism in group CC4; phenylpropanoid biosynthesis, protein digestion and absorption, aminobenzoate degradation, toluene degradation, and biosynthesis of various plant secondary metabolites in group CC7, respectively.

Notably, as shown in Figure 3, biosynthesis of siderophore group non-ribosomal peptides, styrene degradation, butanoate metabolism, glycolysis/gluconeogenesis, naphthalene degradation, and polycyclic aromatic hydrocarbon degradation was all boosted in groups CC4 and CC7. Further analysis showed that alpha-linolenic acid pathway was downregulated in group CC1, while phenolic acids produced from L-phenylalanine were upregulated in groups CC4 and CC7. This indicated that the metabolic pathways of CC1 plants were different from that of CC4 and CC7 plants, and the metabolic pathways of CC4 and CC7 plants were dominated by the synthesis of autotoxins (e.g., phenols and coumarins).

10.3389/fmicb.2023.1318586

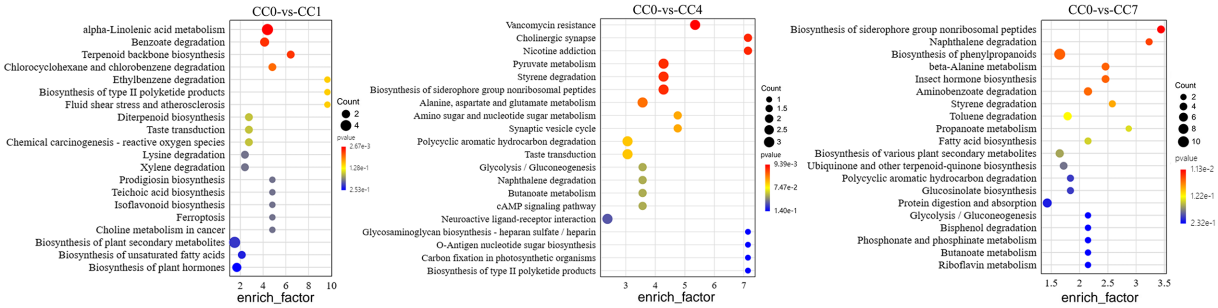

FIGURE 2
KEGG map of metabolic pathways with significant enrichment of DEMs between groups CC0 and CC1, CC4, and CC7. The x-axis is the enrich factor of the DEMs enriched in the pathway, and the y-axis lists the names of the pathways; the color depth of the dot represents the *p*-value, the redder the color, the more significant the enrichment, and the size of the dot represents the number of DMEs enriched.

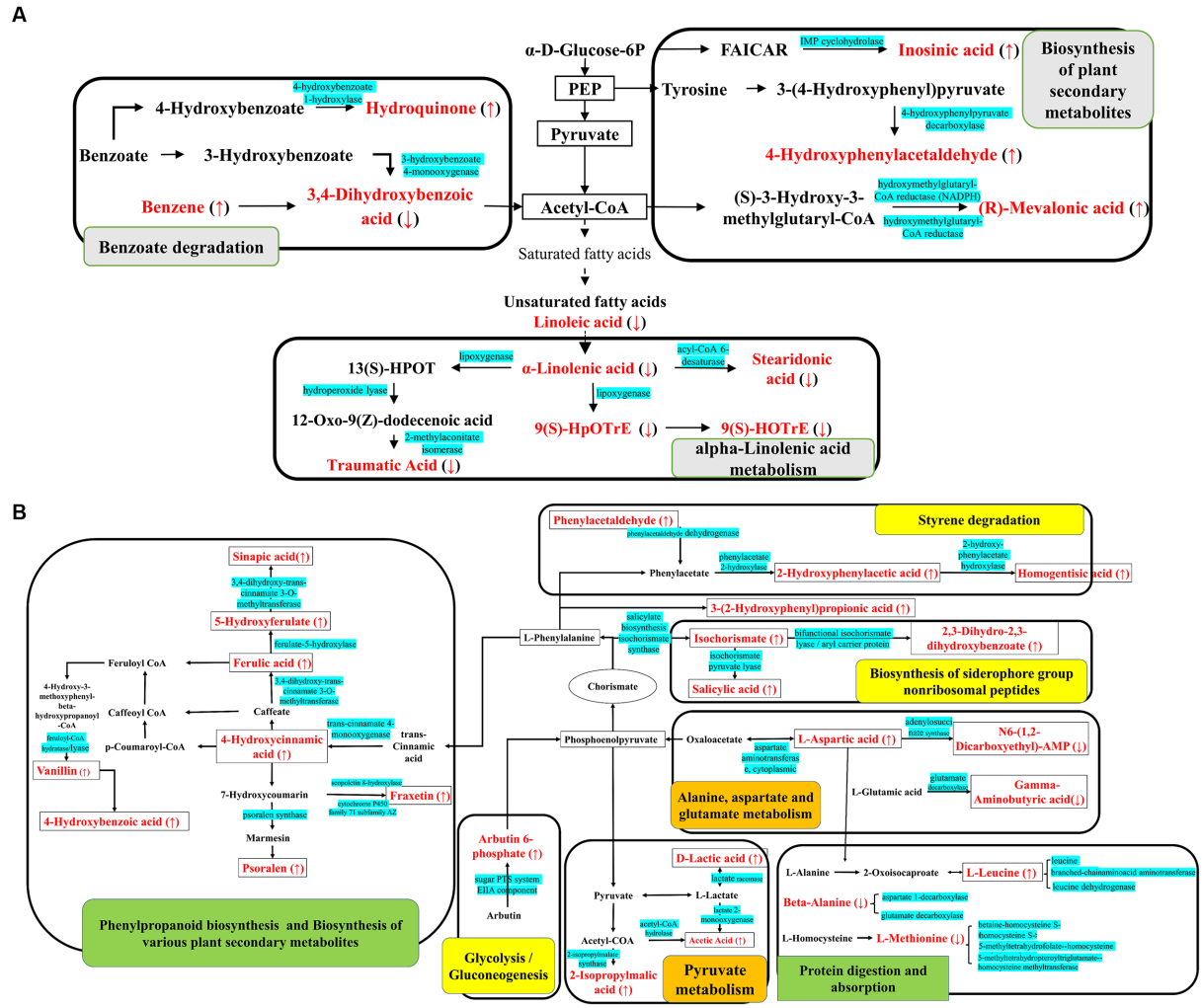

FIGURE 3
KEGG metabolic pathway map of **(A)** CC1 and **(B)** CC4 and CC7. The red marked are the DEMs, with ↑ indicating upregulated and ↓ indicating downregulated, and the blue marked are the enzymes involved in the synthesis of the metabolites. Gray shows the specific metabolic pathway in CC1, green shows the specific metabolic pathway in CC7, orange shows the specific metabolic pathway in CC4, and yellow shows the common metabolic pathways in both CC4 and CC7.

3.4 Analysis of rhizosphere microbial communities in different CC groups

As shown in Figures 4A,B NMDS analyses of rhizosphere bacteria and fungi showed that groups CC4 and CC7 clustered closely together, and clearly separated from groups CC0 and CC1, indicating continuous cropping significantly changed the microbial community structure in the RS soil, especially as the CC years grew.

Bacterial LEfSe analysis (Figure 4C) showed that *RB41*, *Nitrospira,* and *uncultured-bacterium-f-Blastocatellaceae* were significantly elevated, while *uncultured-bacterium-c-S0134-terrestrial-group* and *uncultured-bacterium-c-Acidimicrobiia* were significantly decreased in group CC1. *Bacteroides, Lactobacillus, uncultured-bacterium-f-Enterobacteriaceae, Lactococcus, Coccophora langsdorfii, Cetobacterium, Lachnospiraceae-NK4A136-group, and Pantoea* were significantly elevated while *uncultured-bacterium-c-Subgroup-6*, *Sphingomonas*, *uncultured-bacterium-f-Microscillaceae*, *uncultured-bacterium-c-S0134-terrestrial-group*, *Altererythrobacter*, *uncultured-bacterium-o-Rokubacteriales,* and *uncultured-bacterium-o-Azospirillales* were significantly decreased in group CC4, *uncultured-bacterium-c-JG30-KF-CM45* and *RB41* were significantly elevated while *Sphingomonas*, u*ncultured-bacterium-f-Xanthomonadaceae*, *uncultured-bacterium-c-Acidimicrobiia,* and *Lysobacter* were significantly decreased in group CC7.

Fungal LEfSe analysis (Figure 4D) showed that *Cladosporium* in group CC4, *Plectosphaerella* and *Metarhizium* in group CC7,

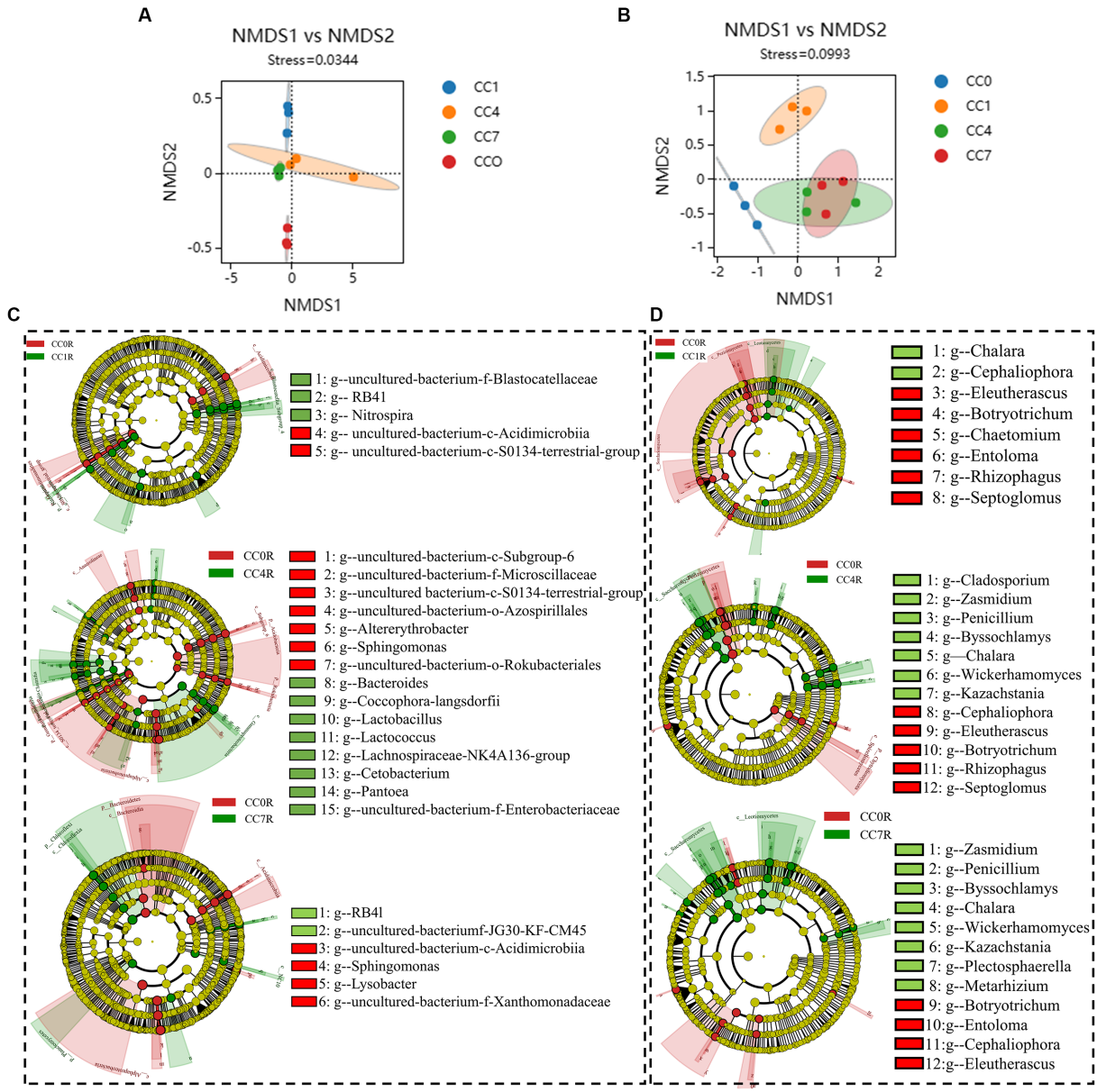

FIGURE 4
Differential analysis of soil microbial communities in group CC. **(A)** Bacterial non-metric multidimensional scaling (NMDS). **(B)** Fungal NMDS, each dot in the graph represents a sample, different colors represent different groups, and the ellipse circle represents its 95% confidence ellipse. **(C)** Bacterial linear discriminant analysis (LDA) effect size (LEfSe) analysis. **(D)** Fungal LEfSe analysis. The figures show the genera with LDA score greater than 3.5.

10.3389/fmicb.2023.1318586

Kazachstania, *Byssochlamys*, *Wickerhamomyces*, *Penicillium,* and *Zasmidium* in both groups CC4 and CC7, *Chalara* in groups CC1, CC4, and CC7 were all significantly elevated after continuous cropping, while *Chaetomium* in group CC1, *Entoloma*, *Rhizophagus* and *Septoglomus* in groups CC4 and CC7, *Cephaliophora*, *Botryotrichum* and *Eleutherascus* in groups CC1, CC4, and CC7 were decreased significantly after continuous cropping.

Analysis of microbial correlation networks was conducted to reveal the key microbial species (e.g., bacteria and fungi) under different continuous cropping conditions. As shown in Figure 5, *Uncultured-bacterium-c-Subgroup-6* was identified to be a key bacterium in all CC groups, *Sphingomonas* was a key bacterium in groups CC0, CC1, and CC7, while its relative abundance reduced to minimum in group CC4. Key fungal species under different continuous cropping conditions were *Iodophanus*, *Funneliformis,* and *Mortierella* in group CC1, *Aspergillus*, *Mortierella,* and *Chalara* in groups CC1 and CC7, *Kazachstania*, *Fusarium* and *Chaetomium* in group CC4, respectively. Notably, CC4 showed different characteristics comparing to CC1 and CC7. It should also be noted that the relative abundance of *Chalara* and *Aspergillus* in groups CC4 and CC7 was all significantly higher than those in group CC0, while the opposite was observed for *Mortierella,* whereas continuous cropping seemed to reduce its relative abundance, which went down from that of CC0, the relative abundance of microorganisms was given in Supplementary Table S7.

3.5 Analysis of rhizosphere via bulk soil microbiota

As shown in Figures 6A,B NMDS analyses showed that the rhizosphere and bulk soil microbial communities of bacteria and fungi in each group were separated clearly, indicating that root exudates significantly influenced the formation of unique rhizosphere microbiota different from that of the bulk soil.

Bacterial LEfSe analysis between rhizosphere and bulk soil of different CC groups (Figure 6C) showed that for CC0, *uncultured-bacterium-f-Gemmatimonadaceae, uncultured-bacterium-o-Saccharimonadales, uncultured-bacterium-o-Gammaproteobacteria-Incertae-Sedis, uncultured-bacterium-c-Subgroup-17, uncultured-bacterium-o-Chloroplast, uncultured-bacterium-o-uncultivated-soil-bacterium-clone-C112, Lechevalieria, Pedobacter, Bacillus, Dongia, Altererythrobacter, Sandaracinobacter, Haliangium, Ellin6067, MND1, Arenimonas, and Luteolibacter* were predominant in the rhizosphere microbiota, while *uncultured-bacterium-f-Gemmatimonadaceae, uncultured-bacterium-o-Saccharimonadales, uncultured-bacterium-o-Gammaproteobacteria-Incertae-Sedis, uncultured-bacterium-c-Subgroup-17, uncultured-bacterium-o-Chloroplast, uncultured-bacterium-o-uncultivated-soil-bacterium-clone-C112, Flaviaesturariibacter, Pontibacter, Gillisia, Salinimicrobium, Gemmatimonas* were predominant in the bulk soil. For CC1, *uncultured-bacterium-o-Saccharimonadales, uncultured-bacterium-c-Subgroup-6, uncultured-bacterium-o-C0119, Sphingobium, Nitrospira, Sphingobium*, and *Altererythrobacter* were predominant in the rhizosphere, while *uncultured-bacterium-o-Gaiellales* and *Gaiella* were predominant in the bulk soil. For CC4, *uncultured-bacterium-o-Chloroplast* was predominant in the rhizosphere, while uncultured-bacterium-f-TRA3-20, *uncultured-bacterium-f-Sphingomonadaceae, uncultured-bacterium-f-67-14, uncultured-bacterium-f-Blastocatellaceae, uncultured-bacterium-o-Gaiellales,uncultured-bacterium-c-S0134-terrestrial-group,Uncultured-bacterium-f-Longimicrobiaceae, Solirubrobacter, Gaiella*, and *Massilia* were predominant in the bulk soil. For CC7,

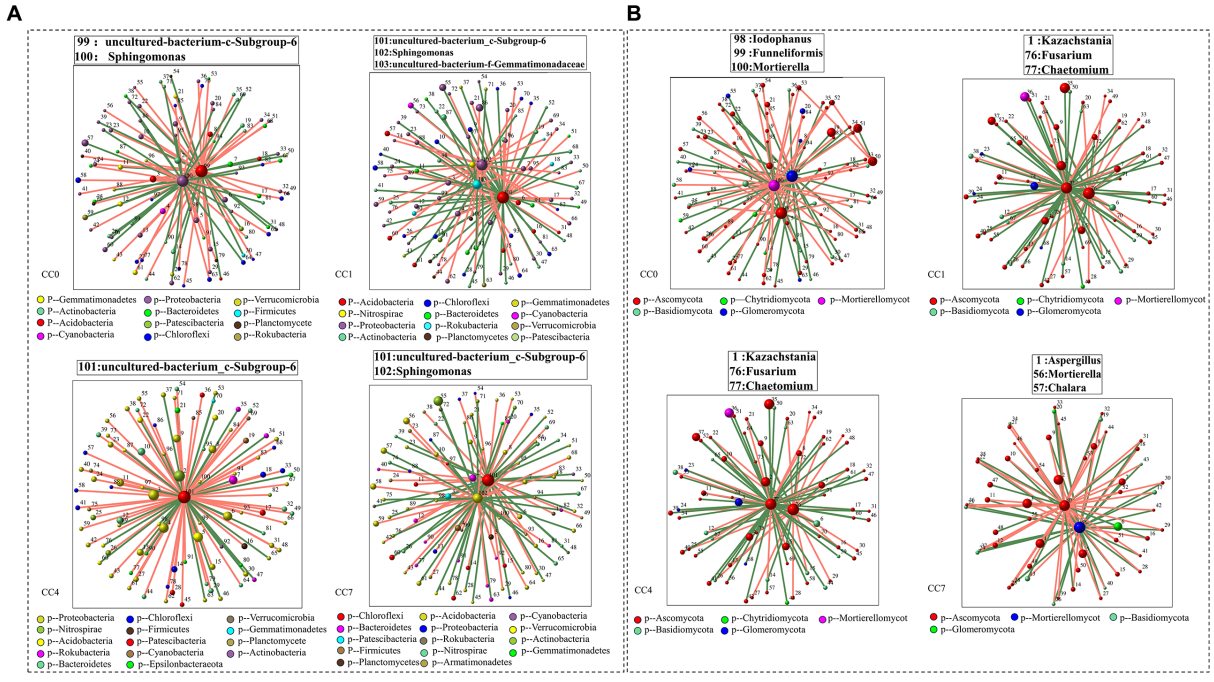

FIGURE 5
Correlation network diagram of each group [**(A)** bacteria; **(B)** fungi]. Red lines represent significant positive relationships (Spearman's correlation, $r > 0.8$ and $p < 0.01$), and green lines denote negative relationships (Spearman's correlation, $r < 0.8$ and $p < 0.01$). The genera shown on these figures are the module hub in each network diagram (ZI > 2.5 and PI < 0.62).

10.3389/fmicb.2023.1318586

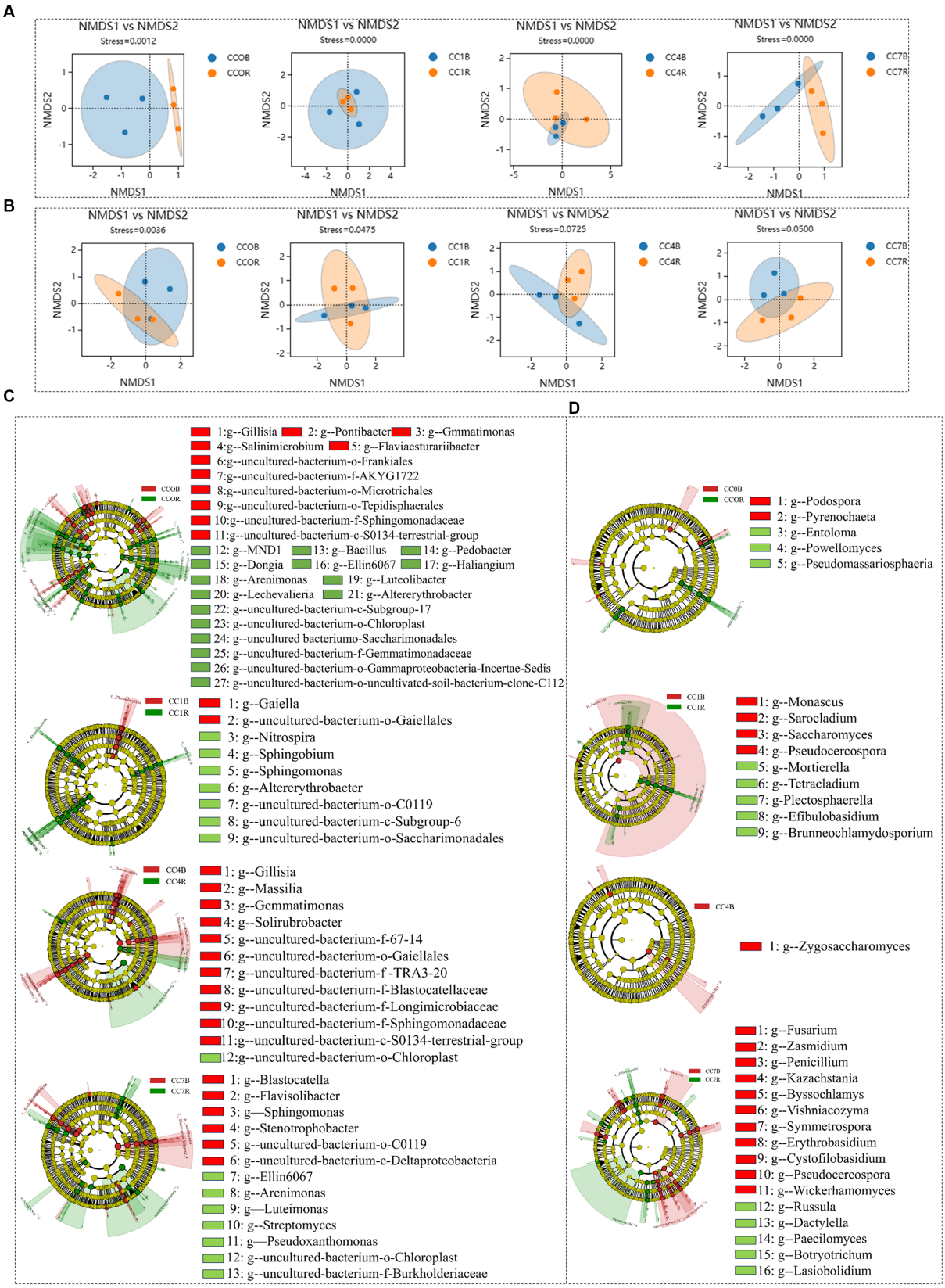

FIGURE 6
Differential analysis between rhizosphere and bulk soil microbiota in each group. **(A)** Bacterial non-metric multidimensional scaling (NMDS). **(B)** fungal NMDS, each dot in the graph represents a sample, different colors represent different groups, and the ellipse circle represents its 95% confidence. **(C)** Bacterial linear discriminant analysis (LDA) effect size (LEfSe) analysis. **(D)** Fungal LEfSe analysis, the genera with LDA score greater than 3.0.

uncultured-bacterium-o-Chloroplast, Arenimonas, Pseudoxanthomonas, Streptomyces, Ellin6067, Litorilinea, and *Luteimonas* were predominant in the rhizosphere, while uncultured-bacterium-o-C0119, *uncultured-bacterium-c-Deltaproteobacteria, Stenotrophobacter, Corynebacterium-1, Blastocatella, Flavisolibacter, Sphingomonas* were predominant in the bulk soil.

Fungal LEfSe analysis between rhizosphere and bulk soil of different CC groups (Figure 6D) showed that for CC0, *Powellomyces*, *Pseudomassariosphaeria*, and *Entoloma* were predominant in the rhizosphere, while *Pyrenochaeta* was predominant in the bulk soil; For CC1, *Mortierella*, *Brunneochlamydosporium*, *Tetracladium*, *Efibulobasidium*, and *Plectosphaerella* were predominant in the rhizosphere, while *Monascus*, *Pseudocercospora*, *Sarocladium*, and *Neodidymella* were predominant in the bulk soil; for CC4, *Zygosaccharomyces* was predominant in the bulk soil; for CC7, *Paecilomyces*, *Botryotrichum*, *Russula*, *Lasiobolidium*, and *Dactylella* were predominant in the rhizosphere, while *Symmetrospora*, *Pseudocercospora*, *Phialophora*, *Bipolaris*, *Vishniacozyma*, *Byssochlamys*, *Penicillium*, *Zasmidium*, *Wickerhamomyces*, *Erythrobasidium*, *Fusarium*, and *Kazachstania* were predominant in the bulk soil. As a general observation, it was discovered that in CC1 (1 year of continuous cropping), beneficial bacteria were enriched in the rhizosphere, while in CC7, pathogens and yeasts such as *Fusarium*, *Pseudocercospora*, and *Wickerhamomyces* became predominant in the bulk soil, which could be a significant contributor to the reduction in potato yield.

3.6 The relationships between microbiota and DEMs in different CC groups

Correlation network between top 20 microbes (based on relative abundance) and DEMs involved in metabolic pathways was generated. As shown in Figures 7A,B connections between rhizosphere microflora (both bacteria and fungi) to DEMs could be identified to suggest that the changes of potential autotoxins could be originated from changes of rhizosphere microflora due to continuous cropping.

3.6.1 The relationships between rhizosphere bacterial communities and metabolites

As shown in Figure 7A, in group CC1, key DEMs were produced via the metabolic pathways of α-linolenic acid metabolism, biosynthesis of plant secondary metabolites, and benzoate degradation. These 12 DEMs (e.g., fatty acids, benzene and derivatives, phenols, and purine nucleotides (linoleic acid, α-linolenic acid, (R)-mevalonic acid, traumatic acid, etc.)) were shown to be significantly ($p \leq 0.05$) or extremely significantly ($p \leq 0.01$) correlated with 11 bacterial genera. For example, *Nitrospira* was positively correlated with 4-hydroxyphenylacetaldehyde, (R)-mevalonic acid, hydroquinone, and inosinic acid and negatively correlated with 9S-hydroperoxy-10E,12Z,15Z-octadecatrienoic acid (9(S)-HpOTrE), stearidonic acid, 9(S)-hydroxy-10(E),12(Z),15(Z)-octadecatrienoic acid (9(S)-HOTrE), and α-linolenic acid; *RB41* was negatively correlated with traumatic acid, stearidonic acid, and linoleic acid.

In group CC4, metabolic pathways of pyruvate metabolism, alanine, aspartate and glutamate metabolism, biosynthesis of siderophore group non-ribosomal peptides, styrene degradation, and glycolysis/gluconeogenesis were the key processes accounting for 13 DEMs of importance (e.g., benzene and substituted derivatives, carboxylic acids and derivatives, hydroxyl acids and derivatives, and fatty acids [salicylic acid, homogentisic acid, 2-hydroxyphenylacetic acid, L-aspartic acid, etc.]). They were significantly ($p \leq 0.05$) or extremely significantly ($p \leq 0.01$) correlated with 12 bacterial genera. Among them, *uncultured-bacterium-c-Subgroup-6* was negatively correlated with arbutin 6-phosphate, salicylic acid, L-aspartic acid, 2-hydroxyphenylacetic acid, and homogentisic acid and positively correlated with gamma-aminobutyric acid, N6-(1,2-dicarboxyethyl)-AMP. *Lactobacillus* and *uncultured-bacterium-f-Enterobacteriaceae* were positively correlated with (2S,3S)-2,3-dihydro-2,3-dihydroxybenzoate, L-aspartic acid, 2-hydroxyphenylacetic acid, phenylacetaldehyde, and homogentisic acid and negatively correlated with N6-(1,2-dicarboxyethyl)-AMP, D-lactic acid, acetic acid, while *Sphingomonas* was the opposite. *Nitrospira* was positively correlated with N6-(1,2-dicarboxyethyl)-AMP, while negatively correlated with L-aspartic acid, 2-hydroxyphenylacetic acid, phenylacetaldehyde, and homogentisic acid. *Coccophora-langsdorfii* was negatively correlated with N6-(1,2-dicarboxyethyl)-AMP, while positively correlated with L-aspartic acid, 2-hydroxyphenylacetic acid, phenylacetaldehyde, and homogentisic acid.

In group CC7, metabolic pathways of phenylpropanoid biosynthesis, protein digestion and absorption, biosynthesis of various plant secondary metabolites, biosynthesis of siderophore group non-ribosomal peptides, styrene degradation, and glycolysis/gluconeogenesis were the key processes accounting for 23 DEMs of importance (e.g., benzene and substituted derivatives, phenylpropionic acid, phenols, carboxylic acid and derivatives, hydroxy acid and derivatives, cinnamic acid and derivatives, coumarin and derivatives [vanillin, fraxetin, ferulic acid, sinapic acid, salicylic acid, 4-hydroxybenzoic acid, etc.]). They were significantly ($p \leq 0.05$) or extremely significantly ($p \leq 0.01$) correlated with 12 bacterial genera. For example, *uncultured-bacterium-f-JG30-KF-CM45* was positively correlated with salicylic acid, and 5-hydroxyferulate, and *uncultured-bacterium-c-Acidimicrobiia* was negatively correlated with vanillin, (2S,3S)-2,3-dihydro-2,3-dihydroxybenzoate, 4-hydroxycinnamic acid, and 3-(2-hydroxyphenyl) propionic acid. *Sphingomonas* was negatively correlated with (2S,3S)-2,3-dihydro-2,3-dihydroxybenzoate, 3-(2-hydroxyphenyl) propionic acid. *Lysobacter* was negatively correlated with salicylic acid, 5-hydroxyferulate, and 4-hydroxybenzoic acid; *uncultured-bacterium-f-Gemmatimonadaceae* was positively correlated with ferulic acid and salicylic acid; *uncultured-bacterium-f-Xanthomonadaceae* was negatively correlated with sinapic acid, fraxetin, ferulic acid, salicylic acid, and 5-hydroxyferulate.

3.6.2 The correlations between rhizosphere fungi and metabolites

Same as for rhizosphere bacteria, analyses were conducted to reveal the connections between key metabolic pathways producing DEMs and rhizosphere fungal communities for the different CC groups, as shown in Figure 7B. In CC1, 12 DEMs were significantly ($p \leq 0.05$) or extremely significantly ($p < 0.01$) correlated with 7 fungal genera. Among them, *Chaetomium* was negatively correlated with (R)-mevalonic acid, inosinic acid, hydroquinone, and 4-hydroxyphenylacetaldehyde and positively correlated with 9(S)-HpOTrE, stearidonic acid, 9(S)-HOTrE, and alpha-linolenic acid.

10.3389/fmicb.2023.1318586

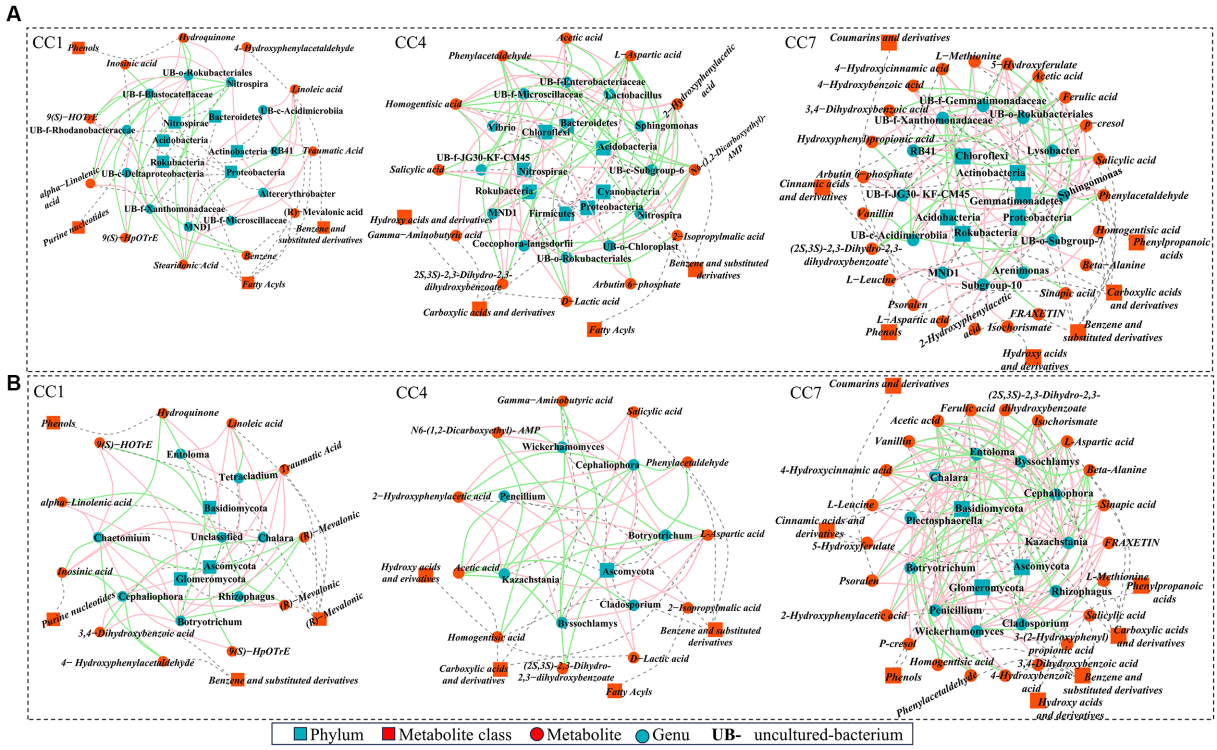

FIGURE 7
High-level correlation network analysis (Spearman's correlation, $r > 0.8$ and $p < 0.05$) between top 20 rhizosphere microbes [**(A)** bacteria; **(B)** fungi] and the differentially expressed metabolites (DEMs) involved in metabolic pathways. Red and green lines denote positive and negative relationships, blue squares and dots represent microbe phylum and genus, red squares and dots represent metabolite class and metabolites, and gray dashed line represents affiliation.

Chalara was positively correlated with (R)-mevalonic acid and inosinic acid and negatively correlated with 3,4-dihydroxybenzoic acid. *Cephaliophora* was negatively correlated with 4-hydroxyphenylacetaldehyde, (R)-mevalonic acid, and inosinic acid and positively correlated with traumatic acid, linoleic acid, and 3,4-dihydroxybenzoic acid. *Botryotrichum* was negatively correlated with (R)-mevalonic acid, hydroquinone, and inosinic acid and was positively correlated with traumatic acid, linoleic acid, 9(S)-HOTrE, 3,4-dihydroxybenzoic acid, and alpha-linolenic acid. *Entoloma* was positively correlated with traumatic acid, linoleic acid. *Rhizophagus* was positively correlated with traumatic acid, stearidonic acid, linoleic acid.

In group CC4, 13 DEMs were shown to be significantly ($p \leq 0.05$) or extremely significantly ($p \leq 0.01$) correlated with 7 genera. Among them, *Botryotrichum* and *Cephaliophora* were negatively correlated with (2S,3S)-2,3-dihydro-2,3-dihydroxybenzoate, 2-hydroxypheny lacetic acid, homogentisic acid, L-aspartic acid, and phenylacetaldehyde and positively correlated with acetic acid, d-lactic acid, and N6-(1,2-dicarboxyethyl)-AMP. *Cladosporium* was positively correlated with L-aspartic acid and negatively correlated with acetic acid. *Kazachstania* and *Byssochlamys* were positively correlated with salicylic acid, L-aspartic acid, and 2-hydroxyphenylacetic acid and negatively correlated with gamma-aminobutyric acid, N6-(1,2-Dicarboxyethyl)-AMP, acetic acid. *Botryotrichum* and *Cephaliophora* were negatively correlated with (2S,3S)-2,3-dihydro-2,3-dihydroxybenzoate, L-aspartic acid, 2-hydroxyphenylacetic acid, phenylacetaldehyde, and homogentisic acid and positively correlated with D-lactic acid, acetic acid, and N6-(1,2-dicarboxyethyl)-AMP. *Wickerhamomyces* was positively correlated with salicylic acid, 2-hydroxyphenylacetic acid, and 2-isopropylmalic acid and negatively correlated with gamma-aminobutyric acid and N6-(1,2-dicarboxyethyl)-AMP. *Penicillium* was positively correlated with L-aspartic acid and phenylacetaldehyde and negatively correlated with acetic acid.

In group CC7, 23 DEMs were shown to be significantly ($p \leq 0.05$) or extremely significantly ($p \leq 0.01$) correlated with 11 genera in group D. *Cladosporium* was positively correlated with fraxetin, ferulic acid, sinapic acid, L-aspartic acid, 4-hydroxycinnamic acid, and isochorismate and negatively correlated with beta-alanine and acetic acid. *Chalara* was positively correlated with (2S,3S)-2,3-dihydro-2,3-dihydroxybenzoate, ferulic acid, 4-hydroxybenzoic acid, L-aspartic acid, phenylacetaldehyde, and isochorismate. *Kazachstania* and *Byssochlamys* were positively correlated with vanillin, fraxetin, ferulic acid, L-leucine, 5-hydroxyferulate, sinapic acid, psoralen, L-aspartic acid, 2-hydroxyphenylacetic acid, 4-hydroxycinnamic acid, and isochorismate. *Cephaliophora* was negatively correlated with (2S,3S)-2,3-dihydro-2,3-dihydroxybenzoate, fraxetin, ferulic acid, L-leucine, sinapic acid, psoralen, L-aspartic acid, 2-hydroxyphenylacetic acid, 4-hydroxycinnamic acid, isochorismate, and homogentisic acid. *Plectosphaerella* was positively correlated with ferulic acid, salicylic acid, and phenylacetaldehyde and negatively correlated with acetic acid. *Botryotrichum* was negatively correlated with (2S,3S)-2,3-dihydro-2,3-dihydroxybenzoate, ferulic acid, 4-hydroxybenzoic acid, L-aspartic acid, phenylacetaldehyde, and isochorismate. *Penicillium*

was positively correlated with vanillin, (2S,3S)-2,3-dihydro-2,3-dihydroxybenzoate, fraxetin, ferulic acid, sinapic acid, L-aspartic acid, 4-hydroxycinnamic acid, and isochorismate and negatively correlated with beta-alanine and acetic acid. *Wickerhamomyces* was positively correlated with vanillin, fraxetin, L-leucine, salicylic acid, 5-hydroxyferulate, sinapic acid, 4-hydroxybenzoic acid, psoralen, and 2-hydroxyphenylacetic acid and negatively correlated with beta-alanine and L-methionine. *Entoloma* was negatively correlated with vanillin, (2S,3S)-2,3-dihydro-2,3-dihydroxybenzoate, L-aspartic acid, 4-hydroxycinnamic acid, isochorismate, homogentisic acid, and 3-(2-hydroxyphenyl) propionic acid.

3.7 The relationships between DEMs and microbiota in the spatial dimension

Figure 8A shows the correlation between GDEMs and the bacteria in different CC groups (CC1–CC7), which were significantly different between rhizosphere (in vicinity of roots) and bulk soil (further away from roots; $p \leq 0.05$). It should be noted that the bacterial genera shown were the ones that were significantly different between rhizosphere (in vicinity of roots) and bulk soil (further away from roots; $p \leq 0.05$). *Sphingobium* was negatively correlated with nonanoylcarnitine, 3-(3-methylbutylidene)-1(3 h)-isobenzofuranone and positively correlated with 2-methyl-2-phenyl-undecane. *Uncultured-bacterium-f-Longimicrobiaceae* was negatively correlated with 2-methyl-2-phenyl-undecane, serine, tyrosine, serine, and cysteine (Ser, Tyr, Ser, Cys) and positively correlated with podecdysone B, (2R)-3-(icosanoyloxy)-2-[(9Z,12Z)-octadeca-9, and 12-dienoyloxy] propyl 2-(trimethylammonio) ethyl phosphate (pc (o-18: 2(9Z,12Z)/20:0)); *Stenotrophobacter* and *Blastocatella* were negatively correlated with 3-hydroxy-4-methoxyphenylacetic acid and 2-methyl-2-phenyl-undecane and positively correlated with alpha-solamarine, pc (o-18:2(9Z,12Z)/20:0) and 4beta-methylzymosterol-4alpha-carboxylic acid; *Flavisolibacter* and *Corynebacterium-1* were negatively correlated with decenoylcarnitine, while *Litorilinea* was positively correlated with decenoylcarnitine.

Figure 8B shows the correlation between the correlation between GDEMs and the fungal genera in different CC groups (CC1–CC7), which were significantly different between rhizosphere (in vicinity of roots) and bulk soil (further away from roots; $p \leq 0.05$). *Mortierella* was negatively correlated with 4,8-dimethyl-1,3(e),7-nonatriene, thujane skeleton, 2-methylisoborneol, 5-ethyl-3-methyl-2e,4e,6e-nonatriene, L-Ala-D-Glu-Meso-A2pm, and triamcinolone diacetate; *Brunneochlamydosporium* was negatively correlated with 4beta-methylzymosterol-4alpha-carboxylic acid and positively correlated with phosphocholine; *Monascus* was positively correlated with 3-(3-methylbutylidene)-1(3 h)-isobenzofuranone; *Sarocladium* was

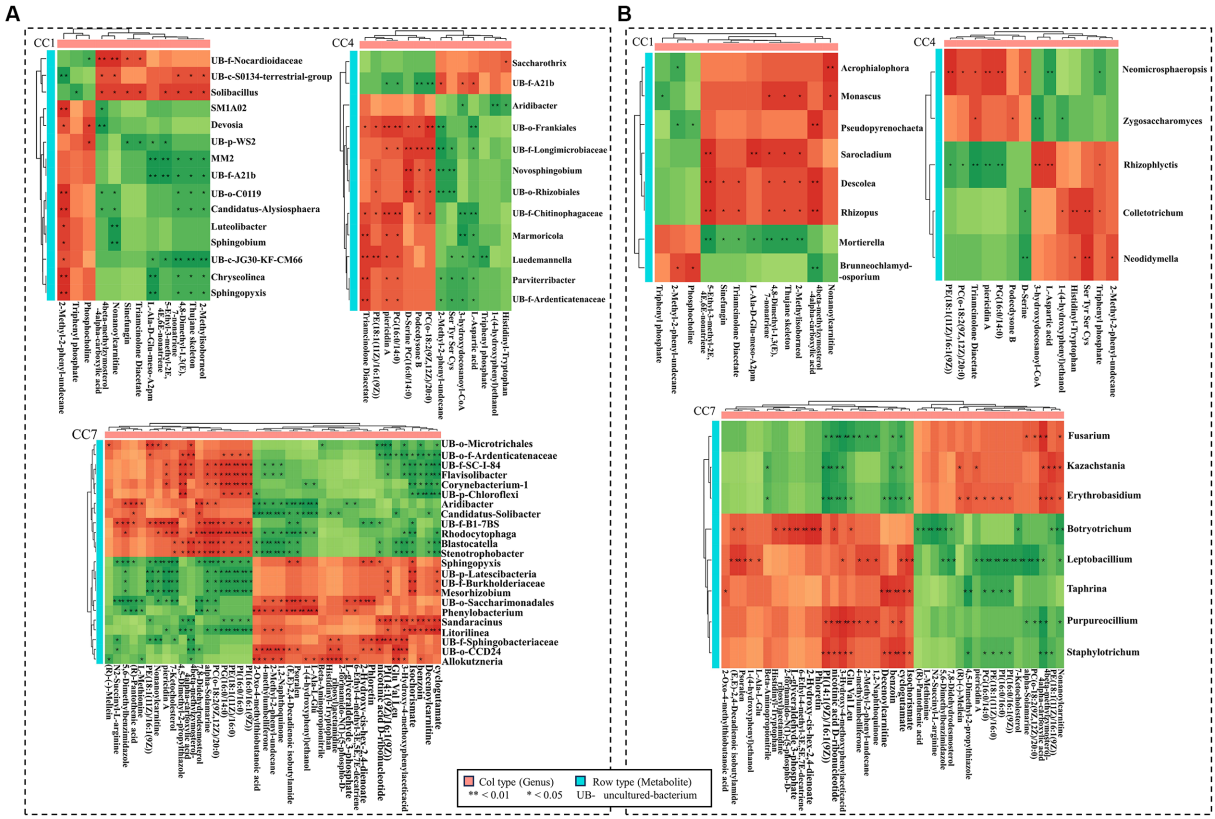

FIGURE 8
Correlation heatmap between GDEMs and the microbiota for rhizosphere and bulk soil. **(A)** The correlation heatmap between bacteria and the greatly differentially expressed metabolites (GDEMs). **(B)** The correlation heatmap between fungi and GDEMs. Every line is the significantly differentiated genus from rhizosphere and bulk soil with *t*-test ($p < 0.05$). Each column is GDEMs, green indicates negative correlation, red indicates positive correlation, *indicates $p < 0.05$, and **indicates $p < 0.01$.

positively correlated with 5-ethyl-3-methyl-2e,4e,6e-nonatriene and L-Ala-D-Glu-Meso-A2pm; *Zygosaccharomyces* was negatively correlated with 3-hydroxydocosanoyl-CoA and positively correlated with triamcinolone diacetate, podecdysone B; *Botryotrichum* was negatively correlated with nonanoylcarnitine and positively correlated with 2-hydroxy-cis-hex-2,4-dienoate; *Fusarium* was positively correlated with 4beta-methylzymosterol-4alpha-carboxylic acid and negatively correlated with 3-hydroxy-4-methoxyphenylacetic acid, nicotinic acid d-ribonucleotide, glutamic acid, valine, and leucine (Glu, Val, Leu); *Kazachstania* was negatively correlated with 1-(9Z-tetradecenoyl)-2-(9Z-hexadecenoyl)-glycero-3-phospho-(1′-myo-inositol) (PI(14:1(9Z)/16:1(9Z))) and nicotinic acid d-ribonucleotide. In general, these results suggested that the root exudates of potato caused chemotaxis in these genera of microorganisms in soil, and their distribution in soil as a function of spatial dimension (close or away from roots) is an indication of their responses to chemical stimuli from the roots.

4 Discussion

Continuous cropping obstacles (CCOs) widely exist in crops, and the mechanisms are very complex. More and more studies indicated that autotoxins secreted by roots combine with rhizosphere microbial imbalance induced by root exudates were the main reasons of CCOs (Jin et al., 2019). Autotoxin secretion is controlled by plant metabolism, and microbiota changes in rhizosphere and bulk soil are responses to it. Both factors were investigated in this study for potato CCOs. It is reasonable to believe that the analytical methods developed in this study would be equally effective for assessment of CCOs for crops other than potato.

4.1 Metabolic pathways in potato controlling root exudates affected by continuous cropping

Root exudates often change when plants are under duress and responding to environmental stressors. The resulted autotoxicity of root exudates was regarded as one of the main reasons of CCOs. As in the cases of *Angelica sinensis*, *Lilium davidii* var. *unicolor*, *Panax quinquefolium*, *Nicotiana tabacum* L., and *P. notoginseng*, the increase of autotoxic allelochemicals in root exudates due to CC was identified as a key reason for failure of replanting (He et al., 2009; Wu Z. J. et al., 2015; Yang et al., 2015; Deng et al., 2017; Xin et al., 2019). In this study, it was discovered that potato root exudates were significantly changed as a function of CC years. Compared with rotation control (CC0), the changes of root exudates of potato from group CC1 could be attributed to α-linolenic acid metabolism, benzoate degradation, biosynthesis of plant secondary metabolites, and biosynthesis of plant hormones. Especially, α-linolenic acid synthesis was downregulated. Linolenic acid was the precursor of jasmonic acid (JA), and JA is a lipogenic plant hormone that regulates the defensive responses of plants to biological and abiotic stresses (Zhao et al., 2014; Balfagon et al., 2019; Zhu et al., 2021; Pyo et al., 2022). Downregulated linolenic acid may suggest that stress levels in potato plants of group CC1 were not increased very much compared to that of group CC0. Meanwhile, for groups CC4 and CC7, metabolic pathways of styrene degradation and biosynthesis of siderophore group non-ribosomal peptides were significantly altered, and the production of phenolic acids (e.g., homogentisic acid and salicylic acid) went up significantly. Homogentisic acid is the precursor for the biosynthesis of α-tocopherol, which regulates the concentration of reactive oxygen and plant hormones in response to stress (Munné-Bosch and Alegre, 2002). Its upregulation was in sharp contrast to the downregulation of linolenic acid-JA synthesis in plants of group CC1. The effects of salicylic acid were concentration-dependent; when the concentration exceeded 0.5 mM, it was shown to significantly affect the mineral absorption of plants (Harper and Balke, 1981), stomatal movement, and chlorophyll content (Manthe et al., 1992; Pancheva et al., 1996). It was also shown to reduce protein content and photosynthetic rate in barley plants (Pancheva et al., 1996). In the range of 3–5 mM, it was shown to completely inhibit the germination of maize embryo (Guan and Scandalios, 1995). In group CC7, metabolic pathway of phenylpropanoid biosynthesis and biosynthesis of various plant secondary metabolites were also significantly changed, and the production of phenolic acids (e.g., sinapic acid, ferulic acid, 4-hydroxycinnamic acid, 4-hydroxybenzoic acid, and vanillin) and coumarin (e.g., psoralen and fraxetin) went up. Vanillin was shown to be connected to changes in microbial communities of the cucumber rhizosphere and the replant failure of eggplant due to CCOs (Chen et al., 2011; Jia et al., 2018; Zhang et al., 2018). Oxidative stress arising from elevated ferulic acid was connected to cellular dysfunction and cell death, and inhibition of the growth of the seedlings (Pergo and Ishii-Iwamoto, 2011; Mandavikia et al., 2017). 4-Hydroxybenzoic acid was shown to regulate grapevine secretion and could cause replant disease (Wang et al., 2019). Psoralen and fraxetin are coumarins, whose effects on plant growth were also dosage-dependent. When the concentration of coumarin was at ~680 μM, the root growth of cucumber and maize seedlings was completely inhibited (Pergo et al., 2008). 4-Hydroxycinnamic acid (p-coumaric acid) could also significantly inhibit crop growth, such as cucumber (Zhou and Wu, 2012), strawberry (Chen et al., 2020), and asparagus (Kato-Noguchi et al., 2017). The elevation of phenolic acids and coumarin production in groups CC7 clearly was one of the main reasons of yield drop in this group. These observations also confirmed that none of these autotoxic allelochemicals were unique to potato, they belong to a group of compounds that could affect various plants, and monitoring their levels could hold keys to understand CCOs in various crops.

In addition to the DEMs involved in the above metabolic pathways, other DEMs increased in a CC-year dependent pattern (Supplementary Table S8), including potential autotoxins: phenols (1-(4-hydroxyphenyl) ethanol, homogentisic acid, 2-aminophenol, purpurogallin), alkaloids (conhydrine), flavonoids (phloretin), coumarins (psoralen), as well as 5-phenyl-4-pentenyl-hydroperoxide (PPHP), 2,5-diketo-d-gluconate, 5-methylaminomethyl-2-thiouridine, N-acetyl-D-proline, benzoin, urodiolenone, and benzyl butyl phthalate. Among them, 1-(4-hydroxyphenyl) ethanol was increased in group CC4, while 1,2-naphthoquinone, 4-methylumbelliferone, 1-(4-hydroxyphenyl) ethanol, phloretin, psoralen, and beta-aminopropionitrile were all significantly increased in group CC7. Studies have found that in addition to coumarins (Yan et al., 2016), phenols (Chaki et al., 2020) and alkaloids (Lei et al., 2021) also indicate that the plants were under oxidative stress. PPHP is a hydroperoxide, an initial product of lipid peroxidation (Weller et al., 1985), and lipid peroxidation is a major indicator of oxidative damage

in plants (Chen et al., 2021; Fardus et al., 2021). 2,5-Diketo-d-gluconate is a key intermediate in the production of l-ascorbic acid (vitamin C; Son et al., 2022), which is a main antioxidant in plants and plays important roles in alleviating excessive activities of oxidative free radicals caused by many abiotic stresses (Gallie, 2013). Exogenous application of 4-methylumbelliferone to *Arabidopsis thaliana* seeds before seedling formation could affect seed germination, resulting in reduced primary root growth, root hair formation, irregular root cap shedding, and reorganization of actin cytoskeleton in root tip (Li et al., 2011). Phloretin also significantly inhibited the growth of primary roots, lateral roots, and leaves of *Arabidopsis thaliana* (Smailagic et al., 2022). The changes in these DEMs related to plant stress responses all indicated the effects of CC on the potato plants. As a general trend, the more CC years, the more autotoxin production in potato plants.

4.2 Microflora changes affected by continuous cropping

Changes in microflora and its imbalance were also important contributing factors to CCOs (Tan et al., 2017; Shen et al., 2018; Li X. G. et al., 2020). Studies found that harmful fungi increased and beneficial bacteria and actinomycetes decreased in soil of potato field undergoing contentious cropping (Qin et al., 2017a; Zhao et al., 2020); consequently, the microbial community structure in soil became unbalanced, with overgrowth of harmful microorganisms such as *Fusaria*, and inhibited plant root growth (Qin et al., 2017a). This study also found that beneficial bacteria (*Sphingomonas*, *Lysobacter*, *Altererythrobacter*, *Rhizophagus*, *Septoglomus*, *Mortierella,* and *Funneliformis*) all were significantly reduced, and harmful fungi (*Cladosporium*, *Plectosphaerella*, *Zasmidium*, *Aspergillus*, and *Chalara*), on the other hand, were significantly increased under CC, especially in groups CC4 and CC7. Among them, *Sphingomonas* was plant growth-promoting endophytic bacteria (PGPEB; Khan et al., 2017), which plays a role in promoting plant growth (Khan et al., 2014; Pan et al., 2016). *Lysobacter* spp. were reported to reduce diseases caused by plant pathogens in *Cucumis sativus* Linn (Folman et al., 2004; Postma et al., 2008), *Oryza sativa* (Ji et al., 2008), *Piper nigrum* Linn (Ko et al., 2009), *Vitis vinifera* (Puopolo et al., 2014), *Spinacia oleracea* L. (Islam et al., 2005), and *Lycopersicon esculentum* (Puopolo et al., 2010). *Altererythrobacter* is genera of bacteria involved in C cycling (An et al., 2022) that could bring ecological benefits (Liu et al., 2022). *Septoglomus*, *Funneliformis,* and *Rhizophagus* (Rodriguez-Caballero et al., 2017; Cui et al., 2018; Todeschini et al., 2018) could colonize on the roots of most terrestrial plant species and improve plant growth, nutrient uptake, and biotic/abiotic stress resistance and tolerance. *Mortierella alpina* was reported to help *Panax ginseng* resist *Fusarium oxysporum* infection by regulating the fungal community in the root (Wang Y. et al., 2022), and *Mortierella capitata* was reported to promote crop growth directly by altering gene expression levels in the plant roots and indirectly via interacting with indigenous rhizosphere bacteria (Li F. et al., 2020). *Cladosporium* (Virginia et al., 2021; Wang T. et al., 2022), *Plectosphaerella* (Garibaldi et al., 2010; Xu et al., 2014), *Zasmidium* (Laranjeira et al., 2020), *Aspergillus* (Ali et al., 2022), and *Chalara* (Wang et al., 2021) were all plant pathogens, which mainly presented in rhizosphere soil and significantly increased with CC years as shown in this study.

4.3 Correlation between root exudates and microflora

Root exudates as substrates and/or signal molecules for microbe are the main driver of rhizosphere microflora (Zhalnina et al., 2018). Plant–microbe interactions mediated by root exudates could facilitate plant CCO and resulted in plant diseases (Wu et al., 2023). For instance, ginseng roots exudates could trigger bloom of the ginseng soft-rot bacteria, which is the culprit for one of major bacterial diseases that affect ginseng plants and the cause for drop in both the yield and quality of ginseng roots (Lei et al., 2017). In tobacco root exudates, cinnamic, myristic, and fumaric acids were identified as attractants to induce the colonization and infection of the roots by *Ralstonia solanacearum*, which led to one of the most serious soil-borne diseases in tobacco cultivation (Li et al., 2017). Previous study found that the root exudates of *Rehmannia glutinosa* could inhibit the growth of *Pseudomonas* sp. W12, a beneficial bacterium and promote the growth and toxin production of pathogenic *Fusarium oxysporum* (Wu L. K. et al., 2015). In the soil of monocropping field of *Radix pseudostellariae*, vanillin (e.g., phenols) was shown to promote the colonization and growth of *Kosakonia sacchari*, the pathogen of *R. pseudostellariae*, and increased the probability of disease occurrence (Wu et al., 2017). In this study, significant ($p \leq 0.05$) or extremely significant ($p \leq 0.01$) positive correlations were established for potato crops between pathogenic microbes and root exudates; *Cladosporium* was positively correlated with ferulic acid (phenolic acids; $p \leq 0.01$), sinapic acid (phenolic acids; $p \leq 0.01$), L-aspartic acid (amino acid; $p \leq 0.05$), 4-hydroxycinnamic acid (phenolic acids; $p \leq 0.05$), fraxetin (coumarin; $p \leq 0.05$), and isochorismate ($p \leq 0.05$), *Chalara* was positively correlated with ferulic acid ($p \leq 0.01$), 4-hydroxybenzoic acid (phenolic acids; $p \leq 0.05$), L-aspartic acid ($p \leq 0.01$), and isochorismate ($p \leq 0.01$), and *Plectosphaerella* was positively correlated with ferulic acid ($p \leq 0.01$) and salicylic acid ($p \leq 0.05$). In contrast, the opposite was true for beneficial bacteria; *Sphingomonas* was negatively correlated with 2-hydroxyphenylacetic acid (phenolic acids; $p \leq 0.05$), phenylacetaldehyde ($p \leq 0.01$), and homogentisic acid (phenolic acids; $p \leq 0.05$), and *Nitrospira* was negatively correlated with 2-hydroxyphenylacetic acid ($p \leq 0.05$), phenylacetaldehyde ($p \leq 0.05$), and homogentisic acid ($p \leq 0.05$). *Lysobacter* was negatively correlated with salicylic acid ($p \leq 0.01$), 5-hydroxyferulate ($p \leq 0.01$), and 4-hydroxybenzoic acid ($p \leq 0.05$), and *Sphingomonas* was negatively correlated with 2-phenylacetaldehyde ($p \leq 0.01$).

Closer investigation revealed some complex patterns. For example, the relative abundance of *Fusarium* in the rhizosphere of CC crops, surprisingly, did not peak in group CC7 but in group CC4. Furthermore, *Fusarium* were significantly enriched in the bulk soil of group CC7. This "puzzle" could be solved from the spatial correlations between DEMs and microbiota. Our study showed that the increase of 4-methylumbelliferon (from bulk to rhizosphere) was negatively correlated with the changes in relative abundance of *Fusarium* in the bulk soil, which could be attributed to coumarins. Studies have shown that coumarin could have a strong inhibitory effect on *Fusarium* in a dosage-dependent way. At high concentrations, they could inhibit mycelial growth, sporulation, and pathogenicity-related enzyme activities (Wu et al., 2008). Hence, the accumulation of high coumarins in the rhizosphere of group CC7 could inhibit the growth of *Fusarium*. However, *Fusarium* was still highly enriched in the bulk soil, which attributed to the much-reduced yield of potato from the group CC7.

Finally, stimulation of psoralen accumulation by biotic elicitors such as yeast extract and chitosan has previously been observed in the cell cultures of plant species, *viz.*, *Calendula officinalis* (Wu et al., 2008), *Sorbus aucuparia* (Gaid et al., 2011), and *Abrus precatorius* (Karwasara and Dixit, 2009; Karwasara et al., 2011). In this study, psoralen was shown to be positively correlated with *Kazachstania* ($p \leq 0.05$), *Byssochlamys* ($p \leq 0.05$), and *Wickerhamomyces* ($p \leq 0.01$), and these fungi were reported to promote plant growth by producing plant hormones and other growth regulators (Nassar et al., 2005; Cloete et al., 2009; Xin et al., 2009; Amprayn et al., 2012; Nutaratat et al., 2014) or interacted indirectly with symbiotic microorganisms such as arbuscular mycorrhizal fungi (AMF; Fracchia et al., 2003; Boby et al., 2008). In general, the knowledge gained on relationships between metabolites and microbial communities could provide guidance for the regulation/manipulation of rhizosphere microflora via biotechnology (e.g., microbial fertilizer) to overcome continuous cropping obstacles and improve both yield and quality of potato crops.

5 Conclusion

The results showed continuous cropping of potato changed the metabolic pathways in potato that significantly changed alpha-linolenic acid metabolism in plants from 1 year CC field, styrene degradation, biosynthesis of siderophore group non-ribosomal peptides, phenylpropanoid biosynthesis, and biosynthesis of various plant secondary metabolites in plants from 4 to 7 years CC field, and increased phenols, flavonoids, coumarins, and alkaloids in root exudates. Continuous cropping of potato beyond 4 years changed their metabolism as reflected in the plant root exudates to drive rhizosphere microflora toward the direction of reducing beneficial bacteria and promoting harmful fungi, which need to be better controlled to reduce the impact of CCO on potato production.

Data availability statement

The datasets presented in this study can be found in online repositories. The names of the repository/repositories and accession number(s) can be found in the article/Supplementary material.

Author contributions

YX: Data curation, Formal analysis, Funding acquisition, Investigation, Writing – original draft. PZ: Funding acquisition, Methodology, Project administration, Writing – original draft. WZ: Conceptualization, Funding acquisition, Investigation, Methodology, Project administration, Supervision, Writing – original draft, Writing – review & editing. CY: Formal analysis, Methodology, Writing – review & editing. ZL: Conceptualization, Supervision, Writing – review & editing.

Funding

The author(s) declare financial support was received for the research, authorship, and/or publication of this article. This study was supported by the National Natural Science Foundation of China [32060717], Key Research and Development Plan of Gansu Province [20YF3WA010], Agricultural Science and Technology Innovation Special Project of Gansu Academy of Agricultural Sciences [2022GAAS25], and the 2023 "Star of Innovation" project for postgraduate from the Department of Education of Gansu Province [2023CXZX-695].

Conflict of interest

The authors declare that the research was conducted in the absence of any commercial or financial relationships that could be construed as a potential conflict of interest.

Publisher's note

Supplementary material

The Supplementary material for this article can be found online at: https://www.frontiersin.org/articles/10.3389/fmicb.2023.1318586/full#supplementary-material

References

Ali, A., Elrys, A. S., Liu, L. L., Iqbal, M., Zhao, J., Huang, X. Q., et al. (2022). Cover plants-mediated suppression of fusarium wilt and root-knot incidence of cucumber is associated with the changes of rhizosphere fungal microbiome structure-under plastic shed system of North China. *Front. Microbiol.* 13:17. doi: 10.3389/fmicb.2022.697815

Amprayn, K. O., Rose, M. T., Kecskes, M., Pereg, L., Nguyen, H. T., and Kennedy, I. R. (2012). Plant growth promoting characteristics of soil yeast (*Candida tropicalis* HY) and its effectiveness for promoting rice growth. *Appl. Soil Ecol.* 61, 295–299. doi: 10.1016/j.apsoil.2011.11.009

An, X. C., Wang, Z. F., Teng, X. M., Zhou, R. R., Wang, X. X., Xu, M., et al. (2022). Rhizosphere bacterial diversity and environmental function prediction of wild salt-tolerant plants in coastal silt soil. *Ecol. Indic.* 134:108503. doi: 10.1016/j.ecolind.2021.108503

Balfagon, D., Sengupta, S., Gomez-Cadenas, A., Fritschi, F. B., Azad, R. K., Mittler, R., et al. (2019). Jasmonic acid is required for plant acclimation to a combination of high light and heat stress. *Plant Physiol.* 181, 1668–1682. doi: 10.1104/pp.19.00956

Boby, V. U., Balakrishna, A. N., and Bagyaraj, D. J. (2008). Interaction between Glomus mosseae and soil yeasts on growth and nutrition of cowpea. *Microbiol. Res.* 163, 693–700. doi: 10.1016/j.micres.2006.10.004

Bonanomi, G., De Filippis, F., Cesarano, G., La Storia, A., Ercolini, D., and Scala, F. (2016). Organic farming induces changes in soil microbiota that affect agro-ecosystem functions. *Soil Biol. Biochem.* 103, 327–336. doi: 10.1016/j.soilbio.2016.09.005

Camire, M. E., Kubow, S., and Donnelly, D. J. (2009). Potatoes and human health. *Crit. Rev. Food Sci. Nutr.* 49, 823–840. doi: 10.1080/10408390903041996

Chaki, M., Begara-Morales, J. C., and Barroso, J. B. (2020). Oxidative stress in plants. *Antioxidants* 9:4. doi: 10.3390/antiox9060481

Chen, L. L., Shan, W., Cai, D. L., Chen, J. Y., Lu, W. J., Su, X. G., et al. (2021). Postharvest application of glycine betaine ameliorates chilling injury in cold-stored banana fruit by enhancing antioxidant system. *Sci. Hortic.* 287:110264. doi: 10.1016/j.scienta.2021.110264

Chen, P., Wang, Y. Z., Liu, Q. Z., Zhang, Y. T., Li, X. Y., Li, H. Q., et al. (2020). Phase changes of continuous cropping obstacles in strawberry (*Fragaria x ananassa* Duch.) production. *Appl. Soil Ecol.* 155:103626. doi: 10.1016/j.apsoil.2020.103626

Chen, S. L., Zhou, B. L., Lin, S. S., Li, X., and Ye, X. L. (2011). Accumulation of cinnamic acid and vanillin in eggplant root exudates and the relationship with continuous cropping obstacle. *Afr. J. Biotechnol.* 10, 2659–2665. doi: 10.5897/AJB10.1338

Cloete, K. J., Valentine, A. J., Stander, M. A., Blomerus, L. M., and Botha, A. (2009). Evidence of Symbiosis between the soil yeast Cryptococcus laurentii and a Sclerophyllous medicinal shrub, *Agathosma betulina* (berg.) Pillans. *Microb. Ecol.* 57, 624–632. doi: 10.1007/s00248-008-9457-9

Cui, J. Q., Sun, H. B., Sun, M. B., Liang, R. T., Jie, W. G., and Cai, B. Y. (2018). Effects of Funneliformis mosseae on root metabolites and rhizosphere soil properties to continuously-cropped soybean in the potted-experiments. *Int. J. Mol. Sci.* 19:16. doi: 10.3390/ijms19082160

Deng, J. J., Zhang, Y. L., Hu, J. W., Jiao, J. G., Hu, F., Li, H. X., et al. (2017). Autotoxicity of phthalate esters in tobacco root exudates: effects on seed germination and seedling growth. *Pedosphere* 27, 1073–1082. doi: 10.1016/s1002-0160(17)60374-6

Dunn, W. B., Broadhurst, D., Begley, P., Zelena, E., Francis-McIntyre, S., Anderson, N., et al. (2011). Procedures for large-scale metabolic profiling of serum and plasma using gas chromatography and liquid chromatography coupled to mass spectrometry. *Nat. Protoc.* 6, 1060–1083. doi: 10.1038/nprot.2011.335

Fardus, J., Hossain, M. S., and Fujita, M. (2021). Modulation of the antioxidant defense system by exogenous l-glutamic acid application enhances salt tolerance in lentil (*Lens culinaris* Medik.). *Biomol. Ther.* 11:15. doi: 10.3390/biom11040587

Folman, L. B., De Klein, M. J. E. M., Postma, J., and van Veen, J. A. (2004). Production of antifungal compounds by *Lysobacter enzymogenes* isolate 3.1T8 under different conditions in relation to its efficacy as a biocontrol agent of *Pythium aphanidermatum* in cucumber. *Biol. Control* 31, 145–154. doi: 10.1016/j.biocontrol.2004.03.008

Fracchia, S., Godeas, A., Scervino, J. M., Sampedro, I., Ocampo, J. A., and Garcia-Romera, I. (2003). Interaction between the soil yeast Rhodotorula mucilaginosa and the arbuscular mycorrhizal fungi Glomus mosseae and Gigaspora rosea. *Soil Biol. Biochem.* 35, 701–707. doi: 10.1016/s0038-0717(03)00086-5

Gaid, M. M., Scharnhop, H., Ramadan, H., Beuerle, T., and Beerhues, L. (2011). 4-Coumarate: CoA ligase family members from elicitor-treated *Sorbus aucuparia* cell cultures. *J. Plant Physiol.* 168, 944–951. doi: 10.1016/j.jplph.2010.11.021

Gallie, D. R. (2013). The role of L-ascorbic acid recycling in responding to environmental stress and in promoting plant growth. *J. Exp. Bot.* 64, 433–443. doi: 10.1093/jxb/ers330

Gao, Z. Y., Han, M. K., Hu, Y. Y., Li, Z. Q., Liu, C. F., Wang, X., et al. (2019). Effects of continuous cropping of sweet potato on the fungal community structure in Rhizospheric soil. *Front. Microbiol.* 10:11. doi: 10.3389/fmicb.2019.02269

Gao, Z. Y., Hu, Y. Y., Han, M. K., Xu, J. J., Wang, X., Liu, L. F., et al. (2021). Effects of continuous cropping of sweet potatoes on the bacterial community structure in rhizospheric soil. *BMC Microbiol.* 21:102. doi: 10.1186/s12866-021-02120-6

Garibaldi, A., Gilardi, G., and Gullino, M. L. (2010). First report of leaf spot caused by Phoma multirostrata on Fuchsia x hybrida in Italy. *Plant Dis.* 94:382. doi: 10.1094/pdis-94-3-0382a

Guan, L., and Scandalios, J. G. (1995). Developmentally related responses of maize catalase genes to salicylic acid. *Proc. Natl. Acad. Sci. U. S. A.* 92, 5930–5934. doi: 10.1073/pnas.92.13.5930

Han, T., Mi, Z. R., Chen, Z., Zhao, J. J., Zhang, H. G., Lv, Y., et al. (2022). Multi-omics analysis reveals the influence of tetracycline on the growth of ryegrass root. *J. Hazard. Mater.* 435:129019. doi: 10.1016/j.jhazmat.2022.129019

Harper, J. R., and Balke, N. E. (1981). Characterization of the inhibition of k absorption in oat roots by salicylic acid. *Plant Physiol.* 68, 1349–1353. doi: 10.1104/pp.68.6.1349

He, C. N., Gao, W. W., Yang, J. X., Bi, W., Zhang, X. S., and Zhao, Y. J. (2009). Identification of autotoxic compounds from fibrous roots of Panax quinquefolium L. *Plant Soil* 318, 63–72. doi: 10.1007/s11104-008-9817-8

Huang, W. J., Sun, D. L., Fu, J. T., Zhao, H. H., Wang, R. H., and An, Y. X. (2020). Effects of continuous sugar beet cropping on Rhizospheric microbial communities. *Genes* 11:13. doi: 10.3390/genes11010013

Huo, C. F., Lu, J. Y., Yin, L. M., Wang, P., and Cheng, W. X. (2022). Coupled of carbon and nitrogen mineralization in rhizosphere soils along a temperate forest altitudinal gradient. *Plant Soil* 15, 1–15. doi: 10.1007/s11104-022-05611-1

Islam, M. T., Hashidoko, Y., Deora, A., Ito, T., and Tahara, S. (2005). Suppression of damping-off disease in host plants by the rhizoplane bacterium Lysobacter sp. strain SB-K88 is linked to plant colonization and antibiosis against soilborne Peronosporomycetes. *Appl. Environ. Microbiol.* 71, 3786–3796. doi: 10.1128/aem.71.7.3786-3796.2005

Ji, G.-H., Wei, L.-F., He, Y.-Q., Wu, Y.-P., and Bai, X.-H. (2008). Biological control of rice bacterial blight by *Lysobacter antibioticus* strain 13-1. *Biol. Control* 45, 288–296. doi: 10.1016/j.biocontrol.2008.01.004

Jia, H. T., Chen, S. C., Yang, S. Y., Shen, Y. H., Qiao, P. L., Wu, F. Z., et al. (2018). Effects of vanillin on cucumber rhizosphere bacterial community. *Allelopath. J.* 44, 191–200. doi: 10.26651/allelo.j/2018-44-2-1164

Jin, X., Shi, Y. J., Tan, S. C., Ma, C. L., Wu, F. Z., Pan, K., et al. (2019). Effects of cucumber root exudates components on soil bacterial community structure and abundance. *Allelopath. J.* 48, 167–174. doi: 10.26651/allelo.j/2019-48-2-1252

Kang, S. M., Radhakrishnan, R., Lee, S. M., Park, Y. G., Kim, A. Y., Seo, C. W., et al. (2015). *Enterobacter* sp SE992-induced regulation of amino acids, sugars, and hormones in cucumber plants improves salt tolerance. *Acta Physiol. Plant.* 37, 1–10. doi: 10.1007/s11738-015-1895-7

Karwasara, V. S., and Dixit, V. K. (2009). Genetic transformation and elicitation as yield enhancement strategy for glycyrrhizin production by cell cultures of *Abrus precatorius* L. *New Biotechnol.* 25:S308. doi: 10.1016/j.nbt.2009.06.882

Karwasara, V. S., Tomar, P., and Dixit, V. K. (2011). Influence of fungal elicitation on glycyrrhizin production in transformed cell cultures of *Abrus precatorius* Linn. *Pharmacogn. Mag.* 7, 307–313. doi: 10.4103/0973-1296.90411

Kato-Noguchi, H., Nakamura, K., Ohno, O., Suenaga, K., and Okuda, N. (2017). Asparagus decline: autotoxicity and autotoxic compounds in asparagus rhizomes. *J. Plant Physiol.* 213, 23–29. doi: 10.1016/j.jplph.2017.02.011

Khademi, Z., Jones, D. L., Malakouti, M. J., and Asadi, F. (2010). Organic acids differ in enhancing phosphorus uptake by *Triticum aestivum* L.-effects of rhizosphere concentration and counterion. *Plant Soil* 334, 151–159. doi: 10.1007/s11104-009-0215-7

Khan, A. L., Waqas, M., Asaf, S., Kamran, M., Shahzad, R., Bilal, S., et al. (2017). Plant growth-promoting endophyte *Sphingomonas* sp LK11 alleviates salinity stress in *Solanum pimpinellifolium*. *Environ. Exp. Bot.* 133, 58–69. doi: 10.1016/j.envexpbot.2016.09.009

Khan, A. L., Waqas, M., Kang, S. M., Al-Harrasi, A., Hussain, J., Al-Rawahi, A., et al. (2014). Bacterial endophyte *Sphingomonas* sp LK11 produces gibberellins and IAA and promotes tomato plant growth. *J. Microbiol.* 52, 689–695. doi: 10.1007/s12275-014-4002-7

Ko, H.-S., Jin, R.-D., Krishnan, H. B., Lee, S.-B., and Kim, K.-Y. (2009). Biocontrol ability of *Lysobacter antibioticus* HS124 against phytophthora blight is mediated by the production of 4-hydroxyphenylacetic acid and several lytic enzymes. *Curr. Microbiol.* 59, 608–615. doi: 10.1007/s00284-009-9481-0

Laranjeira, F. F., Silva, S. X. B., Murray-Watson, R. E., Soares, A. C. F., Santos, H. P., and Cunniffe, N. J. (2020). Spatiotemporal dynamics and modelling support the case for area-wide management of citrus greasy spot in a Brazilian smallholder farming region. *Plant Pathol.* 69, 467–483. doi: 10.1111/ppa.13146

Lei, F. J., Fu, J. F., Zhou, R. J., Wang, D., Zhang, A. H., Ma, W. L., et al. (2017). Chemotactic response of ginseng bacterial soft-rot to ginseng root exudates. *Saudi J. Biol. Sci.* 24, 1620–1625. doi: 10.1016/j.sjbs.2017.05.006

Lei, L. J., Zhao, Y., Shi, K., Liu, Y., Hu, Y. X., and Shao, H. (2021). Phytotoxic activity of alkaloids in the desert plant Sophora alopecuroides. *Toxins* 13:18. doi: 10.3390/toxins13100706

Li, X., Gruber, M. Y., Hegedus, D. D., Lydiate, D. J., and Gao, M. J. (2011). Effects of a Coumarin derivative, 4-Methylumbelliferone, on seed germination and seedling establishment in Arabidopsis. *J. Chem. Ecol.* 37, 880–890. doi: 10.1007/s10886-011-9987-3

Li, X. G., Panke-Buisse, K., Yao, X. D., Coleman-Derr, D., Ding, C. F., Wang, X. X., et al. (2020). Peanut plant growth was altered by monocropping-associated microbial enrichment of rhizosphere microbiome. *Plant Soil* 446, 655–669. doi: 10.1007/s11104-019-04379-1

Li, S. L., Xu, C., Wang, J., Guo, B., Yang, L., Chen, J. N., et al. (2017). Cinnamic, myristic and fumaric acids in tobacco root exudates induce the infection of plants by *Ralstonia solanacearum*. *Plant Soil* 412, 381–395. doi: 10.1007/s11104-016-3060-5

Li, F., Zhang, S. Q., Wang, Y., Li, Y., Li, P. P., Chen, L., et al. (2020). Rare fungus, Mortierella capitata, promotes crop growth by stimulating primary metabolisms related genes and reshaping rhizosphere bacterial community. *Soil Biol. Biochem.* 151:108017. doi: 10.1016/j.soilbio.2020.108017

Liu, C. J., Lin, H., He, P. D., Li, X. Y., Geng, Y., Tuerhong, A., et al. (2022). Peat and bentonite amendments assisted soilless revegetation of oligotrophic and heavy metal contaminated nonferrous metallic tailing. *Chemosphere* 287:132101. doi: 10.1016/j.chemosphere.2021.132101

Mandavikia, F., Saharkhiz, M. J., and Karami, A. (2017). Defensive response of radish seedlings to the oxidative stress arising from phenolic compounds in the extract of peppermint (*Mentha x piperita* L.). *Sci. Hortic.* 214, 133–140. doi: 10.1016/j.scienta.2016.11.029

Manthe, B., Schulz, M., and Schnabl, H. (1992). Effects of salicylic acid on growth and stomatal movements of *Vicia faba* L.: evidence for salicylic acid metabolization. *J. Chem. Ecol.* 18, 1525–1539. doi: 10.1007/bf00993226

Munné-Bosch, S., and Alegre, L. (2002). The function of tocopherols and tocotrienols in plants. *Crit. Rev. Plant Sci.* 21, 31–57. doi: 10.1080/0735-260291044179

Nassar, A. H., El-Tarabily, K. A., and Sivasithamparam, K. (2005). Promotion of plant growth by an auxin-producing isolate of the yeast Williopsis saturnus endophytic in maize (*Zea mays* L.) roots. *Biol. Fertil. Soils* 42, 97–108. doi: 10.1007/s00374-005-0008-y

Nutaratat, P., Srisuk, N., Arunrattiyakorn, P., and Limtong, S. (2014). Plant growth-promoting traits of epiphytic and endophytic yeasts isolated from rice and sugar cane leaves in Thailand. *Fungal Biol.* 118, 683–694. doi: 10.1016/j.funbio.2014.04.010

Pan, F. S., Meng, Q., Wang, Q., Luo, S., Chen, B., Khan, K. Y., et al. (2016). Endophytic bacterium *Sphingomonas* SaMR12 promotes cadmium accumulation by increasing glutathione biosynthesis in Sedum alfredii Hance. *Chemosphere* 154, 358–366. doi: 10.1016/j.chemosphere.2016.03.120

Pancheva, T. V., Popova, L. P., and Uzunova, A. N. (1996). Effects of salicylic acid on growth and photosynthesis in barley plants. *J. Plant Physiol.* 149, 57–63. doi: 10.1016/S0176-1617(96)80173-8

Pergo, E. M., Abrahim, D., Soares da Silva, P. C., Kern, K. A., Da Silva, L. J., Voll, E., et al. (2008). *Bidens pilosa* L. exhibits high sensitivity to coumarin in comparison with three other weed species. *J. Chem. Ecol.* 34, 499–507. doi: 10.1007/s10886-008-9449-8

Pergo, E. M., and Ishii-Iwamoto, E. L. (2011). Changes in energy metabolism and antioxidant defense systems during seed germination of the weed species *Ipomoea triloba* L. and the responses to Allelochemicals. *J. Chem. Ecol.* 37, 500–513. doi: 10.1007/s10886-011-9945-0

Postma, J., Stevens, L. H., Wiegers, G. L., Davelaar, E., and Nijhuis, E. H. (2008). Biological control of *Pythium aphanidermatum* in cucumber with a combined application of *Lysobacter enzymogenes* strain 3.1T8 and chitosan. *Biol. Control* 48, 301–309. doi: 10.1016/j.biocontrol.2008.11.006

Puopolo, G., Giovannini, O., and Pertot, I. (2014). *Lysobacter capsici* AZ78 can be combined with copper to effectively control Plasmopara viticola on grapevine. *Microbiol. Res.* 169, 633–642. doi: 10.1016/j.micres.2013.09.013

Puopolo, G., Raio, A., and Zoina, A. (2010). Identification and characterization of *Lysobacter capsici* strain PG4: a new plant health-promoting rhizobacterium. *J. Plant Pathol.* 92, 157–164. doi: 10.4454/jpp.v92i1.25

Pyo, Y., Moon, H., Nugroho, A. B. D., Yang, S. W., Jung, I., and Kim, D. H. (2022). Transcriptome analysis revealed that jasmonic acid biosynthesis/signaling is involved in plant response to strontium stress. *Ecotoxicol. Environ. Saf.* 237:113552. doi: 10.1016/j.ecoenv.2022.113552

Qin, S. H., Yeboah, S., Cao, L., Zhang, J. L., Shi, S. L., and Liu, Y. H. (2017a). Breaking continuous potato cropping with legumes improves soil microbial communities, enzyme activities and tuber yield. *PLoS One* 12:e0175934. doi: 10.1371/journal.pone.0175934

Qin, S. H., Yeboah, S., Xu, X. X., Liu, Y. H., and Yu, B. (2017b). Analysis on fungal diversity in rhizosphere soil of continuous cropping potato subjected to different furrow-ridge mulching managements. *Front. Microbiol.* 8:10. doi: 10.3389/fmicb.2017.00845

Quast, C., Pruesse, E., Yilmaz, P., Gerken, J., Schweer, T., Yarza, P., et al. (2013). The SILVA ribosomal RNA gene database project: improved data processing and web-based tools. *Nucleic Acids Res.* 41, D590–D596. doi: 10.1093/nar/gks1219

Rodriguez-Caballero, G., Caravaca, F., Fernandez-Gonzalez, A. J., Alguacil, M. M., Fernandez-Lopez, M., and Roldan, A. (2017). Arbuscular mycorrhizal fungi inoculation mediated changes in rhizosphere bacterial community structure while promoting revegetation in a semiarid ecosystem. *Sci. Total Environ.* 584-585, 838–848. doi: 10.1016/j.scitotenv.2017.01.128

Segata, N., Izard, J., Waldron, L., Gevers, D., Miropolsky, L., Garrett, W. S., et al. (2011). Metagenomic biomarker discovery and explanation. *Genome Biol.* 12:R60. doi: 10.1186/gb-2011-12-6-r60

Shannon, P., Markiel, A., Ozier, O., Baliga, N. S., Wang, J. T., Ramage, D., et al. (2003). Cytoscape: a software environment for integrated models of biomolecular interaction networks. *Genome Res.* 13, 2498–2504. doi: 10.1101/gr.1239303

Shen, Z. Z., Penton, C. R., Lv, N., Xue, C., Yuan, X. F., Ruan, Y. Z., et al. (2018). Banana fusarium wilt disease incidence is influenced by shifts of soil microbial communities under different monoculture spans. *Microb. Ecol.* 75, 739–750. doi: 10.1007/s00248-017-1052-5

Smailagic, D., Banjac, N., Ninkovic, S., Savic, J., Cosic, T., Pencik, A., et al. (2022). New insights into the activity of apple Dihydrochalcone Phloretin: disturbance of auxin homeostasis as physiological basis of Phloretin phytotoxic action. *Front. Plant Sci.* 13:17. doi: 10.3389/fpls.2022.875528

Soltys-Kalina, D., Murawska, Z., Strzelczyk-Zyta, D., Wasilewicz-Flis, I., and Marczewski, W. (2019). Phytotoxic potential of cultivated and wild potato species (Solanum sp.): role of glycoalkaloids, phenolics and flavonoids in phytotoxicity against mustard (*Sinapis alba* L.). *Acta Physiol. Plant.* 41:9. doi: 10.1007/s11738-019-2848-3

Son, H., Han, S. U., and Lee, K. (2022). 2,5-Diketo-D-gluconate Hyperproducing *Gluconobacter sphaericus* SJF2-1 with reporting multiple genes encoding the membrane-associated Flavoprotein-cytochrome c complexed dehydrogenases. *Microorganisms* 10:13. doi: 10.3390/microorganisms10112130

Szajko, K., Smyda-Dajmund, P., Ciekot, J., Marczewski, W., and Soltys-Kalina, D. (2023). Glycoalkaloid composition and flavonoid content as driving forces of Phytotoxicity in diploid potato. *Int. J. Mol. Sci.* 24:14. doi: 10.3390/ijms24021657

Tan, Y., Cui, Y., Li, H., Kuang, A., Li, X., Wei, Y., et al. (2017). Rhizospheric soil and root endogenous fungal diversity and composition in response to continuous *Panax notoginseng* cropping practices. *Microbiol. Res.* 194, 10–19. doi: 10.1016/j.micres.2016.09.009

Todeschini, V., Ait Lahmidi, N., Mazzucco, E., Marsano, F., Gosetti, F., Robotti, E., et al. (2018). Impact of beneficial microorganisms on strawberry growth, fruit production, nutritional quality, and Volatilome. *Front. Plant Sci.* 9:22. doi: 10.3389/fpls.2018.01611

Topalovic, O., Hussain, M., and Heuer, H. (2020). Plants and associated soil microbiota cooperatively suppress plant-parasitic nematodes. *Front. Microbiol.* 11:15. doi: 10.3389/fmicb.2020.00313

Virginia, T. C., Nestor, A. J., Dario, C. A., and Noemi, P. G. (2021). Cladosporium species causing "Cladosporium rot" on "bosc" pear fruit in Argentina. *Rev. Argent. Microbiol.* 53, 75–77. doi: 10.1016/j.ram.2019.11.006

Wang, Y., Wang, L. W., Suo, M., Qiu, Z. J., Wu, H., Zhao, M., et al. (2022). Regulating root fungal community using Mortierella alpina for *Fusarium oxysporum* resistance in *Panax ginseng*. *Front. Microbiol.* 13:17. doi: 10.3389/fmicb.2022.850917

Wang, B. Y., Xia, Q., Li, Y. L., Zhao, J., Yang, S. Z., Wei, F. G., et al. (2021). Root rot-infected Sanqi ginseng rhizosphere harbors dynamically pathogenic microbiotas driven by the shift of phenolic acids. *Plant Soil* 465, 385–402. doi: 10.1007/s11104-021-05034-4

Wang, M. X., Xue, J., Ma, J. J., Feng, X. H., Ying, H. J., and Xu, H. (2020). *Streptomyces lydicus* M01 regulates soil microbial community and alleviates foliar disease caused by *Alternaria alternata* on cucumbers. *Front. Microbiol.* 11:13. doi: 10.3389/fmicb.2020.00942

Wang, T., Yang, K. X., Ma, Q. Y., Jiang, X., Zhou, Y. Q., Kong, D. L., et al. (2022). Rhizosphere microbial community diversity and function analysis of cut Chrysanthemum during continuous Monocropping. *Front. Microbiol.* 13:16. doi: 10.3389/fmicb.2022.801546

Wang, B., Zhou, T., Li, K., Guo, X. W., Guo, Y. S., Liu, Z. D., et al. (2019). Bacterial communities that metabolize 4-Hydroxybenzoic acid in grape (*Vitis vinifera* L.) rhizosphere soil. *Allelopath. J.* 46, 41–54. doi: 10.26651/allelo.j/2019-46-1-1197

Weller, P. E., Markey, C. M., and Marnett, L. J. (1985). Enzymatic reduction of 5-phenyl-4-pentenyl-hydroperoxide: detection of peroxidases and identification of peroxidase reducing substrates. *Arch. Biochem. Biophys.* 243, 633–643. doi: 10.1016/0003-9861(85)90541-7

Wu, L. K., Chen, J., Xiao, Z. G., Zhu, X. C., Wang, J. Y., Wu, H. M., et al. (2018). Barcoded pyrosequencing reveals a shift in the bacterial community in the rhizosphere and rhizoplane of *Rehmannia glutinosa* under consecutive monoculture. *Int. J. Mol. Sci.* 19:17. doi: 10.3390/ijms19030850

Wu, C. C., Ma, Y. J., Wang, D., Shan, Y. P., Song, X. P., Hu, H. Y., et al. (2022). Integrated microbiology and metabolomics analysis reveal plastic mulch film residue affects soil microorganisms and their metabolic functions. *J. Hazard. Mater.* 423:127258. doi: 10.1016/j.jhazmat.2021.127258

Wu, H.-S., Raza, W., Liu, D.-Y., Wu, C.-L., Mao, Z.-S., Xu, Y.-C., et al. (2008). Allelopathic impact of artificially applied coumarin on *Fusarium oxysporum* f. sp. *niveum*. *World J. Microbiol. Biotechnol.* 24, 1297–1304. doi: 10.1007/s11274-007-9602-5

Wu, L. K., Wang, J. Y., Huang, W. M., Wu, H. M., Chen, J., Yang, Y. Q., et al. (2015). Plant-microbe rhizosphere interactions mediated by *Rehmannia glutinosa* root exudates under consecutive monoculture. *Sci. Rep.* 5:11. doi: 10.1038/srep15871

Wu, L. K., Weston, L. A., Zhu, S. S., and Zhou, X. A. (2023). Rhizosphere interactions: root exudates and the rhizosphere microbiome. *Front. Plant Sci.* 14:4. doi: 10.3389/fpls.2023.1281010

Wu, Z. J., Xie, Z. K., Yang, L., Wang, R. Y., Guo, Z. H., Zhang, Y. B., et al. (2015). Identification of autotoxins from root exudates of Lanzhou lily (*Lilium davidii* var. *unicolor*). *Allelopath. J.* 35, 35–48.

Wu, H. M., Xu, J. J., Wang, J. Y., Qin, X. J., Wu, L. K., Li, Z. C., et al. (2017). Insights into the mechanism of proliferation on the special microbes mediated by phenolic acids in the Radix pseudostellariae rhizosphere under continuous monoculture regimes. *Front. Plant Sci.* 8:15. doi: 10.3389/fpls.2017.00659

Xia, Z. C., Kong, C. H., Chen, L. C., and Wang, S. L. (2015). Allelochemical-mediated soil microbial community in long-term monospecific Chinese fir forest plantations. *Appl. Soil Ecol.* 96, 52–59. doi: 10.1016/j.apsoil.2015.07.012

Xiang, W., Chen, J. H., Zhang, F. Y., Huang, R. S., and Li, L. B. (2022). Autotoxicity in *Panax notoginseng* of root exudatesand their allelochemicals. *Front. Plant Sci.* 13:10. doi: 10.3389/fpls.2022.1020626

Xin, G., Glawe, D., and Doty, S. L. (2009). Characterization of three endophytic, indole-3-acetic acid-producing yeasts occurring in Populus trees. *Mycol. Res.* 113, 973–980. doi: 10.1016/j.mycres.2009.06.001

Xin, A. Y., Jin, H., Yang, X. Y., Guan, J. F., Hui, H. P., Liu, H. Y., et al. (2022). Allelochemicals from the rhizosphere soil of potato (*Solanum tuberosum* L.) and their interactions with the Soilborne pathogens. *Plants Basel* 11:17. doi: 10.3390/plants11151934

Xin, A. Y., Li, X. Z., Jin, H., Yang, X. Y., Zhao, R. M., Liu, J. K., et al. (2019). The accumulation of reactive oxygen species in root tips caused by autotoxic allelochemicals – a significant factor for replant problem of *Angelica sinensis* (Oliv.) diels. *Ind. Crop. Prod.* 138:111432. doi: 10.1016/j.indcrop.2019.05.081

Xu, J., Xu, X. D., Cao, Y. Y., and Zhang, W. M. (2014). First report of greenhouse tomato wilt caused by *Plectosphaerella cucumerina* in China. *Plant Dis.* 98, 158–159. doi: 10.1094/pdis-05-13-0566-pdn

Yan, Z. Q., Wang, D. D., Cui, H. Y., Zhang, D. H., Sun, Y. H., Jin, H., et al. (2016). Phytotoxicity mechanisms of two coumarin allelochemicals from *Stellera chamaejasme* in lettuce seedlings. *Acta Physiol. Plant.* 38:10. doi: 10.1007/s11738-016-2270-z

Yang, Y., Dou, Y. X., Huang, Y. M., and An, S. S. (2017). Links between soil fungal diversity and plant and soil properties on the loess plateau. *Front. Microbiol.* 8:13. doi: 10.3389/fmicb.2017.02198

Yang, M., Zhang, X. D., Xu, Y. G., Mei, X. Y., Jiang, B. B., Liao, J. J., et al. (2015). Autotoxic ginsenosides in the rhizosphere contribute to the replant failure of *Panax notoginseng*. *PLoS One* 10:e0118555. doi: 10.1371/journal.pone.0118555

Zhalnina, K., Louie, K. B., Hao, Z., Mansoori, N., da Rocha, U. N., Shi, S. J., et al. (2018). Dynamic root exudate chemistry and microbial substrate preferences drive patterns in rhizosphere microbial community assembly. *Nat. Microbiol.* 3, 470–480. doi: 10.1038/s41564-018-0129-3

Zhang, J. W., Liang, L., Xie, Y. D., Zhao, Z., Su, L. H., Tang, Y., et al. (2022). Corrigendum: transcriptome and metabolome analyses reveal molecular responses of two pepper (*Capsicum annuum* L.) cultivars to cold stress. *Front. Plant Sci.* 13:975330. doi: 10.3389/fpls.2022.975330

Zhang, J. H., Yu, H. J., Ge, X., Pan, D. D., Shen, Y. H., Qiao, P. L., et al. (2018). Effects of vanillin on cucumber (*Cucumis sativus* L.) seedling rhizosphere fungal community composition. *Allelopath. J.* 44, 169–180. doi: 10.26651/allelo.j/2018-44-2-1162

Zhao, Y., Dong, W., Zhang, N. B., Ai, X. H., Wang, M. C., Huang, Z. G., et al. (2014). A wheat Allene oxide cyclase gene enhances salinity tolerance via Jasmonate signaling. *Plant Physiol.* 164, 1068–1076. doi: 10.1104/pp.113.227595

Zhao, J., Zhang, D., Yang, Y. Q., Pan, Y., Zhao, D. M., Zhu, J. H., et al. (2020). Dissecting the effect of continuous cropping of potato on soil bacterial communities as revealed by high-throughput sequencing. *PLoS One* 15:e0233356. doi: 10.1371/journal.pone.0233356

Zheng, W., Zhao, Z. Y., Gong, Q. L., Zhai, B. N., and Li, Z. Y. (2018). Responses of fungal-bacterial community and network to organic inputs vary among different spatial habitats in soil. *Soil Biol. Biochem.* 125, 54–63. doi: 10.1016/j.soilbio.2018.06.029

Zhou, X. G., and Wu, F. Z. (2012). P-Coumaric acid influenced cucumber rhizosphere soil microbial communities and the growth of *Fusarium oxysporum* f. sp *cucumerinum* Owen. *PLoS One* 7:11. doi: 10.1371/journal.pone.0048288

Zhu, Y. T., Hu, X. Q., Wang, P., Gao, L. Y., Pei, Y. K., Ge, Z. Y., et al. (2021). GhPLP2 positively regulates cotton resistance to Verticillium wilt by modulating fatty acid accumulation and Jasmonic acid signaling pathway. Frontiers. *Plant Sci.* 12:18. doi: 10.3389/fpls.2021.749630

frontiers | Frontiers in Microbiology

TYPE Original Research
PUBLISHED 15 January 2024
DOI 10.3389/fmicb.2023.1326057

OPEN ACCESS

EDITED BY
Jeanette M. Norton,
Utah State University, United States

REVIEWED BY
Madjid Morsli,
Centre Hospitalier Universitaire de Nîmes, France
Wenting Feng,
Chinese Academy of Agricultural Sciences, China

*CORRESPONDENCE
Qi Deng
✉ dengqi@scbg.ac.cn

RECEIVED 22 October 2023
ACCEPTED 31 December 2023
PUBLISHED 15 January 2024

CITATION
Hu M, Zhou S, Xiong X, Wang X, Sun Y, Meng Z, Hui D, Li J, Zhang D and Deng Q (2024) Dynamics of soil microbial communities involved in carbon cycling along three successional forests in southern China.
Front. Microbiol. 14:1326057.
doi: 10.3389/fmicb.2023.1326057

Dynamics of soil microbial communities involved in carbon cycling along three successional forests in southern China

Minghui Hu[1,2,3], Shuyidan Zhou[1,2], Xin Xiong[1,2,4], Xuan Wang[1,2], Yu Sun[5], Ze Meng[1], Dafeng Hui[6], Jianling Li[1,2], Deqiang Zhang[1,2] and Qi Deng[1,2]*

[1]Key Laboratory of Vegetation Restoration and Management of Degraded Ecosystems, Guangdong Provincial Key Laboratory of Applied Botany, South China Botanical Garden, Chinese Academy of Sciences, Guangzhou, Guangdong, China, [2]South China National Botanical Garden, Guangzhou, Guangdong, China, [3]University of Chinese Academy of Sciences, Beijing, China, [4]College of Life Sciences, South China Agricultural University, Guangzhou, Guangdong, China, [5]Lushan Botanical Garden, Chinese Academy of Sciences, Jiujiang, China, [6]Department of Biological Sciences, Tennessee State University, Nashville, TN, United States

Dynamics of plant communities during forest succession have been received great attention in the past decades, yet information about soil microbial communities that are involved in carbon cycling remains limited. Here we investigated soil microbial community composition and carbohydrate degradation potential using metagenomic analysis and examined their influencing factors in three successional subtropical forests in southern China. Results showed that the abundances of soil bacteria and fungi increased ($p \leq 0.05$ for both) with forest succession in relation to both soil and litter characteristics, whereas the bacterial diversity did not change ($p > 0.05$) and the fungal diversity of Shannon-Wiener index even decreased ($p \leq 0.05$). The abundances of microbial carbohydrate degradation functional genes of cellulase, hemicellulase, and pectinase also increased with forest succession ($p \leq 0.05$ for all). However, the chitinase gene abundance did not change with forest succession ($p > 0.05$) and the amylase gene abundance decreased firstly in middle-succession forest and then increased in late-succession forest. Further analysis indicated that changes of functional gene abundance in cellulase, hemicellulase, and pectinase were primarily affected by soil organic carbon, soil total nitrogen, and soil moisture, whereas the variation of amylase gene abundance was well explained by soil phosphorus and litterfall. Overall, we created a metagenome profile of soil microbes in subtropical forest succession and fostered our understanding of microbially-mediated soil carbon cycling.

KEYWORDS

carbohydrate degradation, forest succession, metagenomics, microbial community, microbial diversity

1 Introduction

Forests play an important role in the global carbon cycle, and forest soil carbon pool accounts for 73% of global soil carbon storage (more than 1,500 Pg) (Post et al., 1982; Jobbagy and Jackson, 2000). Forests at different succession stages may have different accumulation rates of soil organic carbon (Zhou et al., 2006b). Microorganisms are the direct factors driving soil

organic carbon turnover and are essential to soil functions (Liang et al., 2017; Zhong et al., 2018). It has been estimated that microbial mineralization process of organic matter releases about 58 Pg carbon to atmosphere per year (Houghton, 2007). Moreover, microbial activities significantly contribute to litter decomposition, soil nutrient transformation and plant nutrient supply (Carney and Matson, 2006; van der Heijden et al., 2008; Zhu et al., 2012). Therefore, a comprehensive understanding of microbial community structure and function involved in soil carbon cycling during forest succession is crucial for better predicting of soil carbon sequestration in forest ecosystems.

During forest succession, plant types have a great impact on soil microbial community structure and diversity (Cline and Zak, 2015). The quality and quantity of organic matter input into the soil by different plant types vary with forest succession and affect the composition and diversity of the soil microbial community (Zak et al., 2003). According to ecosystem succession theory of Odum (1969), r-strategy species with faster growth rate and higher turnover rate predominate in early successional stage, while K-strategy species with a slower growth rate, lower turnover rate, and higher competitive capacity predominate in late successional stage (Yan et al., 2020). Soil microorganisms such as bacteria and fungi play major roles in soil carbon metabolism, particularly the decomposition process of soil organic carbon, such as desorption, depolymerization, and dissolution with secretory enzymes (Conant et al., 2011). Broadly speaking, fungi are considered to be K- strategist, while bacteria are considered to be r-strategist (Bardgett et al., 2005; Kaiser et al., 2014; Cheng et al., 2016). A meta-analysis of global 85 age sequences found that the fungi: bacteria ratio increased with succession (Zhou et al., 2017), suggesting that bacteria shift from r-strategist to K-strategist with the process of succession, and fungi show the opposite trend. Meanwhile, in bacterial community, phylum of *Proteobacteria* and *Bacteroidetes* are regarded as r-strategist, whereas phylum of *Acidobacteria* and *Actinobacteria* are regarded as K-strategists (Fierer et al., 2007; Zechmeister-Boltenstern et al., 2015). It has been reported that the *Acidobacteri*a and *Actinobacteria* dominated in the late successional stage (Zechmeister-Boltenstern et al., 2015), and the ratio of *Acidobacteria* + *Actinobacteria* to *Proteobacteria* + *Bacteroidetes* increased significantly with succession. However, Zhou et al. (2018) did not find a positive trend in the *Acidobacteria* + *Actinobacteria* to *Proteobacteria* + *Bacteroidetes* ratio as succession proceeds. Moreover, some studies reported that fungal community shifted from r-strategy (*Ascomycota*) to K-strategy (*Basidiomycota*) (Yan et al., 2020; Zhu et al., 2022). Moreover, some studies reported that the strategy of fungi did not show significantly change with forest succession (Ren et al., 2019; Zhong et al., 2019). Ecosystems heterogeneity may lead to differences in microbial successional patterns, and the successional pattern of microbial strategies in the subtropical high nitrogen deposition region of south China remains to be further explored.

The accumulation of soil organic carbon in successional forests is mainly the results of the action of carbon input and output, which is jointly regulated by vegetation and soil microorganisms. Soil carbon input mainly originate from litter and root exudates (Kramer et al., 2010; Clemmensen et al., 2013), while soil carbon output is mainly controlled by soil microbial community in relation to environmental factors. The changes in dominant aboveground vegetation leads to changes in soil nutrient cycling and carbon storage through their complex influence on the soil microbial community (Kelly et al., 2021). Previous studies were mainly concentrated on the variation of soil microbial community structure in successional forests (Sokolowska et al., 2020; Jiang et al., 2021; Shang et al., 2021; Wang et al., 2022), whereas the succession pattern of soil carbohydrate metabolism by microorganisms at the genetic level have received little attention. In general, soil organic carbon degradation is a microbial process driven by functional genes participating in carbohydrate metabolism. Difference in the expression of specific carbon degradation genes in different ecosystems determine nutrient availability, organic carbon turnover, and ultimate carbon retention in soil (Trivedi et al., 2016; Kelly et al., 2021). Exploring the variation of microbial functional genes in successional forests can provide a more intuitive understanding of microbially-mediated soil organic carbon turnover.

In this study, the composition and diversity of soil microbial communities as well as their potential functional changes were studied using a high-throughput sequencing technology in three representative forest types of the successional sequences in the south subtropical region of China. We aimed to determine: (1) whether the composition and diversity of soil microbial communities varied along the forest succession; (2) and what were the patterns of soil microbial functional potential of carbohydrate degradation shifts; (3) and what factors influence the microbial functional potential of carbohydrate degradation.

2 Materials and methods

2.1 Study sites

The study was conducted at Dinghushan Biosphere Reserve in Guangdong Province, China (23°09′21″-23°11′30″ N, 112°30′39″-112°33′41″ E). The area of this region covers approximately 1,133 ha of forests. The annual average temperature is 20.9°C, with the highest and lowest temperatures of 38°C and −0.2°C, respectively. The annual rainfall in this area is 1,950 mm, and the main rainfall season is from April to September, accounting for approximately 70% of the annual rainfall. The mean annual relative humidity is 80.3%. The forest coverage rate of Dinghushan Biosphere Reserve reaches 98.7%. The three types of successional forests studied in this experiment are as follows: (1) *Pinus massoniana* forest (approximately 70 years old, PMF). The dominant species is *P. massoniana*, and the canopy density is approximately 50%; (2) Pine and broadleaf mixed forest (approximately 100 years old, PBMF). The dominant species are *P. massoniana*, *Schima superba*, and *Castanopsis chinensi*, and the canopy density is approximately 90%; and (3) Monsoon evergreen broadleaf forest (approximately 400 years old, MEBF). The dominant species are *C. chinensis*, *Cryptocarya concinna*, *S. superba*, and *Machilus chinensis*, and the canopy density is approximately 95%. These three types of forests represent the early, middle, and late succession of the Dinghushan forest ecosystem, respectively.

2.2 Soil and litter sampling

The experiment and soil sampling were initiated in August 2019. Before sampling, we removed humus, litter, and other impurities from the topsoil. Five scattered soil samples were collected from 0–10 cm

soil layer and mixed into one sample each time using a soil auger (5 cm inner diameter). Five replications were collected in each forest, obtaining 15 soil samples in total. All soil samples were screened with a 2-mm sieve to remove roots and gravel. Each soil sample was divided into two parts; one part was stored in the freezer at −80°C for subsequent soil metagenomic determination, and the other was air-dried for measuring soil physicochemical properties. The litterfall of three successional forests was collected in 1 m × 1 m collection frame, and we recorded the total dry weight in each frame.

2.3 Soil and litter properties measurements

The content of soil organic carbon (SOC) and total nitrogen (TN) were determined using a high sample throughput automatic elemental analyzer (Vario max cube, Elementar, Germany). The content of total phosphorus (TP) was determined using sulfuric-perchloric acid digestion and molybdenum-antimony colorimetry. The pH of soil samples was determined using potentiometric method, and the ratio of water to soil was 1:2.5. Soil readily oxidized organic carbon (ROC) was defined as the organic carbon that can be oxidized by a potassium permanganate ($KMnO_4$) solution with a concentration of 333 mMol/L, and was determined using Blair et al.'s (1995) method. Soil dissolved organic carbon (DOC) was determined using Marten's (1995) method. Soil temperature and moisture was determined by Time domain reflectometry (TDR, Campbell, USA). Litterfall (plant dead organic material such as leaves, branches, fruit (flower) drops, bark, and mosses and lichens) data comes from Dinghushan Forest Ecosystem Research Station, in which litter carbon content was determined by Total Carbon Analysis (TOC-VCPH SHIMADZU, Japan) and litter nitrogen content was analyzed by Kjeldahl method.

2.4 DNA extraction, library construction, and metagenomic sequencing

Total genomic DNA was extracted from 0.5 g of soil samples using the FastDNA® Spin Kit for Soil (MP Biomedicals, Norcross, GA, USA) according to the manufacturer's instructions. The concentration and purity of extracted DNA were determined by TBS-380 (Turner BioSystems Inc., USA) and NanoDrop2000 (Thermo Fisher Scientific, USA), respectively. DNA extract quality was detected on 1% agarose gel.

The average size of extracted DNA samples were sonicated [Covaris M220 (Gene Company Limited, China)] resulting in an average size of 400 bp and these were used to construct the paired-end library. The paired-end library was constructed using NEXTFLEX Rapid DNA-Seq (Bioo Scientific, Austin, TX, USA). Adapters containing the full complement of sequencing primer hybridisation sites were connected to the blunt-end fragments. A dual indexed barcoding information for sample identification and differentiation was incorporated into the library preparation process. Paired-end sequencing was performed on Illumina NovaSeq (Illumina Inc., San Diego, CA, USA) at Majorbio Bio-Pharm Technology (Shanghai, China) using NovaSeq Reagent Kits according to the manufacturer's instructions. The sequencing produced paired-end reads of 150 bp. All sequences associated with this project have been submitted in the NCBI Short Read Archive database (Accession Number: PRJNA782859).

2.5 Genome assembly, construction of non-redundant gene catalog, and functional annotation

The adapter sequences of paired-end Illumina reads were trimmed using fastp (Chen et al., 2020).[1] For ensuring the quality of our metagenomic data, we processed the raw reads using a 5-bp sliding window, trimming sequences with a quality score lower than Q20. This threshold, indicative of a read accuracy of at least 99%, was employed to eliminate low-quality sequences and retain high-quality pair-end and single-end reads for subsequent analyses. The reads with a length of less than 50 bp after trimming process were removed from further analysis. Metagenomics data were assembled using MEGAHIT (Li et al., 2015)[2] based on the principle of the succinct de Bruijn graphs (Supplementary Table S2). Since contigs shorter than 300 bp are often considered less reliable for providing accurate genomic insights due to the limited sequence context they offer (Sameith et al., 2017), only contigs with a length of or over 300 bp were selected as the final assembling result and used for further gene prediction and annotation. Open reading frames (ORFs) prediction of each assembled contig was performed using MetaGene (Noguchi et al., 2006).[3] The predicted ORFs with a length of or over 100 bp were selected and translated into amino acid sequences using the National Center for Biotechnology Information (NCBI) translation table.

CD-HIT (Fu et al., 2012)[4] was used to construct a non-redundant gene catalog (parameters: 90% sequence identity and 90% coverage). High-quality reads were mapped to the non-redundant gene catalog with 95% identity using SOAPaligner (Li et al., 2008),[5] and gene abundance in each sample was evaluated. The representative sequences of non-redundant gene catalog were aligned with the NCBI NR database for taxonomic annotations using Diamond (Buchfink et al., 2015),[6] and the cut-off e-value was $1e^{-5}$. The KEGG annotation was performed using the Kyoto Encyclopedia of Genes and Genomes database[7] using Diamond (Buchfink et al., 2015) (see Footnote 6) with an e-value cut-off of $1e^{-5}$.

2.6 Statistical analyses

The species information about bacteria and fungi were selected from the NR database, while the functional genes were selected from the KEGG database (Supplementary Tables S4–S6). Reads per kilobase per million mapped reads (RPKM) values were employed to calculate alpha diversity and all gene abundance values and compared between different samples; the gene abundance values in replicated samples were averaged.

1 https://github.com/OpenGene/fastp, version 0.20.0.
2 https://github.com/voutcn/megahit, version 1.1.2.
3 http://metagene.cb.k.u-tokyo.ac.jp/
4 http://www.bioinformatics.org/cd-hit/, version 4.6.1.
5 http://soap.genomics.org.cn/, version 2.21.
6 http://www.diamondsearch.org/index.php, version 0.8.35.
7 http://www.genome.jp/keeg/, version 94.2.

10.3389/fmicb.2023.1326057

TABLE 1 Soil physicochemical properties in successional forests.

Property	PMF	PBMF	MEBF
SOC (g/kg)	22.41 ± 3.08 (a)	28.06 ± 1.53 (b)	35.04 ± 2.85 (c)
DOC (g/kg)	0.55 ± 0.1 (a)	0.64 ± 0.11 (ab)	0.74 ± 0.14 (b)
ROC (g/kg)	11.85 ± 0.42	11.65 ± 0.64	12.32 ± 0.29
ROC/SOC	0.54 ± 0.07 (c)	0.42 ± 0.01 (b)	0.35 ± 0.02 (a)
TN (g/kg)	1.47 ± 0.14 (a)	2.04 ± 0.12 (b)	2.71 ± 0.17 (c)
TP (g/kg)	0.22 ± 0.02 (a)	0.41 ± 0.04 (c)	0.31 ± 0.04 (b)
pH	3.91 ± 0.09 (a)	4.06 ± 0.09 (b)	3.97 ± 0.07 (ab)
SM (% Vol.)	0.21 ± 0.02 (a)	0.31 ± 0.02 (b)	0.46 ± 0.05 (c)
ST (°C)	25.98 ± 0.36	26.12 ± 0.31	25.96 ± 0.34
Litterfall (g/m^2/yr)	1083.24 ± 36.11 (c)	661.05 ± 47.44 (a)	788.19 ± 46.14 (b)
Litter C/N	40.2 ± 7 (b)	28.68 ± 3.12 (a)	24.37 ± 2.42 (a)

PMF, *Pinus massoniana* forest; PBMF, pine and broadleaf mixed forest; MEBF, monsoon evergreen broadleaf forest; SOC, total soil organic carbon; DOC, dissolved organic carbon; ROC, readily oxidized organic carbon; TN, total nitrogen; TP, total phosphorus; SM, soil moisture; ST, soil temperature; Litter C/N, the ratio of litter C to litter N. Mean values ± standard deviations are given ($n = 5$). Different lowercase letters (in brackets) indicate a significant difference ($p \leq 0.05$) among the forest types.

One-way analysis of variances and Duncan's multiple range test were conducted using IBM SPSS 21.0 (IBM Corporation, Armonk, NY, USA) to explore the differences in soil physicochemical properties and functional genes abundance. Chao1 index, Shannon–Wiener index, and Simpson index was used to evaluate microbial α-diversity in successional forests, and the significant differences were set at $p \leq 0.05$.

To visualize the differences of microbial community composition and functional genes' abundance, principal coordinate analysis (PCoA) based on Bray–Curtis distance was employed (R vegan package v2.5-6) in R v4.1.0. Analysis of similarities (ANOSIM) based on Bray–Curtis distance was performed to test the differences (microbial community composition and functional genes' abundance) between groups and the differences within groups (R vegan package v2.5-6). Mantel test results were used to explore correlations among environmental factors and microbial community and the microbial carbohydrate degradation genes based on the Spearman correlation coefficient in R v4.1.0. Correlation heatmap with signs was performed using R v4.1.0. Metabolic pathways are based on information from KEGG database,[8] we use the Spearman correlation coefficient to specific environmental factors in the process of metabolic pathways. Random Forest models were used to identified the most important environmental variables, and the importance of variables was evaluated by classifying multiple decision tree (Breiman, 2001). The analyses were conducted using the randomForest package (Liaw and Wiener, 2002) in R v4.1.0. The A3 package were used to evaluate the significance of the model and the cross-validation R^2, and the rfPermute package was used to assess the importance of each predictor to soil carbohydrate degradation functional genes.

Distance-based redundancy analysis (db-RDA) was used to evaluate the effects of soil physicochemical properties on microbial functional genes' abundance (R vegan package v2.5-6). We calculated the β-diversity of species and functional genes using linear regression analysis to assess the conformance between species and functional genes, respectively (R vegan package v2.5-6). Further, to quantify the functional contribution of specific phylums and species, the correlation analysis between species and function relative abundance was conducted based on the corresponding relationship between species and functions in the samples (R vegan package v2.5-6).

8 https://www.genome.jp/kegg/pathway.html, version 94.2.

3 Results

3.1 Soil physicochemical and litter characteristics

With forest succession, the soil physicochemical properties and litter characteristics showed different changing patterns (Table 1). The soil physicochemical properties varied significant among the three forest types (Table 1). SOC, DOC, NROC, TN, and SM showed an upward trend with forest succession ($p \leq 0.05$ for all). Compared with PMF, TP and soil pH significantly increased in PBMF but decreased in MEBF (Table 1). The litter characteristics changed significantly as well (Table 1). Litterfall decreased significantly in PBMF and increased in MEBF compared to PMF. The highest litter C/N were observed in the PMF.

3.2 Soil microbial community composition

Taxonomic annotation information of sample species was obtained and compared with the NR database. A total of eight kingdoms, 135 phyla, 292 classes, 683 orders, 1,295 families, 3,275 genera, and 17,379 species were detected in PMF, PBMF, and MEBF. Both soil bacterial and fungal abundances increased significantly along the gradient of forest succession (Figure 1A, $p \leq 0.05$ for both).

The Chao1 index, Shannon–Wiener index, and Simpson index of bacterial community showed no significant difference with succession (Figures 1B–D; $p > 0.05$ for all). The Chao1 index of fungal community also did not differ among the three forests (Figure 1B). The Shannon–Wiener index of fungal community decreased significantly with succession (Figure 1C; $p \leq 0.05$), while the Simpson index increased significantly (Figure 1D; $p \leq 0.05$). The photographs of each stage of successional forests are shown in Figure 2A. At the phylum level, soil bacterial communities were mainly composed of *Proteobacteria* (36.06–41.63%), *Actinobacteria* (28.38–41.51%), and *Acidobacteria* (28.38–41.51%) during all stages (Figure 2B; Supplementary Table S1). Venn diagrams showed that 11,938 species of bacteria and 402 species of fungi were shared in the three successional forests, respectively (Supplementary Figure S2). Soil fungal communities were mainly composed of *Ascomycota* (69.69–71.38%) and *Basidiomycota* (21.45–23.35%) (Figure 2C; Supplementary Table S1).

The ANOSIM analysis revealed that the differences between bacterial and fungal communities in successional forests were significantly greater than those within the groups (Supplementary Figures S1A,B). The PCoA results showed significant differences among bacterial and fungal communities (Figures 3A,B), which were related to soil physicochemical properties and litter characteristics (Supplementary Figures S3A,B; Table 2).

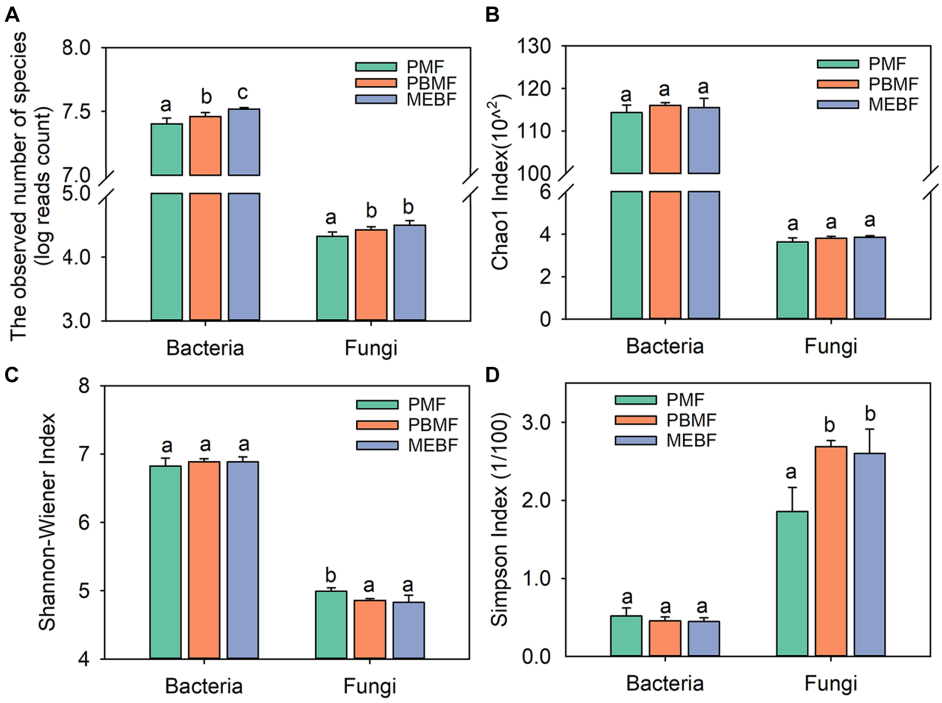

FIGURE 1
Relative abundances of soil bacterial and fungal based on reads counts **(A)**, derived from sequence alignment using SOAPaligner, Chao1 index **(B)**, Shannon–Wiener index **(C)**, and Simpson index **(D)** in successional forests. The values are the means of five replicates (± standard deviations), and different lowercase letters represent significant differences. PMF, *Pinus massoniana* forest; PBMF, pine and broadleaf mixed forest; MEBF, monsoon evergreen broadleaf forest.

3.3 Microbial genes involved in soil carbohydrate decomposition

Using the KEGG database to obtain the KEGG annotation profile corresponding to the genes present in the samples, we found a total of 9,885 KEGG orthologous genes from PMF, PBMF, and MEBF. Soil microbial functional genes related to degradation of soil carbohydrates were selected from the KEGG database (Supplementary Table S3). PCoA results illustrated that the functional potential in soil carbohydrate degradation was statistically significantly different among the three forests (Figure 3C). As shown in Figure 4, the gene abundance of amylase was highest in PMF and lowest in PBMF (Figure 4A). The gene abundance of pectinase did not change significantly in PBMF, but increased significantly in MEBF (Figure 4C). The gene abundance of hemicellulase and cellulase increased significantly in each stage of succession (Figures 4B,D). However, the gene abundance for chitinase showed no significantly difference with succession (Figure 4E).

Fifteen specific genes, coding for amylase, pectinase, hemicellulase, cellulase and chitinase, responded significantly to soil physicochemical and litter characteristics (Figure 5). There were significant correlations between the relative abundance of genes encoding amylase (amyA, malZ, and SGA1) and TP ($n = 3$ genes), pH ($n = 1$ gene), and litterfall ($n = 3$ genes) (Figure 5). The Random Forest model suggested that litterfall, TP, SM, TN, SOC and litter C/N were the most important predictors of amylase gene in successional forests (Overall model: $R^2 = 0.766$, $p = 0.001$; environment variable $p \leq 0.05$, Figure 6A). The relative abundance of genes encoding hemicellulase (xynD, xynB) were significantly correlated with SOC ($n = 2$ genes), ROC ($n = 1$ gene), TN ($n = 1$ gene), SM ($n = 1$ gene) and litterfall ($n = 1$ gene) (Figure 5). The Random Forest model suggested that SOC, SM and TN were the most important predictors of hemicellulase gene in successional forests (Overall model: $R^2 = 0.64$, $p = 0.001$; environment variable $p \leq 0.05$, Figure 6B). The relative abundance of genes encoding pectinase (Polygalacturonase, E3.2.1.67 and pectinesterase) were significantly correlated with SOC ($n = 3$ genes), TN ($n = 3$ genes) and SM ($n = 3$ genes) (Figure 5). The Random Forest model suggested that SOC, SM and TN were the most important predictors of pectinase gene in successional forests (Overall model: $R^2 = 0.729$, $p = 0.001$; environment variable $p \leq 0.05$, Figure 6C). The relative abundance of genes encoding cellulase (beta-glucosidase, CBH and endoglucanase) were significantly correlated with SOC ($n = 3$ genes), ROC ($n = 1$ gene), DOC ($n = 1$ gene), TN ($n = 3$ genes) and SM ($n = 3$ genes) (Figure 5). The Random Forest model suggested that SOC, SM, TN and litterfall were the most important predictors of cellulase gene in successional forests (Overall model: $R^2 = 0.899$, $p = 0.001$; environment variable $p \leq 0.05$, Figure 6D). The metabolic pathway of soil carbohydrate degradation and related environmental factors are shown in Figure 7.

3.4 Link between soil carbohydrate degradation and functional genes

To evaluate the consistency between microbial communities and functions, we performed a linear regression analysis using Bray-Curtis distance based on the β-diversity of microbial communities and

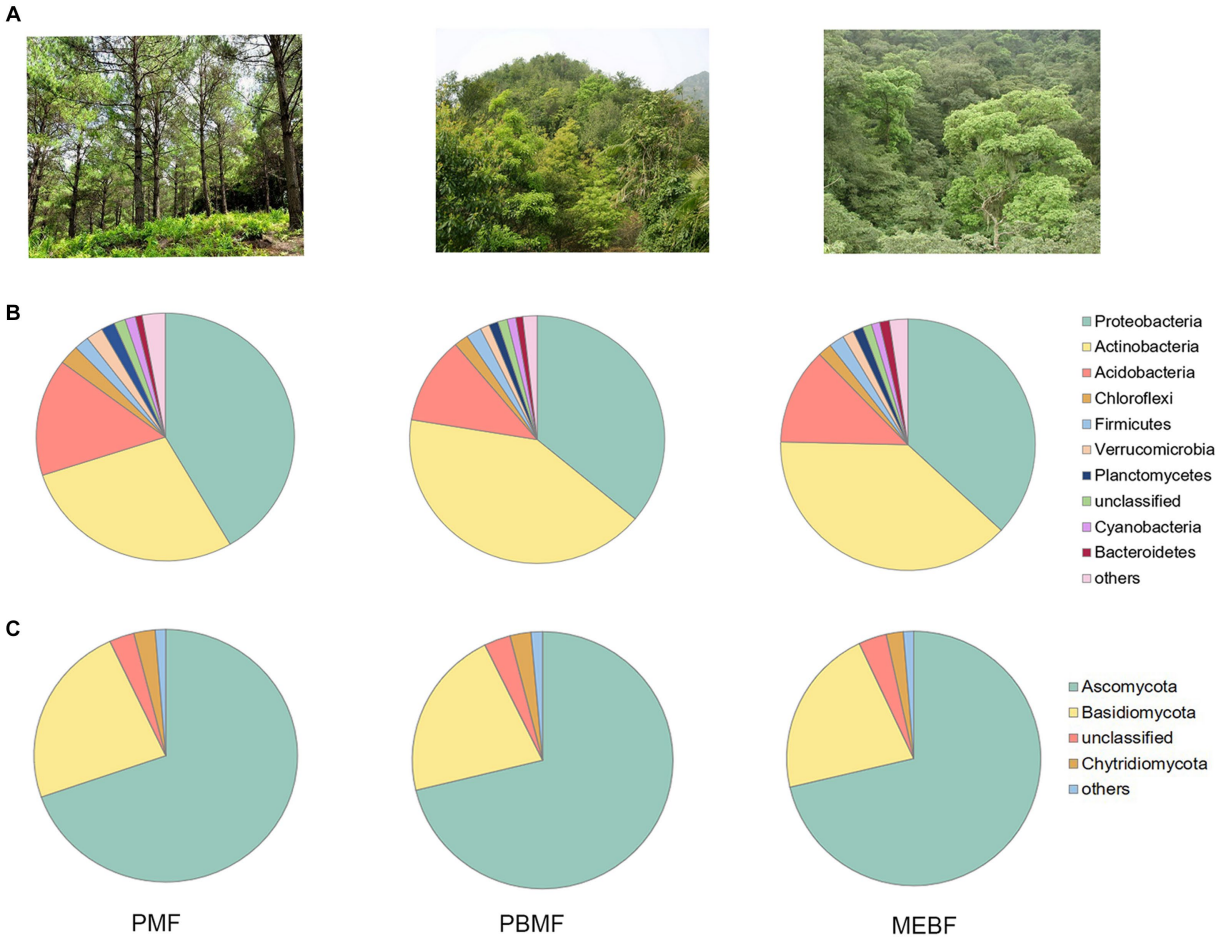

FIGURE 2
Photographs of each stage of successional forests **(A)**. Composition of major taxa of bacteria **(B)** and fungi **(C)** at the phylum level in successional forests. PMF, *Pinus massoniana* forest; PBMF, pine and broadleaf mixed forest; MEBF, monsoon evergreen broadleaf forest.

functions. We observed a significant and positive linear relationship, which indicates that the change of microbial community composition will change the functional composition ($R^2 = 0.67$, $p = 0.001$, Supplementary Figure S4A).

To visualize the association between species and functions in the samples, we mapped species (in phylum and species level) to functional genes to discover the contribution of species to specific functions. Functional genes encoding for carbohydrate degradation were clustered at level 2 on KEGG (Supplementary Figure S4A). *Actinobacteria*, *Proteobacteria* and *Acidobacteria* were the main contributor of carbohydrate degradation in microbial communities across successional forests (Supplementary Figure S4). As it shown in Supplementary Figure S5, at species level, *Thermomonospora curvata* was the main contributor of starch degradation, accounting for 2.71%~3.95%; *Silvibacterium bohemicum* was the main contributor of hemicellulose degradation, accounting for 9.5% ~11.42%; *Actinospica robiniae* was the main contributor of hemicellulose degradation, accounting for 4.64%~6.37%; *Terracidiphilus gabretensis* was the main contributor of hemicellulose degradation, accounting for 16.72%~21.6%; *Candidatus Koribacter versatilis* was the main contributor of hemicellulose degradation, accounting for 3.93%~9.38%. As for individual carbohydrate degradation genes, *Terracidiphilus gabretensis* was the main contributor of SGA1, beta-glucosidase, endoglucanase and polygalacturonase, accounting for 3.06%~7.46, 4.23%~5.31, 3.31%~4.19, and 21.58% ~26.58%. *Silvibacterium_bohemicum* was the main contributor of xynB and chitinase.

4 Discussion

4.1 Changes in microbial community structure

The typical forest types at three different succession stages in Dinghushan Biosphere Reserve provide a unique dynamic landscape for studying the succession pattern of microbial community structure and their influencing factors. The continuous increase in bacterial and fungal biomass with forest succession can be attributed in part to the increased availability of soil nutrients (Supplementary Figure S3; Table 2). Both soil physicochemical and litter characteristics were closely associated with soil bacterial and fungal community structure (Supplementary Figure S3; Table 2). During forest succession, due to changes in plant community types, especially in the composition of

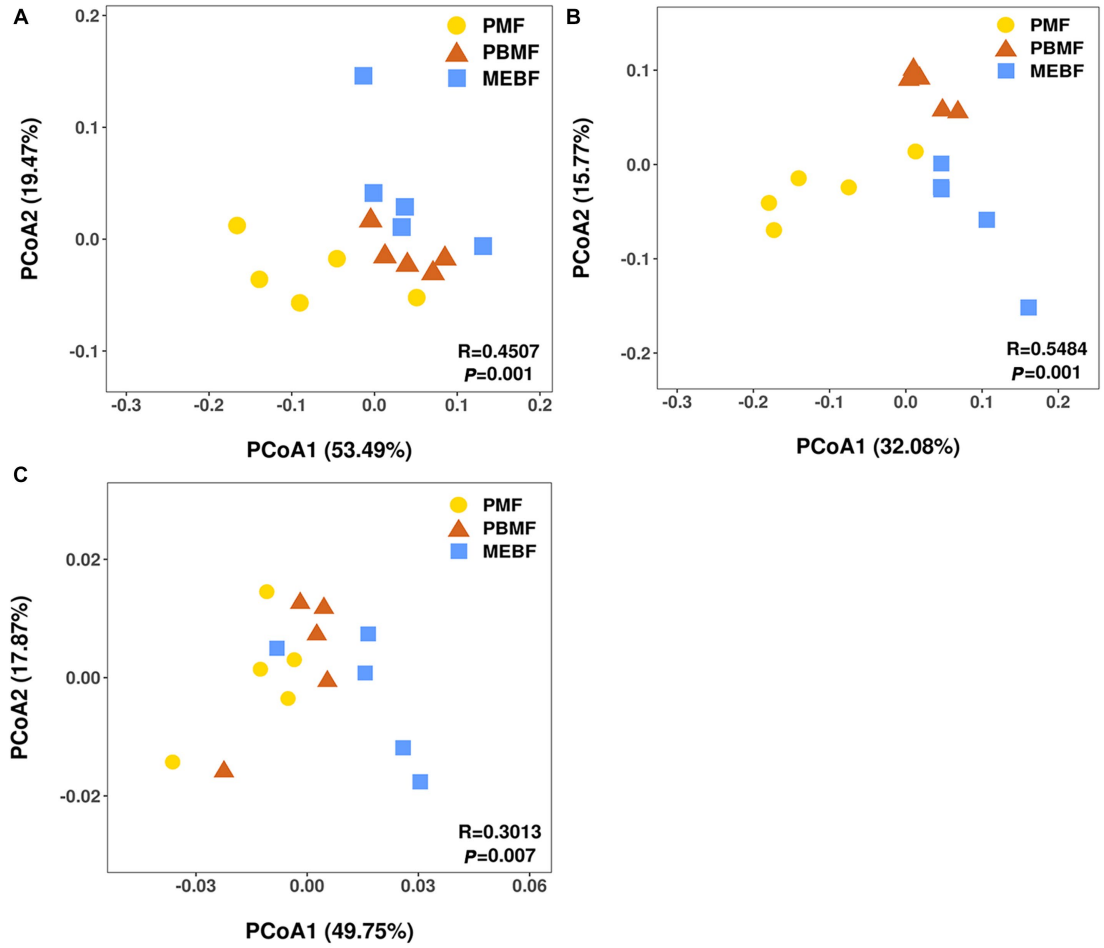

FIGURE 3
Principal coordinate analysis (PCoA) based on the Bray–Curtis distance of samples for bacterial **(A)** and fungal **(B)** communities, carbohydrate degradation gene composition **(C)** in successional forests. PMF, *Pinus massoniana* forest; PBMF, pine and broadleaf mixed forest; MEBF, monsoon evergreen broadleaf forest.

TABLE 2 Mantel test results based on the Bray–Curtis distance that were used to explore correlations among carbohydrate degradation genes, bacterial communities, fungal communities, soil physicochemical characteristics (SOC, DOC, ROC, TN, TP, pH, SM, and ST), and litter characteristics (litterfall and litter C/N).

	Soil characteristics	Litter characteristics	Bacterial communities	Fungal communities	Carbohydrate degradation genes
Soil characteristics	1				
Litter characteristics	0.3466**	1			
Bacterial communities	0.3104*	0.3002*	1		
Fungal communities	0.3836*	0.2977**	0.8471***	1	
Carbohydrate degradation genes	0.4465**	0.3357*	0.2878*	0.3605**	1

*Indicates $p \leq 0.05$; **indicates $p \leq 0.01$, ***indicates $p \leq 0.001$.

dominant tree species, litter characteristics and soil physicochemical changed correspondingly (Wedin and Tilman, 1996). Soil provides the substrate for microbial growth, and the quantity and quality of litter regulate the rate of microbial decomposition (Crow et al., 2009; Scheibe et al., 2015).

In our study, *Proteobacteria* and *Actinobacteria* accounted for a large proportion of the soil microbial community in successional forests (Figures 2B,C). Compared with the early stage of succession, the abundance of *Proteobacteria* (r-strategist) decreased significantly and abundance of *Actinobacteria* (K-strategist) increased significantly in the middle stage (Supplementary Table S1). In addition, the ratio of (*Actinobacteria* + *Acidobacteria*) to (*Proteobacteria* + *Bacteroidetes*) increased significantly in the middle stage of succession (Supplementary Table S1). This phenomenon indicated that the middle forest succession leads to the transformation of bacterial community from the dominant r strategists to the dominant

10.3389/fmicb.2023.1326057

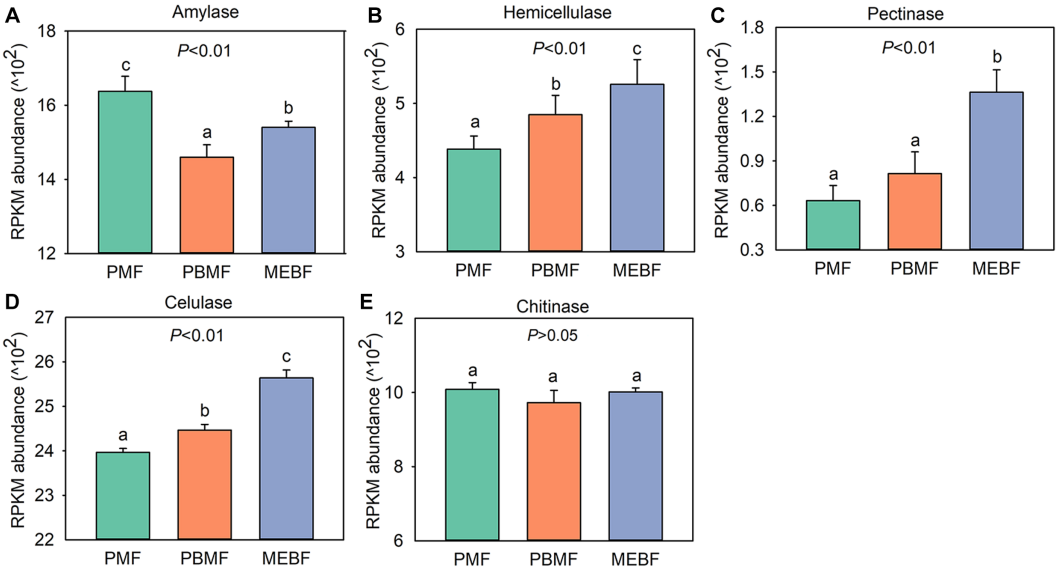

FIGURE 4
Abundance of functional genes in soil carbohydrate degradation in successional forests. **(A)** Amylase; **(B)** hemicellulose; **(C)** pectinase; **(D)** cellulase; **(E)** chitinase. RPKM values are calculated as the number of reads mapped to a gene per kilobase of its transcript length, scaled to a million mapped reads for each sample. The data are means ± standard deviations, and $n = 5$. Different lowercase letters represent significant differences among forest types. PMF, *Pinus massoniana* forest; PBMF, pine and broadleaf mixed forest; MEBF, monsoon evergreen broadleaf forest.

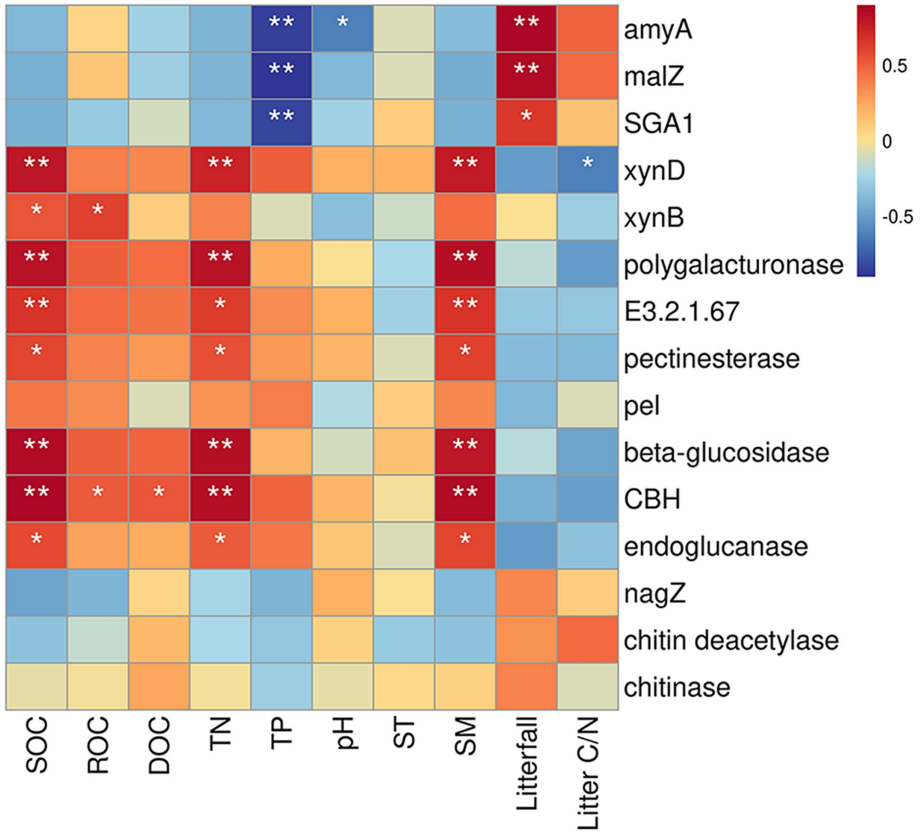

FIGURE 5
Correlation between environmental factors and soil carbohydrate degradation genes based on the Spearman correlation coefficient. The color gradients represented Spearman correlation coefficient: red indicates positive correlation, and blue indicates negative correlation. *Indicates $p \leq 0.05$; ** indicates $p \leq 0.01$.

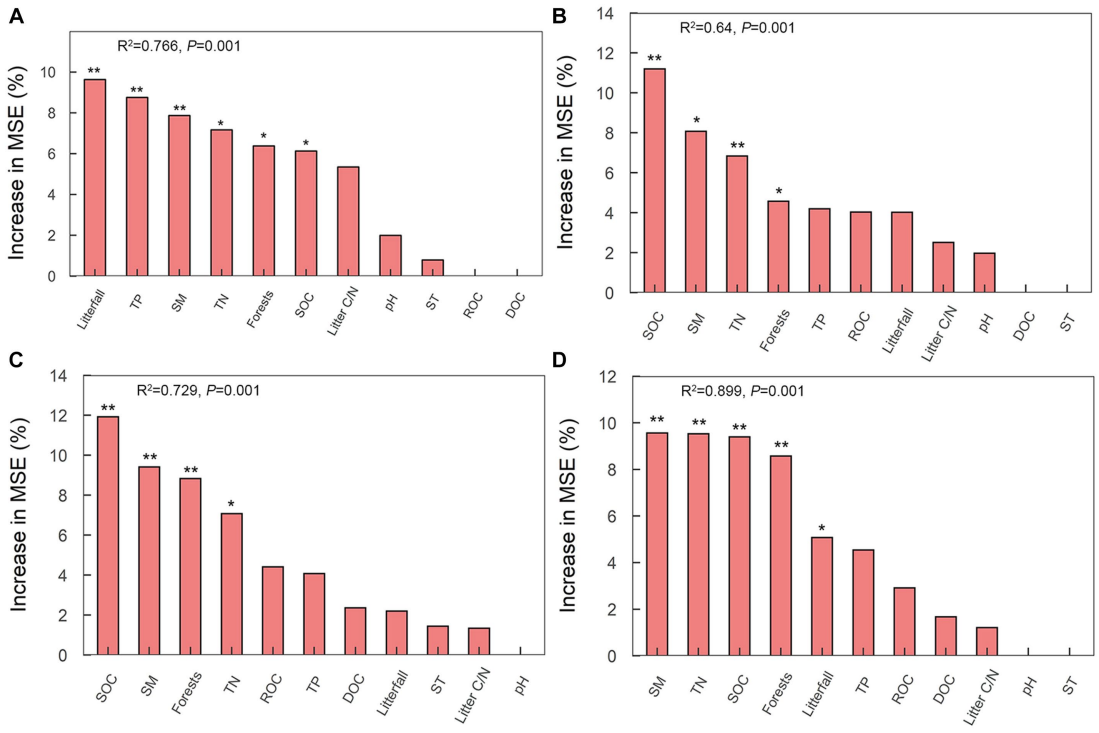

FIGURE 6
Random forest model of relationships between environmental factors and soil carbohydrate degradation genes in successional forests. The model shows the average predictive importance (mean square error (MSE) increase percentage) for each environmental factor for soil carbohydrate degradation genes. **(A)** Amylase; **(B)** hemicellulase; **(C)** pectinase; **(D)** cellulase. *Indicates $p \leq 0.05$; ** indicates $p \leq 0.01$.

K-strategists (Yan et al., 2020). However, the r-strategists of bacteria did not show a decline trend in the late succession, which was not consistent with the Odum's (1969) theory on ecosystem succession. We speculate that the high input of litterfall in the late forest succession provided more substrate for microbial decomposition, which may lead to a slight increase of r-strategists' bacteria.

We did not find increasing trend of the relative abundance of *Acidobacteria* in successional forests (Supplementary Table S1). This result suggested that other environmental factors may play a more important role in microbial ecological strategies (Dai et al., 2021). The dominance of *Acidobacteria* may be related to the acidic soil of Dinghushan (pH value reached 3–4.5) (Liu et al., 2001), which promoted the growth of *Acidobacteria* (Dai et al., 2018). Fierer and Jackson (2006) found that soil pH value had important effects on soil bacterial community across different forest types. The negative correlation between the relative abundance of *Acidobacteria* and soil pH explained the highest relative abundance in the early stage of forest succession that had the lowest soil pH (Supplementary Figure S6).

Interestingly, fungal α-diversity decreased significantly in PBMF and MEBF compared with PMF, while fungal abundance increased significantly (Figure 1A), suggesting that microbial abundance and species diversity did not always respond the same way along the forest succession. It has been reported that the composition and abundance of soil fungal communities were affected by differences in litter composition and quality (Aponte et al., 2013; Prescott and Grayston, 2013). The decrease of fungi diversity in late-successional forest was also reported in previous studies (Zhang et al., 2018; Zhong et al., 2018). One possible explanation for this pattern is that certain fungal taxa within the dominant phyla are more efficient in utilizing available resources and have a competitive advantage in the nutrient-rich conditions of middle and late successional forests (Ghoul and Mitri, 2016; Chu et al., 2021). These dominant fungal taxa may exhibit higher growth rates and biomass accumulation, leading to an overall increase in fungal biomass despite a decrease in α-diversity. Meanwhile, less competitive or specialized fungal species may experience reduced abundance and diversity due to niche exclusion or resource competition with the dominant taxa (Pontarp and Petchey, 2018). Despite the α-diversity changed in middle and late successional forests, the ecological functions performed by the fungal communities may remain relatively unchanged. The relative abundance of fungal phyla may not change significantly because functionally similar species replace each other over time. In this case, even though fungi α-diversity decreases, the ecosystem may still maintain key ecological processes due to functional redundancy among the fungal species.

4.2 Variation of carbohydrate degradation potential of microbial community with succession

In the KEGG database, carbohydrate degradation genes changed significantly in different succession stages (Figure 3C), which was related to different plant communities formed by long-term forest succession. The carbohydrate degradation genes were significantly related to soil characteristics, litter characteristics, and microbial communities (Table 2), which was consistent with the research result (Ding et al., 2015). The correlation may be due to the difference in plant community structure and soil development degree during forest

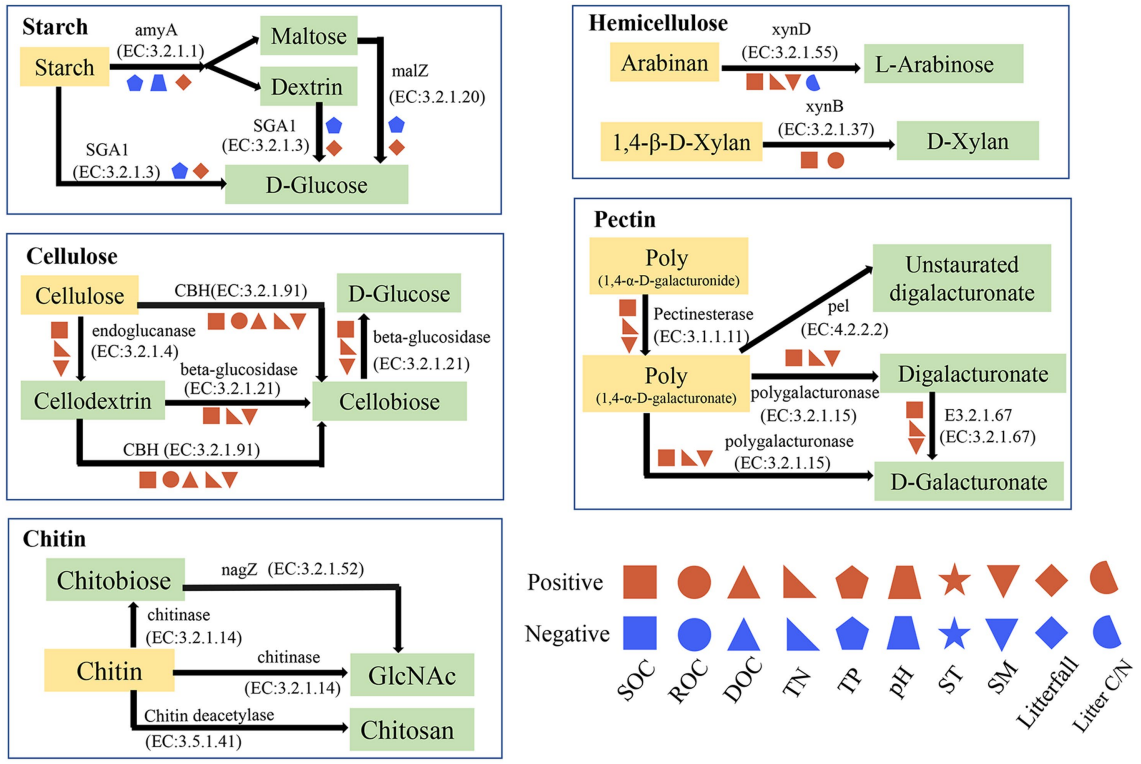

FIGURE 7
Metabolic pathway of soil carbohydrate degradation and related environmental factors. SOC, total soil organic carbon; DOC, dissolved organic carbon; ROC, readily oxidized organic carbon; TN, total nitrogen; TP, total phosphorus; SM, soil moisture; ST, soil temperature; Litter C/N, the ratio of litter C to litter N. The *p* values less than or equal to 0.05 are presented.

succession, which leads to the difference in microenvironment and soil nutrients (Lange et al., 2015), and then affects the microbial community structure and function (Wang et al., 2017).

This study revealed the environmental factors affecting the microbial community and functional diversity of soil organic carbon turnover. The significant changes in the carbohydrate degradation genes along the forest succession sequence indicated the existence of a succession distribution pattern of microbial functional diversity (Kelly et al., 2021). In general, the order of soil carbohydrate degradation is starch (the most mineralized), hemicellulose, pectin, cellulose, chitin, and lignin (Weil and Brady, 2016; Xie et al., 2022). Since we did not find lignin degradation genes in the KEGG database, we will not discuss.

In terrestrial ecosystems, litter decomposition is a key process of carbon exchange between plant carbon pool and soil carbon pool (Cusack et al., 2009). The gradual decomposition of litter returns carbon to soil and provides nutrients for plant and microbial growth (van der Heijden et al., 2008). In this study, we found that the amylase gene abundance was highest in PMF, and was positively correlated with litterfall and negatively correlated with TP (Figures 5, 6A). In general, the growth of microorganisms in the early stage of succession was mainly restricted by soil nutrient, but the large increase of litters could enhance the activity and growth of r-strategy microorganisms (Fontaine et al., 2003) and alleviate the low availability of soil nutrients. Dimassi et al. (2014) found that the priming effect of fresh organic matter was stronger in the soil with low nutrient content, but weaker in the soil with high nutrient content.

At the early stage of succession, the low soil phosphorus content led to tendency of r-strategy microorganisms to rapidly secrete enzymes to degrade litters to obtain phosphorus for growth and activity, which may lead to the rapid increase of soil amylase gene abundance. Compared with the early stage of succession, the increase of soil p content in the middle and late stages of succession led to the direct acquisition of phosphorus by microorganisms for the growth and activities in the soil, and the demand for nutrients from litter sources decreased, which may lead to the reduction of soil amylase gene abundance. R-strategy microorganisms tend to use fresh exogenous organic matter (Bremer and Kuikman, 1994). After substrate exhaustion, r-strategists die or become dormant because they are unable to use SOM (Fontaine et al., 2003). Moreover, the quantity of litter in the middle and late stage was significantly lower than that in the early stage, which may lead to the decrease of substrate content of r-strategy microorganisms, thus affecting the abundance of soil amylase gene. As the main contributor of amylase degradation, the relative abundance and relative contribution of *Proteobacteria* (r-strategist) reduced significantly in PBMF and MEBF compared with PMF, which further demonstrated our conclusion.

By contrast, gene abundance of hemicellulase, cellulase, and pectinase showed an upward trend with forest succession and had the highest degradation potential in MEBF (Figure 4), indicating the highest turnover rate of carbohydrates in the late-successional stage. We attributed it to the difference in soil carbon pool content. Previous studies reported that the late successional old-growth forests can still accumulate carbon in soil (Zhou et al., 2006a). Although the amount of

exogenous input litter was significantly lower in MEBF than in PMF, the long-term forest succession resulted in significantly higher soil carbon content in MEBF than in PMF, which provided sufficient substrates for microorganisms to degrade soil refractory organic carbon in MEBF. Moreover, *Actinobacteria* and *Acidobacteria* (K-strategists) accounted for a large proportion of the contribution in the degradation of hemicellulose, cellulose, and pectin, and the gene abundance of hemicellulose, cellulase, and pectinase were mainly affected by SOC, TN, and SM (Figure 6). In our study, the strategy of the bacterial communities changed in the middle succession stage. The relative proportion of r strategists (*Proteobacteria*) decreased while the sum of the relative proportion of K-strategists (*Actinobacteria* and *Acidobacteria*) increased (Supplementary Table S1). Although the proportion of K-strategists did not change significantly in the late succession stage, the significant increase of total bacterial community elevated the degradation potential of K-strategists to a certain extent. Compared with r-strategists, which tend to use fresh exogenous organic matter (Bremer and Kuikman, 1994), K-strategists grow slowly and mainly use inexhaustible soil organic matter (Fontaine et al., 2003). Moreover, K-strategists can degrade the non-readily oxidation organic carbon to obtain nutrients required for its growth (Blagodatskaya et al., 2007), thus gradually dominating forest succession. When the abundance of K-strategists increases, the degradation of SOC will be promoted. Under the maximum SOC, SM, and TN values, the degradation potential of hemicellulase, cellulase, and pectinase genes was highest (Figures 5, 6), suggesting that the increase of soil SOC, SM, and TN may increase the K-strategy microbial biomass and activity, thus accelerating the decomposition of recalcitrant organic C.

5 Conclusion

Using metagenomic analysis, we investigated changes in soil bacterial and fungal community compositions in three subtropical successional forests and linked to the genetic potential for soil carbohydrate degradation. Soil bacterial and fungal communities showed increasing trends with forest succession, which were positively associated with soil and litter characteristics. Across all the successional stages, *Proteobacteria* and *Actinobacteria* dominated the bacterial community while *Ascomycota* maintained an absolute dominance in the fungal community. The strategy of bacteria transformed from r to K in middle succession stage, while the fungi strategy did not change during forest succession. However, the α-diversity of soil bacteria did not change during forest succession, and the α-diversity of soil fungi even decreased in the late-successional stage. Soil carbohydrate degradation functional genes such as hemicellulase, cellulase, and pectinase increased with forest succession, which were mainly affected by soil organic carbon, soil total nitrogen, and soil moisture, while the gene abundance of amylase was mainly affected by soil total phosphorus and litterfall. These findings emphasized the importance of soil microbial communities and their functions in forest soil carbon turnover and provided a better understanding of the mechanisms by which soil microbes and soil environments interactively drive soil carbon storage during subtropical forest succession.

Data availability statement

The datasets presented in this study can be found in online repositories. The names of the repository/repositories and accession number(s) can be found in the article/Supplementary material.

Author contributions

MH: Writing – original draft. SZ: Writing – review & editing. XX: Writing – review & editing. XW: Writing – review & editing. YS: Writing – review & editing. ZM: Writing – review & editing. DH: Writing – review & editing. JL: Writing – review & editing. DZ: Writing – review & editing. QD: Writing – review & editing.

Funding

The author(s) declare financial support was received for the research, authorship, and/or publication of this article. The study was supported by the Science and Technology Planning Project of Guangdong Province (2021B1212110004), the National Natural Science Foundation of China (no. 41773088, 42107269, 31870461), the China Postdoctoral Science Foundation (no. 2020M682951), the "Hundred Talent Program" of South China Botanical Garden at the Chinese Academy of Sciences (no. Y761031001), and the "Young Top-notch Talent" in Pearl River talent plan of Guangdong Province (no. 2019QN01L763).

Acknowledgments

We wish to thank Xiaoping Pan, Xiaoying You, and Hui Mo for their help in laboratory work. We gratefully acknowledge Dinghushan Forest Ecosystem Research Station (http://dhf.cern.ac.cn/) for providing litter, soil temperate and moisture data and Majorbio Bio-Pharm Technology (http://www.majorbio.com/) for supporting in metagenomic sequencing.

Conflict of interest

The authors declare that the research was conducted in the absence of any commercial or financial relationships that could be construed as a potential conflict of interest.

Publisher's note

Supplementary material

The Supplementary material for this article can be found online at: https://www.frontiersin.org/articles/10.3389/fmicb.2023.1326057/full#supplementary-material

References

Aponte, C., Garcia, L. V., and Maranon, T. (2013). Tree species effects on nutrient cycling and soil biota: a feedback mechanism favouring species coexistence. *For. Ecol. Manag.* 309, 36–46. doi: 10.1016/j.foreco.2013.05.035

Bardgett, R. D., Bowman, W. D., Kaufmann, R., and Schmidt, S. K. (2005). A temporal approach to linking aboveground and belowground ecology. *Trends Ecol. Evol.* 20, 634–641. doi: 10.1016/j.tree.2005.08.005

Blagodatskaya, E. V., Blagodatsky, S. A., Anderson, T. H., and Kuzyakov, Y. (2007). Priming effects in Chernozem induced by glucose and N in relation to microbial growth strategies. *Appl. Soil Ecol.* 37, 95–105. doi: 10.1016/j.apsoil.2007.05.002

Blair, G. J., Lefroy, R. D. B., and Lise, L. (1995). Soil carbon fractions based on their degree of oxidation, and the development of a carbon management index for agricultural systems. *Aust. J. Agric. Res.* 46, 1459–1466. doi: 10.1071/Ar9951459

Breiman, L. (2001). Random forests. *Mach. Learn.* 45, 5–32. doi: 10.1023/a:1010933404324

Bremer, E., and Kuikman, P. (1994). Microbial utilization of 14C[U]glucose in soil is affected by the amount and timing of glucose additions. *Soil Biol. Biochem.* 26, 511–517. doi: 10.1016/0038-0717(94)90184-8

Buchfink, B., Xie, C., and Huson, D. H. (2015). Fast and sensitive protein alignment using DIAMOND. *Nat. Methods* 12, 59–60. doi: 10.1038/nmeth.3176

Carney, K. M., and Matson, P. A. (2006). The influence of tropical plant diversity and composition on soil microbial communities. *Microbial Ecol.* 52, 226–238. doi: 10.1007/s00248-006-9115-z

Chen, H., Li, C., Liu, T., Chen, S., and Xiao, H. (2020). A metagenomic study of intestinal microbial diversity in relation to feeding habits of surface and cave-dwelling Sinocyclocheilus species. *Microbial Ecol.* 79, 299–311. doi: 10.1007/s00248-019-01409-4

Cheng, J., Jing, G., Wei, L., and Jing, Z. (2016). Long-term grazing exclusion effects on vegetation characteristics, soil properties and bacterial communities in the semi-arid grasslands of China. *Ecol. Eng.* 97, 170–178. doi: 10.1016/j.ecoleng.2016.09.003

Chu, X. L., Zhang, Q. G., Buckling, A., and Castledine, M. (2021). Interspecific niche competition increases morphological diversity in multi-species microbial communities. *Front. Microbiol.* 12:699190. doi: 10.3389/fmicb.2021.699190

Clemmensen, K. E., Bahr, A., Ovaskainen, O., Dahlberg, A., Ekblad, A., Wallander, H., et al. (2013). Roots and associated fungi drive long-term carbon sequestration in boreal forest. *Science* 339, 1615–1618. doi: 10.1126/science.1231923

Cline, L. C., and Zak, D. R. (2015). Soil microbial communities are shaped by plant-driven changes in resource availability during secondary succession. *Ecology* 96, 3374–3385. doi: 10.1890/15-0184.1

Conant, R. T., Ryan, M. G., Agren, G. I., Birge, H. E., Davidson, E. A., Eliasson, P. E., et al. (2011). Temperature and soil organic matter decomposition rates – synthesis of current knowledge and a way forward. *Glob. Chang. Biol.* 17, 3392–3404. doi: 10.1111/j.1365-2486.2011.02496.x

Crow, S. E., Lajtha, K., Filley, T. R., Swanston, C. W., Bowden, R. D., and Caldwell, B. A. (2009). Sources of plant-derived carbon and stability of organic matter in soil: implications for global change. *Glob. Chang. Biol.* 15, 2003–2019. doi: 10.1111/j.1365-2486.2009.01850.x

Cusack, D. F., Chou, W. W., Yang, W. H., Harmon, M. E., Silver, W. L., and Lidet, T. (2009). Controls on long-term root and leaf litter decomposition in neotropical forests. *Glob. Chang. Biol.* 15, 1339–1355. doi: 10.1111/j.1365-2486.2008.01781.x

Dai, Z., Su, W., Chen, H., Barberan, A., Zhao, H., Yu, M., et al. (2018). Long-term nitrogen fertilization decreases bacterial diversity and favors the growth of Actinobacteria and Proteobacteria in agro-ecosystems across the globe. *Glob. Chang. Biol.* 24, 3452–3461. doi: 10.1111/gcb.14163

Dai, Z., Zang, H., Chen, J., Fu, Y., Wang, X., Liu, H., et al. (2021). Metagenomic insights into soil microbial communities involved in carbon cycling along an elevation climosequences. *Environ. Microbiol.* 23, 4631–4645. doi: 10.1111/1462-2920.15655

Dimassi, B., Mary, B., Fontaine, S., Perveen, N., Revaillot, S., and Cohan, J.-P. (2014). Effect of nutrients availability and long-term tillage on priming effect and soil C mineralization. *Soil Biol. Biochem.* 78, 332–339. doi: 10.1016/j.soilbio.2014.07.016

Ding, J., Zhang, Y., Wang, M., Sun, X., Cong, J., Deng, Y., et al. (2015). Soil organic matter quantity and quality shape microbial community compositions of subtropical broadleaved forests. *Mol. Ecol.* 24, 5175–5185. doi: 10.1111/mec.13384

Fierer, N., Bradford, M. A., and Jackson, R. B. (2007). Toward an ecological classification of soil bacteria. *Ecology* 88, 1354–1364. doi: 10.1890/05-1839

Fierer, N., and Jackson, R. B. (2006). The diversity and biogeography of soil bacterial communities. *Proc. Natl. Acad. Sci. U.S.A.* 103, 626–631. doi: 10.1073/pnas.0507535103

Fontaine, S., Mariotti, A., and Abbadie, L. (2003). The priming effect of organic matter: a question of microbial competition? *Soil Biol Biochemist* 35, 837–843. doi: 10.1016/s0038-0717(03)00123-8

Fu, L., Niu, B., Zhu, Z., Wu, S., and Li, W. (2012). CD-HIT: accelerated for clustering the next-generation sequencing data. *Bioinformatics* 28, 3150–3152. doi: 10.1093/bioinformatics/bts565

Ghoul, M., and Mitri, S. (2016). The ecology and evolution of microbial competition. *Trends Microbiol.* 24, 833–845. doi: 10.1016/j.tim.2016.06.011

Houghton, R. A. (2007). Balancing the global carbon budget. *Annu. Rev. Earth Planet. Sci.* 35, 313–347. doi: 10.1146/annurev.earth.35.031306.140057

Jiang, S., Xing, Y., Liu, G., Hu, C., Wang, X., Yan, G., et al. (2021). Changes in soil bacterial and fungal community composition and functional groups during the succession of boreal forests. *Soil Biol. Biochem.* 161:108393. doi: 10.1016/j.soilbio.2021.108393

Jobbagy, E. G., and Jackson, R. B. (2000). Global controls of forest line elevation in the northern and southern hemispheres. *Glob. Ecol. Biogeogr.* 9, 253–268. doi: 10.1046/j.1365-2699.2000.00162.x

Kaiser, C., Franklin, O., Dieckmann, U., and Richter, A. (2014). Microbial community dynamics alleviate stoichiometric constraints during litter decay. *Ecol. Lett.* 17, 680–690. doi: 10.1111/ele.12269

Kelly, C. N., Schwaner, G. W., Cumming, J. R., and Driscoll, T. P. (2021). Metagenomic reconstruction of nitrogen and carbon cycling pathways in forest soil: influence of different hardwood tree species. *Soil Biol. Biochem.* 156:108226. doi: 10.1016/j.soilbio.2021.108226

Kramer, C., Trumbore, S., Froeberg, M., Dozal, L. M. C., Zhang, D., Xu, X., et al. (2010). Recent (< 4 year old) leaf litter is not a major source of microbial carbon in a temperate forest mineral soil. *Soil Biol. Biochem.* 42, 1028–1037. doi: 10.1016/j.soilbio.2010.02.021

Lange, M., Eisenhauer, N., Sierra, C. A., Bessler, H., Engels, C., Griffiths, R. I., et al. (2015). Plant diversity increases soil microbial activity and soil carbon storage. *Nat. Commun.* 6:6707. doi: 10.1038/ncomms7707

Li, R., Li, Y., Kristiansen, K., and Wang, J. (2008). SOAP: short oligonucleotide alignment program. *Bioinformatics* 24, 713–714. doi: 10.1093/bioinformatics/btn025

Li, D., Liu, C.-M., Luo, R., Sadakane, K., and Lam, T.-W. (2015). MEGAHIT: an ultra-fast single-node solution for large and complex metagenomics assembly via succinct de Bruijn graph. *Bioinformatics* 31, 1674–1676. doi: 10.1093/bioinformatics/btv033

Liang, C., Schimel, J. P., and Jastrow, J. D. (2017). The importance of anabolism in microbial control over soil carbon storage. *Nat. Microbiol.* 2:17105. doi: 10.1038/nmicrobiol.2017.105

Liaw, A., and Wiener, M. (2002). Classification and regression by random forest. *R News* 23, 18–22. doi: 10.1057/9780230509993

Liu, J. X., Yu, Q. F., Chu, G. W., Zhou, G. Y., and Wen, D. Z. (2001). The dynamic change of soil pH value in major forests in Dinghushan. *Soil Environ. Sci.* 10, 39–41. (In Chinese with English abstract)

Martens, R. (1995). Current methods for measuring microbial biomass-C in soil – potentials and limitations. *Biol. Fertil. Soils* 19, 87–99. doi: 10.1007/Bf00336142

Noguchi, H., Park, J., and Takagi, T. (2006). MetaGene: prokaryotic gene finding from environmental genome shotgun sequences. *Nucleic Acids Res.* 34, 5623–5630. doi: 10.1093/nar/gkl723

Odum, E. P. (1969). Strategy of ecosystem development. *Science* 164:262-+. doi: 10.1126/science.164.3877.262

Pontarp, M., and Petchey, O. L. (2018). Ecological opportunity and predator-prey interactions: linking eco-evolutionary processes and diversification in adaptive radiations. *Proc. R. Soc. B* 285:2550. doi: 10.1098/rspb.2017.2550

Post, W. M., Emanuel, W. R., Zinke, P. J., and Stangenberger, A. G. (1982). Soil carbon pools and world life zones. *Nature* 298, 156–159. doi: 10.1038/298156a0

Prescott, C. E., and Grayston, S. J. (2013). Tree species influence on microbial communities in litter and soil: current knowledge and research needs. *For. Ecol. Manag.* 309, 19–27. doi: 10.1016/j.foreco.2013.02.034

Ren, C., Liu, W., Zhao, F., Zhong, Z., Deng, J., Han, X., et al. (2019). Soil bacterial and fungal diversity and compositions respond differently to forest development. *Catena* 181:104071. doi: 10.1016/j.catena.2019.104071

Sameith, K., Roscito, J. G., and Hiller, M. (2017). Iterative error correction of long sequencing reads maximizes accuracy and improves contig assembly. *Brief. Bioinform.* 18, 1–8. doi: 10.1093/bib/bbw003

Scheibe, A., Steffens, C., Seven, J., Jacob, A., Hertel, D., Leuschner, C., et al. (2015). Effects of tree identity dominate over tree diversity on the soil microbial community structure. *Soil Biol. Biochem.* 81, 219–227. doi: 10.1016/j.soilbio.2014.11.020

Shang, R., Li, S., Huang, X., Liu, W., Lang, X., and Su, J. (2021). Effects of soil properties and plant diversity on soil microbial community composition and diversity during secondary succession. *Forests* 12:805. doi: 10.3390/f12060805

Sokolowska, J., Jozefowska, A., Woznica, K., and Zaleski, T. (2020). Succession from meadow to mature forest: impacts on soil biological, chemical and physical properties-evidence from the Pieniny Mountains, Poland. *Catena* 189:104503. doi: 10.1016/j.catena.2020.104503

Trivedi, P., Delgado-Baquerizo, M., Trivedi, C., Hu, H., Anderson, I. C., Jeffries, T. C., et al. (2016). Microbial regulation of the soil carbon cycle: evidence from gene-enzyme relationships. *ISME J.* 10, 2593–2604. doi: 10.1038/ismej.2016.65

van der Heijden, M. G. A., Bardgett, R. D., and van Straalen, N. M. (2008). The unseen majority: soil microbes as drivers of plant diversity and productivity in terrestrial ecosystems. *Ecol. Lett.* 11, 296–310. doi: 10.1111/j.1461-0248.2007.01139.x

Wang, Z., Bai, Y., Hou, J., Li, F., Li, X., Cao, R., et al. (2022). The changes in soil microbial communities across a subalpine forest successional series. *Forests* 13:289. doi: 10.3390/f13020289

Wang, J., Ren, C., Cheng, H., Zou, Y., Bughio, M. A., and Li, Q. (2017). Conversion of rainforest into agroforestry andmonoculture plantation in China: consequences for soil phosphorus forms and microbial community. *Sci. Total Environ.* 595, 769–778. doi: 10.1016/j.scitotenv.2017.04.012

Wedin, D. A., and Tilman, D. (1996). Influence of nitrogen loading and species composition on the carbon balance of grasslands. *Science* 274, 1720–1723. doi: 10.1126/science.274.5293.1720

Weil, R. R., and Brady, N. C. (2016). *The nature and properties of soils*, *15th Edn* Upper Saddle River, NJ: Soil Science Society of America Journal, Pearson Press.

Xie, Z., Yu, Z., Li, Y., Wang, G., Liu, X., Tang, C., et al. (2022). Soil microbial metabolism on carbon and nitrogen transformation links the crop-residue contribution to soil organic carbon. *NPJ Biofilms Microbiomes* 8:14. doi: 10.1038/s41522-022-00277-0

Yan, B., Sun, L., Li, J., Liang, C., Wei, F., Xue, S., et al. (2020). Change in composition and potential functional genes of soil bacterial and fungal communities with secondary succession in Quercus liaotwigensis forests of the loess plateau, western China. *Geoderma* 364:114199. doi: 10.1016/j.geoderma.2020.114199

Zak, D. R., Holmes, W. E., White, D. C., Peacock, A. D., and Tilman, D. (2003). Plant diversity, soil microbial communities, and ecosystem function: are there any links? *Ecology* 84, 2042–2050. doi: 10.1890/02-0433

Zechmeister-Boltenstern, S., Keiblinger, K. M., Mooshammer, M., Penuelas, J., Richter, A., Sardans, J., et al. (2015). The application of ecological stoichiometry to plant-microbial-soil organic matter transformations. *Ecol. Monogr.* 85, 133–155. doi: 10.1890/14-0777.1

Zhang, K. R., Cheng, X. L., Shu, X., Liu, Y., and Zhang, Q. F. (2018). Linking soil bacterial and fungal communities to vegetation succession following agricultural abandonment. *Plant Soil* 431, 19–36. doi: 10.1007/s11104-018-3743-1

Zhong, Z., Wang, X., Zhang, X., Zhang, W., and Yang, G. (2019). Edaphic factors but not plant characteristics mainly alter soil microbial properties along a restoration chronosequence of Pinus tabulaeformis stands on Mt. Ziwuling, China. *For. Ecol. Manag.* 453:117625. doi: 10.1016/j.foreco.2019.117625

Zhong, Y. Q. W., Yan, W. M., Wang, R. W., Wang, W., and Shangguan, Z. P. (2018). Decreased occurrence of carbon cycle functions in microbial communities along with long-term secondary succession. *Soil Biol. Biochem.* 123, 207–217. doi: 10.1016/j.soilbio.2018.05.017

Zhou, G. Y., Liu, S. G., Li, Z., Zhang, D. Q., Tang, X. L., Zhou, C. Y., et al. (2006a). Old-growth forests can accumulate carbon in soils. *Science* 314:1417. doi: 10.1126/science.1130168

Zhou, Z., Wang, C., Jiang, L., and Luo, Y. (2017). Trends in soil microbial communities during secondary succession. *Soil Biol. Biochem.* 115, 92–99. doi: 10.1016/j.soilbio.2017.08.014

Zhou, Z., Wang, C., and Luo, Y. (2018). Effects of forest degradation on microbial communities and soil carbon cycling: a global meta-analysis. *Glob. Ecol. Biogeogr.* 27, 110–124. doi: 10.1111/geb.12663

Zhou, G. Y., Zhou, C. Y., Liu, S. G., Tang, X. L., Ouyang, X. J., Zhang, D. Q., et al. (2006b). Belowground carbon balance and carbon accumulation rate in the successional series of monsoon evergreen broad-leaved forest. *Sci. China Ser. D-Earth Sci.* 49, 311–321. doi: 10.1007/s11430-006-0311-y

Zhu, H., He, X., Wang, K., Su, Y., and Wu, J. (2012). Interactions of vegetation succession, soil bio-chemical properties and microbial communities in a karst ecosystem. *Eur. J. Soil Biol.* 51, 1–7. doi: 10.1016/j.ejsobi.2012.03.003

Zhu, K., Wang, Q., Zhang, Y., Zarif, N., Ma, S., and Xu, L. (2022). Variation in soil bacterial and fungal community composition at different successional stages of a broad-leaved Korean pine forest in the lesser Hinggan mountains. *Forests* 13:625. doi: 10.3390/f13040625

frontiers | Frontiers in Microbiology

TYPE Original Research
PUBLISHED 02 February 2024
DOI 10.3389/fmicb.2024.1321059

OPEN ACCESS

EDITED BY
Romy Chakraborty,
Berkeley Lab (DOE), United States

REVIEWED BY
Lars Wadso,
Lund University, Sweden
Marko Popovic,
University of Belgrade, Serbia
Nieves Barros Pena,
University of Santiago de Compostela, Spain

*CORRESPONDENCE
Thomas Maskow
✉ thomas.maskow@ufz.de

†These authors have contributed equally to this work and share first authorship

RECEIVED 13 October 2023
ACCEPTED 04 January 2024
PUBLISHED 02 February 2024

CITATION
Yang S, Di Lodovico E, Rupp A, Harms H, Fricke C, Miltner A, Kästner M and Maskow T (2024) Enhancing insights: exploring the information content of calorespirometric ratio in dynamic soil microbial growth processes through calorimetry.
Front. Microbiol. 15:1321059.
doi: 10.3389/fmicb.2024.1321059

Enhancing insights: exploring the information content of calorespirometric ratio in dynamic soil microbial growth processes through calorimetry

Shiyue Yang[1†], Eliana Di Lodovico[1,2†], Alina Rupp[1], Hauke Harms[1], Christian Fricke[2], Anja Miltner[1], Matthias Kästner[1] and Thomas Maskow[1*]

[1]Helmholtz Centre for Environmental Research – UFZ, Leipzig, Germany, [2]Rheinland-Pfälzische Technische Universität Kaiserslautern-Landau (RPTU), Landau in der Pfalz, Germany

Catalytic activity of microbial communities maintains the services and functions of soils. Microbial communities require energy and carbon for microbial growth, which they obtain by transforming organic matter (OM), oxidizing a fraction of it and transferring the electrons to various terminal acceptors. Quantifying the relations between matter and energy fluxes is possible when key parameters such as reaction enthalpy ($\Delta_r H$), energy use efficiency (related to enthalpy) (EUE), carbon use efficiency (CUE), calorespirometric ratio (CR), carbon dioxide evolution rate (CER), and the apparent specific growth rate (μ_{app}) are known. However, the determination of these parameters suffers from unsatisfying accuracy at the technical (sample size, instrument sensitivity), experimental (sample aeration) and data processing levels thus affecting the precise quantification of relationships between carbon and energy fluxes. To address these questions under controlled conditions, we analyzed microbial turnover processes in a model soil amended using a readily metabolizable substrate (glucose) and three commercial isothermal microcalorimeters (MC-Cal/100P, TAM Air and TAM III) with different sample sizes meaning varying volume-related thermal detection limits (LOD_v) (0.05–1 mW L^{-1}). We conducted aeration experiments (aerated and un-aerated calorimetric ampoules) to investigate the influence of oxygen limitation and thermal perturbation on the measurement signal. We monitored the CER by measuring the additional heat caused by CO_2 absorption using a NaOH solution acting as a CO_2 trap. The range of errors associated with the calorimetrically derived μ_{app}, EUE, and CR was determined and compared with the requirements for quantifying CUE and the degree of anaerobicity (η_A). Calorimetrically derived μ_{app} and EUE were independent of the instrument used. However, instruments with a low LOD_v yielded the most accurate results. Opening and closing the ampoules for oxygen and CO_2 exchange did not significantly affect metabolic heats. However, regular opening during calorimetrically derived CER measurements caused significant measuring errors due to strong thermal perturbation of the measurement signal. Comparisons between experimentally determined CR, CUE, η_A, and modeling indicate that the evaluation of CR should be performed with caution.

KEYWORDS

calorimetry, biothermodynamics, energy use efficiency, carbon use efficiency, growth rate, calorespirometric ratio, soil systems

1 Introduction

Calorimetry is a non-destructive technique that was initially used to measure the heat released by small rodents (Crawford, 1788; Lavoisier and DeLaplace, 1994). The results sparked scientists' interest, leading to the development of more sensitive and high-throughput calorimeters (Sunner and Wadsö, 1959; Hofelich et al., 2001; Wadsö et al., 2010; Paufler et al., 2013; Wadso, 2015; Wadsö et al., 2017) for application to various life-forms, such as animals and plants (Kemp and Guan, 1997), microbes (Gustafsson, 1991; von Stockar et al., 1993; Fricke et al., 2019), as well as entire soil systems (Dijkerman, 1974; Ljungholm et al., 1979; Herrmann and Bölscher, 2015).

Soil plays an essential role in maintaining the Earth's carbon balance. This balance heavily depends on catalytic functions performed by microbial communities on soil organic matter (SOM), whose activity obeys the rules of thermodynamics for an open system. A crucial state function for testing and evaluating thermodynamic models is the reaction enthalpy $\Delta_r H$, which can be determined by isothermal microcalorimetry. The measured heat production rate P (in W) contains both kinetic and stoichiometric information, and the integral of the heat production rate provides (under constant pressure) the reaction enthalpy ($\Delta_r H = Q$).

In soil systems, organic matter (OM) can be utilized for growth through microbial assimilation in anabolic reactions or dissipated as CO_2 to the environment in catabolic reactions. The catabolic reactions provide the energy for the anabolic reactions (Kästner et al., 2021) and essentially determine the overall heat production rate of the overall reactions (Canfield et al., 2005; von Stockar, 2010). This explains the frequently observed relation between the CR and the yield coefficient in biotechnology or the CUE in soil science (Von Stockar and Birou, 1989; Hansen et al., 2004; Herrmann and Bölscher, 2015; Wadsö and Hansen, 2015).

A simple calorimetric experiment can provide many important and valuable thermodynamic, kinetic and stoichiometric variables (a detailed derivation is given in section 2.4). For example, P is equal to the product of the growth rate multiplied by the reaction enthalpy. The slope of the natural logarithm of P vs. time corresponds to the apparent growth rate (μ_{app}). In the simplest case, the slope is constant over a certain time. $\Delta_r H$ is linked to the growth reaction stoichiometry via the law of Hess (Braissant et al., 2010; Maskow and Paufler, 2015). Applying the law of Hess requires both calorimetric information and information about matter fluxes. To link the two pieces of information, a combination of calorimetry and respirometry, also known as calorespirometry is required. From such coupled measurements, the calorespirometric ratio (CR) is obtained, which represents the ratio of the specific heat production rate P_m (in $W\,g^{-1}$) to the specific CO_2 evolution rate CER (in $mol\,g^{-1}\,s^{-1}$) or the ratio of the specific total heat Q_m (in $J\,g^{-1}$) to the specific total evolved CO_2 (in $mol\,g^{-1}$). Thus, the CR has the dimension of $J\,mol^{-1}$.

Three options of measuring CR have recently been discussed. Firstly, the heat production rate of soil samples with (P_{SN}) and without (P_S) a CO_2 trap (filled with a trap solution, usually NaOH) can be continuously monitored calorimetrically. A simple setup is shown in Figure 1. Additional heat is released by the absorption reaction between CO_2 and NaOH ($2NaOH + CO_2 \rightarrow Na_2CO_3 + H_2O$) causing an increase in P_{SN} compared to P_S in vials without NaOH trap. The CER is calculated from the difference between both signals and the known reaction enthalpy for the CO_2 trapping reaction ($\Delta_{abs}H$) (Critter et al., 2001; Barros et al., 2010). Secondly, like the first approach, a CO_2 trap can be positioned in a calorimetric ampoule or a backup reactor, and the trap can be sampled at defined time points and the trapped CO_2 quantified, for example by titration or a dissolved inorganic carbon analyzer. In all cases, the total inorganic carbon in the trap is a measure of the CER (Barros et al., 2011). Thirdly, the heat production rate of soil samples can be monitored in a calorimeter, and the headspace of the calorimetric ampoules or of parallel back-up reactors can be sampled at defined time points and quantified by alternative analytics, such as gas-chromatography, as discussed in Pushp et al., 2021.

To link calorespirometric data and energy and matter turnover in soil systems, thermodynamic models are being developed to investigate the link between CR, CUE and EUE. Hansen et al. (2004) established a quantitative model linking CR with CUE, which is widely used today. To achieve this connection, Hansen et al. (2004) simplified the intricate soil processes by assuming aerobic metabolisms, concentrating on a single substrate, and disregarding interactions of OM with minerals. Furthermore, Chakrawal et al. (2020) extended Hansen's model to encompass anaerobic, fermentative processes that result in the production of ethanol and lactic acid. This expansion allows for a more comprehensive understanding of the relationship between CR and CUE, considering a broader range of metabolic pathways and conditions. This is particularly important in complex, heterogeneous and dynamic systems such as soil. Other models were established to predict the fate of carbon (Trapp et al., 2018) as well as the conversion rates of SOM (Ugalde-Salas et al., 2020).

However, based on the overall turnover reactions, energy and mass balances depend on the microbial growth, decaying of cells, CO_2 formation and transformation from necromass to SOM (Kästner et al., 2021). Deriving energy turnover parameters in soil samples using isothermal microcalorimeters (IMCs) and applying them to thermodynamic models is still challenging for the following reasons. First, 1 g of soil can contain approximately 10^9 microbial cells from 4,000 different microbial taxa (Raynaud and Nunan, 2014; Chaudhary et al., 2019). However, a large fraction of them is in a dormant state at any given time (Blagodatsky and Richter, 1998), with a metabolism limited to basic maintenance of the cells. The heat output of these resting soil microbes is so low that highly sensitive calorimeters are required, or the sample sizes increased to make it measurable. Second, natural spatial heterogeneities and complexity in different soils influence the accuracy of the heat signal. This influence can be reduced by measuring large soil samples. The combined effect of the minimal thermal limit of detection and maximal sample size can be considered by comparing the minimum volume-related declared thermal limit of detection (LOD_V) of different devices, Third, oxygen depletion triggered by microbial activities might results in anaerobic conditions in the sample ampoules. Thus, during the measurements, it is common to open the calorimetric ampoules from time to time, not only to sample the NaOH solution or to renew the CO_2 trap but also to counteract the consumption of oxygen to avoid anaerobic conditions (see Figure 1). Aeration becomes important when the experiments run for long periods (e.g., weeks or months) or the microorganisms are highly active. However, a weekness of opening the ampoules is the thermal disturbance caused by a sudden temperature change when removing and replacing the ampoule on the Peltier sensor. This is

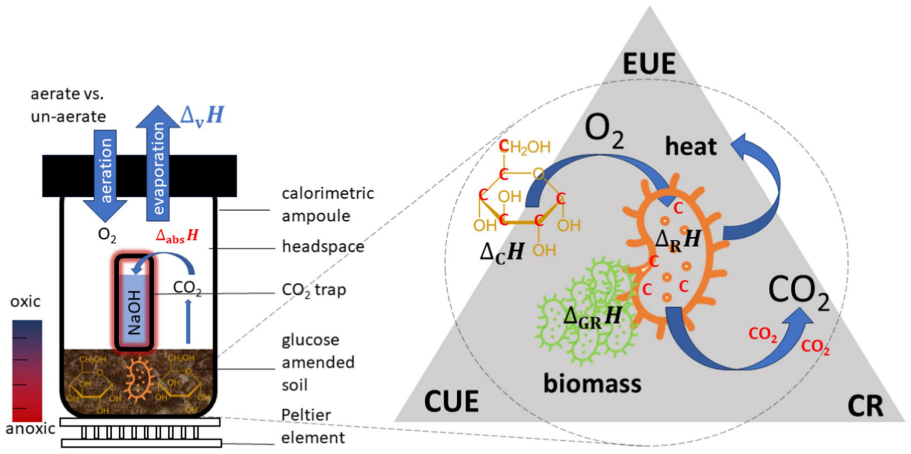

FIGURE 1
Setup of a common calorespirometric measuring system to monitor simultaneously *P* and CER **(left)**. Fundamental mechanism for microbial turnover of substrates in soil and underlying key variables for evaluating the efficiency of such processes **(right)**.

particularly important for signals in the microwatt range (Wadsö, 2001).

A few aspects need to be considered to prevent over- and mis-interpretation of the calorimetric signals in soil research: (i) how accurately can the CR be determined in the best case using commercially available IMCs, (ii) what influences do the LOD_V and the regular opening of the calorimetric measuring chamber have on the determination of kinetic (μ_{app}) and thermodynamic parameters ($\Delta_r H$, EUE, CR), (iii) do rates or integrated values give the most reliable CR, and (iv) what are the consequences of the experimental error of the CR determination for the calculation of CUE and the degree of anaerobicity (η_A) are?

This study thus aims at maximizing the achievable information about energy turnover from calorimetric experiments with soil samples. For this purpose, substrate-induced growth experiments on soil samples were performed with glucose as a readily metabolizable substrate, which is expected to rapidly give clear calorespirometric signals. The experiments were conducted with different instruments with soil treated in the same way. We tested different ways to analyze the data. Theoretical expectation on the relation between the CR and the CUE or the η_A and minimum requirements for CR accuracy determination are also discussed.

2 Materials and methods

2.1 Technical and preparative framework

The three different types of commercial available IMCs provide the technical framework for this study, and are intended to evaluate the combined effects of sample sizes and thermal detection limits on both, the calorimetric signal itself and the derived values (e.g., CUE, CER, EUE, μ_{app}, CR). For an optimal performance of the IMCs, two factors are crucial: high thermal sensitivity and large soil sample size. This is expressed by the LOD_V. Further technical details regarding these instruments are provided in Table 1, with references to the respective sources (operational manuals from manufacturers).

In order to avoid unknown heat losses to the environment or to minimize the impact of water evaporation, calorimetric measurements are conducted in air-tight closed ampoules (Figure 1). However, due to the rapid depletion of oxygen by active microbial communities within the closed ampoules, oxygen might get limited, shifting the metabolism toward anaerobic processes, with lower $\Delta_r H$. A potential limitation by insufficient oxygen supply can be mitigated by periodically aerating the ampoules. To quantify the impact of regularly aerating the ampoules, two types of experiments were performed: one with aeration (indexed as A) and another permanently un-aerated (indexed as U) using the calorimeter with the lowest LOD_V (TAM III). Oxygen limitation can simply be estimated assuming ideal gas behavior as described in Eq. 1.

$$n_{O_2} = \frac{p \cdot V}{\chi_{O_2,air} \cdot R \cdot T} \quad (1)$$

Here, p, V, $\chi_{O_2,air}$, R, T stand for the pressure (101,325 Pa), the gas volume of the ampoule, the mole fraction of oxygen in the air (0.2094) (Lemmon et al., 2000), the universal gas constant (8.314 J mol^{-1} K^{-1}) and the temperature in K, respectively. The maximum required oxygen can be estimated assuming a complete oxidation of glucose (see Eq. 2).

$$C_6H_{12}O_6 + 6O_2 \rightarrow 6CO_2 + 6H_2O \quad (2)$$

We added 900 µg (0.005 mmol) glucose or 360 µg (0.03 mmol) C per g dw-soil. Thus, we expect a maximum oxygen consumption of 0.03 mmol g^{-1} dw-soil. For the estimation of oxygen availability, the compact volume of the soil needs to be considered as soil is a porous structure. Thus, oxygen within soil particles pores should also be considered. The density of the dry soil particles is estimated to be 2.65 g cm^{-3} (Schjønning et al., 2017). Table 2 compares the available amount of oxygen with the required amount of oxygen as well as the maximum expected CO_2 concentration in the headspace. The calculations are provided in the Supplementary material. The estimation indicates that oxygen consumption may be significant, and oxygen limitation might become an issue if all glucose is respired.

TABLE 1 Technical comparison of the calorimeters used (LOD-thermal limit of detection, LOD_V minimum thermal limit of detection).

Instrument	Maximum number of channels	*LOD* µW	Declared signal drift over 24 h µW	Volume of the reaction vessel mL	LOD_V mW L^{-1}
MC-Cal/100P	12	20	<40	20	1
TAM Air	8	4	<40	20	0.2
TAM III	24	0.2	<0.2	4	0.05

TABLE 2 Summary of the oxygen availability and maximum expected CO_2 concentration in all calorimeters used.

Calorimeter	Volume of the ampoule ml	Available air volume ml	Estimated O_2 availability mmol	Maximum required O_2 mmol	Maximum CO_2 concentration %
MC-Cal/100 P	20	17.92	0.16	0.12	15.0
TAM Air	20	17.92	0.16	0.12	15.0
TAM III	4	3.58	0.03	0.02	15.0

2.2 Soil preparation

As an example, farmyard manure soil from the Dikopshof long-term experiment (since 1904) from INRES (Institute of Crop Science and Resource Conservation), Bonn University was used in these experiments. The soil is classified as Haplic Luvisol (Parabraunerde), with a silt loam texture, pH 6.3, 0.74% organic carbon and a water holding capacity of 31% (w dw^{-1} soil). The soil has been treated with farmyard manure fertilizer annually and it is aggregated moderately with a moderate usable field capacity. Further physicochemical parameters of the soil are well-documented and can be found here https://www.lap.uni-bonn.de/en/research/projects/long-term-experiment-dikopshof (Huging, 1904).

In order to prepare the soil samples, they were air-dried and stored at room temperature (approximately 20°C). The air-dried soil was initially sieved through a 2-mm sieve, with larger aggregates crushed and stones removed. The sieved soil was then transferred into a glass beaker. Roots, seeds, and other organic material were carefully taken out. To obtain around 14% (w dw^{-1} soil) water content for the pre-incubation, deionized water was added stepwise to the dried soil and manually stirred for homogeneous distribution. A smaller glass beaker, partially filled with water, was placed on the soil surface to maintain the moisture. The larger glass beaker was sealed with parafilm and pre-incubated for 7 days at 20°C.

2.3 Calorimetric soil incubation experiments

In the following study, the IMCs TAM III (Minicalorimeter/Multi 4 mL), TAM Air (TA Instruments, New Castle, USA) equipped with 12 and 8 channels, respectively, as well as the MC-Cal/100P (C3 Prozess- und Analysetechnik GmbH, Munich, Germany) equipped with 12 measuring channels and 2 reference channels were used to perform the substrate-induced soil experiments. The three calorimeters differ in a few main characteristics, which can be found in Table 1. After the pre-incubation period, a glucose solution (200 g L^{-1}) was added to the pre-incubated soil using a pipette aiming for a concentration of 360 µg C g^{-1} DW soil, which corresponds to four times the microbial carbon content quantified via chloroform fumigation extraction. With the addition of the glucose solution, a water content of 16% was reached. In control samples, 16% water content was reached via the addition of deionized water. The entire calorimetric incubations were performed at 20°C.

In our first research question, we would like to investigate what influences the LOD_V of different IMCs have on the determination of kinetic (μ_{app}) and thermodynamic parameters. Soil was prepared following the same method mentioned previously. Afterwards, the glucose amended soil (min. 99%, CHEMSOLUTE) and unamended soil were distributed equally into the different calorimetric glass ampoules in order to make full use of all channels in each device, various numbers of replicates were used in different IMCs, which can be found in Table 3. We aimed at providing sufficient oxygen for aerobic microbial activity while having sufficient soil to obtain a good heat signal. Moreover, we maintained the air/soil volume ratio in all experiments at 4.44. Therefore, 4.5 g of wet soil (16% water content) were used for 20 mL glass ampoules (TAM Air and MC-Cal/100 P), while 0.9 g of wet soil (16% water content) were used for 4 mL glass ampoules (TAM III).

Secondly, to figure out the influence of aeration on the heat production rate (P_m) and metabolic heat (Q_m) measurement and CER calculation, aeration experiment was conducted in TAM III. Aeration could have huge thermal disturbance on calorimetric signals. Therefore, IMCs with most stable temperature control was utilized to conduct experiments and answer this research question to avoid misinterpretation of the result. Triplicates were used for each treatment. At each aeration time (t = 8, 22, 30, 50 h), calorimetric ampoules were taken out from TAM III to prevent oxygen depletion. NaOH containers were also moved and NaOH solution was renewed to avoid saturation. Lids were opened and ampoules were left open for aeration under 20°C room temperature for 5 min. Afterwards, the ampoules were closed tightly and introduced again into the original channels. Half of the ampoules contained a small vial with 700 µL, 0.4 M NaOH (≥ 98%, Carl Roth GmbH) to measure the combined heat of metabolism and absorption of CO_2.

In the case of the TAM III instrument, the prepared ampoules were placed into the channels of the calorimeter and allowed to thermally equilibrate for 15 min in the pre-heating position. After another 45 min for thermal equilibration in the measuring position,

TABLE 3 Experimental set-up.

Abbreviation	Set-up	Influence of LOD_v			Influence of aeration
		MC-Cal/100P	TAM Air	TAM III	TAM III
$P_S(t)$	Soil, un-aerated	($n = 3$)	($n = 4$)	($n = 6$)	($n = 2$)
$P_{SN}(t)$	Soil, NaOH, un-aerated	/	/	/	/
$P_{SG}(t)$	Soil, Glucose, un-aerated	($n = 3$)	($n = 4$)	($n = 6$)	($n = 2$)
$P_{SGA}(t)$	Soil, Glucose, reg. aerated	/	/	/	($n = 2$)
$P_{SGNU}(t)$	Soil, Glucose, NaOH, un-aerated	/	/	/	($n = 3$)
$P_{SGNA}(t)$	Soil, Glucose, NaOH, reg. aerated	/	/	/	($n = 3$)

P was recorded. Regular gain calibration was performed to ensure the measurement precision. This involves generating heat pulses in each channel using an integrated electrical calibration heater (Joule heat). The resulting calibration data provided gain factors and offsets for each channel, which were applied by the instrument. The TAM III instrument has fixed installed reference directly below the measurement channel. For TAM Air, the baseline automatically started and was recorded for 30 min (time needed to have a stable signal according to the experimental wizard's criteria). Afterwards, both measuring and reference ampoules were placed directly in the measuring position. Heat production rate recording commenced after 45 min when the data were considered correct by the software (thermal equilibration). As with the TAM III, calibration resulted in gain factors and offsets for each channel, ensuring accurate measurements. For the MC-Cal/100P instrument, an internal electrical calibration was performed before conducting the experiments. The instrument automatically determined and applied gain factors and offsets of each channel. The prepared ampoules were directly placed in the measuring position, which required a longer time (60 min) until the instrument provided stable data. One channel per block was selected as a reference and contained a reference ampoule.

The reference ampoules for TAM Air and MC-Cal/100P were filled with 1.362 mL deionized water to give a heat capacity similar to the soil samples. All measurements were conducted at 20°C. We stopped all experiments when all calorimetric signals were constant over time. However, for comparison, we evaluated the signals until 70 h.

Table 3 summarizes the different set-ups in the respective calorimeters and the number of replicated used (n); note that not all the set-ups were replicated in all the devices.

2.4 Theoretical framework

Based on the experimental data that was obtained from the calorespirometric measurements a theoretical framework can be developed to derive important and valuable thermodynamic and kinetic parameters of soil microbial processes. The heat production rate $P(t)$ is linked to the rate $r_i(t)$ of all i occurring reactions and their respective reaction enthalpies $\Delta_r H_i$ using Eq. 3 (Assael et al., 2023).

$$P(t) = \sum_{i=1}^{n} r_i(t) \cdot \Delta_r H_i \tag{3}$$

The total heat, $Q(t)$, results from the integration of the heat production rate, as given in Eq. 4.

$$Q(t) = \int_{t=0}^{t} P(t)\mathrm{d}t \tag{4}$$

Performing integration to the end of the reaction and dividing the total heat by the amount of substrate consumed yields the reaction enthalpy $\Delta_r H$, which contains stoichiometric information (Eq. 5). It is typically assumed that glucose is a rapidly and almost completely degraded substrate (Yang et al., 2016). Therefore, n^e is assumed in this work to be 0 after 70 h.

$$\Delta_r H = \frac{\int_{t_0}^{t^e} P(t)\mathrm{d}t}{n_0 - n^e} = -\sum_{i=1}^{n} Y_{i/S} \cdot \Delta_C H_i \tag{5}$$

Here, t_0, t^e, n_0, n^e, $Y_{i/S}$, $\Delta_C H_i$ stand for the time of the beginning and end of the metabolic reaction, the amount of the substrate before and after the reaction, the yield coefficient, and the combustion enthalpy of the compound i, respectively. The yield coefficient expresses the amount of the component i required or formed during the conversion of one mol consumed substrate. In soil sciences, energy use efficiency (EUE) is an important parameter which can be defined in different ways. In the following, we will define EUE as shown by Eq. 6.

$$\mathrm{EUE} = 1 - \frac{Q}{\left(n_0 - n^e\right) \cdot \Delta_c H_{\mathrm{Glucose}}} \tag{6}$$

Here, Q, n_0, n^e, $\Delta_C H_{\mathrm{Glucose}}$ stand for the measured total heat over the whole reaction, the amount of added glucose, the amount of glucose after the reaction, and the combustion enthalpy of glucose, respectively.

In the simplest case of a pure microbial culture, when putting all metabolic reactions together and assuming exponential growth after the addition of the substrate, an exponential curve with an apparent specific growth rate μ_{app} is expected and indeed, this is mostly observed after adding a C- and energy source (Eq. 7). In the case of soil samples, we observe an exponential growth phase, but it is the results of overlapping metabolisms, due to the complexity of the soil system. Sometimes a lag phase is observed which for simplicity, is not reflected in the following equation. If a lag phase is present, it would mainly affect the timing, but not the slope of the curve of $\ln(P(t))$ vs. t.

$$P(t) = P_0 \cdot \exp(\mu_{app} \cdot t) \quad (7)$$

This means that plotting the ln($P(t)$) vs. t gives a straight line with the slope of the apparent specific growth rate μ_{app} (Figure 1). In order to capture the metabolic heat production rate, $P(t)$, after substrate addition, both heat production rates of soil amended with glucose (SG) ($P_{SG}(t)$), and unamended soil(S), ($P_S(t)$) must be measured and the metabolic heat production rate of substrate metabolization is the difference between ($P_{SG}(t)$) and $P_S(t)$ (Eq. 8).

$$P(t) = P_{SG}(t) - P_S(t) \quad (8)$$

An important parameter in thermodynamic soil research is the calorespirometric ratio (CR), which correlates the released heat with the evolved carbon dioxide. It can be defined from the P and CER (CR_P, Eq. 9), or from Q and the accumulated amount of released CO_2, (CR_Q, Eq. 10). Both approaches were tested and discussed in the respective sections.

$$CR_P = \frac{P(t)}{CER(t)} \quad (9)$$

$$CR_Q = \frac{Q(t)}{\int_{t=0}^{t} CER(\tilde{t})\, d\tilde{t}} \quad (10)$$

The CR is important since under aerobic conditions it is thought to contain information about the CUE (Hansen et al., 2004; Maskow et al., 2011). Additionally, newer modeling research revealed that the CR contains also information about the ratio of aerobic to anaerobic metabolisms (Chakrawal et al., 2020). However, for calculation of the CR, the CER needs to be measured, which is often done by equipping a calorimetric ampoule with a CO_2 trap (NaOH solution, subscript N) and monitoring the additional heat of the CO_2 absorption reaction ($\Delta_{abs}H = 108.4\ kJ\ mol^{-1}$) (Criddle et al., 1991). P_{SN} is the heat production rate of unamended soil equipped with CO_2 trap and P_S is the heat production rate of unamended soil. P_{SGN} is the heat production rate of glucose-amended soil equipped with CO_2 trap and P_{SG} is the heat production rate of glucose-amended soil. In the case of unamended (S) and glucose amended (SG) soil, the CER can be calculated according to Eqs. 11, 12.

$$CER_S(t) = \frac{P_{SN}(t) - P_S(t)}{\Delta_{abs}H} \quad (11)$$

$$CER_{SG}(t) = \frac{P_{SGN}(t) - P_{SG}(t)}{\Delta_{abs}H} \quad (12)$$

2.5 Statistical analysis

The statistical analysis (Kruskal-Wallis test for ≥ 2 nonparametric groups and Wilcoxon test for two independent and nonparametric groups) and the plots creation were performed using the software R.

3 Results

3.1 Apparent specific growth rate derived from calorimetric measurements

Calorimetrically derived μ_{app} were calculated as the slope of the curve ln($P(t)$) vs. time during the exponential growth phase from P_m. Details are given in the SM. Table 4 compares μ_{app} determined with the different IMCs using closed ampoules after amendment with glucose.

The instruments with a medium LOD_V (TAM Air) $\mu_{app} = (0.138 \pm 0.008)\ h^{-1}$ and a high LOD_V (MC-Cal/100P) $\mu_{app} = (0.144 \pm 0.013)\ h^{-1}$ show statistically the same μ_{app}, whereas the low LOD_V instrument (TAM III) $\mu_{app} = (0.131 \pm 0.003)\ h^{-1}$ provides a slightly smaller value. Although the difference between the results obtained with MC-Cal/100P and TAM III was small, it was significant.

3.2 Influence of sample size and calorimetric instrument on specific metabolic heat

P from soil amended with glucose solution were measured with three calorimeters differing in LOD_V. Q resulted from the integration of P (Eq. 4). Figure 2A illustrates $P_{m,SG}$ in $\mu W\ g^{-1}$ soil. For MC-Cal/100P, a peak maximum of $(98.0 \pm 8.6)\ \mu W\ g^{-1}$ is observed after approx. 19.2 h. For TAM Air, $P_{m,SG}$ reaches its peak maximum at $(70.0 \pm 7.7)\ \mu W\ g^{-1}$ after approx. 15.2 h. $P_{m,SG}$, measured by TAM III reached $(77.1 \pm 3.0)\ \mu W\ g^{-1}$ after approx. 18.1 h.

Figure 2B displays the Q_m in $J\ g^{-1}$, with values of $(5.34 \pm 0.69)\ J\ g^{-1}$ for MC-Cal/100P, $(4.25 \pm 1.42)\ J\ g^{-1}$ for TAM Air, and $(3.42 \pm 0.18)\ J\ g^{-1}$ for TAM III. A statistically significant difference was found only between the IMC with a low LOD_V (TAM III) and the IMC with a high LOD_V (MC-Cal/100P), as seen in Figure 2C.

3.3 Influence of aeration on the thermal signal

The following comparison intends to answer the question of whether aerating calorimetric ampoules to prevent oxygen depletion affects the thermal signal. For better comparability, the experiments were performed with the IMC with the lowest LOD_V (TAM III) adding glucose for two different treatments (aerated vs. un-aerated). The ampoules were aerated for 5 min, causing a thermal disturbance which lasted for approximately 2 h. To integrate the P (for obtaining the Q),

TABLE 4 Apparent specific growth rate for different calorimeters.

IMC	LOD_V $mW\ L^{-1}$	$\mu_{app}\ h^{-1}$	Standard error h^{-1}
MC-Cal/100P	1	0.145[a]	0.007
TAM Air	0.2	0.138[ab]	0.004
TAM III	0.05	0.131[b]	0.001

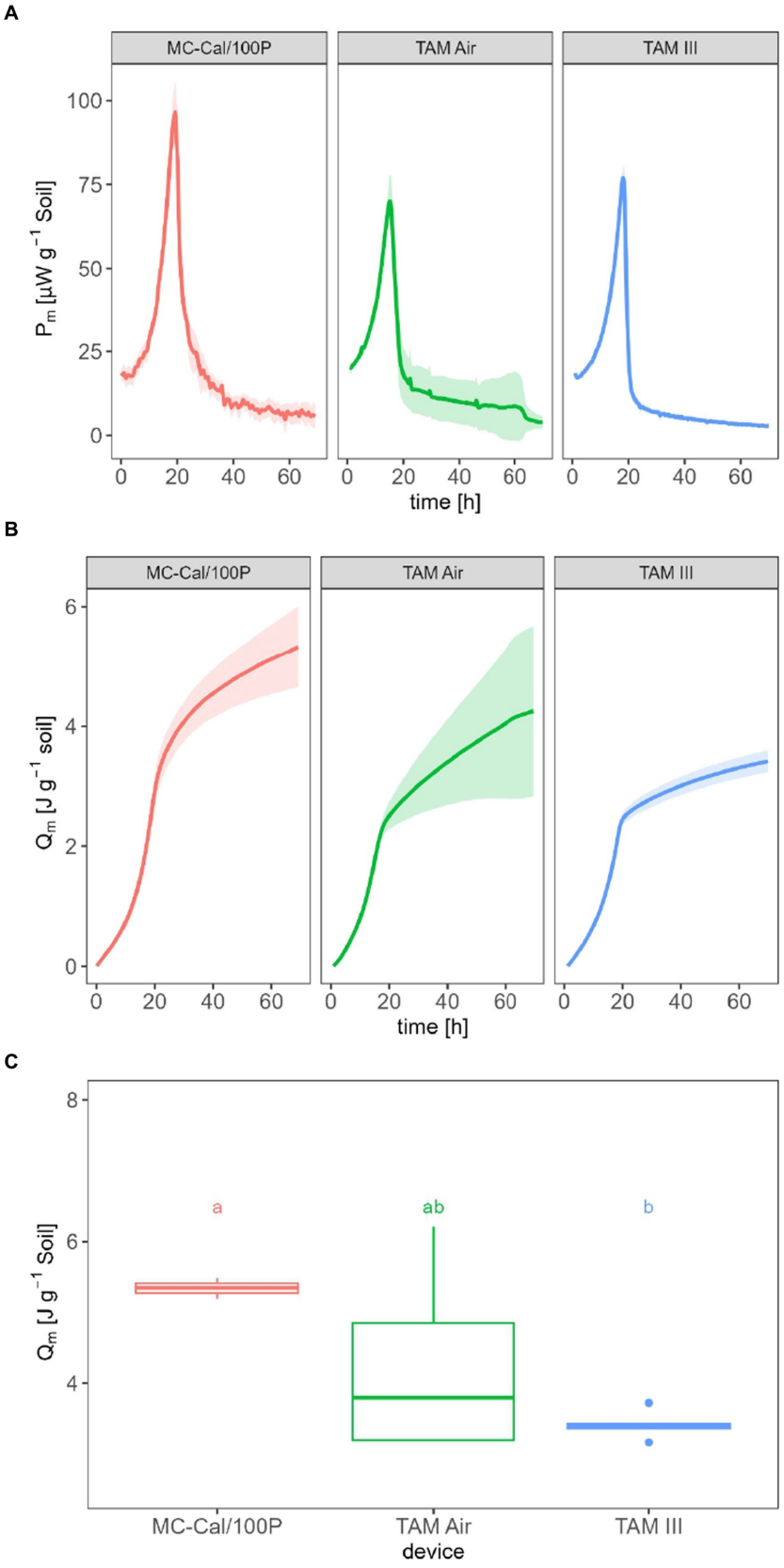

FIGURE 2
Specific heat production rate $P_{m,SG}$ **(A)**, specific heat Q_m **(B)** and Q_m after 70 h of glucose-amended soil for the three applied calorimeters with different LOD_V **(C)**.

the discontinuities caused by opening of the ampoule were mathematically treated by a linear interpolation of the signal during this time. However, if we focus on the interpolated signal, there was no statistically significant difference between the permanently un-aerated and transiently aerated treatments. The maximum $P_{m,SG}$ for the un-aerated treatment was (71.4 ± 19.8) μW g^{-1} after 18.9 h, and (84.8 ± 11.7) μW g^{-1} after 18.7 h for the aerated treatment (Figure 3A). Q_m for the un-aerated and aerated treatment was (3.62 ± 0.84) J g^{-1} and (4.02 ± 1.22) J g^{-1} after 70 h (Figure 3B), respectively. Q_m does not show a significant difference (Figure 3C).

3.4 Influence of the aeration on the calorimetrically derived CO_2 evolution rate

The following comparison intends to reveal the impact of aeration of calorimetric ampoules on the calculation of calorimetrically derived CER. This comparison was done with the same instrument (TAM III) and glucose concentration as in the previous experiment. The opening of ampoules led to an increase in peak $P_{m,SG}$ for soil amended with glucose (87.1 μW g^{-1} at t = 18.7 h) compared with un-aerated ampoules (74.5 μW g^{-1} at t = 19.0 h) but a decrease in peak $P_{m,SG}$ for soil amended with glucose equipped with CO2 traps (88.0 μW g^{-1} at t = 18.3 h) in comparison with un-aerated ampoules (105 μW g^{-1} at t = 19.7 h) as shown in Figure 4A.

The CER was calculated according to Eq. 11. In the un-aerated ampoules, the CER reached a peak maximum of 4.47·10^{-7} mmol s^{-1} g^{-1} at t = 20.3 h. In the aerated case, the CER decreased below 0 since t = 10.7 h and increased until the peak value, which equals 1.24·10^{-7} mmol s^{-1} g^{-1} at t = 21 h, which was approx. 25% of CER in the un-aerated systems. After approx. 25 h, CER for un-aerated systems tended to around 0 mmol s^{-1} g^{-1} whereas CER for un-aerated system remained at approx. 5.00·10^{-8} mmol s^{-1} g^{-1}.

3.5 Calorespirometric ratio of dynamic or integrated signals

The CR was calculated either from P (Eq. 9) or Q (Eq. 10) observed during the exponential growth phase. The CR was 568 kJ mol^{-1} and 578 kJ mol^{-1} during exponential phase (8.48–19.0 h) for P-derived and Q-derived method, respectively (Figure 5A). Figure 5B shows that there is no statistically significant difference between the CR ratio calculated by both methods. The distribution of all CR data points also reflects the dispersion of this value around the average CR. Nevertheless, CR derived from the heat production rate started to decrease to 108.8 kJ mol^{-1} and then increased sharply again. CR derived from total heat presented a slight and smooth drop, it reached approx. 375 kJ mol^{-1} after 30 h. For CR, we focus on the first 30 h only, because thereafter, both the heat signal as well as the calorimetrically derived CER had dropped so much that only a very uncertain CR ratio resulted.

4 Discussion

Independent of the technical, preparative and data processing level of the calorimetric measurements, calorimetry delivers reliable and accurate key parameters such as $\Delta_r H$ for a better understanding of the relations between matter and energy fluxes in soil systems. Other essential key parameters such as CUE, CR, CER, and μ_{app}, can reliably and practically be derived from calorimetric measurements for growth on rapidly metabolized substrates.

However, if over- and misinterpretations of calorimetric results are to be avoided in future thermodynamic soil research, the following questions need to be addressed. How accurately can the respective parameters be determined under the best measuring conditions? What influences do technical conditions, sample preparation and data evaluation exert on the results? What are the consequences of the calorimetric measurement accuracy for the derived parameters such as CUE, CR, CER, EUE, μ_{app}, and η_A? This will be discussed in the following using the respective parameters.

4.1 Kinetic data interpretation

In principle, P corresponds to the product of a reaction rate and the associated reaction enthalpy (Eq. 3). $\Delta_r H$ is linked to the reaction stoichiometry via the law of Hess (Eq. 5). Calorimetric experiments thus provide both kinetic and stoichiometric information. Here, we first discuss the kinetic information expressed by μ_{app}, calculated from the heat production rates during the exponential growth phase. Table 4 shows μ_{app} with the corresponding error for the different IMCs with respective LOD_V. All calorimetrically derived μ_{app} values are similar and exhibit good agreement within the range reported in previous studies with comparable experimental setups (Barros et al., 2000; Koga et al., 2003). Comparison with literature values has its limits because the kinetics of soil processes depend on physical conditions, microbial communities, SOM, minerals etc. However, our values (Table 4) are in the upper range of the literature data from 0.035 h^{-1} to 0.157 h^{-1} (Barros et al., 2000). The μ_{app} values derived from the instruments with a low and medium LOD_V (TAM III and TAM Air) cannot be statistically distinguished. However, the μ_{app} value obtained from MC-Cal/100P was significantly higher than the value derived from the TAM III (Table 4). Our observed variations in μ_{app} are assumed to be influenced by the interactive effects of the calorimeter's thermal limits of detection and the sample sizes employed, which are expressed by the parameter LOD_V. The literature data used for the comparison of μ_{app} were determined using a TAM 2277 with a thermal LOD of 0.15 mW and a calorimetric vessel of 5 mL and therefore a LOD_V of 30 mW L^{-1}. The difference in signal drift between TAM III (< 0.2 μW over 24 h) and MC-Cal/100P (< 40 μW over 24 h) could be a further reason for the observed deviation.

4.2 Determination of the metabolic heat

The second point to be discussed is the metabolic heat. In the case of Q_m, the results obtained with the IMCs with different LOD_V are within a small range, spanning from 3.42 to 5.34 J g^{-1} (Figure 2). By considering the amendment of 900 μg (0.005 mmol) of glucose per g-DW soil or 0.0043 mmol per g-wet soil and the combustion enthalpy of glucose (−2,808 kJ mol^{-1}) (Kabo et al., 2013), a maximum enthalpy input into the soil of 12.1 J g^{-1} can be calculated. Assuming that (i) the difference between these energy values represents the energy content of freshly formed biomass, (ii) all added glucose is completely

10.3389/fmicb.2024.1321059

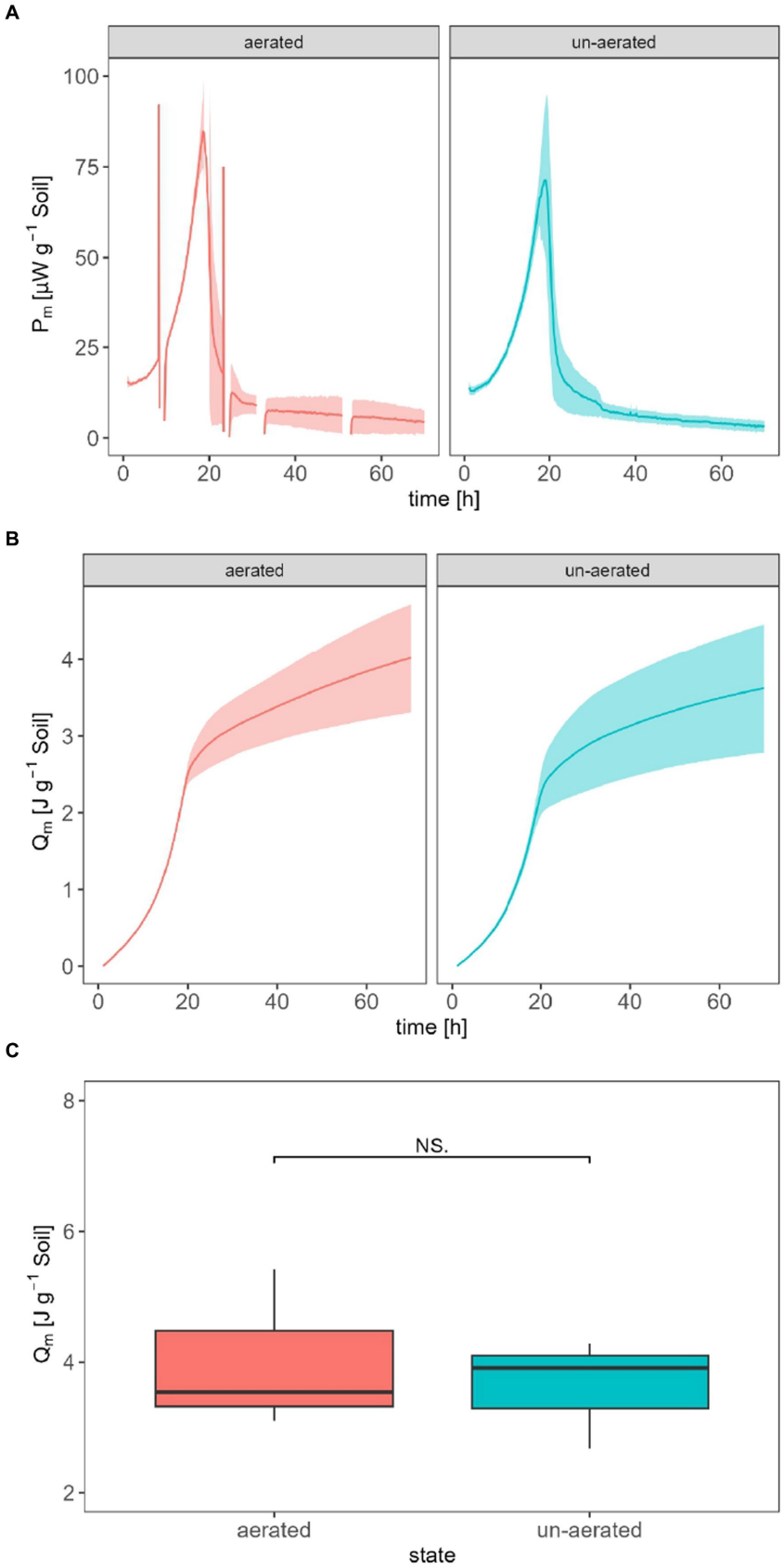

FIGURE 3
Influence of aeration on the specific heat production rate $P_{m,SG}$ **(A)**, the specific heat Q_m **(B)**, and the statistic comparison of Q_m after 70 h for aerated and un-aerated treatment **(C)**.

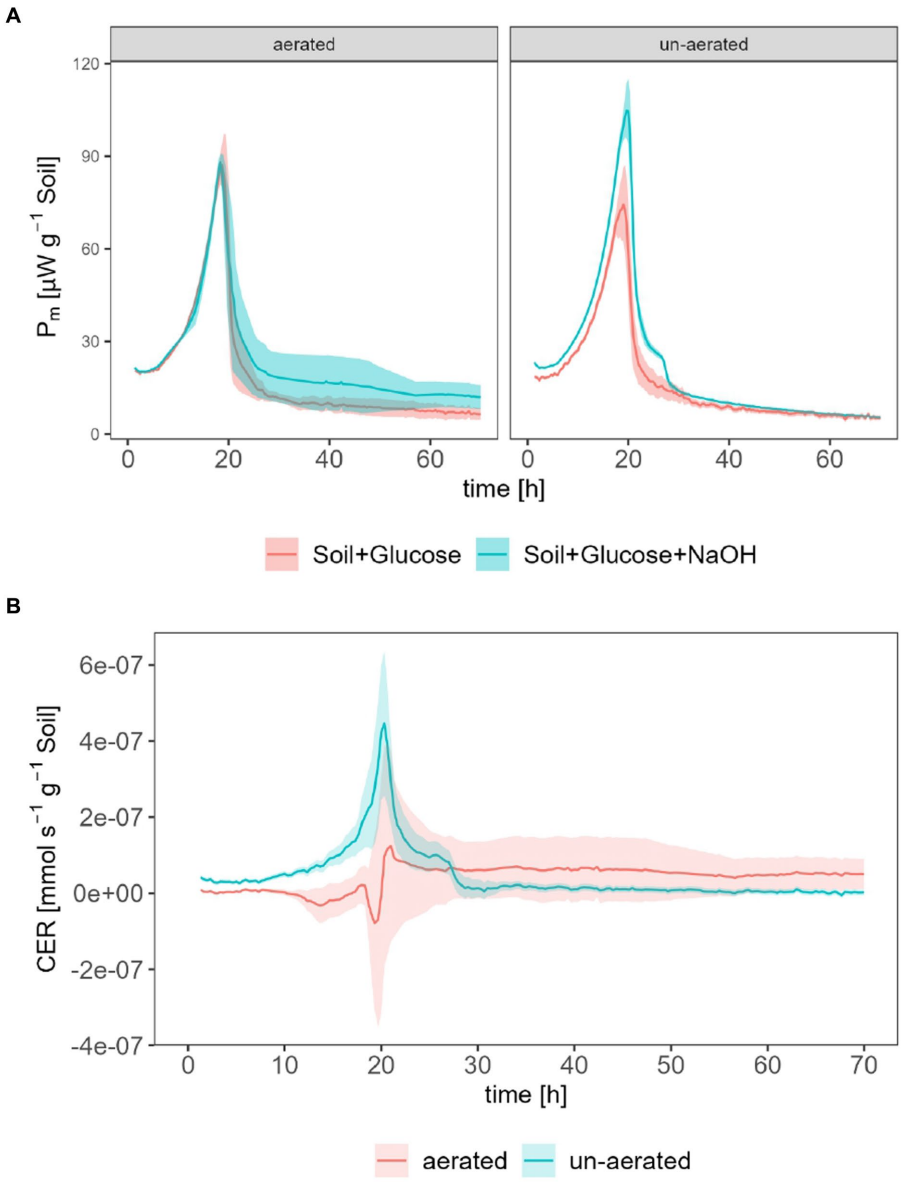

FIGURE 4
Calorimetrically derived CER; **(A)** shows P_m for measurements with ($P_{m,SGN}$) and without ($P_{m,SG}$) CO_2 traps for aerated and un-aerated systems, **(B)** shows the derived CER for aerated and un-aerated systems.

consumed, and (iii) energy contributions from SOM or necromass can be neglected, an energy use efficiency (EUE) between 55.9 and 71.7% is obtained using Eq. 6. These values are at the upper end of reported data in soil, which range from 15.6 to 63.1% (Barros and Feijoo, 2003).

Significant differences in Q_m were observed between MC-Cal/100P and TAM III, as depicted in Figure 2C. Once again, the different LOD_V values can be considered as potential reasons for these discrepancies. Therefore, it is recommended to use the instrument with the lowest LOD_V provided that the size of the soil sample is large enough to obtain homogeneous replicates.

Aeration of the calorimetric ampoules may be necessary to replenish the consumed oxygen and remove the evolved CO_2 to prevent adverse effects on microbial activities (Figure 6). It has already been reported that oxygen depletion and the accumulation of CO_2 in the headspace inhibit microbial activity (Neilson and Pepper, 1990). Figure 3A demonstrates that aeration introduces some thermal disturbances causing discontinuities in the thermal signal; however, no statistically significant difference was observed between aerated and non-aerated measurements (Figure 3C). This is surprising as about three-fourth (75%) of the oxygen in the ampoules might have been used assuming complete mineralization of the added glucose (see Table 2). Such a strong reduction of the oxygen concentration should have resulted in a decrease in aerobic microbial activity and a shift toward anaerobic processes, which should have been reflected in the heat signal. Obviously, a sufficiently large soil volume remained aerobic to support the observed unchanged heat production. During the integration of the heat production rate, the disturbances were mathematically treated by linear interpolations between the undisturbed signals, making data evaluation more complex. Hence, whenever possible, it is advisable to avoid opening the ampoules. To

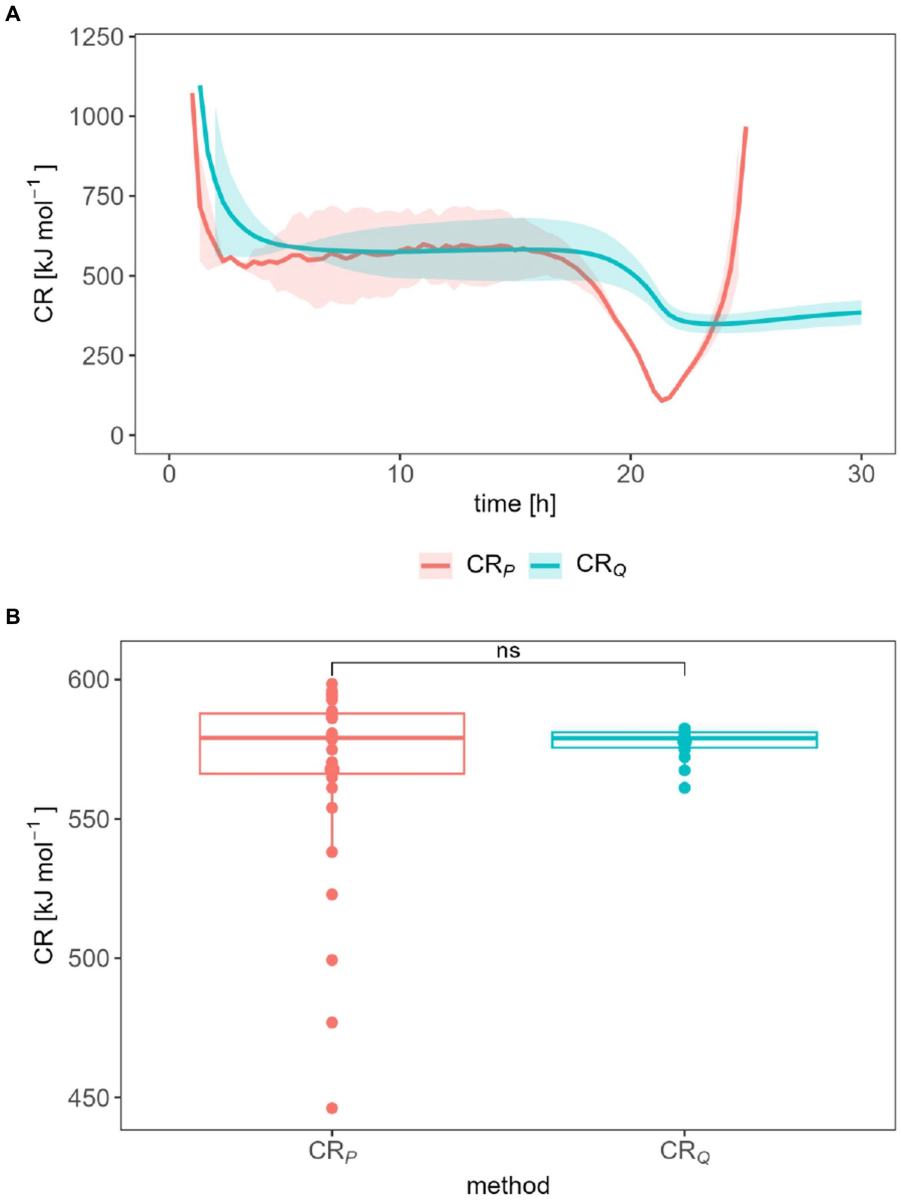

FIGURE 5
Influence of the data treatment on the CR **(A)** and statistical measurement error of the CR determination **(B)** during the exponential growth phase.

make decisions regarding whether an ampoule should be aerated or not, the calculations discussed in section 2.1 can be consulted.

4.3 Determination of the carbon dioxide evolution rate in the calorimeter

The shape of the calorimetrically derived CER, as depicted in Figure 4, supports the concept of utilizing the difference in heat production rates with (P_{SGN}) and without (P_{SG}) CO_2 traps in closed systems. However, during the exponential growth phase, inconsistencies were observed in the calorimetrically derived CO_2 values for regularly opened ampoules, particularly with unexpectedly negative values of CER. While the exact reasons for these observations are unknown, several factors may have contributed. Firstly, the aeration of channels led to temperature fluctuations in response to the ambient environment, resulting in arbitrary and unpredictable heat production rate measurements (up to 0.45 W) within a short time (approx. 2 h). This necessitated omission of data and interpolation, introducing the potential for manual and non-reproducible errors during the data analysis process. Additionally, the calorimeter required a certain amount of time to return to its original signal level following the opening of calorimetric ampoules and returning to measuring channels. This delay in returning to the original signal level could potentially introduce deviations in the measured data, particularly for short-term experiments. Furthermore, previous studies confirmed this deviation in CER by inserting and removing CO_2 traps at a regular time interval (Barros et al., 2011). These findings align with the observations made in this study regarding inconsistencies in the calorimetrically determined CER.

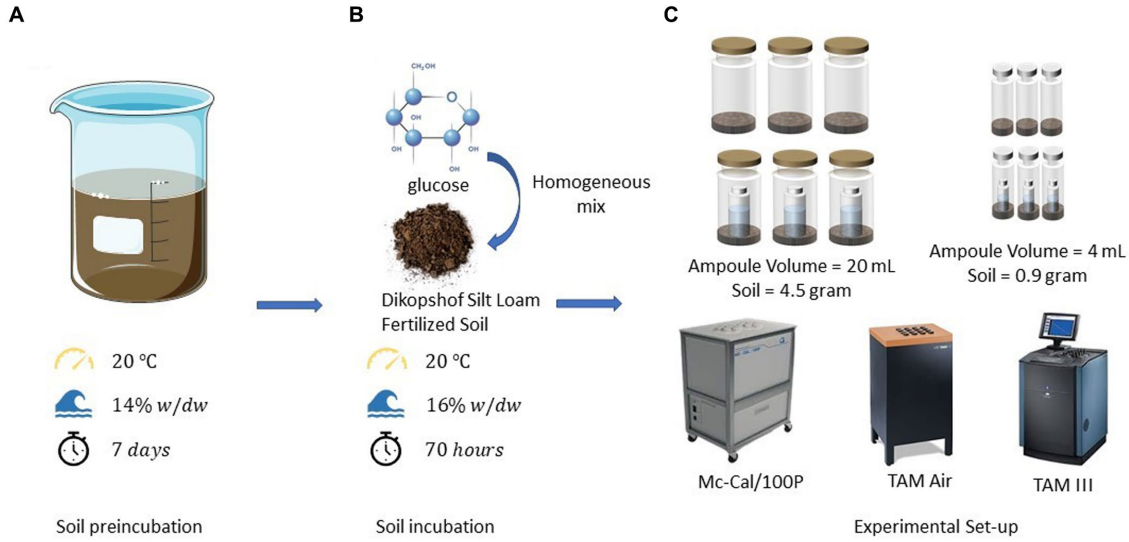

FIGURE 6
(A) Pre-incubation conditions and duration of the experiments, **(B)** environmental conditions, procedures, materials, and durations for soil incubations, and **(C)** experimental set-ups and devices utilized in calorimetric incubation experiments.

Another significant factor to consider is the act of opening the ampoules, which exchanges the air inside the ampoule with ambient air (as shown in Figure 6). These two atmospheres both differ in temperature and water content. When the ampoule is closed again, this can lead to the evaporation of water, resulting in an associated endothermic effect. The highest endothermic impact of opening the ampoule (15.3 μW) was observed in experiments involving glucose and the CO_2 trap. Using the evaporation enthalpy of water at 20°C (44.2 kJ mol^{-1}, Hodgman, 1951), we can estimate an evaporation rate of $0.35{\cdot}10^{-9}$ mol s^{-1} or $6.23{\cdot}10^{-9}$ g s^{-1}. The water content of the air space in the applied ampoule after water saturation, assuming equilibrium, is 17.3 g m^{-3} at 20°C (Hodgman, 1951), corresponding to $6.19{\cdot}10^{-5}$ g in the vial. Taking this value and dividing it by the evaporation rate results in an evaporation duration of 2.76 h. Consequently, the observed maximum endothermic deviation could explain a vaporization of 2.76 h until the saturation of completely dry air is achieved. Although this rough estimate does not take into account the substantial water content in the soil sample (0.144 g), as its vaporization extent is more difficult to estimate, it emphasizes the importance of water evaporation on the heat signal.

Lastly, the absorption of CO_2 by NaOH leads to a reduced partial pressure of CO_2. This reduction has the potential to interfere with the growth of specific microorganisms that rely on CO_2 fixation as a vital component of their growth. However, due to the regular aeration, the system becomes dynamic, preventing CO_2 accumulation and avoiding limitations in O_2 availability for growth. These factors may contribute to varying outcomes in C mineralization, as observed in a study by Hopkins (2008). On the other hand, several studies have explored the comparison of respiration rates in soil systems between well-aerated and static closed systems. Their findings demonstrated that well-aerated systems yielded higher respiration rates than static closed systems (Sakamoto and Yoshida, 1988; Jensen et al., 1996; Rochette et al., 1997; Suh et al., 2006).

It is important to consider these factors when interpreting and analyzing the CO_2 data in closed, static calorimetric experiments, as they can introduce uncertainties and potential sources of error. To sum up, it is not advisable to aerate the ampoules during experiments when oxygen is not a limiting factor for soil microorganisms. Opening the ampoules can introduce biases in the calorimetrically derived CO_2 results, affecting the accuracy and reliability of the measurements. The question of whether oxygen could potentially be limiting can be estimated by calculating the oxygen content of the ampoule.

To achieve simultaneous measurement of *P* and CO_2 with minimal disturbance, it is necessary to explore alternative approaches. The combination of the calorimetric measurement principle with a Warburg apparatus might be a solution. The conventional Warburg apparatus is a device for measuring the pressure of a gas at constant volume and constant temperature so that the pressure is a measure of the quantity of gas and changes in pressure reflect the production and absorption of gas (Oesper, 1964). Another option might be the incorporation of a CO_2 sensor into the calorimetric ampoule, if the potential heat evolution of the sensor itself does not interfere with the measuring signal. Wadso (2015) developed a new calorimetric-respirometric ampoule using a valve on the ampoule that allows opening and closing (aeration) inside the calorimeter for short-term processes. As a result, the calorimetric measurement is not disturbed and gives more reliable results. Calorimetric ampoules need to be covered to prevent water evaporation interfering with the calorimetric signal by the large evaporation enthalpy of water. However, the calorimetric ampoule could be closed with gas separation membranes being impermeable to water but allowing the transport of oxygen (Valappil et al., 2021). Both ideas could be part of future calorespirometer developments.

4.4 Influence of data evaluation on the calorespirometric ratio

The CR shows a similar range between 100 and 1,200 kJ mol^{-1} and trends regardless of the evaluation method used. CR between 0 and

600 kJ mol^{-1} and extreme values of 1,500 kJ mol^{-1} are reported (Hansen et al., 2004). The CR value drops in the first 3 h and is then approximately constant until the 18th or 20th hour. When the heat production rate decreases, so does the CR. After the 20th to 21st hour, the CR (derived from the heat production rate) increases or remains constant at about 375 kJ mol^{-1}. Thus, our trend is similar to those observed by Barros et al. (2010). The CR drop at the beginning of the measurement should be considered carefully. Currently, both signals (P_m and CER or Q_m and accumulated CO_2) are very small and thus the quotient of the two quantities is strongly error prone. The same applies to the signals after the 20th hour. The constant average CR of 577.7 kJ mol^{-1} (from Q_m) or 567.6 kJ mol^{-1} (from P_m) speaks for a constant growth stoichiometry. For these values, the signal evaluation seems to be without relevance.

4.5 Limitations of the informative content of the calorespirometric ratio

Assuming an aerobic metabolism and the validity of the oxycaloric equivalent (−455 kJ mol^{-1} O_2) (Gnaiger and Kemp, 1990), the CUE can be calculated from the measured CR (Hansen et al., 2004; Colombi et al., 2022). For that purpose, we extended the equation of Hansen et al. (2004) by including the enthalpy of the nitrogen source (NH_4^+, Eq. 13) to complete the energy balance. The derivation of Eq. 13. is provided in the supporting material.

$$CUE = \frac{\frac{4 \cdot CR}{455\ \text{kJ mol}^{-1}} - \gamma_S}{n_N^X \cdot \gamma_N - \gamma_X + \frac{4 \cdot CR}{455\ \text{kJ mol}^{-1}}} \quad (13)$$

Here γ_S, γ_N, γ_X stand for the relative degree of reduction of the substrate, the nitrogen source, and the biomass, respectively. n_N^X stands for the molecular nitrogen content of biomass. If we now ask ourselves what measurement accuracy is required for CR in the context of this theory in order to achieve a certain accuracy for CUE, we need to look at the derivative of CUE with respect to CR (Eq. 14).

$$\Delta CR = \left|\frac{dCR}{dCUE}\right| \Delta CUE = \left|\frac{n_N^X \cdot \gamma_N - \gamma_X + \gamma_S}{4 \cdot (1 - CUE)^2} \cdot 455\ \text{kJ mol}^{-1}\right| \Delta CUE \quad (14)$$

Figure 7 depicts this relation and the uncertainty (assuming that the CUE needs to be determined with 5% accuracy) for two different biomass compositions. We considered two elemental biomass compositions because the C/N in soil microbial biomass is different from that growing in liquid culture. A C:N ratio of 7:1 is a generally accepted average for soil (Xu et al., 2013; Mooshammer et al., 2014). Different biomass compositions cause different γ_X and thus different combustion enthalpies of the biomass (see SM). $C_1H_{1.6}O_{0.5}N_{0.25}$ is suggested for bacteria growing in liquid culture in bioreactors (Babel et al., 1993), while $C_1H_{1.571}O_{0.429}N_{0.143}$ takes the C/N ratio in soil microbial biomass into account.

The average CR we obtained from heat measurements was 577.7 kJ mol^{-1}, and CR from heat production rate measurements was 567.6 kJ mol^{-1}. These values correspond to CUE values of 0.878 or 0.868, respectively, which seem unrealistically high. These calculations were based on a biomass composition of $C_1H_{1.6}O_{0.5}N_{0.25}$. However, when considering a biomass composition of $C_1H_{1.571}O_{0.429}N_{0.143}$, such high CR values become simply impossible. Qiao et al. (2019) reports about a wide range of CUE with a global average of 0.5 ± 0.25. However, the CUE obtained with glucose also depended on the applied method. For instance, the CUE tended to be lower (<0.4) under identical incubation conditions using ^{18}O incorporation and stoichiometric modeling. Substrate-dependent ^{13}C-based methods, calorespirometry, and metabolic flux modeling provides often higher CUE (>0.6) (Geyer et al., 2019). Barros et al. (2010) reported CUE values in the range of 0.75–0.77 applying the same method as in our study. Neglecting the simultaneous metabolism of SOM components could be a potential reason for the high CUE values derived from Eq. 13.

Furthermore, Eq. 13 assumes that oxygen is the terminal electron acceptor. Therefore, it is only applicable in oxic, non-water-saturated soils, where glucose and other sugars derived from starch or (hemi-) celluloses are mainly oxidized with oxygen as the terminal electron acceptor.

In soils under partially anoxic conditions, the theory cannot be applied. Soil redox conditions can strongly fluctuate both temporarily and spatially. For instance, after (heavy) rain events, the topsoil becomes partly water-saturated for a period, leading to a quick limitation of oxygen. Furthermore, anoxic conditions can exist even at microsites in soil due to the combination of high microbial activities and slow oxygen diffusion. The influence of anaerobic metabolism on CR will be discussed below using a combination of the acetate fermentation ($C_6H_{12}O_6 + 2H_2O \rightarrow 2C_2H_4O_2 + 2CO_2 + 4H_2$) with the acetogenesis ($2CO_2 + 4H_2 \rightarrow C_2H_4O_2 + 2H_2O$) yielding the reaction shown in Eq. 15. Acetate is a good example because it is often formed in soil under anoxic conditions. In order to analyze the influence of the transition from oxic to anoxic conditions on the CR, we consider the combination of the catabolic oxic glucose oxidation and anoxic conversion to acetate expressed as the degree of anaerobiosis, η_A, ranging from 0 (complete oxic conditions) to 1 (complete anoxic conditions) (Figure 8, Eq. 15). The $\Delta_{OX}H$ represents the combustion enthalpy of glucose (−2813.6 kJ mol^{-1}) and $\Delta_{ANOX}H$ were calculated using the law of Hess [−((3·-873.4) +2813.6) = −193.4 kJ mol^{-1}] and the combustion enthalpy of glucose and of acetate (−873.4 kJ mol^{-1}). The combustion enthalpies of compounds in the water dissolved state was taken from (von Stockar et al., 1993).

Oxic metabolism: $C_6H_{12}O_6 + 6\,O_2 \rightarrow 6CO_2 + 6\,H_2O$, $\Delta_{OX}H = -2813.6$ kJ / mol

Anoxic metabolism: $C_6H_{12}O_6 \rightarrow 3CH_3COOH$, $\Delta_{ANOX}H = -193.4$ kJ / mol

$$CR = \frac{\eta_A \cdot \Delta_{ANOX}H + (1 - \eta_A) \cdot \Delta_{OX}H}{(1 - \eta_A) \cdot 6} \quad (15)$$

The maximum error of CR caused by the error of η_A is estimated using Eq. 16.

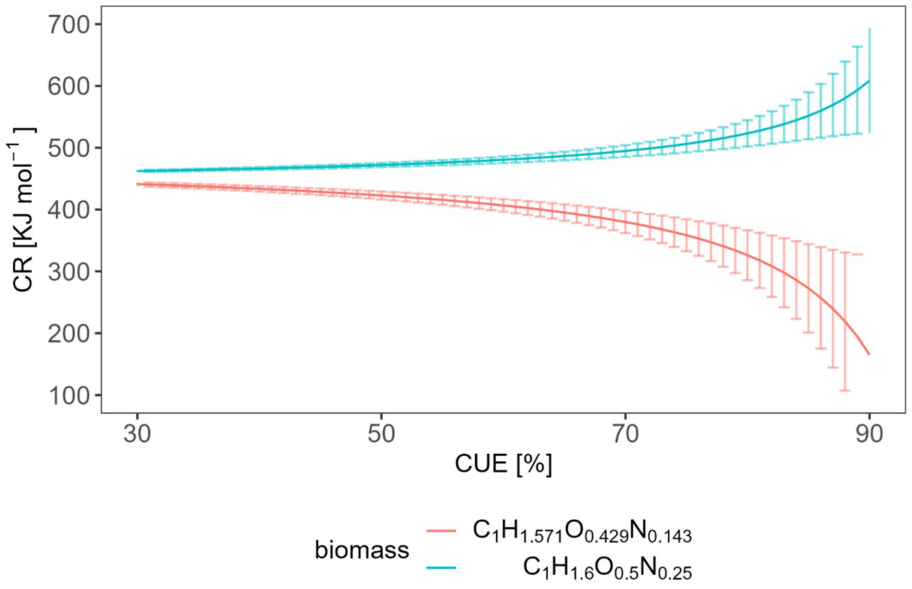

FIGURE 7
Expected relation and uncertainty between the CR and the CUE with two different biomass compositions.

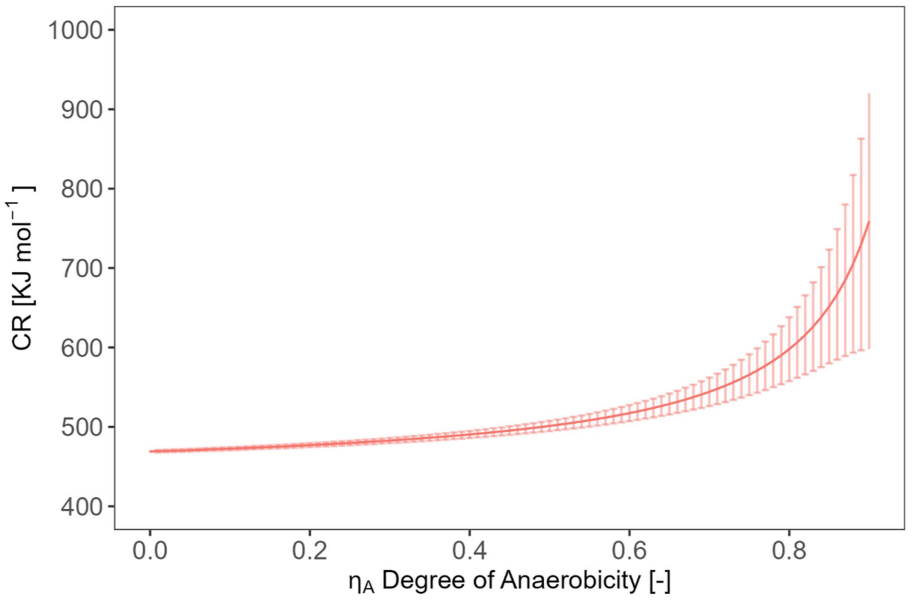

FIGURE 8
Expected relation and uncertainty between the CR and the degree of anaerobicity.

$$\Delta CR = \left|\frac{\mathrm{d}CR}{\mathrm{d}\eta_A}\right| \Delta\eta_A = \left|\frac{\Delta_{ANOX} H}{6(1-\eta_A)^2}\right| \Delta\eta_A \qquad (16)$$

Our simple model (Eqs. 14, 16) allows estimating the required accuracy in measuring CR to obtain statements with an error < 5% on CUE or η_A. For example, if we aim to determine a typical CUE of 0.5 with 5% error for a biomass composition $C_1H_{1.6}O_{0.5}N_{0.25}$, we will need to measure a CR value with an accuracy of (472.1 ± 3.4) kJ mol^{-1}. In the case of a biomass composition of $C_1H_{1.571}O_{0.429}N_{0.143}$, a CR value of (422.8 ± 6.4) kJ mol^{-1} would be required. Similarly, if our goal is to calculate η_A with a value of 0.5 and 5% error using CR, we should be able to measure CR values with an accuracy of (501.2 ± 10.1) kJ mol^{-1} (assuming a biomass composition of $C_1H_{1.6}O_{0.5}N_{0.25}$). However, the actual measuring error is 5.52 kJ mol^{-1} using the integrated values or 21.6 kJ mol^{-1} using the rates (interquartile range). The measuring error obtained with integrated value falls within the range of requirements while using the rates not fit the requirement. It is important to note that the substrate we analyzed in our test had a high conversion rate, which

may have contributed to these relatively favorable evaluations. More complex substrates with lower energy content or slower conversion rates will lead to smaller signals which are more influenced by the signal noise and more difficult to integrate. Such material calls for higher accuracy in measuring CR to achieve the desired precision in estimation CUE and η_A.

In conclusion, the simple model offers valuable insights into the required measurement accuracy for determining CUE or η_A with a given error margin. However, the complexity of real-world scenarios, including variations in biomass composition and substrate characteristics, demands careful consideration and further investigation to ensure accurate and reliable estimations as well as striving for the development of improved calorespirometers.

5 Conclusion

The calorimetric determination of the apparent specific growth rate μ_{app}, the metabolic heat Q simultaneously with the CER via CO_2 trap method is possible and provides plausible data for an easily degradable substrate (e.g., glucose) added to the soil. However, several variables affect the results. Firstly, volume-related declared thermal limit of detection (LOD_V) represents the integrated effect of thermal calorimeter sensitivity and sample size. In order to obtain more reliable and reproducible data, it is recommended to use an IMC with a low LOD_V. For calorimeters with a comparable LOD_V, the instrument with a larger calorimetric ampoule should be preferred to better cover soil heterogeneities and to achieve results representative for the soil under study.

Regular aeration of the calorimetric vessel is considered as a method to counteract oxygen depletion. Despite the thermal disturbances caused by this, no significant differences in the thermal signal were observed between analyses with and without regular aeration. However, in the case of the simultaneous measurement of P and CER, the difference between the two calorimetric signals with and without CO_2 traps must be evaluated. In such cases, the aeration of the calorimeter causes a significant error.

Equation 13 shows a tight link between the CR and the CUE. The comparison between accuracy requirements from this model for CR with the real errors of determination reveals that only in the best case the currently available instruments are sensitive enough to infer the CUE from the CR. The same holds true for the link between the CR and the proportion of anaerobic processes from the CR. With more complex substances such as polymeric carbohydrates, plant debris, non-viable bacteria, chitin etc., slower mass conversions and thus more error-prone CR values are to be expected. This means that novel types of calorimeters should be developed that either have better thermal sensitivity or allow larger soil samples to be measured. The second point is significant because a larger soil sample size can counteract the influence of soil heterogeneity on the thermal signal and is probably technically the most feasible. Furthermore, larger calorimetric ampoules facilitate the insertion of gas sensors for a better combination of calorimetry and respirometry. The analysis of small samples, however, might be interesting for the study of processes in selected microhabitats, e.g., the rhizosphere or different aggregate fractions.

The discrepancies between the CUE values or η_A derived from the experimental CR values and the expectations from the models of Hansen et al. (2004) and Chakrawal et al. (2020) result from the simplifying basic assumptions of both models, which are discussed in section 4.5. This argues for the application of more complex numerical models, which include a certain proportion of anaerobic reactions, the usage of energy and "building blocks" from the SOM, the interaction of the OM with soil minerals, etc. The extension of the models to other factors will provide a better understanding of the intricate processes influencing carbon and energy utilization in soil systems.

The surprising result that a small variation of the elemental biomass composition can even change the trend of the CUE/CR relation shows that changes in the microbial community may not only affect the kinetics of the matter and energy fluxes as expected but also the process stoichiometry and thus the CUE/CR relation. Consequently, future numerical models should also take this effect into account.

List of symbols

Symbol	Property	Unit
CER	CO_2 evolution rate	$mol\,g^{-1}\,s^{-1}$
CR	Calorespirometric ratio	$J\,mol^{-1}$
CUE	Carbon use efficiency	$mol\,mol^{-1}$
DW	Dry weight	g
EUE	Energy use efficiency	$J\,J^{-1}$
LOD_V	Volume-related thermal limit of detection	$W\,L^{-1}$
P	Heat production rate	W
P_m	Specific metabolic heat production rate	$W\,g^{-1}$
Q	Heat	J
Q_m	Specific total metabolic heat	$J\,g^{-1}$
(S)OM	(Soil) Organic matter	g
WHC	Water holding capacity	$g\,g^{-1}$
$\Delta_{abs}H$	Enthalpy of absorption	$J\,mol^{-1}$
$\Delta_c H$	Combustion enthalpy	$J\,mol^{-1}$
$\Delta_r H$	Reaction enthalpy	$J\,mol^{-1}$
η_A	Degree of anaerobicity	---
μ_{app}	Apparent specific growth rate	s^{-1}
Subscripts	**Meaning**	
a	aerated	
G	Glucose added	
N	Equipped with CO_2 trap (NaOH)	
S	Soil	
u	un-aerated	

Data availability statement

The link with the datasets is the following: https:/doi.org/10.48758/ufz.14030.

Author contributions

SY: Conceptualization, Data curation, Formal analysis, Investigation, Methodology, Validation, Visualization, Writing – original draft. ED: Conceptualization, Data curation, Formal analysis, Investigation, Methodology, Validation, Visualization, Writing – original draft. AR: Data curation, Writing – review & editing. HH: Supervision, Writing – review & editing. CF: Supervision, Writing – review & editing, Visualization. AM: Supervision, Writing – review & editing. MK: Supervision, Writing – review & editing. TM: Conceptualization, Data curation, Funding acquisition, Project administration, Supervision, Writing – review & editing.

Funding

The author(s) declare financial support was received for the research, authorship, and/or publication of this article. This work was funded by the Helmholtz-Centre for Environmental Research UFZ and the German Research Foundation (SPP2322) with the projects: DFG-TherMic (MI 598/9-1; MA 3746/8-1), and DFG-DriverPool (MA 3746/9-1, SCHA 849/22-1).

Acknowledgments

We wish to thank Sven Paufler (UFZ, Department of Environmental Microbiology) for technical support. For this work, data obtained within the DFG Priority Program 2322 "SoilSystems" has been used. Soils were provided by S. J. Seidel and H. Hüging (University of Bonn, Germany). We would also like to thank the three reviewers who contributed significantly to improving the readability of the article.

Conflict of interest

The authors declare that the research was conducted in the absence of any commercial or financial relationships that could be construed as a potential conflict of interest.

The author(s) declared that they were an editorial board member of Frontiers, at the time of submission. This had no impact on the peer review process and the final decision.

Publisher's note

Supplementary material

The Supplementary material for this article can be found online at: https://www.frontiersin.org/articles/10.3389/fmicb.2024.1321059/full#supplementary-material

References

Assael, M. J., Maitland, G. C., Maskow, T., Wakeham, W. A., and Will, S. (2023) *Commonly asked questions in thermodynamics*. Boca Raton, London, New York: CRC Press

Babel, W., Brinkmann, U., and Muller, R. H. (1993). The auxiliary substrate concept-an approach for overcoming limits of microbial performances. *Acta Biotechnol.* 13, 211–242. doi: 10.1002/abio.370130302

Barros, N., and Feijoo, S. (2003). A combined mass and energy balance to provide bioindicators of soil microbiological quality. *Biophys. Chem.* 104, 561–572. doi: 10.1016/S0301-4622(03)00059-0

Barros, N., Feijóo, S., and Hansen, L. D. (2011). Calorimetric determination of metabolic heat, CO2 rates and the calorespirometric ratio of soil basal metabolism. *Geoderma* 160, 542–547. doi: 10.1016/j.geoderma.2010.11.002

Barros, N., Feijóo, S., Simoni, A., Critter, S. A. M., and Airoldi, C. (2000). Interpretation of the metabolic enthalpy change, ΔHmet, calculated for microbial growth reactions in soils. *J. Therm. Anal. Calorim.* 63, 577–588. doi: 10.1023/A:1010162425574

Barros, N., Salgado, J., Rodríguez-Añón, J. A., Proupín, J., Villanueva, M., and Hansen, L. D. (2010). Calorimetric approach to metabolic carbon conversion efficiency in soils. *J. Therm. Anal. Calorim.* 99, 771–777. doi: 10.1007/s10973-010-0673-4

Blagodatsky, S. A., and Richter, O. (1998). Microbial growth in soil and nitrogen turnover: a theoretical model considering the activity state of microorganisms. *Soil Biol. Biochem.* 30, 1743–1755. doi: 10.1016/S0038-0717(98)00028-5

Braissant, O., Wirz, D., Goepfert, B., and Daniels, A. U. (2010). Use of isothermal microcalorimetry to monitor microbial activities. *FEMS Microbiol. Lett.* 303, 1–8. doi: 10.1111/j.1574-6968.2009.01819.x

Canfield, D. E., Kristensen, E., and Thamdrup, B. (2005). Thermodynamics and microbial metabolism. *Adv. Mar. Biol.* 48, 65–94. doi: 10.1016/S0065-2881(05)48003-7

Chakrawal, A., Herrmann, A. M., Šantrůčková, H., and Manzoni, S. (2020). Quantifying microbial metabolism in soils using calorespirometry — a bioenergetics perspective. *Soil Biol. Biochem.* 148:107945. doi: 10.1016/j.soilbio.2020.107945

Chaudhary, D. K., Khulan, A., and Kim, J. (2019). Development of a novel cultivation technique for uncultured soil bacteria. *Sci. Rep.* 9:6666. doi: 10.1038/s41598-019-43182-x

Colombi, T., Chakrawal, A., and Herrmann, A. M. (2022). Carbon supply–consumption balance in plant roots: effects of carbon use efficiency and root anatomical plasticity. *New Phytol.* 233, 1542–1547. doi: 10.1111/nph.17598

Crawford, A. (1788). *Experiments and observations on animal heat and the inflammation of combustible bodies* Johnson.

Criddle, R. S., Fontana, A. J., Rank, D. R., Paige, D., Hansen, L. D., and Breidenbach, R. W. (1991). Simultaneous measurement of metabolic heat rate, CO2 production, and O2 consumption by microcalorimetry. *Anal. Biochem.* 194, 413–417. doi: 10.1016/0003-2697(91)90250-W

Critter, S. A. M., Freitas, S. S., and Airoldi, C. (2001). Calorimetry versus respirometry for the monitoring of microbial activity in a tropical soil. *Appl. Soil Ecol.* 18, 217–227. doi: 10.1016/S0929-1393(01)00166-4

Dijkerman, J. C. (1974). Pedology as a science: the role of data, models and theories in the study of natural soil systems. *Geoderma* 11, 73–93. doi: 10.1016/0016-7061(74)90009-3

Fricke, C., Harms, H., and Maskow, T. (2019). Rapid calorimetric detection of bacterial contamination: influence of the cultivation technique. *Front. Microbiol.* 10:2530. doi: 10.3389/fmicb.2019.02530

Geyer, K. M., Dijkstra, P., Sinsabaugh, R., and Frey, S. D. (2019). Clarifying the interpretation of carbon use efficiency in soil through methods comparison. *Soil Biol. Biochem.* 128, 79–88. doi: 10.1016/j.soilbio.2018.09.036

Gnaiger, E., and Kemp, R. B. (1990). Anaerobic metabolism in aerobic mammalian cells: information from the ratio of calorimetric heat flux and respirometric oxygen flux. *Biochim. Biophys. Acta Bioenerg.* 1016, 328–332. doi: 10.1016/0005-2728(90)90164-Y

Gustafsson, L. (1991). Microbiological calorimetry. *Thermochim. Acta* 193, 145–171. doi: 10.1016/0040-6031(91)80181-H

Hansen, L. D., Macfarlane, C., Mckinnon, N., Smith, B. N., and Criddle, R. S. (2004). Use of calorespirometric ratios, heat per CO_2 and heat per O_2, to quantify metabolic paths and energetics of growing cells. *Thermochim. Acta* 422, 55–61. doi: 10.1016/j.tca.2004.05.033

Herrmann, A. M., and Bölscher, T. (2015). Simultaneous screening of microbial energetics and CO2 respiration in soil samples from different ecosystems. *Soil Biol. Biochem.* 83, 88–92. doi: 10.1016/j.soilbio.2015.01.020

Hodgman, C. D. (1951). Handbook of chemistry and physics. *LWW* 71:246. doi: 10.1097/00010694-195103000-00018

Hofelich, T., Wadsö, L., Smith, A. L., Shirazi, H., and Mulligan, S. R. (2001). The isothermal heat conduction calorimeter: a versatile instrument for studying processes in physics, chemistry, and biology. *J. Chem. Educ.* 78:1080. doi: 10.1021/ed078p1080

Hopkins, D. W. (2008). "Carbon mineralization" in *Soil sampling and methods of analysis*. 2nd ed. Eds. M. R. Carter and E. G. Gregorich (Taylor & Francis/CRC Press). 589–598.

Huging, H. (1904), Long-term experiment Dikopshof. in eds E. G. Gregorich and M. H. Beare. Available at: https://www.lap.uni-bonn.de/en/research/projects/long-term-experiment-dikopshof

Jensen, L. S., Mueller, T., Tate, K. R., Ross, D. J., Magid, J., and Nielsen, N. E. (1996). Soil surface CO2 flux as an index of soil respiration in situ: a comparison of two chamber methods. *Soil Biol. Biochem.* 28, 1297–1306. doi: 10.1016/S0038-0717(96)00136-8

Kabo, G. J., Voitkevich, O. V., Blokhin, A. V., Kohut, S. V., Stepurko, E. N., and Paulechka, Y. U. (2013). Thermodynamic properties of starch and glucose. *J. Chem. Thermodyn.* 59, 87–93. doi: 10.1016/j.jct.2012.11.031

Kästner, M., Miltner, A., Thiele-Bruhn, S., and Liang, C. (2021). Microbial necromass in soils—linking microbes to soil processes and carbon turnover. *Front. Environ. Sci.* 9:597. doi: 10.3389/fenvs.2021.756378

Kemp, R. B., and Guan, Y. (1997). Heat flux and the calorimetric-respirometric ratio as measures of catabolic flux in mammalian cells. *Thermochim. Acta* 300, 199–211. doi: 10.1016/S0040-6031(96)03125-5

Koga, K., Suehiro, Y., Matsuoka, S.-T., and Takahashi, K. (2003). Evaluation of growth activity of microbes in tea field soil using microbial calorimetry. *J. Biosci. Bioeng.* 95, 429–434. doi: 10.1016/S1389-1723(03)80040-3

Lavoisier, A. -L., and DeLaplace, P. (1994). Memoir on heat REad to the royal acedemy of sciences. *Obes. Res.* 2, 189–202. doi: 10.1002/j.1550-8528.194.tb00646.x

Lemmon, E. W., Jacobsen, R. T., Penoncello, S. G., and Friend, D. G. (2000). Thermodynamic properties of air and mixtures of nitrogen, argon, and oxygen from 60 to 2000 K at pressures to 2000 MPa. *J. Phys. Chem. Ref. Data* 29, 331–385. doi: 10.1063/1.1285884

Ljungholm, K., Norén, B., and Wadsö, I. (1979). Microcalorimetric observations of microbial activity in normal and acidified soils. *Oikos* 33, 24–30. doi: 10.2307/3544507

Maskow, T., and Paufler, S. (2015). What does calorimetry and thermodynamics of living cells tell us? *Methods* 76, 3–10. doi: 10.1016/j.ymeth.2014.10.035

Maskow, T., Schubert, T., Wolf, A., Buchholz, F., Regestein, L., Buechs, J., et al. (2011). Potentials and limitations of miniaturized calorimeters for bioprocess monitoring. *Appl. Microbiol. Biotechnol.* 92, 55–66. doi: 10.1007/s00253-011-3497-7

Mooshammer, M., Wanek, W., Zechmeister-Boltenstern, S., and Richter, A. (2014). Stoichiometric imbalances between terrestrial decomposer communities and their resources: mechanisms and implications of microbial adaptations to their resources. *Front. Microbiol.* 5, 1–10. doi: 10.3389/fmicb.2014.00022

Neilson, J. W., and Pepper, I. L. (1990). Soil respiration as an index of soil aeration. *Soil Sci. Soc. Am. J.* 54, 428–432. doi: 10.2136/sssaj1990.03615995005400020022x

Oesper, P. (1964). The history of the Warburg apparatus. *J. Chem. Educ.*:41.

Paufler, S., Weichler, M.-T., Harms, H., and Maskow, T. (2013). Simple improvement of the sensitivity of a heat flux reaction calorimeter to monitor bioprocesses with weak heat production. *Thermochim. Acta* 569, 71–77. doi: 10.1016/j.tca.2013.07.001

Pushp, M., Lönnermark, A., Hedenqvist, M., and Vikegard, P. (2021). Heat production in municipal and industrial waste as revealed by isothermal microcalorimetry. *J. Therm. Anal. Calorim.* 147, 8271–8278. doi: 10.1007/s10973-021-11117-2

Qiao, Y., Wang, J., Liang, G., Du, Z., Zhou, J., Zhu, C., et al. (2019). Global variation of soil microbial carbon-use efficiency in relation to growth temperature and substrate supply. *Sci. Rep.* 9:5621. doi: 10.1038/s41598-019-42145-6

Raynaud, X., and Nunan, N. (2014). Spatial ecology of bacteria at the microscale in soil. *PLoS One* 9:e87217. doi: 10.1371/journal.pone.0087217

Rochette, P., Ellert, B., Gregorich, E. G., Desjardins, R. L., Pattey, E., Lessard, R., et al. (1997). Description of a dynamic closed chamber for measuring soil respiration and its comparison with other techniques. *Can. J. Soil Sci.* 77, 195–203. doi: 10.4141/S96-110

Sakamoto, K., and Yoshida, T. (1988). In situ measurement of soil respiration rate by a dynamic method. *Soil Sci. Plant Nutr.* 34, 195–202. doi: 10.1080/00380768.1988.10415673

Schjønning, P., Mcbride, R. A., Keller, T., and Obour, P. B. (2017). Predicting soil particle density from clay and soil organic matter contents. *Geoderma* 286, 83–87. doi: 10.1016/j.geoderma.2016.10.020

Suh, S. U., Chun, Y. M., Chae, N. Y., Kim, J., Lim, J. H., Yokozawa, M., et al. (2006). A chamber system with automatic opening and closing for continuously measuring soil respiration based on an open-flow dynamic method. *Ecol. Res.* 21, 405–414. doi: 10.1007/s11284-005-0137-7

Sunner, S., and Wadsö, I. (1959). On the design and efficiency of isothermal reaction calorimeters. *Acta Chem. Scand.* 13, 97–108. doi: 10.3891/acta.chem.scand.13-0097

Trapp, S., Brock, A. L., Nowak, K., and Kästner, M. (2018). Prediction of the formation of biogenic nonextractable residues during degradation of environmental chemicals from biomass yields. *Environ. Sci. Technol.* 52, 663–672. doi: 10.1021/acs.est.7b04275

Ugalde-Salas, P., Desmond-Le Quéméner, E., Harmand, J., Rapaport, A., and Bouchez, T. (2020). Insights from microbial transition state theory on Monod's affinity constant. *Sci. Rep.*:10.

Valappil, R. S. K., Ghasem, N., and Al-Marzouqi, M. (2021). Current and future trends in polymer membrane-based gas separation technology: a comprehensive review. *J. Ind. Eng. Chem.* 98, 103–129. doi: 10.1016/j.jiec.2021.03.030

von Stockar, U. (2010). Biothermodynamics of live cells: a tool for biotechnology and biochemical engineering. *J. Non-Equilib. Thermodyn.* 35, 415–475. doi: 10.1515/jnetdy.2010.024

von Stockar, U., and Birou, B. (1989). The heat generated by yeast cultures with a mixed metabolism in the transition between respiration and fermentation. *Biotechnol. Bioeng.* 34, 86–101. doi: 10.1002/bit.260340112

von Stockar, U., Gustafsson, L., Larsson, C., Marison, I., Tissot, P., and Gnaiger, E. (1993). Thermodynamic considerations in constructing energy balances for cellular growth. *Biochim. Biophys. Acta* 1183, 221–240. doi: 10.1016/0005-2728(93)90225-5

Wadsö, L. (2001). Isothermal microcalorimetry. Current problems and prospects. *J. Therm. Anal. Calorim.* 64, 75–84. doi: 10.1023/A:1011576710913

Wadso, L. (2015). A method for time-resolved calorespirometry of terrestrial samples. *Methods* 76, 20–26. doi: 10.1016/j.ymeth.2014.10.001

Wadsö, I., Hallén, D., Jansson, M., Suurkuusk, J., Wenzler, T., and Braissant, O. (2017). A well-plate format isothermal multi-channel microcalorimeter for monitoring the activity of living cells and tissues. *Thermochim. Acta* 652, 141–149. doi: 10.1016/j.tca.2017.03.010

Wadsö, L., and Hansen, L. D. (2015). Calorespirometry of terrestrial organisms and ecosystems. *Methods* 76, 11–19. doi: 10.1016/j.ymeth.2014.10.024

Wadsö, L., Salamanca, Y., and Johansson, S. (2010). Biological applications of a new isothermal calorimeter that simultaneously measures at four temperatures. *J. Therm. Anal. Calorim.* 104, 119–126. doi: 10.1007/s10973-010-1140-y

Xu, X., Thornton, P. E., and Post, W. M. (2013). A global analysis of soilmicrobial biomass carbon, nitrogen and phosphorus interrestrial ecosystems. *Glob. Ecol. Biogeogr.* 22, 737–749. doi: 10.1111/geb.12029

Yang, Z., Wullschleger, S. D., Liang, L., Graham, D. E., and Gu, B. (2016). Effects of warming on the degradation and production of low-molecular-weight labile organic carbon in an Arctic tundra soil. *Soil Biol. Biochem.* 95, 202–211. doi: 10.1016/j.soilbio.2015.12.022

frontiers | Frontiers in Microbiology

TYPE Opinion
PUBLISHED 23 February 2024
DOI 10.3389/fmicb.2024.1364487

OPEN ACCESS

EDITED BY
Ruibo Sun,
Anhui Agricultural University, China

REVIEWED BY
Gang Fu,
Chinese Academy of Sciences (CAS), China
Yunhui Zhang,
Tongji University, China
Jin Wu,
Beijing University of Technology, China

*CORRESPONDENCE
Haoming Chen
✉ chenhaoming89@hotmail.com
Zhen Li
✉ lizhen@njau.edu.cn

†These authors have contributed equally to this work

RECEIVED 02 January 2024
ACCEPTED 12 February 2024
PUBLISHED 23 February 2024

CITATION
Li L, Yang S, Hu X, Li Z and Chen H (2024) The combined application of salt-alkali tolerant phosphate solubilizing microorganisms and phosphogypsum is an excellent measure for the future improvement of saline-alkali soils. *Front. Microbiol.* 15:1364487. doi: 10.3389/fmicb.2024.1364487

The combined application of salt-alkali tolerant phosphate solubilizing microorganisms and phosphogypsum is an excellent measure for the future improvement of saline-alkali soils

Lingli Li[1†], Shiqi Yang[1†], Xin Hu[1], Zhen Li[2*] and Haoming Chen[1*]

[1]School of Environmental and Biological Engineering, Nanjing University of Science and Technology, Nanjing, China, [2]College of Resources and Environmental Sciences, Nanjing Agricultural University, Nanjing, Jiangsu, China

KEYWORDS

microbial remediation, salt and alkali stress, co-remediation, phosphogypsum, organic acids, dissolution and release

1 Introduction

1.1 Saline-alkali soils not only affect food security but also hinder human social development

Soil salinization has always been a major threat to the sustainable development of agriculture and the improvement of land use efficiency (Meena et al., 2019; Kumawat et al., 2022). Salt-alkali soil, characterized by the accumulation of salt in the surface layer and an excessively high pH level, can be broadly categorized into three types: saline-alkali soil, alkaline soil, and saline-alkali soil. When the soil salt ion content is higher than 0.1%, the soil pH is higher than 8.0 or the sodium alkalinity is higher than 5%, it can be called saline-alkali soil. In nature, soil salinization and alkalization often occur simultaneously. Soil salinization is divided into primary salinization and secondary salinization. Primary salinization is mostly caused by climate, hydrology, and topography, while secondary salinization is mostly caused by the overuse of fertilizers and pesticides as well as irrational irrigation methods (Negacz et al., 2022). High salinity and elevated pH levels exert multifaceted negative impacts on soil. Firstly, salt ions attract and immobilize soil particles, resulting in soil compaction and decreased porosity, which in turn hinders the exchange of water, air, and nutrients with plant roots. Additionally, high salinity diminishes the soil's capacity to absorb beneficial nutrients. Secondly, elevated pH levels cause cations to bind to soil particles, further contributing to soil compaction and affecting the availability of micronutrients as well as organic matter decomposition. Ultimately, these negative impacts severely constrain soil fertility and plant growth. Currently, more than 100 countries around the world are affected by soil salinization. The most severe soil salinization is primarily found in regions such as North, East, and Southern Africa, the western United States, the Middle East, Central Asia, western China, the Yellow River basin, as well as Australia (Li et al., 2019; Negacz et al., 2022). The global map of saline-alkali soils in 2021 shows that 20–50% of irrigated soils in all continents have excessive salinity (FAO, 2021), which means that more than 1.5 billion people around the world are facing significant challenges in food production due to soil degradation. Moreover, about 1.5 million hectares

of irrigated land are rendered unfit for cultivation due to severe salinization every year (Dey et al., 2021). Hence, the urgent need arises for the improvement and utilization of saline-alkali soils, given their significance as a crucial reserve land resource for food production and ecological environment construction.

1.2 Difficulty in utilizing phosphorus (P) is a non-negligible problem in soil salinization

The negative impact of salinization on soil is multifaceted. Firstly, the high salt content and high pH value of saline-alkali soil lead to soil hardening, reducing the soil's porosity and nutrient retention capacity (Negacz et al., 2022). Additionally, soil salinization also reduces the activity of soil microorganisms, affecting soil respiration and the activity of various enzymes such as alkaline phosphatase, urease, and catalase (Kumawat et al., 2022). In terms of plant growth, the high osmotic pressure of saline-alkali soil can interfere with the water absorption capacity of root cells, leading to cell dehydration and thus affecting the normal growth of plants. Additionally, saline-alkali soil can also increase plant uptake of soluble salt ions, which may have a negative impact on the material stability within plant cells, reducing photosynthetic rates and leading to plant wilting or even death (Parida and Das, 2005). More in-depth research has shown that increased salinity can lead to a series of problems such as ion toxicity, nutrient limitation, high osmotic stress, and oxidative stress. These problems can cause serious damage to processes such as enzyme activity, DNA, RNA, cell division, and protein synthesis in plants (Zhang et al., 2015; Kumawat et al., 2022).

The issue of P immobilization in saline-alkali soils should be given high priority because P is an essential element for plant and microbial growth. Although the total P content in some saline-alkali soils is relatively high, most of the P (60–90%) is fixed in the form of cations such as calcium phosphate, magnesium phosphate, aluminum phosphate, and iron phosphate (Jiang et al., 2019; Dey et al., 2021). Moreover, phosphorus fertilizers applied to saline-alkali soils tend to be preferentially fixed in the inorganic phosphorus pool, rather than being directly utilized by plants. To mitigate these effects, further research is needed to investigate how to improve the utilization efficiency of P in soil and mitigate the negative impact of salinization on plant growth by improving soil conditions.

2 Microbial remediation and mineral amelioration have received much attention in the remediation of saline-alkali soils

Currently, scholars at home and abroad have proposed a series of improvement measures for saline-alkali soil, including water conservancy, physics, chemistry, and biology. Physical improvement is usually achieved by reducing soil salinity, mainly based on the principles of water and salt movement. Basic methods include soil leaching, which involves the dissolution of salts in saline-alkali soils through freshwater irrigation. The resulting salt components are then transported to deeper soil layers through infiltration or drained away through drainage measures. These methods can also be classified as water conservancy engineering restoration technologies (Kumawat et al., 2022). The chemical improvement method for saline-alkali soil is mainly achieved by adding chemical reagents that react with salt-alkali ions (mainly Na^{+}) in the soil. This reduces the content of soil salt-alkali components and improves the physical and chemical properties and soil structure. Commonly used chemical reagents include gypsum/phosphogypsum, humic acid, superphosphate, peat, and vinegar residue, etc. The biological improvement method (mainly plants and microorganisms) can essentially improve the physical and chemical properties of soil, while increasing soil fertility. It is a technology that integrates economic, environmental, and ecological effects. Among them, soil microorganisms are the most dynamic component of soil, affecting soil energy flow and material circulation through metabolic activities. Many salt-tolerant and alkali-tolerant microorganisms can not only reduce soil salinity, but also have the functions of nitrogen fixation, increasing potassium and phosphate dissolution. Meanwhile, these microorganisms secrete active substances, including plant hormones, iron carriers, antioxidants, and extracellular polysaccharides, which can activate the antioxidant enzyme system in plants and promote their growth. Compared to conventional physical and chemical improvement or remediation methods, in agricultural soil improvement, the choice of technology needs to be very cautious, which also leads to many physical and chemical improvement methods being rejected due to cost, environmental protection, etc. In current research, microbial remediation of saline-alkali soil has occupied a major position in most countries. Therefore, the introduction of salt-tolerant functional microorganisms can bolster the remediation of saline-alkali soils and augment plant resistance to salt stress.

3 The difficulty of P utilization in saline-alkali soils gives a place to phosphate solubilizing microorganisms (PSMs)

PSMs are a type of soil functional microorganism that was first discovered in the roots of farmland crops (Dey et al., 2021). It showed that in the community of salt-tolerant microorganisms, most species of PSMs are considered to be key plant growth-promoting microorganisms, which have the ability to solubilize P and K, and produce various metabolites that promote plant growth under saline conditions (such as plant growth hormones, iron carriers, ACC deaminase, and antagonists of plant pathogens) (Su et al., 2023). The most beneficial function of PSMs is to convert non-biologically available sources of P (both organic and inorganic) in soil into bio-available forms: 1. solubilization of inorganic P salts through cell-produced biological functions such as protonation, acidification, chelation, etc. 2. mineralization of organic P salts through enzyme activities (such as phosphatase, phosphonate hydrolase, phytases, and C-P lyase) (Ahemad, 2015; Hu and Chen, 2023). However, we must recognize that high salt concentration environments can lead to cell dehydration, shrinkage, and loss of activity (Rath and Rousk, 2015). Therefore, in order to improve the effect of microorganism's application in saline-alkali soil, it is

necessary to screen out and select highly tolerant PSMs in saline-alkali soil during the process, and to use other technologies to maintain the activity of PSMs and their effect.

4 Phosphogypsum is a low-cost material for ameliorating saline-alkali soils

The application of gypsum in improving saline-alkali soil has been widely recognized, and the key lies in effectively reducing soil salt content through the displacement of Ca^{2+} and Na^{+} (Basak et al., 2022). Non-renewable natural gypsum minerals pose challenges for large-scale agricultural use. Meanwhile, due to industrial growth, government subsidies have decreased (especially in developing countries), and the quality of gypsum raw materials has decreased, leading to high costs of chemical remediation and further impeding the repair of saline-alkali soils (Qadir and Oster, 2004).

With the rapid development of industry, the production of gypsum and its similar by-products (such as PG and desulfurization gypsum) is gradually increasing, and the main component of these by-products is $CaSO_4 \cdot 2H_2O$. PG is a solid waste from the wet phosphoric acid process, and its treatment is difficult. It is usually only stored or discarded in a centralized manner. The environmental hazards of PG mainly come from the release of P and heavy metals that are enriched in the soil or water body after large-scale accumulation, leading to high local concentrations and ecological damage. However, with the progress of process technology and the implementation of relevant policies, the content of polluting elements in PG produced in industrial production has been significantly reduced. For example, the weight percentage of heavy metals such as Pb, Cd and Cr in the PG used in the study of Chen et al. (2021) was $\leq$0.002 wt%. Additionally, countries such as Brazil, Spain and Lebanon have widely used PG as a soil amendment (Abril et al., 2009; Kassir et al., 2011; Costa et al., 2021).

Besides reducing salinity by replacing Na^{+}, PG can also improve soil pore structure, increase water permeability, reduce soil redox potential (reduce negative values), and reduce CH_4 emissions in saline-alkali soils (Khatun et al., 2021). Armstrong (1989) compared the solubility, exchangeable sodium replacement, and clay dispersion inhibition of three calcium amendments (PG, rock gypsum, saturated gypsum solution), and the results showed that PG was the most effective in saline-alkali soil improvement. Additionally, the total P content in PG is about 2.5–7.5%, and its reuse as a P fertilizer can reduce the damage to the environment and natural resources caused by P mining. However, under alkaline soil conditions, the application of PG can lead to the precipitation of Ca–P, thereby limiting the utilization efficiency of P in PG.

5 The combination of PSMs and PG for saline-alkali soil improvement is a measure for resource utilization

It is gratifying that the utilization of PSMs to solubilize insoluble P minerals and enhance P release has been proven to be feasible. The secretion of multiple organic acids makes PSMs more suitable for working with mineral soil adsorbents than other types of plant growth-promoting bacteria. For instance, the PSMs (*Burkholderia* sp. strain PH10) can completely dissolve apatite crystals within 22 h (Fontaine et al., 2016). The phosphate-solubilizing *B. megaterium* (TBRC 1396) can solubilize up to 835.45 $\pm$ 11.76 mg/L phosphorus from struvite in 14 days (Jokkaew et al., 2022).

Multiple studies have confirmed that oxalic acid, citric acid, acetic acid, lactic acid, gluconic acid, and malic acid, which are organic acids secreted by PSMs, are the main means for dissolving inorganic insoluble phosphorus sources because these organic acids have strong acidity. Tian et al. (2022) found that *Aspergillus niger* (ANG) released up to 1,103 mg/L P from PG in 7 days. In addition, the rich P, Ca and organic matter in PG have been confirmed to be useful as fertilizers to promote plant growth. For example, adding 30 g/kg PG and a mixed microbial agent containing phosphate-solubilizing bacteria *Bacillus megaterium* var. phosphaticum and *Pseudomonas fluorescens* to the soil can increase the available phosphorus in the soil by ~80%, and increase the dry weight of corn (mg per plant) from 398 to 624 (Al-Enazy et al., 2017). Meanwhile, the application of PG (9 t ha^{-1}) and bacteria (*A. lipoferum* + *B. circulance*) can significantly improve the physiological status, antioxidant enzyme activity, microbial activity, nutrient absorption, and productivity of maize plants under saline-sodic soil conditions (Khalifa et al., 2021). It is worth noting that the combination of microorganisms and PG can also reduce potentially harmful elements in PG, such as Fe, Al, F, etc., through their own cells and secretions (such as, extracellular polymers) (Jalali et al., 2016; Chen et al., 2021). Therefore, the combined application of PSMs and PG for saline-alkali soil remediation is feasible and effective, as the combination of the two not only leverages their respective advantages, but also leads to mutual enhancement (Figure 1).

6 Prospects for the combined application of PSMs and PG

The improvement of saline-alkali soil with PSMs and PG, and the promotion of plant growth in saline-alkali soil, is a potentially efficient and economic measure in the future. However, when trying to implement both technologies simultaneously in practical engineering applications, we should consider the following aspects. Firstly, attention should be paid to microbial diversity, and the beneficial microbial communities should be protected and utilized to achieve comprehensive soil improvement and ecological restoration. Secondly, the utilization of waste PG should be optimized (including raw material composition, usage amount, application frequency, application process, etc.) to reduce its negative impact on soil and the environment, while exploring its potential phosphorus resource value. Thirdly, long-term effect evaluation should be emphasized, and the impact of improvement measures on soil physical and chemical properties, microbial community structure, crop growth, and other aspects should be continuously monitored to ensure the stability and sustainability of the improvement measures. Fourth, emphasis should be placed on assessing environmental risks, particularly the damage and residual effects of radioactive elements on plants, to ensure that the improvement measures do not have negative impacts on

10.3389/fmicb.2024.1364487

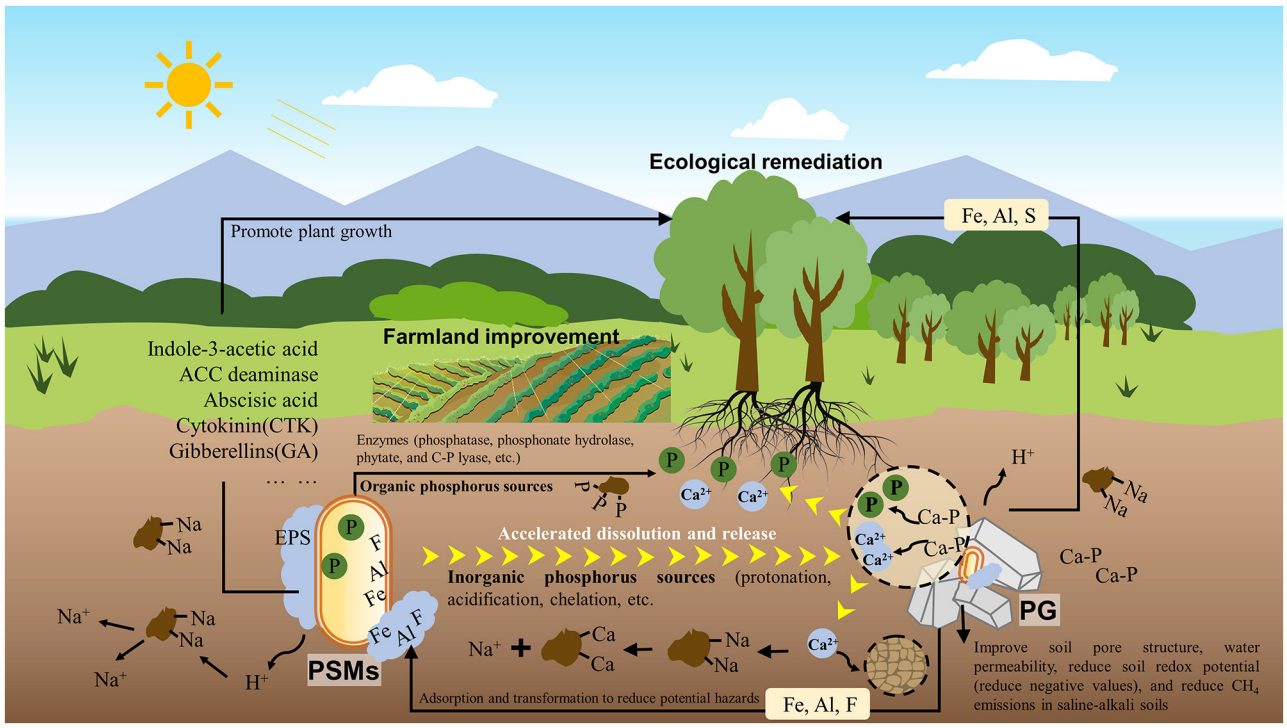

FIGURE 1
Phosphate solubilizing microorganisms (PSMs) combined with phosphogypsum (PG) can effectively repair saline-alkali soil remediation.

the environment and human health. Finally, attention should be paid to technological innovation and application, exploring new composite improvement technologies and methods, and improving the utilization rate and improvement effect of PSMs and PG resources, thus making greater contributions to agricultural sustainable development and ecological environmental protection.

Author contributions

LL: Data curation, Formal analysis, Writing – original draft. SY: Data curation, Methodology, Writing – original draft. XH: Data curation, Methodology, Writing – original draft. ZL: Methodology, Writing – review & editing. HC: Writing – original draft, Writing – review & editing.

Funding

The author(s) declare financial support was received for the research, authorship, and/or publication of this article. This study was supported by the National Natural Science Foundation of China (No. 42007105), Natural Science Foundation of Hebei Province (E2023519001), and the Open Fund for Large Instrumentation of Nanjing University of Science and Technology to HC.

Conflict of interest

The authors declare that the research was conducted in the absence of any commercial or financial relationships that could be construed as a potential conflict of interest.

Publisher's note

All claims expressed in this article are solely those of the authors and do not necessarily represent those of their affiliated organizations, or those of the publisher, the editors and the reviewers. Any product that may be evaluated in this article, or claim that may be made by its manufacturer, is not guaranteed or endorsed by the publisher.

References

Abril, J. M., García-Tenorio, R., Periáñez, R., Enamorado, S. M., Andreu, L., and Delgado, A. (2009). Occupational dosimetric assessment (inhalation pathway) from the application of phosphogypsum in agriculture in South West Spain. *J. Environ. Radioact.* 100, 29–34. doi: 10.1016/j.jenvrad.2008.09.006

Ahemad, M. (2015). Phosphate-solubilizing bacteria-assisted phytoremediation of metalliferous soils: a review. *3 Biotech* 5, 111–121. doi: 10.1007/s13205-014-0206-0

Al-Enazy, A. R., Al-Oud, S. S., Al-Barakah, F. N., and Usman, A. R. A. (2017). Role of microbial inoculation and industrial by-product phosphogypsum in growth and nutrient uptake of maize (Zea mays L.) grown in calcareous soil. *J. Sci. Food Agric.* 97, 3665–3674. doi: 10.1002/jsfa.8226

Armstrong, A. B. (1989). *Salt and Water Dynamics in Saline and Sodic Clay Soils. Vol. I and II*.

Basak, N., Rai, A. K., Sundha, P., Meena, R. L., Bedwal, S., Yadav, R. K., et al. (2022). Assessing soil quality for rehabilitation of salt-affected agroecosystem: a comprehensive review. *Front. Environ. Sci.* 10:935785. doi: 10.3389/fenvs.2022.935785

Chen, H. M., Lu, Y. Q., Zhang, C. N., Min, F. F., and Huo, Z. L. (2021). Red yeast improves the potential safe utilization of solid waste (phosphogypsum and titanogypsum) through bioleaching. *Front. Bioeng. Biotechnol.* 9:13. doi: 10.3389/fbioe.2021.777957

Costa, E. T. D., Guilherme, L. R. G., Lopes, G., De Lima, J. M., and Curi, N. (2021). Sorption of cadmium, lead, arsenate, and phosphate on red mud combined with phosphogypsum. *Int. J. Environ. Res.* 15, 427–444. doi: 10.1007/s41742-021-00319-z

Dey, G., Banerjee, P., Sharma, R. K., Maity, J. P., Etesami, H., Shaw, A. K., et al. (2021). Management of phosphorus in salinity-stressed agriculture for sustainable crop production by salt-tolerant phosphate-solubilizing bacteria—a review. *Agronomy* 11:1552. doi: 10.3390/agronomy11081552

FAO (2021). *Global Map of Salt Affected Soils Version 1.0*. Food and Agriculture Organization of the United Nations. Available online at: https://www.fao.org/soils-portal/data-hub/soil-maps-and-databases/global-map-of-salt-affected-soils/en/

Fontaine, L., Thiffault, N., Paré, D., Fortin, J. A., and Piché, Y. (2016). Phosphate-solubilizing bacteria isolated from ectomycorrhizal mycelium of Picea glaucaare highly efficient at fluorapatite weathering. *Botany* 94, 1183–1193. doi: 10.1139/cjb-2016-0089

Hu, X., and Chen, H. (2023). Phosphate solubilizing microorganism: a green measure to efectively control and regulate heavy metal pollution in agricultural soils. *Front. Microbiol.* 14:1193670. doi: 10.3389/fmicb.2023.1193670

Jalali, J., Magdich, S., Jarboui, R., Loungou, M., and Ammar, E. (2016). Phosphogypsum biotransformation by aerobic bacterial flora and isolated *Trichoderma asperellum* from Tunisian storage piles. *J. Hazard. Mater.* 308, 362–373. doi: 10.1016/j.jhazmat.2016.01.063

Jiang, H. H., Qi, P. S., Wang, T., Chi, X. Y., Wang, M. A., Chen, M. N., et al. (2019). Role of halotolerant phosphate-solubilising bacteria on growth promotion of peanut (*Arachis hypogaea*) under saline soil. *Ann. Appl. Biol.* 174, 20–30. doi: 10.1111/aab.12473

Jokkaew, S., Jantharadej, K., Pokhum, C., Chawengkijwanich, C., and Suwannasilp, B. B. (2022). Free and encapsulated phosphate-solubilizing bacteria for the enhanced dissolution of swine wastewater-derived struvite—an attractive approach for green phosphorus fertilizer. *Sustainability* 14:12627. doi: 10.3390/su141912627

Kassir, L. N., Darwish, T., Shaban, A., Lartiges, B., and Ouaini, N. (2011). Mobility of selected trace elements in Mediterranean red soil amended with phosphogypsum: experimental study. *Environ. Monit. Assess.* 184, 4397–4412. doi: 10.1007/s10661-011-2272-7

Khalifa, T., Elbagory, M., and Omara, A. E.-D. (2021). Salt stress amelioration in maize plants through phosphogypsum application and bacterial inoculation. *Plants* 10:2024. doi: 10.3390/plants10102024

Khatun, L., Ali, M. A., Sumon, M. H., Islam, M. B., and Khatun, F. (2021). Mitigation rice yield scaled methane emission and soil salinity stress with feasible soil amendments. *J. Agric. Chem. Environ.* 10, 16–36. doi: 10.4236/jacen.2021.101002

Kumawat, K. C., Nagpal, S., and Sharma, P. (2022). Potential of plant growth-promoting rhizobacteria-plant interactions in mitigating salt stress for sustainable agriculture: a review. *Pedosphere* 32, 223–245. doi: 10.1016/S1002-0160(21)60070-X

Li, H., Zhao, Q., and Huang, H. (2019). Current states and challenges of salt-affected soil remediation by cyanobacteria. *Sci. Total Environ.* 669, 258–272. doi: 10.1016/j.scitotenv.2019.03.104

Meena, M. D., Yadav, R. K., Narjary, B., Yadav, G., Jat, H. S., Sheoran, P., et al. (2019). Municipal solid waste (MSW): strategies to improve salt affected soil sustainability: a review. *Waste Manag.* 84, 38–53. doi: 10.1016/j.wasman.2018.11.020

Negacz, K., Malek, Ž., De Vos, A., and Vellinga, P. (2022). Saline soils worldwide: identifying the most promising areas for saline agriculture. *J. Arid Environ.* 203:104775. doi: 10.1016/j.jaridenv.2022.104775

Parida, A. K., and Das, A. B. (2005). Salt tolerance and salinity effects on plants: a review. *Ecotoxicol. Environ. Saf.* 60, 324–349. doi: 10.1016/j.ecoenv.2004.06.010

Qadir, M., and Oster, J. (2004). Crop and irrigation management strategies for saline-sodic soils and waters aimed at environmentally sustainable agriculture. *Sci. Total Environ.* 323, 1–19. doi: 10.1016/j.scitotenv.2003.10.012

Rath, K. M., and Rousk, J. (2015). Salt effects on the soil microbial decomposer community and their role in organic carbon cycling: a review. *Soil Biol. Biochem.* 81, 108–123. doi: 10.1016/j.soilbio.2014.11.001

Su, M., Mei, J. J., Mendes, G. O., Tian, D., Zhou, L. M., Hu, S. J., et al. (2023). Alkalinity intensifies phosphorus deficiency in subtropical red soils: An insight from phosphate solubilizing fungi. *Soil Use Manage.* 39, 1504–1516.

Tian, D., Xia, J., Zhou, N., Xu, M., Li, X., Zhang, L., et al. (2022). The utilization of phosphogypsum as a sustainable phosphate-based fertilizer by *Aspergillus niger*. *Agronomy* 12:646. doi: 10.3390/agronomy12030646

Zhang, Y., Zhang, H., Zou, Z. R., Liu, Y., and Hu, X. H. (2015). Deciphering the protective role of spermidine against saline–alkaline stress at physiological and proteomic levels in tomato. *Phytochemistry* 110, 13–21. doi: 10.1016/j.phytochem.2014.12.021

frontiers | Frontiers in Microbiology

TYPE Review
PUBLISHED 12 April 2024
DOI 10.3389/fmicb.2024.1379879

OPEN ACCESS

EDITED BY
Paola Grenni,
National Research Council, Italy

REVIEWED BY
Kalpana Bhatt,
Purdue University, United States
Sudipta Sankar Bora,
Assam Agricultural University, India
Blessing Chidinma Nwachukwu,
University of the Witwatersrand, South Africa

*CORRESPONDENCE
Xiaoyan Zhang
✉ zhangxiaoyan@xtbg.ac.cn
Xiayu Guan
✉ gxy302@126.com
Junzhi Qiu
✉ junzhiqiu@126.com

RECEIVED 31 January 2024
ACCEPTED 03 April 2024
PUBLISHED 12 April 2024

CITATION
Jibola-Shittu MY, Heng Z, Keyhani NO, Dang Y, Chen R, Liu S, Lin Y, Lai P, Chen J, Yang C, Zhang W, Lv H, Wu Z, Huang S, Cao P, Tian L, Qiu Z, Zhang X, Guan X and Qiu J (2024) Understanding and exploring the diversity of soil microorganisms in tea (*Camellia sinensis*) gardens: toward sustainable tea production. *Front. Microbiol.* 15:1379879. doi: 10.3389/fmicb.2024.1379879

Understanding and exploring the diversity of soil microorganisms in tea (*Camellia sinensis*) gardens: toward sustainable tea production

Motunrayo Y. Jibola-Shittu[1], Zhiang Heng[1], Nemat O. Keyhani[2], Yuxiao Dang[1], Ruiya Chen[1], Sen Liu[1], Yongsheng Lin[1], Pengyu Lai[1], Jinhui Chen[1], Chenjie Yang[1], Weibin Zhang[1], Huajun Lv[1], Ziyi Wu[1], Shuaishuai Huang[3], Pengxi Cao[3], Lin Tian[4], Zhenxing Qiu[5], Xiaoyan Zhang[1]*, Xiayu Guan[6]* and Junzhi Qiu[1]*

[1]Key Lab of Biopesticide and Chemical Biology, Ministry of Education, State Key Laboratory of Ecological Pest Control for Fujian and Taiwan Crops, College of Life Sciences, Fujian Agriculture and Forestry University, Fuzhou, China, [2]Department of Biological Sciences, University of Illinois, Chicago, IL, United States, [3]School of Ecology and Environment, Tibet University, Lhasa, China, [4]Tibet Plateau Institute of Biology, Lhasa, China, [5]Fuzhou Technology and Business University, Fuzhou, Fujian, China, [6]College of Horticulture, Fujian Agriculture and Forestry University, Fuzhou, Fujian, China

Leaves of *Camellia sinensis* plants are used to produce tea, one of the most consumed beverages worldwide, containing a wide variety of bioactive compounds that help to promote human health. Tea cultivation is economically important, and its sustainable production can have significant consequences in providing agricultural opportunities and lowering extreme poverty. Soil parameters are well known to affect the quality of the resultant leaves and consequently, the understanding of the diversity and functions of soil microorganisms in tea gardens will provide insight to harnessing soil microbial communities to improve tea yield and quality. Current analyses indicate that tea garden soils possess a rich composition of diverse microorganisms (bacteria and fungi) of which the bacterial Proteobacteria, Actinobacteria, Acidobacteria, Firmicutes and Chloroflexi and fungal Ascomycota, Basidiomycota, Glomeromycota are the prominent groups. When optimized, these microbes' function in keeping garden soil ecosystems balanced by acting on nutrient cycling processes, biofertilizers, biocontrol of pests and pathogens, and bioremediation of persistent organic chemicals. Here, we summarize research on the activities of (tea garden) soil microorganisms as biofertilizers, biological control agents and as bioremediators to improve soil health and consequently, tea yield and quality, focusing mainly on bacterial and fungal members. Recent advances in molecular techniques that characterize the diverse microorganisms in tea gardens are examined. In terms of viruses there is a paucity of information regarding any beneficial functions of soil viruses in tea gardens, although in some instances insect pathogenic viruses have been used to control tea pests. The potential of soil microorganisms is reported here, as well as recent techniques used to study microbial diversity and their genetic manipulation, aimed at improving the yield and quality of tea plants for sustainable production.

KEYWORDS

microbial communities, soil health, soil microorganisms, tea gardens, tea plant

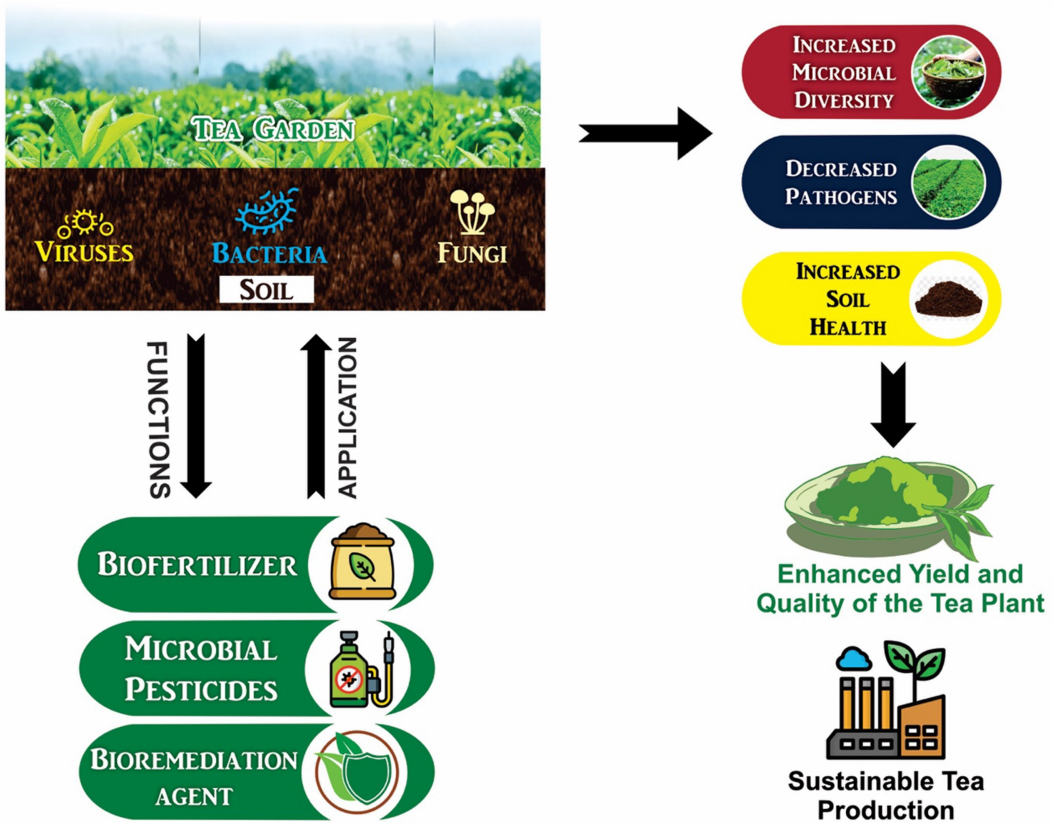

GRAPHICAL ABSTRACT

1 Introduction

Camellia sinensis commonly referred to as the "tea plant" is an economically important crop, belonging to the family Thaeceae (Pandey et al., 2021). As a brewed beverage, it has been consumed for at least several millennia, with initial indications that leaves were first eaten raw or added to soups followed by fermentation and chewing of the leaves. Subsequently, it was turned into a beverage by mixing fresh or cured leaves with hot or boiling water, with early written description of tea drinking dating to at least the 3rd century A.D. in China. Modern tea consumption is second only to water, and tea production is dominated by India/Sri Lanka and China, with the latter accounting for about half of the tea produced in our world today (Xu et al., 2018, 2022). Tea is cultivated predominantly in tropical and subtropical regions of the world (Hazra et al., 2019), and global tea consumption is estimated to have increased ~43% from 2005 to 2020 (FAOSTAT, 2022). This is likely due in part to the many putative beneficial health and medicinal values of tea due to its wide range of bioactive constituents. One well known component of tea is caffeine, which can act as a stimulant increasing alertness, with levels of caffeine affected by leaf harvest time and various forms of post-harvest processing. In addition, tea contains a range of secondary metabolites, some of which may possess antioxidant, digestive, (putative) antimicrobial, and/or other health promoting benefits to the consumers (Pokharel et al., 2023; Ramphinwa et al., 2023). Aside from caffeine, potential bioactive compounds include polyphenols (e.g., flavonoids and catechins) as well as xanthines such as theobromine and theophylline. Tea consumption has been linked cancer-prevention, treatment of various cardiovascular problems, and improved circulation potentially due to the variety of polyphenols, antioxidants, and other compounds they possess, although definitive clinical data is lacking (Perez-Burillo et al., 2019; Abe and Inoue, 2021; Bag et al., 2022). Tea consumption also provides important comfort and social interactions in many societies worldwide. Nevertheless, the demand for tea is projected to see a continuous increase (Xi et al., 2023). Therefore, to effectively cater for the rising demand for tea, research should be aimed at the development of ecologically friendly and sustainable approaches to improving the quality and yield of tea.

Camellia sinensis is native to East Asia, with a purported origin along the Irrawady River, spreading into present day southeast China, India, and later to Sri Lanka. Two main cultivated varieties of traditional tea have thus far been described, *C. sinensis* var. *sinensis* and *C. sinensis var. assamica*, that are separated into distinct clades and likely have different parentages. However, *C. sinensis* var. *assamica* can be separated into two subtypes, namely, Southern Yunnan Assam (China) and Indian Assam (India), which although may have originated from the same parent, appears to represent two independent domestication events. Furthermore, some subvarieties appear to have undergone hybridization with closely related species such as *C. taliensis* and *C. pubicosta* (Mukhopadhyay and Mondal, 2017; Auria et al., 2022). In addition to the occurrence of different regional varieties, tea is further classified post-harvest via the different means and methods for processing of the leaves that result in significant differences in the final consumed product (Auria et al., 2022). These

different post-harvest processing methods result in the commonly referred to black, green, white, oolong, dark, and yellow teas (among others), and involve a series of steps that can include, depending upon the final outcome, the following: (picking), (i) withering—drying of the leaves; under sun for darker teas, in a cool ventilated room for lighter teas, (ii) bruising—crushing, shaking, rolling, and/or other forms of manipulating the leaves; mainly for darker teas, (iii) oxidation—exposure leaves to air for different period of time; darkens teas depending upon time, (iv) heating—after oxidation, leaves are heated to stop oxidation process, also referred to as "fixation," (v) yellowing—light heating in closed chamber, (vi) fermentation—leaves are allowed to ferment for a period of time; results in increase in sweetness, (vii) drying—remove moisture via baking, sun and/or air-drying, (viii) sorting and shaping—stems, seeds, and impurities are removed and the tea "shaped" into various forms, e.g., bricks, circles, etc., for aging and/or storage. Each "type" of tea has its own sequence of specific steps as outlined above, but not all. Thus, "black" tea involves withering, bruising, oxidation, shaping, and drying, "white" tea (freshly picked leaf buds): only withering, heating, shaping, and drying (with white tea often considered the least "processed" of the final tea forms). In addition, many of these steps can have important production differences with respect to leaf treatment for any given step in terms of time, temperature, and other conditions that can result in significant differences in the final products even if all are considered "black" teas (Auria et al., 2022; Aaqil et al., 2023).

Although post-harvest processing is relatively well-described, the soil support used to produce tea has been less studied despite anecdotal and regional recognition that variations in soil "quality" affects plant growth and subsequent leaf quality and production. It is well known that soil microorganisms (bacteria, fungi, and viruses, e.g., the soil microbiome) functions in mediating soil health, and subsequent plant growth and crop yield (Wang et al., 2017; Gu et al., 2019). These effects can be positive or negative with respect to plant health, with beneficial microbes helping to: (i) mobilize otherwise (plant) recalcitrant nutrients, particularly nitrogen and phosphorus, to the plant (often in exchange for carbon), (ii) facilitate plant resistance to abiotic stress including temperature and drought, and (iii) protect plants from infection and disease. In contrast, harmful microbes, e.g., biotrophic and necrotrophic plant pathogens can cause disease, and competition with some microbes may decrease overall plant access to nutrients. Overall, however, the diversity of soil microbial communities can serve as an indicator of soil fertility and soil health (Gui et al., 2022), and poor soil (in terms of mediating plat health) typically showing a reduction in soil microbial community diversity, which can then result in adverse effects on the sustainable utilization of soil resources (Chen et al., 2015). Therefore, maintaining the diversity of soil microbial communities, with an emphasis on identifying and enriching for beneficial microbes, can exert a significant impact on managing soil organic carbon and nutrient availability to plants thus increasing the sustainability of agricultural ecosystems (Bertola et al., 2021; Chauhan et al., 2023), particularly given that several studies have shown that soil microorganisms can have important positive effects on plant growth, plant health, resistance to abiotic stress, and overall agricultural productivity (Trivedi et al., 2020; Qiao et al., 2024). Due to the economic importance of tea plants, it is valuable to build models integrating the nature of soil microorganisms and the vital functions they perform with respect to tea cultivation. Here, we review current information concerning the diversity and potential functions of soil microbial communities in tea gardens, to provide insights into less reported factors that could be explored to improve tea cultivation by examining and potentially manipulating the diversity of soil microorganisms. We also highlight the various techniques used for studying soil microbial diversity within tea gardens. The identification of the diverse groups of soil microorganisms as well as their potential functions will help in meeting the growing demand for the sustainable production of tea plants with high quality and yield.

2 Overview of soil microbiome activities and recent approaches to soil microbiome studies in tea gardens

Soil microbial communities are an essential part of the soil ecosystem, consisting of diverse fungi, bacteria, and viruses (Naylor et al., 2022). Generally, soil microorganisms are involved in key processes in the soil ecosystem; they mediate organic matter decomposition, nutrient cycling, and gaseous fluxes, and impact soil geochemistry including pH, trace metal and other element content, and phosphorus availability, all of which have resultant effects on plant nutrient availability and resistance to stress (Bastida et al., 2021; Hartmann and Six, 2022). Although carbon is gained via photosynthesis, other primary nutrients such as nitrogen, phosphorus, sulphur and potassium, required for plant growth and development, are made available for plant uptake through cycling and transformation processes in the soil. These processes are actively mediated by soil microorganisms, and the availability of these nutrients for plant uptake is a determinant of soil fertility (Basu et al., 2021; Nabi, 2023). Highly fertile soils often exhibit increased bacterial diversity, predominantly those belonging to the Proteobacteria, Nitrospira, Chloroflexi, and Bacteroidetes, in addition to demonstrating enhanced functions such as nitrate reduction, ammonia oxidation and aromatic compound degradation in contrast with low fertile soils (Da Costa et al., 2024). For many crops, bacteria of prominent groups involved in nitrogen-cycling processes and maintaining soil nitrogen balance are indicative of soil fertility, and correlate with crop yield (Bayer et al., 2020; Hayatsu et al., 2021).

In addition, the soil microbiome can participate in the bioremediation of pollutants, heavy metals, and other compounds that can adversely affect plant health or could otherwise affect the quality (and human health safety) of the tea leaves (Bastida et al., 2021; Phillippot et al., 2023). Nitrogen which is a key element involved in the growth and quality tea plants leaves (Ma et al., 2021), is usually recycled by nitrogen-metabolizing microorganisms present in the rhizosphere, providing for enhanced nitrogen absorption of plant usable forms (NO^-_3 and NH^+_4) (Liu et al., 2017, 2022) that can then impact the growth and yield of tea. In tea root systems, ammonia is converted into theanine, a non-protein amino acid that adds a distinct rich flavor to tea as the root absorbs such nitrogen sources from the soil (Cheng et al., 2017; Dong et al., 2019). Theanine is then transported to the leaves and young shoots which are harvested during tea production (Zhang et al., 2023). Within this context, a consortium of nitrogen-metabolizing soil microorganisms predominantly belonging to the Proteobacteria and other phyla such as the Actinobacteria, Firmicutes, Chloroflexi, and Armatimonadetes have been reported in tea roots to help enhance ammonia uptake and

subsequent theanine synthesis, thus contributing to the taste and quality of tea leaves (Xin et al., 2024).

Tea cultivation is unique in that an important number of tea "gardens" or areas of tea cultivation, have existed, i.e., been continuously cultivated with *C. sinensis*, for significant periods of times (generations or even more in some instances). With such relatively continuous cultivation in specific areas, it is likely strong co-interactions between the tea plants and resident microorganisms in the soil have developed, including potentially unique co-adaptations. However, many areas of tea cultivation have also had significant inputs (fertilizer, pesticides, even soil) from other areas that can impact the diversity of both beneficial and harmful (to the plant) microbes (Fu et al., 2021). In addition, tea gardens are faced with a variety of challenges from insect pests and microbial diseases, many of which are vectored by insects (Zhang X. et al., 2022). As suggested, to achieve high yield, significant amounts of fertilizers and pesticides are used in some tea gardens which can, after long term use, cause a decline in soil microbial diversity and hence results in a negative environmental impact (Wang et al., 2020). As tea gardens are usually found on elevated plains, application of chemical fertilizers and pesticides can easily run-off into downstream water bodies, causing eutrophication and pollution of the water (Xie et al., 2021).

Several studies on tea garden soils have revealed the presence of a vast array of microorganisms which are linked to the quality of tea produced from the soil (Fu et al., 2021; Kui et al., 2021; Bag et al., 2022), particularly as soil microbial communities participate in promoting soil health and suppressing plant pathogens (Wu et al., 2023). Based on culture-dependent approach and molecular identification of bacterial isolates through 16S rRNA gene sequencing, keystone bacteria genera such as *Bacillus, Burkholderia, Serratia* and *Arthrobacter* (Table 1) have been reported to display a wide range of growth promoting activities. For example, the phosphorus solubilizing abilities in *Burkholderia* and *Bacillus* isolated from rhizospheric soil samples of tea gardens in West Bengal, India have been characterized (Panda et al., 2017), and isolation of a *Burkholderia pyrrocinia* strain from the tea rhizosphere contributing to abiotic stress tolerance and possessing plant growth promoting activities through phosphorus solubilization and production of phytohormones has also been reported (Han et al., 2021). In addition, a biocontrol strain of *Serratia marcescens* was reportedly isolated from tea rhizosphere displayed significant biocontrol efficacy against fungal root pathogens of tea through the production of hydrolytic enzymes such as chitinase, protease, lipase and cellulase, as well as the production of antibiotics (Dhar Purkayastha et al., 2018). These studies indicate that knowledge concerning the microbial ecosystem of tea soils and the processes by which they help improve tea quality, should be considered an important avenue for further exploration aimed toward enhancing nutrient availability in tea gardens and the resultant yield and quality of tea plants.

Exploring soil microbial diversity is beneficial for the development of agricultural ecosystems as well as testing the effectiveness of restoration measures (Deltedesco et al., 2020). For tea gardens such studies can help in understanding the functions of microorganisms and in harnessing them for better productivity of tea. Recently, the development of culture-independent metagenomics techniques, has contributed greatly to mapping soil microbial phylogeny (Su et al., 2017). The development and refinement of molecular techniques such as the high-throughput sequencing have greatly promoted the study and understanding of diversity and interactions of soil microorganisms (Wei et al., 2018; Song et al., 2023) and has given rise to a significant improvement in terms of both rDNA homology and descriptions of biosynthetic pathways (Wei et al., 2018). Consequently, metagenomic analyses display strong reliability and convenience for characterizing root-associated microorganisms (Bhattacharyya et al., 2016; Busby et al., 2017), and is being applied to characterize soil microbial diversity by directly capturing total soil microbial DNA (Sharma and Kaur, 2021; Parihar et al., 2022) providing a window into functional aspects of soil microorganisms (Wei et al., 2018).

Next,-generation sequencing technologies have also led to insights into various environmental factors contributing to soil microbial diversity (Egidi et al., 2019). As part of this, the majority of microbial species assigned to "RNA similarity groups" can help provide a deeper understanding of the changes in diversity and composition of soil microbial communities (Chen et al., 2017). Similarly, high through-put sequencing technologies have enabled microbiologists to sequence amplified gene markers (e.g., 16S ribosomal RNA), to determine phylogenetic and functional diversity profiles of soil microbial communities (Wu et al., 2015). High-throughput sequencing and molecular ecology network (MEN) analyses have been used to investigate soil microbial diversity, community structure, composition, and interaction networks of tea plantations, revealing the diversity, and dominance of Proteobacteria, Acidobacteria, and Chloroflexi in all tea plantation samples under different management practices (Tan et al., 2019). Although still limited, targeted gene manipulation, e.g., use of CRISPR/Cas technologies has been applied to alter the expression of genes, study genetic diversity, and or produce modified microorganisms, and/or transfer of genes have been applied to tea cultivation research (Bag et al., 2022).

2.1 Fungal communities in tea gardens soils

Fungi are important drivers in soil ecosystems (Francioli et al., 2020); a rich fungal diversity in tea garden soils may help maintain healthy ecological functioning, including by facilitating nutrient cycling, organic matter decomposition, and plant productivity (Ma et al., 2022). In addition, (beneficial) fungi can play important roles in suppressing the activities of (microbial) plant pathogens present in the soil (Bollmann-Giolai et al., 2022). This latter function can be due to a variety of factors including excluding plant pathogen competitors to the production of certain metabolites targeting pathogenic microbes to stimulating plant antimicrobial defenses, thus suppressing tea pathogens, and enhancing tea yield and quality. Xu et al. (2022) have reported that fungal taxa that colonized tea shoots significantly inhibited fungal pathogens. These included fungal taxa corresponding to *Myriangium* and *Mortierella* which have been demonstrated to have plant growth-promoting abilities (Ozimek and Hanaka, 2021). Thus, these abilities may be linked to their ubiquity and potentials to protect plants against pathogens. Zheng et al. (2023) investigated the response of soil microbial communities and functions to long-term tea (*C. sinensis*) planting in a subtropical region and reported the relative abundance of fungal community in tea gardens to be largely dominated by Ascomycota (38.63–55.27%), Basidiomycota (19.45–39.13%), Mortierellomycota (1.8–10.1%), and Rozellomycota (0.12–7.41%). Similarly, Ma et al. (2022) in a study conducted on soils of tea plantations revealed that fungal community predominantly consisted

TABLE 1 Some key microbial species associated with soil ecosystem of tea gardens.

Microbial species	Bacteria phyla	Function	References
Arthrobacter sp. MT436081	Actinobacteria	Phosphorus solubilizing, biocontrol	Bhattacharyya et al. (2020)
Bacillus firmus HNS012 *Bacillus firmus* UST000620-011	Firmicutes	Phosphorus solubilizing	Panda et al. (2017)
Bacillus megaterium MT436102	Firmicutes	Phosphorus solubilizing, ammonia production, protease production, cellulase production	Bhattacharyya et al. (2020)
Bacillus pseudomycoides SN29 (KJ767523)	Firmicutes	Ammonia production, phosphorus solubilizing, production of phytohormones	Dutta et al. (2015)
Bacillus velezensis MT436088 *Bacillus velezensis* MT436091	Firmicutes	Phosphorus solubilizing, ammonia production, protease production	Bhattacharyya et al. (2020)
Brevibacillus agri KX373961	Firmicutes	Phosphorus solubilizing, ammonia production, biocontrol, production of phytohormones	Dutta and Thakur (2017)
Brevibacterium sediminis A6	Actinobacteria	Phosphate solubilizing, ammonia production, biocontrol	Chopra et al. (2020a)
Burkholderia arboris R24201	Proteobacteria	Phosphorus solubilizing	Panda et al. (2017)
Burkholderia cepacia ATCC177759 *Burkholderia cepacia* ATCC 35254	Proteobacteria	Phosphorus solubilizing	Panda et al. (2017)
Burkholderia pyrrocinia P10 (DSM 10685^{T})	Proteobacteria	Abiotic stress tolerance	Han et al. (2021)
Burkholderia sp. J62 *Burkholderia* sp. YXA1-13	Proteobacteria	Phosphorus solubilizing	Panda et al. (2017)
Burkholderia sp. TT6 (KJ767524)	Proteobacteria	Ammonia production, phosphorus solubilizing, production of phytohormones	Dutta et al. (2015)
Burkholderia vietnamiensis TVV70	Proteobacteria	Phosphorus solubilizing	Panda et al. (2017)
Claroideoglomus sp.	Glomeromycota	Nutrient uptake and Leaf food quality	Wu et al. (2019) and Shao et al. (2019)
Enterobacter lignolyticus TG1 (KJ767522)	Proteobacteria	Ammonia production, phosphorus solubilizing, production of phytohormones	Dutta et al. (2015)
Enterobacter sp. KX373977	Proteobacteria	Phosphorus solubilizing, ammonia production, biocontrol, production of phytohormones	Dutta and Thakur (2017)
Glomus sp.	Glomeromycota	Growth promoting activities	Wu et al. (2019); Sun et al. (2020)
Glomus viscosum	Glomeromycota	Nutrient uptake	Wu et al. (2019)
Pseudomonas aeruginosa KH45 (KJ767521)	Proteobacteria	Ammonia production, phosphorus solubilizing, production of phytohormones	Dutta et al. (2015)
Serratia marcescens	Proteobacteria	Phosphorus solubilizing, production of phytohormones. Biocontrol	Panda et al. (2017)
Serratia marcescens ETR17	Proteobacteria	Biocontrol, Phosphorus solubilizing, production of phytohormones	Dhar Purkayastha et al. (2018)

of Ascomycota (44.7%), Mortierellomycota (17.7%) and Basidiomycota (11.4%) and accounted for 73.8% of total composition of fungal communities.

Earlier reports indicated that fungal communities in several tea gardens at the genus level are dominated primarily by *Saitozyma* (Ma et al., 2022; Wang et al., 2023). Members of the *Saitozyma,* have been shown to account for ~30% of the sequences in tea garden soils in the Southeast Asia region, followed by *Mortierella* (20%) and *Pseudogymnoascus* (10%) (Yan P. et al., 2022). Basidiomycota, such as *Saitozyma, Russula* and *Hygrocybe* commonly found in tea gardens, are well known to colonize lignin-rich surfaces and likely play significant roles in the degradation of lignin-rich plant litters (Guo et al., 2018; Kui et al., 2021), transforming these substrates to provide carbon and nitrogen as well as other nutrients for plant growth (Li et al., 2020). In addition, *Penicillium*, *Trichoderma* and *Pseudogymnoascus* are prominent members of the Ascomycota predominantly found in tea gardens (Kui et al., 2021; Wang et al., 2021; Yan L. et al., 2022). The abundance of the Ascomycota among soil fungal communities in tea gardens is perhaps because Ascomycota have been able to successfully evolve mechanisms to dominate soils globally (Egidi et al., 2019). These abilities of the Ascomycota include stress tolerance and production of secondary metabolites which can inhibit other microorganisms (Chen et al., 2017). Moreover, Ascomycota have been known to produce a wide range of antimicrobial agents, which can be advantageous to the protection of plants against pathogens.

The rhizosphere of tea gardens in Southeast Asia have been shown to contain a rich community of Glomeromycota, that include

arbuscular mycorrhizal fungi (AMF), such as *Claroideoglomus, Acaulospora, Rhizophagus* and *Glomus* species. These fungi often colonize and form symbiotic relationships with the roots of tea plants (Bag et al., 2022; Zhang X. et al., 2022). This relationship with tea plant roots likely contributes to the ability of tea plants to thrive successfully for many years even under adverse environmental conditions that can include drought, salinity, and temperature. In particular, various AMF are known to provide host plants with essential mineral elements, confer resistance to pests, diseases and abiotic stress and promote plant health (Almario et al., 2022; Zhang X. et al., 2022). AMF members of the *Glomus, Acaulospora* and *Gigaspora* genera have all been reported in cultivated tea lands, e.g., in India and various locations of China (Sharma et al., 2013; Ji et al., 2022; Zhang Z. et al., 2022).

2.2 Bacterial communities in soils of tea gardens

Bacterial communities are diverse and perform numerous functions in soils. Kui et al. (2021), through the direct extraction of total soil DNA from soil samples and sequencing using high through-put 16S rRNA and internal transcribed spacer amplicon sequencing techniques, characterized the soil microbiome in ancient tea plantations in Southwest region, China, identifiying Acidobacteria, Actinobacteria, and Proteobacteria phyla as the dominant bacterial community. As tea farming often occurs in one place over many generations and sometimes hundreds of years the dominance of Acidobacteria may indicate their importance in key ecological processes such as regulation of biogeochemical cycles and growth promoting activities (Kalam et al., 2020) in tea gardens. The relative abundance of Acidobacteria in tea garden soils is linked to increased age of tea plants (Wang et al., 2019). The long-term use of pesticides and fertilizers which contributes to the acidification of tea soil enables the Acidobacteria to thrive through many mechanisms they have developed. These mechanisms are genetically controlled and include acid tolerance, secondary metabolites, nitrogen metabolism, exopolysaccharide synthesis, hopanoids synthesis, siderophore synthesis (Kalam et al., 2020; Yadav et al., 2021).

Furthermore, using Illumina Miseq sequencing of the 16S rRNA targeting rhizospheric soil bacteria, Zi et al. (2020) found the bacterial community to be dominated by Proteobacteria, Acidobacteria and Actinobacteria with the relative abundance of 43.12, 21.61, and 14.84%, respectively, in Southwest tea cultivation region of China. The dominance of Proteobacteria in soils of tea gardens may be linked to their functioning in carbon and nitrogen cycling because these bacteria are known to be involved in ammonia oxidation and nitrification (Zhang Z. et al., 2022; Wang et al., 2023). Besides, the use of nitrogen-based fertilizers to increase yield in tea gardens could be responsible for the abundance of Proteobacteria in soil because they are actively involved in nitrogen conversions in soil. Likewise, a recent study conducted by Zheng et al. (2023) through the direct extraction of soil DNA and high-throughput sequencing to investigate soil microbial communities structure in tea plantations in the Southeast region of China, reported the relative abundance of bacterial phyla corresponding to Proteobacteria (20.96–41.40%), Acidobacteria (9.41–28.42%), Firmicutes (6.39–16.03%), Bacteriodetes (6.05–13.80%), Chloroflexi (3.35–13.27%) and Actinobacteria (2.37–11.52%) being dominant phyla. Lynn et al. (2017), through the direct extraction of soil microbial DNA and 16S rRNA sequencing also demonstrated that Actinobacteria, Chloroflexi, Acidobacteria, Proteobacteria, Firmicutes dominated the diverse bacterial communities in tea plantations found in Southern region of China. Actinobacteria have evolved mechanisms such as production of secondary metabolites, production of phytohormones, production of antimicrobials and stress tolerance, enabling them to thrive successfully in various soil ecosystem including adverse conditions, this may explain their high level of occurrence. The presence of Actinobacteria in tea gardens may also be helpful for the growth and successful yield of tea plants over the years. Actinobacteria have been reported to produce enzymes and secondary metabolites including a range of antibiotics some of which have been successfully exploited commercially and industrially (Barka et al., 2016; Jose et al., 2021). They are also known to act as biopesticides for agricultural benefit and play important roles in bioremediation of chemical pesticides, heavy metals, and other toxins (Alvarez et al., 2017; Banik et al., 2019). The rich abundance of Actinobacteria in soils of tea gardens likely helps account for the ability of tea plants to resist a wide range of phytopathogens, *i.e*, through their production of antimicrobial metabolites (Shan et al., 2018).

In addition, bacteria belonging to diverse genera known as the "mycorrhizal helper bacteria" (MHB) exist in soils. Frequently, these bacteria have a tripartite association with arbuscular mycorrhizal fungi and tea roots (Bidondo et al., 2016; Gupta and Chakraborty, 2020). Although their activities in tea gardens are poorly understood, these bacterial AMF enhancers generally have been reported to promote the functions of arbuscular mycorrhizal fungi leading to a better uptake of nutrients by plants and potentially increasing their ability to survive biotic and abiotic stresses (Sangwan and Prasanna, 2022). These bacteria may also benefit the AMF which would then benefit the plant. Bacteria that function actively as mycorrhizal fungal enhancers are found in (1) the Proteobacteria, specifically within the bacteria genera: *Pseudomonas*, *Agrobacterium*, *Azospirillum*, *Azotobacter*, *Burkholderia*, *Bradyrhizobium*, *Enterobacter*, *Klebsiella* and *Rhizobium* species, (2) the Actinobacteria including *Rhodococcus*, *Streptomyces* and *Arthrobacter* sp., and (3) the Firmicutes that include *Bacillus*, *Brevibacillus* and *Paenibacillus* sp. (Martin, 2016; Nasslahsen et al., 2022). These mycorrhizal helper bacteria may also perform several other functions not limited to enhancing AMF, such as plant growth promoting activities through the production of phytohormones (Sangwan and Prasanna, 2022), and they are widespread in tea garden soils.

2.3 Viral communities in soils of tea gardens

Viruses are likely the most abundant and diverse organisms on earth, many of whom affect soil microbial communities and their functions (Berliner et al., 2018; Jansson and Wu, 2022). Examination of soil viruses remains understudied; however, it is known that viruses can regulate soil microbial communities (Chevallereau et al., 2021; Liao et al., 2022) and contribute significantly to soil ecological processes such as nutrient cycling (Bi et al., 2022). In particular, there is paucity of reports on specific activities of soil viruses in tea gardens, viruses can be very important as they infect other microbial

communities such as the bacteria and fungi, hence shaping microbial composition, metabolism and probably influence major soil activities (Roux and Emerson, 2022). Since viruses are host specific, viruses that infect pathogenic bacteria, fungi, and insects, have been isolated and used as biocontrol agents targeting their respective hosts (Kizheva et al., 2021). In terms of insect pests, two viruses: *Ectropis obliqua* single-nucleocapsid nucleopolyhedrovirus (EcobSNPV) and *Ectropis obliqua* picorna-like viruses (EoPV) have been commercially used with high efficacy against *E. obiqua* which is a common pest of tea plants (Idris et al., 2020). However, effective viruses for other tea pests, e.g., *Helopeltis theivora* and *Gyropsylla spegazziniana*, have not yet been commercialized, and overall, the specific contributions of soil viruses to (tea) soil fertility and plant health remains unknown.

3 Functions of soil microorganisms in tea gardens

Depending upon the member community, soil microorganisms in tea garden could have beneficial or detrimental effects on tea plants (Figure 1). Beneficial microorganisms, such as members of the *Bacillus*, *Rhizobium, Actinomycetes, Trichoderma*, and *Glomus* promote soil health and enhance plant productivity through improving soil structure and promoting organic matter recycling (Hicks et al., 2021; Wei et al., 2024), e.g., functioning as decomposers of leaf litters and dead plant materials in tea gardens (Schroeter et al., 2022; Wang et al., 2023).

Microbial communities can also help plant disease resistance, decrease soil load of (plant) pathogens, and increase (plant) environmental stress tolerances (Zhang X. et al., 2022). For example, beneficial microbes such as *Bacillus* spp. and Actinomycetes can help tea plants resist a range of fungal diseases, i.e., leaf blight and scab disease (Wang et al., 2021). Arbuscular AMF colonization in the tea rhizosphere, e.g., by *Glomus*, *Rhizophagus*, and *Acaulospora*, likely contributes to enhanced disease resistance in host tea plants. Tea roots colonization by AMF can also help tea plants to survive under adverse conditions, enhance photosynthesis, and increase nutrient (e.g., phosphorus) absorption (Bag et al., 2021; Almario et al., 2022). Conversely, some soil microorganisms, e.g., *Fusarium* and *Pseudopestalotiopsis*, can cause disease to tea plants (Arafat et al., 2020; Pandey et al., 2023), and cultivation methods such as long-term applications of chemical fertilizers (e.g., Urea- N and NPK) may result in enrichment of pathogenic fungi (e.g., *Fusarium* and *Pseudopestalotiopsis*) in tea gardens (Wang et al., 2023; Zheng et al., 2023).

Nitrosphaeraceae also play important roles in nitrogen cycling (Amoo and Babalola, 2017; Zhang Z. et al., 2022), and the rhizosphere of tea plants are frequently colonized by nitrogen fixing and ammonia oxidizing bacteria (e.g., *Azotobacter* and *Nitrosomonas*, respectively) which affect nutrient cycling in the soil and can regulate nutrient utilization in tea plants (Wright and Lehvirta-Morley, 2023). Beneficial bacteria such as *Bacillus*, *Azotobacter* and *Pseudomonas* have also been proven to be of great potential in soil remediation (Xiang et al., 2022). However, there is no information of their specific application in remediation of tea soils.

Viral lysis of microbial cells can release materials which are transformed into dissolved organic matters (Chen X. et al., 2022), thus impacting nutrient cycling processes. In addition, viruses can reprogram host metabolism by expressing virus-contained auxiliary metabolic genes during infection. These auxiliary metabolic genes are sometimes involved in numerous metabolic pathways and could boost host metabolism and supply energy, thereby enhancing viral propagation, consequently impacting biogeochemical cycles (Hurwitz and U'Ren, 2016; Bi et al., 2022). Several studies have demonstrated the presence of auxiliary metabolic genes in soils, particularly agricultural soils (Wang et al., 2016; Han et al., 2017). For example, viral-encoded carbon metabolism was identified in high organic matter peatsoils, demonstrating potential viral roles in carbon cycling processes (Emerson et al., 2018; Trubl et al., 2018). Viruses can also influence microbial/plant/animal evolution as agents of horizontal gene transfer by encoding other functional genes and mediating the transfer of genes between hosts (Trubl et al., 2018). Although assumed for many years that the tea plant was virus-free, Hao et al. (2018) reported two novel viruses belonging to the *Blunervirus* and *Ilarvirus* genera from tea plants using metagenomic analysis. These viruses infected the tea plant causing necrotic ring and discoloration of tea leaves, reducing the quality and yield of tea leaves.

4 Mechanisms of actions of microbial communities in tea garden soils

Some soil microorganisms' exhibit positive plant growth promoting (PGP) traits that impact the productivity of the plants that grows on such soils (Bag et al., 2022). Growth promoting traits in soil microorganisms (e.g., *Bacillus subtilis*, *Trichoderma viridae*, and *Streptomyces griseus*) in tea garden soils (Tables 2, 3) have been shown to impact phosphate solubilization, nitrogen fixation, siderophore production, antagonism to the pathogen, and act in the production of plant auxin hormone production, e.g., indole-3-acetic acid (Bhattacharyya and Sarmah, 2018; Kolandasamy et al., 2023), with tea rhizosphere bacteria also found to promote the growth of rice and maize seedlings (Bhattacharyya et al., 2020). A significant positive relationship between Nitrososphaeraceae in tea garden soils with ammonia oxidation and nitrification processes has been reported, suggesting the importance of these bacteria in sustaining nitrogen fixation (Zhang Z. et al., 2022). These results suggest that exploitation of identified beneficial tea rhizosphere microorganisms has the potential to be used as microbial-based fertilizers. A two-year field experiment comparing the effects of bio-organic fertilizers (*Bacillus megaterium*-based bio-organic fertilizer, *Bacillus colloid*-based bio-organic fertilizer and *Bacillus subtilis*-based bio-organic fertilizer) and conventional chemical fertilizers, reported that the microbial-based fertilizers increased significantly the contents of tea polyphenols, amino acids and caffeine compared with the conventional chemical fertilizer (Liu et al., 2023), perhaps, through nitrogen metabolism and nutrient solubilization processes which enhanced nutrient availability and uptake by tea roots. Similarly, a study conducted by Xin et al. (2024) reported that the inoculation of soil with a synthetic community (SynCom21) of 21 bacterial strains belonging to the phyla Proteobacteria and Actinobacteria isolated from the rhizosphere of highly productive tea plants, was able to enhance ammonia uptake and transport in tea plants, facilitate the synthesis of theanine and increase theanine content of the tea leaves in comparison with the controls. Thus, application of tea rhizosphere bacteria as microbial-based fertilizer can promote nutrient availability and absorption

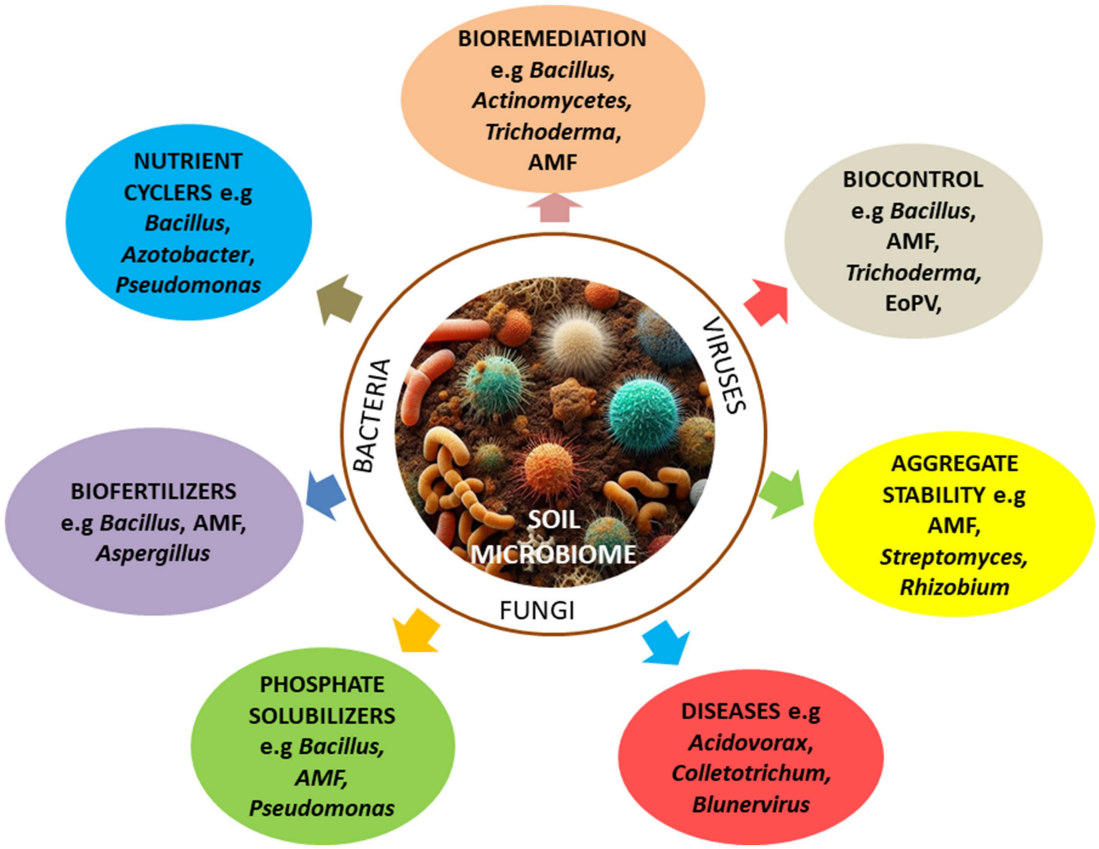

FIGURE 1
Composition and functions of soil microbial communities in tea garden.

resulting in enhanced tea polyphenols and theanine content, increasing the quality of tea leaves.

Soil microbe degradation of soil pollutants is another key ecological function that entails regulated gene expression and the activities of multiple enzymes (Wang et al., 2023). A variety of chemical pesticides, especially organochlorine pesticides (OCPs) such as Dichloro-diphenyl-trichloroethanes (DDT), Endosulfan and Dicofol to target tea scale insect, mites and tea mosquito bug are routinely used in tea plantations, resulting in residues on the tea plants themselves as well as in the soil (Lu et al., 2015; Fernandes et al., 2023). These chemicals can decrease the quality of both the tea and the soil, with such persistent organic pollutants (POPs), accumulating due to their low natural degradation rates (Negrete-Bolagay et al., 2021), potentially carcinogenic (Fernandes et al., 2023). However, rhizosphere microorganisms, through the action of degradative enzymes, have been reported to be able to degrade such persistent organic pollutants (Bishnu et al., 2012; Shi et al., 2015) in the soil of tea plants. The specific microorganisms involved in the degradation of organic pollutants in tea gardens have not been reported, but tea plant root secretions such as catechin, glucose, arginine and oxalic acid, have been reported to significantly influence the degradative abilities of soil microorganisms against persistent organic pollutants (POPs) by tea plant rhizosphere microorganisms. This was explained by the reduction in the binding energy of the complex protein to POP molecules in the presence of these root secretions (Du et al., 2022). These root secretions likely also attract and stimulate select microorganisms to produce degradative enzymes such as polyphenol oxidase, hydrolases, catalase and laccase (Wei et al., 2024), which can catalyze the degradation of the POPs. Moreover, root secretions can influence microorganisms present in the rhizosphere by acting as stimulants, signaling molecules or repellants (Olanrewaju et al., 2019; Xin et al., 2024). Various plant growth promoting microorganisms including *Bacillus*, *Pseudomonas*, and *Trichoderma* have also been shown to be involved in the remediation of pollutants and heavy metals in soil (Gond et al., 2021; Ren et al., 2023). The ability of bacteria such Acidobacteria and Chloroflexi to utilize complex organic compounds has been shown to increase with the age of tea planting (Wang et al., 2020). These data indicate that metabolic activities of microorganisms in the soil of tea gardens could potentially remove and degrade harmful substances such as chemical pesticides, heavy metals and organic pollutants in the soil.

Microorganisms also help maintain soil aggregates that are important to soil structure and fertility, root penetration and crop yield, through secretions of extracellular polymeric substances and other compounds including polysaccharides, polyuronic, and amino acids with adhesive properties which can bind soil particles together (Hartmann and Six, 2022). The soil fungal community can promote aggregate stability because of their filamentous growth and their hyphal networks in soil (Morris et al., 2019). Particularly, AMF produce hyphal networks and gromalin, a putative abundantly produced glycoprotein, which aids in soil resistance to erosion, and helps increase carbon storage and water-holding capacity (Rashid

TABLE 2 Regulation of the functions of major soil bacterial communities in tea gardens.

Functions	Mechanisms	Phyla of microorganisms	Examples (Genera)	References
Biofertilizers (Plant growth promoters)	Indole-3- acetic acid production	Firmicutes, Proteobacteria, Actinobacteria Acidobacteria	*Bacillus, Pseudomonas, Enterobacter, Brevibacillus, Burkholderia, Leifsonia, Achromobacter, Klebsiella Staphylococcus, Nocardia, Ochrabactrum, Micrococcus, Arthrobacter, Streptomyces*	Dutta and Thakur (2017), Shan et al. (2018), and Bhattacharyya et al. (2020)
	Siderophore production	Firmicutes, Proteobacteria, Actinobacteria, Acidobacteria	*Bacillus, Pseudomonas, Enterobacter, Brevibacillus, Burkholderia, Leifsonia, Achromobacter, Klebsiella Staphylococcus, Arthrobacter, Micrococcus, Ochrabactrum, Streptomyces*	Dutta and Thakur (2017), Bhattacharyya et al. (2020), and Kolandasamy et al. (2023)
	ACC deaminase production	Actinobacteria Firmicutes, Acidobacteria Proteobacteria	*Bacillus, Pseudomonas, Enterobacter, Brevibacillus, Burkholderia, Streptomyces, Achromobacter, Klebsiella Staphylococcus, Ochrabactrum, Micrococcus,*	Dutta and Thakur (2017), Shan et al. (2018), Bhattacharyya et al. (2020), and Kolandasamy et al. (2023)
Biofertilizers (Nutrient cycling)	Phosphate solubilization	Firmicutes, Proteobacteria, Actinobacteria, Acidobacteria	*Bacillus, Pseudomonas, Enterobacter, Brevibacillus, Burkholderia, Arthrobacter, Achromobacter, Klebsiella Staphylococcus, Leifsonia, Ochrabactrum, Micrococcus, Streptomyces*	Dutta and Thakur (2017), Bhattacharyya et al. (2020), and Kolandasamy et al. (2023)
	Potassium solubilizing	Firmicutes, Proteobacteria, Acidobacteria, Actinobacteria	*Bacillus, Burkholderia, Pseudomonas, Paenibacillus, Acidothiobacillus, Rhizobium, Azospirillium, Arthrobacter*	Bagyalakshmi et al. (2017), Bhattacharyya and Sarmah (2018), and Zhang X. C. et al., 2022
	Ammonia production	Firmicutes, Proteobacteria, Actinobacteria,	*Bacillus, Pseudomonas, Enterobacter, Brevibacillus, Arthrobacter, Burkholderia, Ochrabactrum, Micrococcus, Achromobacter, Klebsiella, Leifsonia, Staphylococcus,*	Dutta and Thakur (2017) and Bhattacharyya et al. (2020)
	Nitrogen fixation	Proteobacteria, Firmicutes, Acidobacteria, Actinobacteria	*Burkholderia, Azospirillum, Pseudomonas, AcidocapsaMethylobacterium, Azotobacter, Acinetobacter, Streptomyces, Klebsiella*	Bhaduri et al. (2018), Yan et al. (2018), and Cernava et al. (2019)
Biocontrol	biosurfactant production	Actinobacteria, Firmicutes, Acidobacteria,	*Bacillus, Brevibacterium, Pseudomonas*	Banik et al. (2019) and Chopra et al. (2020a,b)
	antifungal/antibiotics production	Actinobacteria, Firmicutes Acidobacteria	*Bacillus, Pseudomonas, Enterobacter, Brevibacillus, Burkholderia, Actinomadura,Achromobacter, Klebsiella Staphylococcus, Serratia, Streptomyces*	Dutta and Thakur (2017), Dhar Purkayastha et al. (2018), Shan et al. (2018), and Kolandasamy et al. (2023)
Soil structure	Stabilizing soil aggregates	Actinobacteria, Firmicutes, Chloroflexi, Proteobacteria	*Streptomyces, Nocardia, Actinomadura, Rhizobium*	Wang et al. (2021) and Wang et al. (2023)
Tolerance to stress	Enhances resistance to abiotic stress	Firmicutes Actinobacteria Acidobacteria	*Pseudomonas, Bacillus, Streptomyces, Leifsonia, Ochrabactrum, Micrococcus, Arthrobacter, Nocardia, Actinomadura*	Bhattacharyya et al. (2020), Bag et al. (2021), and Kolandasamy et al. (2023)

et al., 2016). AMF also increase the stability of soil macroaggregates in the soil ecosystem of tea gardens (Morris et al., 2019). A report on the dynamics of soil bacterial community diversity and composition at aggregate scales in tea gardens, revealed that soil aggregates exhibited complex bacterial communities which could provide biological buffering which could prevent individual bacterial species from gaining superiority via competition or predation (Wang et al., 2021). Because stable soils can provide a valuable ecosystem for tea plants to thrive, future studies should explore the potentials of microorganisms, particularly AMF stabilization of soil ecosystem in tea gardens.

Furthermore, some soil microorganisms colonizing the root of tea plants exhibit strong biocontrol activity against plant pathogens and pests (Bag et al., 2022). Plant growth promoting fungi such as *Aspergillus*, *Fusarium, Trichoderma* and bacteria such as *Azotobacter*, *Azospirillum*, *Pseudomonas* sp., have been shown to help increase tea plant growth and can help control soil-borne plant pathogens (Thabah and Joshi, 2022), as well as potentially improving tea plant resistance to diseases (Zhang X. et al., 2022). For instance, bacterial *Bacillus* and fungal *Trichoderma* strains isolated from the tea rhizosphere have been shown to display high biocontrol efficacy against *Phomopsis theae,* a fungi pathogen causing stem canker in tea plants (Kolandasamy et al., 2023). Similarly, isolates of *B. subtilis* has been reported to significantly improve the resistance of tea against several diseases including black rot, branch canker, blister blight and root diseases (Bhattacharyya et al., 2020; Bora and Bora, 2021). Actimomycetes such as *Streptomyces*, *Microbacterium*, and *Norcardia* sp. have been reported to produce secondary metabolites with

TABLE 3 Mechanisms of the functions of major soil fungal communities in tea gardens.

Functions	Mechanisms	Phyla of Microorganisms	Examples (Genera)	References
Biofertilizers (Plant growth promoters)	Indole-3- acetic acid production	Glomeromycota Ascomycota	*Penicillium, Aspergillus, Trichoderma, AMF*	Nath et al. (2015), Chen et al. (2023), and Kolandasamy et al. (2023)
	Siderophore production	Ascomycota	*Trichoderma*	Kolandasamy et al. (2023)
	ACC deaminase production	Ascomycota	*Trichoderma*	Kolandasamy et al. (2023)
	Uptake of nutrients	Glomeromycota	*Glomus, Claroideoglomus*	Shao et al. (2018) and Li et al. (2020)
Biofertilizers (Nutrient cycling)	Phosphate Solubilizing	Glomeromycota Ascomycota	*Penicillium, Aspergillus, Fusarium, Trichoderma, Rhizophagus*	Nath et al. (2015), Bhattacharyya and Sarmah (2018), Zhang Z. et al. (2022), and Kolandasamy et al. (2023)
	Potassium solubilizing	Ascomycota, Glomeromycota,	*Penicillium, Aspergillus, Fusarium*	Nath et al. (2015)
	Ammonia production	Ascomycota	*Trichoderma*	Kolandasamy et al. (2023)
Biocontrol	Production of antibiotics/ antifungals	Ascomycota, Basidiomycota, Glomeromycota	*Trichoderma, Glomus, Rhizophagus*	Chelangat et al. (2021), Chen W. et al. (2022), and Kolandasamy et al. (2023)
Tolerance to stress	Enhances resistance of tea plant to abiotic stress	Glomeromycota	*Trichoderma, Glomus, Glomus, Clariodeoglomus, Rhizophagus*	Chelangat et al. (2021), Chen W. et al. (2021), Kolandasamy et al. (2023), and Gao et al. (2023)

antimicrobial potentials (Shan et al., 2018) and have been proven to be successful in managing tea diseases (Bhattacharyya et al., 2016). These data indicate that healthy and/or manipulation of tea plantations soils can be useful and effective approach toward helping tea plants resist attack by microbial pathogens.

5 Factors that influence soil microbial communities of tea gardens

Tea is a perennial plant that is usually propagated through seedlings developed from seeds by hardening in a nursery through stepwise exposure to full daylight. Tea plant is frequently pruned to enable the development of new shoots and maintain the shape and height and can take up to two years to maturity. The leaves are harvested by plucking new leaves and terminal buds from the tip of the branches at regular intervals from the second year onwards (Mukhopadhyay and Mondal, 2017; Auria et al., 2022). The plucking of the new leaves also enables the emergence of new buds and leaves. Tea soil ecosystem functions are often affected by multiple biotic and abiotic factors. The intensity and duration of tea planting have a significant impact on the microbial community structure, biomass, and its function (Kui et al., 2021), also impacting the soil physicochemical properties.

Soil physicochemical properties like temperature, humidity and pH values influence microbial community diversity in tea garden soils (Muneer et al., 2022). Bacterial and fungal communities during tea planting are strongly affected by changes in soil pH (Zheng et al., 2023) that can occur due to the long-term use of chemical fertilizers. Soil pH in tea gardens can be altered by agricultural practices such as the addition of fertilizers and pesticides. The heavy use of chemical fertilizers can decrease soil pH while the use of organic fertilizers can regulate soil pH. Ye et al. (2022) reported that the long-term use of chemical fertilizer led to a continuous decrease in soil pH from 3.07–2.82 in tea plantations in Southeast China while the long-term use of organic fertilizer led to a stable pH of 5.13–5.33, which is suitable for growth, improved yield, and quality of tea. Persistent decreases in soil pH in addition to decreasing microbial diversity, may result in the denaturing of soil enzymes, and lowered nutrient solubility and availability to plants, as well as increased aluminium and/or heavy metals toxicity as lowered soil pH can increase solubility of certain toxic chemicals, resulting both direct plant toxicity, decreased soil microbial diversity, and equally important in terms of relevance to human consumption, accumulation of toxic metals by the plant (Yan et al., 2021; Naz et al., 2022).

Like many metals, low levels of aluminium, copper, manganese, and others are needed by the plant and promote tea plant growth, however at high concentrations coupled to lowered pH, they can induce toxicity (in the plant and/or to the consumer) as insoluble forms, e.g., for aluminium, dissociate at $pH < 5$ and releasing (Al^{3+}) ions into the soil, which can form complexes with the other compounds (e.g., phosphates) found in the rhizosphere of tea plants (Ray et al., 2022), which would not only increase metal contents in the plants, but could also reduce the availability of phosphorus to plants. As mentioned, decreases soil pH can lead to the accumulation of metals in the tea plant leaves (de Silva et al., 2016; Peng et al., 2018; Yan et al., 2018), that when cycled, leads to a further decrease in soil pH, successively affecting soil microbial community structure and function, and ultimately impairing healthy plant growth and reducing the quality of the tea leaves. Decreased pH would favor acidophilic bacteria, i.e., those that encode genes regulating acid tolerance and/or prefer acidic conditions for their growth such as Acidobacteria (Kalam et al., 2020), and the abundance of microorganisms such as Acidobacteria and Ascomycota in tea gardens was increased with lower soil pH (Zhang Z. et al., 2022).

Similarly, agricultural management practices (e.g., the use of pesticides, mulch, fertilizers, Figure 2) can have beneficial or detrimental effect on the health of (beneficial) soil microbial communities, leading to increased or decreased tea plants yields,

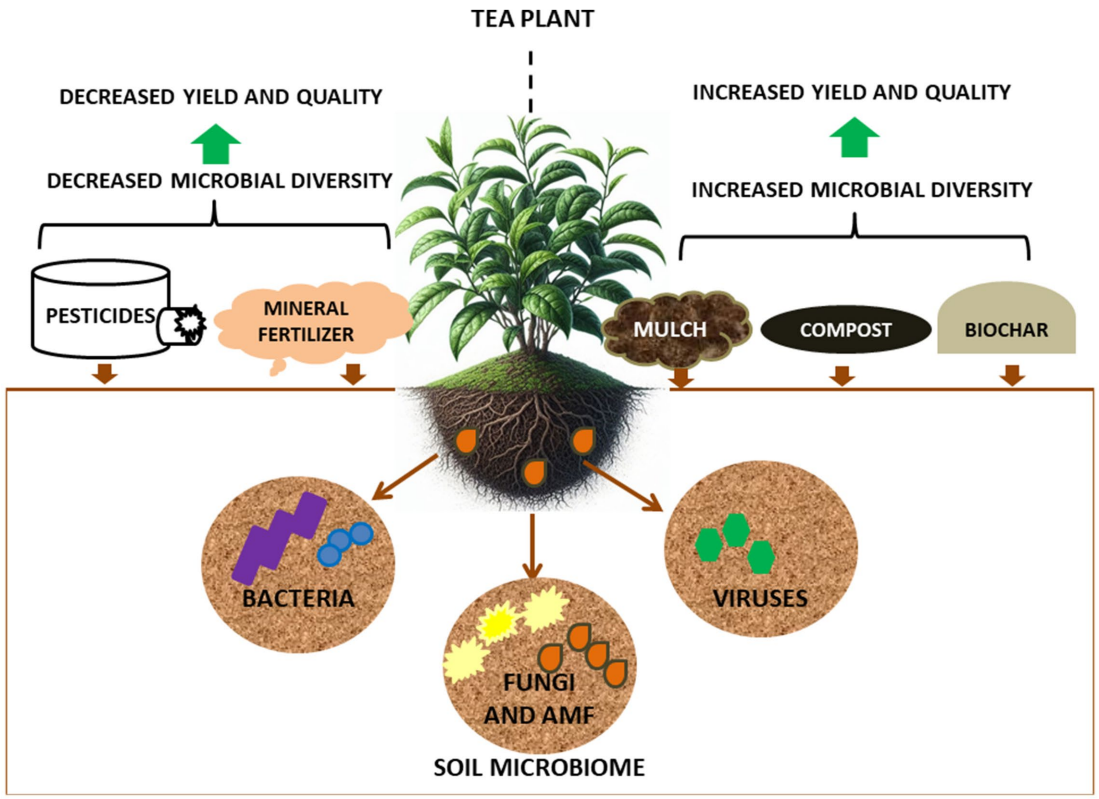

FIGURE 2
Agricultural management factors influencing microbial diversity in soils of tea gardens.

respectively. Fertilizer and pesticide applications can affect the microbial communities of the rhizosphere (Liu et al., 2021), with nitrogen fertilizers improving tea yields but leading to rapid and continuous acidification of tea garden soils (Yan et al., 2020). This acidification can result in loss of important soil microorganisms which is exacerbated by continuous tea cultivation in the same soil, which can lead to erosion of tea quality and yield (Li et al., 2016; Yang et al., 2018; Ye et al., 2022). To combat this, there has been increasing use organic fertilizers/compost as these have been to improve (i.e., help alkalinize) acidified soils, improving soil microbial community health including enzyme activities that improve soil quality (Li et al., 2018; Lin et al., 2019; Xie et al., 2021). Thus, addition of organic fertilizers to tea garden soil can be one method for the remediation of acidified soil (Ye et al., 2022). Within this context, the application of a combination of compost and nitrogen fertilizer has been shown to increase soil microbial diversity, demonstrating the compatibility of this combined approach for promoting soil and subsequent plant health (Taha et al., 2016).

A study on the effect of organic mulching in tea plantations, reported that bacteria of the phylum Nitrospirae were more numerous in peanut hull mulched soils (3.24%) as compared to polyethylene mulched soils (1.21%) (Zhang et al., 2020). The abundance of Nitrospirae indicates the presence of ammonia-and nitrate-oxidizing bacteria which are important for nitrogen cycling processes (Chen Y. P. et al., 2021). Fungal Mortierellomycota and Basidiomycota were also higher in peanut mulched soils (33.72, 21.93%) as compared to polyethylene mulched soils (14.88, 6.53%) (Zhang et al., 2020), indicating that organic mulching of tea garden soils could have a positive effect on soil microbial communities, helping to improve soil fertility for higher tea plant yields.

More recently, the biochar, which consists of carbon, volatile matter, mineral matter (ash) and moisture, created by thermal burning of biomass has been applied to soils with the aim of improving soils (Armah et al., 2023). This innovation has gained prominence as an effective soil amendment for decreasing plant disease incidence and helping promote beneficial microbial populations in continuous cropping soils (Ge et al., 2023). Biochar application to soil has been reported to increase tea plant productivity and soil nutrient contents (Zou et al., 2023). Bamboo and rice straw biochar has also been shown to significantly improve tea growth, increase tea nutrients and reduced heavy metals in tea (Yan et al., 2021). Although the mechanism of biochar mediated effects on soil microorganisms in tea gardens remains unclear, biochar application has been shown to shape the tea soil fungal community (Zheng et al., 2019), which may be because fungi play important roles in organic matter turnover (Chen et al., 2014). The mechanism of how biochar influences specific soil microbial communities for improved tea yield is an important emerging field for sustainable tea production.

6 Conclusions and future perspectives

Tea cultivation has considerable economic and medicinal value, and to ensure sustainable tea production, it is necessary to study the role that soil microorganism play, including promoting an increase in

the diversity of beneficial soil microorganisms to improve soil health and tea productivity. Targets of future research include:

(i) Exploiting molecular techniques, including targeted gene manipulation (e.g., CRISPR/Cas) to enhance the beneficial characteristics of soil microorganisms, including their biofertilizing capabilities. For example, the potential of AMFs in soils (which can contribute to increased nutrient acquisition, stress tolerance and/or disease resistance) of tea plantations could be enhanced through the isolation and application of suitable strains for inoculation. In this context, molecular techniques can be used to directly manipulate tea varieties to achieve these desirable characteristics.
(ii) Enhancing the biocontrol activity, especially toward fungal plant pathogens and insect pests, of soil bacteria and fungi in tea gardens to provide an ecologically friendly approaches disease and pest management.
(iii) To explore and commercialize the use of plant growth-promoting microorganisms from other crops for tea cultivation and, conversely, the use of beneficial microbes derived from tea garden soils on other economically important crops for sustainable agriculture.

Author contributions

MJ-S: Conceptualization, Methodology, Writing – original draft. ZH: Resources, Writing – original draft. NK: Writing – review & editing. YD: Data curation, Writing – original draft. RC: Data curation, Writing – original draft. SL: Data curation, Writing – original draft. YL: Data curation, Writing – original draft. PL: Data curation, Writing – original draft. JC: Data curation, Writing – original draft. CY: Data curation, Writing – original draft. WZ: Data curation, Writing – original draft. HL: Resources, Writing – original draft. ZW: Resources, Writing – original draft. SH: Resources, Writing – original draft. PC: Resources, Writing – original draft. LT: Writing – original draft. ZQ: Writing – original draft. XZ: Writing – original draft. XG: Writing – original draft. JQ: Conceptualization, Funding acquisition, Writing – review & editing.

Funding

The author(s) declare financial support was received for the research, authorship, and/or publication of this article. This research was financed by the National Natural Science Foundation of China (no. 32270029, U1803232, 31670026), the National Key R&D Program of China (no. 2017YFE0122000), Social Service Team Support Program Project (no. 11899170165) and Science and Technology Innovation Special Fund (no. KFB23084) of Fujian Agriculture and Forestry University, Fujian Provincial Major Science and Technology Project (no. 2022NZ029017), Key Project from Fujian Provincial Department of Science and Technology (no. 2020N5005), and the Young and Middle-aged Teacher Education Research Project of Fujian Province (no. JAT210075).

Conflict of interest

The authors declare that the research was conducted in the absence of any commercial or financial relationships that could be construed as a potential conflict of interest.

Publisher's note

References

Aaqil, M., Peng, C., Kamal, A., Nawaz, T., Zhang, F., and Gong, J. (2023). Tea harvesting and processing techniques and its effects on phytochemical profile and final quality of black tea: a review. *Food Secur.* 12:4467. doi: 10.3390/foods12244467

Abe, S. K., and Inoue, M. (2021). Green tea and cancer and cardiometabolic diseases: a review of the current epidemiological evidence. *Eur J. Clinical Nutr.* 75, 865–876. doi: 10.1038/s41430-020-00710-7

Almario, J., Fabianska, I., Saridis, G., and Bucher, M. (2022). Unearthing the plant-microbe quid pro quo in root associations with beneficial fungi. *New Phytol.* 234, 1967–1976. doi: 10.1111/nph.18061

Alvarez, A., Saez, J. M., Costa, J. S. D., Colin, V. L., Fuentes, M. S., Cuozzo, S. A., et al. (2017). Actinobacteria: current research and perspectives for bioremediation of pesticides and heavy metals. *Chemosphere* 166, 41–62. doi: 10.1016/j.chemosphere.2016.09.070

Amoo, A. E., and Babalola, O. O. (2017). Ammonia-oxidizing microorganisms: key players in the promotion of plant growth. *J. Soil Sci. Plant Nutr.* 17, 935–947. doi: 10.4067/S0718-95162017000400008

Arafat, Y., Din, I. U., Tayyab, M., Jiang, Y., Chen, T., Cai, Z., et al. (2020). Soil sickness in aged tea plantation is associated with a shift in microbial communities as a result of plant polyphenol accumulation in the tea gardens. *Front. Plant Sci.* 11:601. doi: 10.3389/fpls.2020.00601

Armah, E. K., Chetty, M., Adedeji, J. A., Estrice, D. E., Mutsvene, B., Singh, N., et al. (2023). Biochar: production, application and the future. In: Biochar-productive technologies, properties and applications. Bartoli, M., Giorcelli, M. and Tagliaferro, A. (Eds.). *Intech Open*. pp. 1–26. doi: 10.5772/intechopen.105070

Auria, J. C. D., Cohen, S. P., Leung, J., Glockzin, K., Glockzin, K., Gervay-Hague, J., et al. (2022). United States tea: a synopsis of ongoing tea research and solutions to United States tea production issues. *Front. Plant Sci.* 13:934651. doi: 10.3389/fpls.2022.934651

Bag, S., Mondal, A., and Banik, A. (2022). Exploring tea (*Camellia sinensis*) microbiome: insights into the functional characteristics and their impact on tea growth promotion. *Microbiol. Res.* 254:126890. doi: 10.1016/j.micres.2021.126890

Bag, S., Mondal, A., Majumder, A., and Banik, A. (2021). Tea and its phytochemicals: hidden health benefits and modulation of signaling cascade by phytochemicals. *Food Chem.* 371:131098. doi: 10.1016/j.foodchem.2021.131098

Bagyalakshmi, B., Ponmurugan, P., and Balamurugan, A. (2017). Potassium solubilization, plant growth promoting substances by potassium solubilizing bacteria (KSB) from southern India tea plantation soil. *Biocatal. and Agric. Biotechnol.* 12, 116–124. doi: 10.1016/jbcab.2017.09.011

Banik, A., Chattopadhyay, A., Ganguly, S., and Mukhopadhyay, S. K. (2019). Characterisation of a tea pest specific Bacillus thuringiensis and identification of its toxin by MALDI-TOF mass spectrophotometry. *Indust. Crops and Prod.* 137, 549–556. doi: 10.1016/J.INDCROP.2019.05.051

Barka, E. A., Vatsa, P., Sanchez, L., Gaveau-Vaillant, N., Jacquard, C., Meier-Kolthoff, J. P., et al. (2016). Taxonomy, physiology and natural products of Actinobacteria. *Microbiol. Biol. Rev.* 80, 1–43. doi: 10.1128/mmbr.00019-15

Bastida, F., Eldridge, D. J., Garcia, C., Png, G. K., Bardgett, R. D., and Baquerizo, M. D. (2021). Soil microbial diversity-biomass relationships are driven by soil carbon content across global biomes. *ISME J.* 15, 2081–2091. doi: 10.1038/s41396-021-00906-0

Basu, S., Kumar, G., Chhabra, S., and Prasad, R. (2021). Chapter 13-role of microbes in biogeochemical cycle for enhancing soil fertility. In: New and future developments in microbial biotechnology and bioengineering. Verma, J. P., Macdonald, C. A., Gupta, V. K. and Podile, A. R. (Eds.) *Phytomicrobiome for sustainable agriculture*. Elsevier. pp. 149–157.

Bayer, B., Saito, M. A., Mcllvin, M. R., Luker, S., Moran, D. M., Lankiewicz, T. S., et al. (2020). Metabolic versatility of the nitrite-oxidizing bacterium Nitrospira marina and its proteomic response to oxygen-limited conditions. *ISME J.* 15, 1025–1039. doi: 10.1038/s41396-020-00828-3

Berliner, A. J., Mochizuki, T., and Stedman, K. M. (2018). Astrovirology: viruses at large in the universe. *Astrobiology* 18, 207–223. doi: 10.1089/ast.2017.1649

Bertola, M., Ferrarini, A., and Visioli, G. (2021). Improvement of soil microbial diversity through sustainable agricultural practices and its evaluation by-omics approaches: a perspective for the environment, food quality and human safety. *Microorganisms* 9:1400. doi: 10.3390/microorganisms9071400

Bhaduri, J., Kundu, P., and Roy, S. K. (2018). Identification and molecular phylogeny analysis using random amplification of polymorphic DNA (RAPD) and 16SrRNA sequencing of N_2 fixing tea field soil bacteria from North Bengal tea gardens. *Afr. J. Microbiol. Res.* 12, 655–663. doi: 10.5897/AJMR2018.8872

Bhattacharyya, C., Baberjee, S., Acharya, U., Mitra, A., Mallick, I., Haldar, A., et al. (2020). Evaluation of plant growth promotion properties and induction of oxidative defense mechanism by tea rhizobacteria of Darjeeling. *India. Sci. Rep.* 10:15536. doi: 10.1038/s41598-020-72439-z

Bhattacharyya, P. K. S., Roy, M., Dasa, S., Raya, D., Balachandar, S., Karthikeyan, A. K., et al. (2016). Elucidation of rice rhizosphere metagenome in relation to methane and nitrogen metabolism under elevated carbondioxide and temperature using whole genome metagenomic approach. *Sci. Total Environ.* 542, 886–898. doi: 10.1016/j.scitotenv.2015.10.154

Bhattacharyya, P., and Sarmah, S. R. (2018). "The role of microbes in tea cultivation" in *Global tea science: Current status and future needs*. eds. V. S. Sharma and M. T. Kumudini (Cambridge, UK: Burleigh Dodds Science Publishing), 1–35.

Bi, L., Yu, D., Han, L., Du, S., Yuan, C., He, J., et al. (2022). Unravelling the ecological complexity of soil viromes: challenges and opportunities. *Sci. Total Environ.* 812:152217. doi: 10.1016/j.scitotenv.2021.152217

Bidondo, L. F., Colombo, R., Bompadre, J., Benavides, M., Scorza, V., Silvani, V., et al. (2016). Cultivable bacteria associated with infective propagules of arbuscular mycorrhizal fungi: implications for mycorrhizal activity. *Appl. Soil Ecol.* 105, 86–90. doi: 10.1016/j.apsoil.2016.04.013

Bishnu, A., Chakraborty, A., Chakrabarti, K., and Saha, T. (2012). Ethion degradation and its correlation with microbial and biochemical parameters of tea soils. *Biol. Fert. Soils.* 48, 19–29. doi: 10.1007/s00374-011-0606-9

Bollmann-Giolai, A., Malone, J., and Arora, S. (2022). Diversity, detection and exploitation: linking soil fungi and plant diseases. *Curr. Opin. Microbiol.* 70:102199. doi: 10.1016/j.mib.2022.102199

Bora, P., and Bora, L. C. (2021). Microbial antagonists and botanicals mediated disease management in tea, *Camellia sinensis* (L.) O. Kuntze: An overview. *Crop Protect.* 148:105711. doi: 10.1016/j.cropro.2021.105711

Busby, P. E., Soman, C., Wagner, M. R., Friesen, M. L., Kremer, J., Bennett, A., et al. (2017). Research priorities for harnessing plant microbiomes in sustainable agriculture. *PLoS Biol.* 15:e2001793. doi: 10.1371/journal.pbio.2001793

Cernava, T., Chen, X., Krug, L., Li, H., Yang, M., and Berg, G. (2019). The tea leaf microbiome shows specific responses to chemical pesticides and biocontrol applications. *Sci. Total Environ.* 667, 33–40. doi: 10.1016/j.scitotenv.2019.02.319

Chauhan, P., Sharma, N., Tapwal, A., Kumar, A., Verma, G. S., Meena, M., et al. (2023). Soil microbiome: diversity, benefits and interactions with plants. *Sustain. For.* 15:14643. doi: 10.3390/su151914643

Chelangat, A., Gweyi-Onyango, J. P., Korir, N. K., and Mwangi, M. (2021). Influence of arbuscular mycorrhizae on callusing and root colonization of tea (*Camellia sinensis*) clones in Kenya. *Asian Soil Res. J.* 5, 21–26. doi: 10.9734/ASRJ/2021/v5i130098

Chen, Y., Deng, Y., Ding, J., Hu, H., Xu, T., Li, F., et al. (2017). District microbial communities in the active and permafrost layers on the Tibetan plateau. *Mol. Ecol.* 26, 6608–6620. doi: 10.1111/mec.14396

Chen, L., Hu, X., Yang, W., Xu, Z., Zhang, D., and Gao, S. (2015). The effects of arbuscular mycorrhizal fungi on sex-specific responses to Pb pollution in Populus cathayana. *Ecotoxicol. Environ. Saf.* 113, 460–468. doi: 10.1016/j.ecoenv.2014.12.033

Chen, H., Mothapo, N. V., and Shi, W. (2014). The significant contribution of fungi to soil N_2O production across diverse ecosystems. *Appl. Soil Ecol.* 73, 70–77. doi: 10.1016/j.apsoil.2013.08.011

Chen, W., Shan, W., Niu, T., Ye, T., Sun, Q., and Zhang, J. (2023). Insight into regulation of adventitious root formation by arbuscular mycorrhizal fungus and exogeneous auxin in tea plant (*Camellia sinensis* L.) cuttings. *Front. Plant Sci.* 14:1258410. doi: 10.3389/fpls.2023.1258410

Chen, Y. P., Tsai, C. F., Rekha, P. D., Ghate, S. D., Huang, H. Y., Hsu, Y. H., et al. (2021). Agricultural management practices influence the soil enzyme activity and bacterial community structure in tea plantations. *Bot. Stu.* 62:8. doi: 10.1186/s40529-021-00314-9

Chen, X., Wei, W., Xiao, X., Wallace, D., Hu, C., Zhang, L., et al. (2022). Heterogeneous viral contribution to dissolved organic matter processing in a long-term macrocosm experiment. *Environ. Internat.* 158:106950. doi: 10.1016/j.envint.2021.106950

Chen, W., Ye, T., Sun, Q., Niu, T., and Zhang, J. (2021). Arbuscular mycorrhizal fungus alters root system architecture in *Camellia sinensis* L. as revealed by RNA-Seq analysis. *Front. Plant Sci.* 12:777357. doi: 10.3389/fpls.2021.777357

Chen, W., Ye, T., Sun, Q., Niu, T., and Zhang, J. (2022). Arbuscular mycorrhizal fungus alleviates anthracnose disease in tea seedlings. *Front. Plant Sci.* 13:1058092. doi: 10.3389/fpls.2022.1058092

Cheng, S., Fu, X., Wang, X., Liao, Y., Zeng, L., Dong, F., et al. (2017). Studies on the biochemical formation pathway of the amino acid L-theanine in tea (*Camellia sinensis*) and other plants. *J. Agric. Food Chem.* 65, 7210–7216. doi: 10.1021/acs.jafc.7b02437

Chevallereau, A., Pons, B. J., van Houte, S., and Westra, E. R. (2021). Interactions between bacterial and phage communities in natural environments. *Nat. Rev. Microbiol.* 20, 49–62. doi: 10.1038/s41579-021-00602-y

Chopra, A., Bobate, S., Rahi, P., Banpurkar, A., Mazumder, P. B., and Satpute, S. (2020b). *Pseudomonas aeruginosa* RTE4: a tea rhizobacterium with potential for plant growth promotion and biosurfactant production. *Front. Bioeng. Biotechnol.* 8:861. doi: 10.3389/fbioe.2020.00861

Chopra, A., Vandana, U. K., Rahi, P., Satpute, S., and Mazumder, P. B. (2020a). Plant promoting Brevibacterium sediminis A6 isolated from tea rhizosphere of Assam. *India. Biocatal. Agric. Biotechnol.* 27:101610. doi: 10.1016/j.bcab.2020.101610

Da Costa, D. P., da Silva, T. G. E., Araujo, A. S. F., Pereira, A. P. A., Mendes, L. W., Borges, W. S., et al. (2024). Soil fertility impact on recruitment and diversity of the soil microbiome in sub-humid tropical pastures in northeastern Brazil. *Sci. Rep.* 14:3919. doi: 10.1038/s41598-024-54221-7

De Silva, J., Tuwei, G., and Zhao, F. J. (2016). Environmental factors influencing aluminium accumulation in tea *Camellia sinensis* L. *Plant Soil* 400, 223–230. doi: 10.1007/s11104-015-2729-5

Deltedesco, E., Keiblinger, K. M., Piepho, H. P., Antonielli, L., Potsch, E. M., Zechmeis-Boltenstern, S., et al. (2020). Soil microbial community structure and function mainly respond to indirect effects in multifactorial climate manipulation experiment. *Soil Biol. Biochem.* 142:107704. doi: 10.1016/j.soilbio.2020.107704

Dhar Purkayastha, G., Mangar, P., Saha, A., and Saha, D. (2018). Evaluation of the biocontrol efficacy of *Serratia marcescens* strain indigenous to tea rhizosphere for the management of root rot disease in tea. *PLoS One* 13:e0191761. doi: 10.1371/journal.pone.0191761

Dong, C., Li, F., Yang, T., Feng, L., Zhang, S., Li, F., et al. (2019). Theanine transporters identified in tea plants (*Camellia sinensis* L.). *Plant J.* 101, 57–70. doi: 10.1111/tpj.14517

Du, M., Li, X., Cai, D., Zhao, Y., Li, Q., Wang, J., et al. (2022). *In-silico* study of reducing human health risk of POP residues' direct (from tea) or indirect exposure (from tea garden soil): improved rhizosphere microbial degradation, toxicity control, and mechanism analysis. *Ecotoxicol. Environ. Saf.* 242:113910. doi: 10.1016/j.ecoenv.2022.113910

Dutta, J., Handique, P. J., and Thakur, D. (2015). Assessment of culturable tea rhizobacteria isolated from tea estates of Assam, India for growth promotion in commercial tea cultivars. *Front. Microbiol.* 6:1252. doi: 10.3389/fmicb.2015.01252

Dutta, J., and Thakur, D. (2017). Evaluation of multifarious plant growth promoting traits, antagonistic potential and phylogenetic affiliation of rhizobacteria associated with commercial tea plants grown in Darjeeling, India. *PLoS One* 12:e0182302. doi: 10.1371/journal.pone.0182302

Egidi, E., Delgado-Baquerizo, M., Plett, J. M., Wang, J., Eldridge, D. J., Bargett, R. D., et al. (2019). A few Ascomycota taxa dominate communities worldwide. *Nat. Commun.* 10:2369. doi: 10.1038/s41467-019-10373-z

Emerson, J. B., Roux, S., Brum, J. R., Bolduc, B., Woodcroft, B. J., Jang, H. B., et al. (2018). Host-linked soil viral ecology along a perma frost thaw gradient. *Nat. Microbiol.* 3, 870–880. doi: 10.1038/s41564-018-0190-y

FAOSTAT. (2022). Food and agriculture organization of the United Nations. Available at: https://faostat.fao.org

Fernandes, I. A. A., Maciel, G. M., Bortolini, D. G., Pedro, A. C., Rubio, F. T. B., de Carvalho, K. Q., et al. (2023). The bitter side of tea: pesticide residues and their impact on human health. *Food Chem. Toxicol.* 179:113955. doi: 10.1016/j.fct.2023.113955

Francioli, D., van Ruijven, J., Bakker, L., and Mommer, L. (2020). Drivers of total and pathogenic soil-borne fungal communities in grassland plant species. *Fungal Ecol.* 48:100987. doi: 10.1016/j.funeco.2020.100987

Fu, H., Li, H., Yin, P., Mei, H., Li, J., Zhou, P., et al. (2021). Integrated application of rapeseed cake and green manure enhances soil nutrients and microbial communities in tea garden soil. *Sustain. For.* 13:2967. doi: 10.3390/su13052967

Gao, X., Liu, Y., Liu, C., Guo, C., Zhang, Y., Ma, C., et al. (2023). Individual and combined effects of arbuscular mycorrhizal fungi and phytohormones on the growth and physicochemical characteristics of tea cutting seedlings. *Front. Plant Sci.* 14:1140267. doi: 10.3389/fpls.2023.1140267

Ge, S., Gao, J., Chang, D., He, T., Wang, M., Li, C., et al. (2023). Biochar contributes to resistance against root rot disease by stimulating soil polyphenol oxidase. *Biochar* 5, 1–17. doi: 10.1007/s42773-023-00257-3

Gond, D. P., Jha, S. S., Kumar, A., and Singh, S. K. (2021). Plant growth promoting bacteria and its role in green remediation. *Sustain. Environ. Clean-up*, 149–163. doi: 10.1016/B978-0-12-823828-8.00007-4

Gu, S., Hu, Q., Cheng, Y., Bai, L., Liu, Z., Xiao, W., et al. (2019). Application of organic fertilizer improves microbial community diversity and alters microbial network structure in tea (*Camellia sinensis*) plantation soils. *Soil Tillage Res.* 195:104356. doi: 10.1016/j.still.2019.104356

Gui, H., Fan, L. C., Wang, D. H., Yan, P., Li, X., Pang, Y. H., et al. (2022). Variations in soil nutrient dynamics and bacterial communities after the conversion of forests to long-term tea monoculture systems. *Front. Microbiol.* 13:896530. doi: 10.3389/fmicb.2022.896530

Guo, J. J., Liu, W. B., Zhu, C., Luo, G. W., Kong, Y. L., Ling, N., et al. (2018). Bacterial rather fungal community composition is associated with microbial activities and nutrient-use efficiencies in a paddy soil with short-term organic amendments. *Plant Soil* 424, 335–349. doi: 10.1007/s11104-017-3547-8

Gupta, S. K., and Chakraborty, A. P. (2020). Mycorrhiza helper bacteria: future prospects. *Int. J. Res Rev.* 7, 387–391.

Han, L. L., Yu, D. T., Zhang, L. M., Shen, J. P., and He, J. Z. (2017). Genetic and functional diversity of ubiquitous DNA viruses in selected Chinese agricultural soils. *Sci. Rep.* 7:45142. doi: 10.1038/srep45142

Han, L., Zhang, H., Xu, Y., Li, Y., and Zhou, J. (2021). Biological characteristics and salt-tolerant plant-growth promoting effects of an ACC deaminase-producing *Burkholderia pyrrocinia* strain isolated from the tea rhizosphere. *Arch. Microbiol.* 203, 2279–2290. doi: 10.1007/s00203-021-02204-x

Hao, X., Zhang, W., Zhao, F., Liu, Y., Qian, W., Wang, Y., et al. (2018). Discovery of plant viruses from tea plant (*Camellia sinensis* (L.) O. Kuntze) by metagenomic sequencing. *Front. Microbiol.* 9:2175. doi: 10.3389/fmicb.2018.02175

Hartmann, M., and Six, J. (2022). Soil structure and microbiome functions in agrosystems. *Nat. Rev. Earth Environ.* 4, 4–18. doi: 10.1038/s43017-022-00366-w

Hayatsu, M., Katsuyama, C., and Tago, K. (2021). Overview of recent researches on nitrifying microorganisms in soil. *Soil Sci. Plant Nutri.* 67, 619–632. doi: 10.1080/00380768.2021.1981119

Hazra, A., Dasgupta, N., Sengupta, C., Bera, B., and Das, S. (2019). "Tea: a worthwhile, popular beverage crop since time immemorial" in *Agronomic crops*. ed. M. Hasanuzzaman (Singapore: Springer Publishing), 507–531.

Hicks, L. C., Beat, F., Kjoller, R., Lukac, M., Moora, M., Weedon, J. T., et al. (2021). Toward a function-first framework to make soil microbial ecology perspective. *Ecology* 103:e03594. doi: 10.1002/ecy.3594

Hurwitz, B. L., and U'Ren, J. M. (2016). Viral metabolic reprogramming in marine ecosystems. *Curr. Opin. Microbiol.* 31, 161–168. doi: 10.1016/j.mib.2016.04.002

Idris, A. L., Fan, X., Muhammad, M. H., Guo, Y., Guan, X., and Huang, T. (2020). Ecologically controlling insect and mite pests of tea plants with microbial pesticides: a review. *Arch. Microbiol.* 202, 1275–1284. doi: 10.1007/s00203-020-01862-7

Jansson, J. K., and Wu, R. (2022). Soil viral diversity, ecology and climate change. *Nat. Rev. Microbiol.* 21, 296–311. doi: 10.1038/s41579-022-00811-z

Ji, L., Yang, X., Zhu, C., Ma, L., Chen, Y., Ling, N., et al. (2022). Land-use changes alter the arbuscular mycorrhizal fungal community composition and assembly in the ancient tea forest reserve. *Agric. Ecosyst. Environ.* 339:108142. doi: 10.1016/j.agee.2022.108142

Jose, P. A., Maharshi, A., and Jha, B. (2021). Actinobacteria in natural products research: progress and prospects. *Microbiol. Res.* 246:126708. doi: 10.1016/j.micres.2021.126708

Kalam, S., Basu, A., Ahmad, I., Sayyed, R. Z., El-Enshasy, H. A., Dailin, D. J., et al. (2020). Recent understanding of soil Acidobacteria and their ecological significance: a critical review. *Front. Microbiol.* 11:580024. doi: 10.3389/fmicb.2020.580024

Kizheva, Y., Eftimova, M., Rangelov, R., Micheva, N., Urshev, Z., Rasheva, I., et al. (2021). Broad host range bacteriophages found in rhizosphere soil of a healthy tomato plant in Bulgaria. *Heliyon* 7:e07084. doi: 10.1016/j.heliyon.2021.e07084

Kolandasamy, M., Mandal, A. K. A., Balasubramanian, M. G., and Ponnusamy, P. (2023). Multifaceted plant growth-promoting traits of indigenous rhizospheric microbes against Phomopsis theae, a causal agent of stem canker in tea plants. *World J. Microbiol. Biotechnol.* 39:237. doi: 10.1007/s11274-023-03688-z

Kui, L., Xiang, G., Wang, Y., Wang, Z., Li, G., Li, D., et al. (2021). Large-scale characterization of the soil microbiome in ancient tea plantations using high-throughput 16s rRNA and internal transcribed spacer amplicon sequencing. *Front. Microbiol.* 12:745225. doi: 10.3389/fmicb.2021.745225

Li, Y., Li, Z., Arafat, Y., and Lin, W. (2020). Studies on fungal communities and functional guilds shift in tea continuous cropping soils by high-through put sequencing. *Ann. Microbiol.* 70:7. doi: 10.1186/s13213-020-01555-y

Li, Y. C., Li, Z., Li, Z. W., Jiang, Y. H., Weng, B. Q., and Lin, W. X. (2016). Variations of rhizosphere bacterial communities in tea (*Camellia sinensis* L.) continuous cropping soil by high-throughput pyrosequencing approach. *J. Appl. Microbiol.* 121, 787–799. doi: 10.1111/jam.13225

Li, Y. C., Li, Z. W., Lin, W. W., Jiang, Y. H., Weng, B. Q., and Lin, W. X. (2018). Effects of biochar and sheep manure on rhizospheric soil microbial community in continuous rationing tea orchards. *J. Appl. Ecol.* 29, 1273–1282. doi: 10.13287/j.1001-9332.201804.036

Liao, H., Li, H., Duan, C. S., Zhou, X. Y., Luo, Q. P., An, X. L., et al. (2022). Response of soil viral communities to land use changes. *Nat. Commun.* 13:6027. doi: 10.1038/s41467-022-33771-2

Lin, W., Lin, M., Zhou, H., Wu, H., Li, Z., and Lin, W. (2019). The effects of chemical and organic fertilizer usage on rhizosphere soil in tea orchards. *PLoS One* 14:e0217018. doi: 10.1371/journal.pone.0217018

Liu, M. Y., Burgos, A., Zhang, Q., Tang, D., Shi, Y., Ma, L., et al. (2017). Analyses of transcriptome profiles and selected metabolites unravel the metabolic response of NH^{+}_{4} and NO^{-}_{3} as signaling molecules in tea plant (*Camellia sinensis* L.). *Sci. Hort.* 218, 293–303. doi: 10.1016/j.scienta.2017.02.036

Liu, W., Cui, S., Wu, L., Qi, W., Chen, J., Ye, Z., et al. (2023). Effects of bio-organic fertilizer on soil fertility, yield and quality of tea. *J. Soil Sci. Plant Nutr.* 23, 5109–5121. doi: 10.1007/s42729-023-01195-6

Liu, X., Hu, B., and Chu, C. (2022). Nitrogen assimilation in plants: current status and future prospects. *J. Genetics Genomics.* 49, 394–404. doi: 10.1016/j.jgg.2021.12.006

Liu, J., Li, X., and Yao, M. (2021). Research progress on assembly of plant rhizosphere microbialcommunity. *Acta Microbiol Sin.* 61, 231–248. doi: 10.13343/j.cnkiwsxb.20200154

Lu, Y., Song, S., Wang, R., Liu, Z., Meng, J., Sweetman, A. J., et al. (2015). Impacts of soil and water pollution on food safety and health risks in China. *Environ. Int.* 77, 5–15. doi: 10.1016/j.envint.2014.12.010

Lynn, T. M., Liu, Q., Hu, Y., Yuan, H., Wu, X., Khai, A. A., et al. (2017). Influence of land use on bacteria and archael diversity and community structures in three natural ecosystems and one agricultural soil. *Arch. Microbiol.* 199, 711–721. doi: 10.1007/s00203-017-1347-4

Ma, Z., Tanalgo, K. C., Xu, Q., Li, W., Wu, S., Ji, Q., et al. (2022). Influence of tea-Pleurotus ostreatus intercropping on soil fungal diversity and community structure. *Can. J. Soil Sci.* 102, 359–369. doi: 10.1139/CJSS-2021-0123

Ma, L., Yang, X., Shi, Y., Yi, X., Ji, L., Cheng, Y., et al. (2021). Response of tea yield, quality and soil bacteria characteristics to long-term nitrogen fertilization in an eleven-year field experiment. *Appl. Soil Ecol.* 166:103976. doi: 10.1016/j.apsoil.2021.103976

Martin, F. (2016). *Molecular mycorrhizal symbiosis*. Hoboken, NJ: John Wiley and Sons, Inc.

Morris, E. K., Morris, D. J. P., Vogt, S., Gleber, S. C., Bigalke, M., Wilcke, W., et al. (2019). Visualizing the dynamics of soil aggregation as affected by arbuscular mycorrhizal fungi. *ISME J.* 13, 1639–1646. doi: 10.1038/s41396-019-0369-0

Mukhopadhyay, M., and Mondal, T. K. (2017). Cultivation, improvement and environmental impacts of tea. Oxford Research Encyclopedia of Environmental Science. Oxford University Press. pp. 1–22. doi: 10.1093/acrefore/9780199389414.013.373

Muneer, M. A., Hou, W., Li, J., Huang, X. M., Kayani, M. U. R., Cai, Y. Y., et al. (2022). Soil pH: a key edaphic factor regulating distribution and functions of bacterial community along vertical soil profiles in redsoil of pomelo orchard. *BMC Microbiol.* 23:38. doi: 10.1186/s12866-02202452-x

Nabi, M. (2023). "Chapter eleven-role of microorganisms in plant nutrition and soil health" in *Molecular inventions and advancements for crop improvement. Sustainable Plant Nutrition*, 263–282.

Nasslahsen, B., Prin, Y., Ferhout, H., Smouni, A., and Duponnois, R. (2022). Mycorrhizae helper bacteria for managing the mycorrhizal soil infectivity. *Front. Soil Sci.* 2:979246. doi: 10.3389/fsoil.2022.979246

Nath, R., Sharma, G. D., and Barooah, M. (2015). Plant growth promoting endophytic fungi isolated from tea (*Camellia sinensis*) shrubs of Assam. *India. Appl. Ecol. Environ. Res.* 13, 877–891. doi: 10.15666/aeer/1303_877891

Naylor, D., McClure, R., and Jansson, J. (2022). Trends in microbial community composition and function by soil depth. *Microorganisms* 10:540. doi: 10.3390/microorganisms10030540

Naz, M., Dai, Z., Hussain, S., Tariq, M., Danish, S., Khan, I. U., et al. (2022). The soil pH and heavy metals revealed their impact on soil microbial community. *J. Environ. Manag.* 321:115770. doi: 10.1016/j.envman.2022.115770

Negrete-Bolagay, D., Zamora-Ledezma, C., Chuya-Sumba, C., DeSousa, F. B., Whitehead, D., Alexis, F., et al. (2021). Persistent organic pollutants: the trade-off between potential risks and sustainable remediation methods. *J. Environ. Manag.* 300:113737:113737. doi: 10.1016/j.jenvman.2021.113737

Olanrewaju, O. S., Ayangbenro, A. S., Glick, B. R., and Babalola, O. O. (2019). Plant health: feedback effect of root exudate-rhizobiome interactions. *Appl. Microbial. Biotechnol.* 103, 1155–1166. doi: 10.1007/s00253-018-9556-6

Ozimek, E., and Hanaka, A. (2021). Mortierella species as the plant growth-promoting fungi present in agricultural soils. *Agriculture* 11:7. doi: 10.3390/agriculture11010007

Panda, P., Choudhury, A., Chakraborty, S., Ray, D. P., Deb, S., Patra, P. S., et al. (2017). Phosphorus solubilizing bacteria from tea soils and their phosphate solubilizing abilities. *Int. J. Bioresource Sci.* 4, 113–125. doi: 10.5958/2454-9541.2017.00018.4

Pandey, A. K., Deka, B., Varshney, R., Cheramgoi, E. C., and Babu, A. (2021). Do the beneficial fungi manage phytosalinity problems in tea agro-ecosystem? *Biol. Control* 66, 445–462. doi: 10.1007/s10526-021-10084-9

Pandey, A. K., Hubbali, M., Dutta, V. P., and Babu, A. (2023). Characterisation and identification of fungicide insensitive Pestalotiopsis-like species pathogenic to tea crop in India. *World J. Microbiol. Biotechnol.* 39:34. doi: 10.1007/s11274-022-03474-3

Parihar, J., Parihar, S., Suravajhala, P., and Bagaria, A. (2022). Spatial metagenomic análisis in understanding the microbial diversity of Thar desert. *Biol.* 11:461. doi: 10.3390/biology11030461

Peng, C., Zhu, X. H., Hou, R. Y., Ge, G. F., Hua, R. M., Wan, X. C., et al. (2018). Aluminium and heavy metal accumulation in tea leaves: an interplay of environmental and plant factors and an assessment of exposure risks to consumers. *J. Food Sci.* 83, 1165–1172. doi: 10.1111/1750-3841.14093

Perez-Burillo, S., Jimenez-Zamora, A., Parraga, J., Rufian-Henares, J. A., and Pastoriza, S. (2019). Furosine and 5-hydroxymethylfurfural as chemical markers of tea processing and storage. *Food Control* 99, 73–78. doi: 10.1016/j.foodcont.2018.12.029

Phillippot, L., Chenu, C., Kappler, A., Rillig, M. C., and Fierer, N. (2023). The interplay between microbial communities and soil properties. *Nat. Rev. Microbiol.* 22, 226–239. doi: 10.1038/s41579-023-00980-5

Pokharel, S. S., Yu, H., Fang, W., Parajulee, M. N., and Chen, F. (2023). Intercropping cover crops for a vital ecosystem service: a review of the biocontrol of insect pests in tea agroecosystems. *Plan. Theory* 12:2361. doi: 10.3390/plants12122361

Qiao, Y., Wang, T., Huang, Q., Guo, H., Zhang, H., Xu, Q., et al. (2024). Core species impact plant health by enhancing soil microbial cooperation and network complexity during community coalescence. *Soil Biol. Biochem.* 188:109231. doi: 10.1016/j.soilbio.2023.109231

Ramphinwa, M. L., Mchau, G. R. A., Mashau, M. E., Madala, N. E., Chimonyo, V. G. P., Modi, T. A., et al. (2023). Eco-physiological response of secondary metabolites of teas: review of quality attributes of herbal tea. *Front. Sustain. Food Syst.* 7:990334. doi: 10.3389/fsufs.2023.990334

Rashid, M. I., Mujawar, L. H., Shahzad, T., Almeelbi, T., Ismail, I. M., and Oves, M. (2016). Bacteria and fungi can contribute to nutrients bioavailability and aggregate formation in degraded soils. *Microbiol. Res.* 183, 26–41. doi: 10.1016/j.mcres.2015.11.007

Ray, D., Baruah, P. M., and Agarwala, N. (2022). "Chapter 15-Aluminium in tea plants: phytotoxicity, tolerance and mitigation" in *Harzardous and trace materials in soil and plants*. eds. M. Naeem, T. Aftab, A. A. Ansari, S. S. Gill and A. Macovei (Cambridge, MA: Academic Press), 217–229.

Ren, Z., Cheng, R., Chen, P., Xue, Y., Xu, H., Yin, Y., et al. (2023). Plant-associated microbe system in treatment of heavy metals-contaminated soil: mechanisms and applications. *Water Air Soil Pollut.* 234:39. doi: 10.1007/s11270-023-06061-w

Roux, S., and Emerson, J. B. (2022). Diversity in the soil virosphere: to infinity and beyond? *Trends Microbiol.* 30, 1025–1035. doi: 10.1016/j.tim.2022.05.003

Sangwan, S., and Prasanna, R. (2022). Mycorrhizae helper bacteria: unlocking their potential as bioenhancers of plant-arbuscular mycorrhizal fungal associations. *Fungal Microbiol.* 84, 1–10. doi: 10.1007/s00248-021-01831-7

Schroeter, S. A., Eveillard, D., Chaffron, S., Zoppi, J., Kampe, B., Lohmann, P., et al. (2022). Microbial community functioning during plant litter decomposition. *Sci. Rep.* 12:7451. doi: 10.1038/s41598-022-11485-1

Shan, W., Zhou, Y., Liu, H., and Yu, X. (2018). Endophytic Actinomycetes from tea plants (*Camellia sinensis*): isolation, abundance antimicrobial, and plant-growth-promoting activities. *Biomed. Res. Int.* 2018:1470305. doi: 10.1155/2018/1470305

Shao, Y. D., Zhang, D. J., Hu, X. C., Wu, Q. S., Jiang, C. J., Gao, X. B., et al. (2019). Arbuscular mycorrhiza improves leaf food quality of tea plants. *Not. Bot. Horti. Agrobo.* 47, 1842–4309. doi: 10.15835/nbha47311434

Shao, Y. D., Zhang, D. J., Hu, X. C., Wu, Q. S., Xia, T. J., Gao, X. B., et al. (2018). Mycorrhiza-induced changes in root growth and nutrient absorption of tea plants. *Plant Soil Environ.* 64, 283–289. doi: 10.17221/126/2018-PSE

Sharma, C., Gupta, R. K., Pathak, R. K., and Choudhary, K. K. (2013). Seasonal colonization of arbuscular mycorrhiza fungi in roots of *Camellia sinensis* (tea) in different tea gardens of India. *ISRN Biodiversity* 2013:593087, 1–6. doi: 10.1155/2013/593087

Sharma, S., and Kaur, S. (2021). "Soil microbial diversity and metagenomics" in *Soil nitrogen ecology*. eds. C. Cruz, K. Vishwakarma, D. K. Choudhary and A. Varma, vol. *62* (Cham: Springer), 283–301.

Shi, J., Qu, R., Feng, M., Wang, X., Wang, L., Yang, S., et al. (2015). Oxidative degradation of decabromodiphenyl ether (BDE209) by potassium permanganate: reaction pathways, kinetics, and mechanisms assisted by density functional theory calculations. *Environ. Sci. Technol.* 49, 4209–4217. doi: 10.1021/es505111r

Song, Q., Deng, X., Song, R., and Song, X. (2023). Three plant growth-promoting rhizobacteria regulate the soil microbial community and promote the growth of maize seedlings. *J. Plant Growth Regul.* 42, 7418–7434. doi: 10.1007/s00344-023-11019-7

Su, J., Xia, Y., Yao, H. Y., Li, Y. Y., An, X. L., Singh, B. K., et al. (2017). Metagenomic assembly unravel microbial response to redox fluctuations in acid sulfate soil. *Soil Biol. Biochem.* 105, 244–252. doi: 10.1016/j.soilbio.2016.11.027

Sun, M., Yuan, D., Hu, X., Zhang, D., and Li, Y. (2020). Effects of mycorrhizal fungi on plant growth, nutrient absorption and phytohormones levels in tea under shading condition. *Not. Bot. Horti. Agrobo.* 48, 2006–2020. doi: 10.15835/48412082

Taha, M., Salama, A., El-Seedy, M., Elakhdar, I., Islam, M. S., Barutcular, C., et al. (2016). Potential impact of compost tea on soil microbial properties and performance of radish plant under sandy soil conditions-greenhouse experiments. *Aust. J. Basic Appl. Sci.* 10, 158–165.

Tan, L., Gu, S. S., Li, S., Ren, Z. H., Deng, Y., Liu, Z. H., et al. (2019). Responses of microbial communities and interaction networks to different management practices in tea plantation soils. *Sustain. For.* 11:4428. doi: 10.3390/su11164428

Thabah, S., and Joshi, S. R. (2022). Chapter 17-Plant growth promoting rhizobacteria from the perspectives of tea plantations and diseases. In: *New and future developments in microbial biotechnology and bioengineering and engineering*. Singh, H., Vaishnav, A. (Eds.). Sustainable Agriculture: Microorganisms as Biostimulants. Elsevier. pp. 315–332.

Trivedi, P., Leach, J. E., Tringe, S. G., Sa, T., and Singh, B. K. (2020). Plant–microbiome interactions: from community assembly to plant health. *Nat. Rev. Microbiol.* 18, 607–621. doi: 10.1038/s41579-020-0412-1

Trubl, G., Jang, H. B., Roux, S., Emerson, J. B., Solonenko, N., Vik, D. R., et al. (2018). Soil viruses are underexplored players in ecosystem carbon processing. *mSystems* 3, e00018–e00076. doi: 10.1128/mSystems.00076-18

Wang, Z., Geng, Y., and Liang, T. (2020). Optimization of reduced chemical fertilizer use in tea gardens based on the assessment of related environmental and economic benefits. *Sci. Total Environ.* 713:136439. doi: 10.1016/j.scitotenv.2019.136439

Wang, J., Ji, Y., Yuan, Z., Guan, J., Liu, C., and Lv, L. (2017). Analysis of bacterial community structure and diversity in different restoration methods in Qixing river wetland. *Adv. J. Toxicol. Curr. Res.* 1, 49–55.

Wang, S., Li, T., Zheng, Z., and Chen, H. Y. H. (2019). Soil aggregate associated bacterial metabolic activity and community structure in different aged plantations. *Sci. Total Environ.* 654, 1023–1032. doi: 10.1016/j.scitotenv.2018.11.032

Wang, X., Liu, J., Yu, Z., Jin, J., Liu, X., and Wang, G. (2016). Novel groups and unique distribution of phage phoH genes in paddy waters in Northeast China. *Sci. Rep.* 6:38428. doi: 10.1038/srep38428

Wang, S., Tang, L., and Ye, S. (2021). Dynamics of soil bacterial community diversity and composition at aggregate scales in chronosequence of tea gardens. *Catena* 206:105486. doi: 10.1016/j.catena.2021.105486

Wang, Z., Xu, M., Li, F., Bai, Y., Hou, J., Li, X., et al. (2023). Changes in soil bacterial communities and functional groups beneath coarse woody debris across a subalpine forest successional series. *Global Ecol. Conserv.* 43:e02436. doi: 10.1016/j.geco.2023.e02436

Wei, Z., Niu, S., Wei, Y., Liu, Y., Xu, Y., Yang, Y., et al. (2024). The role of extracellular polymetric substances (EPS) in chemical-degradation of persistent organic pollutants in soil: a review. *Sci. Tot. Environ.* 912:168877. doi: 10.1016/j.scitotenv.2023.168877

Wei, Y., Wu, Y., Yan, Y., Zou, W., Xue, J., Ma, W., et al. (2018). High-throughput sequencing of microbial community diversity in soil, grapes, leaves, grape juice and wine of grapevine from China. *PLoS One* 13:e0193097. doi: 10.1371/journal.pone0193097

Wright, C. L., and Lehvirta-Morley, L. E. (2023). Nitrification and beyond: metabolic versatility of ammonia oxidizing archaea. *ISME J.* 17, 1358–1368. doi: 10.1038/s41396-023-01467-0

Wu, Q. S., Shao, Y. D., Gao, X. B., Xia, T. J., and Kuca, K. (2019). Characterization of AMF-diversity of endosphere versus rhizosphere of tea (*Camellia sinensis*) crops. *Indian J. Agric. Sci.* 89, 348–352. doi: 10.56093/ijas.v89i2.87097

Wu, D., Wang, W., Yao, Y., Li, H., Wang, Q., and Niu, B. (2023). Microbial interactions within beneficial consortia promote soil health. *Sci. Total Environ.* 900:165801. doi: 10.1016/j.scitotenv.2023.165801

Wu, L., Wen, C., Qin, Y., Yin, H., Tu, Q., van Nostrand, J. D., et al. (2015). Phasing amplicon sequencing on illumine Miseq for robust environmental microbial community analysis. *BMC Microbiol.* 15, 1–12. doi: 10.1186/s12866-015-0450-4

Xi, S., Chu, H., Zhou, Z., Li, T., Zhang, S., Xu, X., et al. (2023). Effect of potassium fertilizer on tea yield and quality: a meta analysis. *Eur. J. Agron.* 144:126767. doi: 10.1016/j.eja.2023.126767

Xiang, L., Harindintwali, J. D., Redmile-Gordon, M., Chang, S. X., Fu, Y., He, C., et al. (2022). Integrating biochar, bacteria and plants for sustainable remediation of soils contaminated with organic pollutants. *Environ. Sci. Technol.* 56, 16546–16566. doi: 10.1021/acs.est.2c02976

Xie, S., Yang, F., Feng, H., Yu, Z., Liu, C., Wei, C., et al. (2021). Organic fertilizer reduced carbon and nitrogen in run-off and buffered soil acidification in tea plantations: evidence in nutrient content and isotope fractionations. *Sci. Total Environ.* 762:143059. doi: 10.1016/j.scitotenv.2020.143059

Xin, W., Zhang, J., Yu, Y., Tian, Y., Li, H., Chen, X., et al. (2024). Root microbiota of tea plants regulate nitrogen homeostasis and theanine synthesis to influence tea quality. *Curr. Biol.* 34, 868–880.e6. doi: 10.1016/j.cub.2024.01.044

Xu, P., Fan, X. Y., Mao, Y. X., Cheng, H. Y., Xu, A. A., Lai, W. Y., et al. (2022). Temporal metabolite responsiveness of microbiota in the tea plant phyllosphere promotes continuous suppression of fungal pathogens. *J. Adv. Res.* 39, 49–60. doi: 10.1016/j.jare.2021.10.003

Xu, G., Liu, Y., Long, Z., Hu, S., Zhang, Y., and Jiang, H. (2018). Effects of exotic plantation forests on soil edaphon and organic matter fractions. *Sci. Total Environ.* 626, 59–68. doi: 10.1016/j.scitotenv.2018.01.088

Yadav, A., Borrelli, J. C., Elshahed, M. S., and Youssef, N. H. (2021). Genomic analysis of family UBA6911 (group 18 Acidobacteria) expands the metabolic capacities of the phylum and highlights adaptations to terrestrial habitats. *Appl. Environ. Microbiol.* 87:e0094721. doi: 10.1128/AEM.00947-21

Yan, K., Abbas, M., Meng, L., Cai, H., and Zhao, X. (2021). Analysis of fungal diversity and community structure in Sichuan dark tea pile-fermentation. *Front. Microbiol.* 12:706714. doi: 10.3389/fmicb.2021.706714

Yan, L., Riaz, M., Liu, J., Yu, M., and Cuncang, J. (2022). The aluminium tolerance and detoxification in plants; recent advances and prospects. *Crit. Rev. Environ. Sci. Technol.* 52, 1491–1527. doi: 10.1080/10643389.2020.1859306

Yan, P., Shen, C., Fan, L. C., Li, X., Zhang, L. P., Zhang, L., et al. (2018). Tea planting affects acidification and nitrogen and phosphorus distribution in soil. *Agric. Ecosys. Environ.* 254, 20–25. doi: 10.1016/j.agee.2017.11.015

Yan, P., Shen, C., Zou, Z., Fan, L., Li, X., Zhang, L., et al. (2022). Increased soil fertility in tea gardens lead to declines in fungal diversity and complex subsoils. *Agronomy* 12:1751. doi: 10.3390/agronomy12081751

Yan, P., Wu, L. Q., Wang, D. H., Fu, J., Shen, C., Li, X., et al. (2020). Soil acidification in Chinese tea plantations. *Sci. Total Environ.* 715:136963. doi: 10.1016/j.scitotenv.2020.136963

Yang, X. D., Ni, K., Shi, Y. Z., Yi, X. Y., Zhang, Q. F., Fang, L., et al. (2018). Effects of long-term nitrogen application on soil acidification and solution chemistry of a tea plantation in China. *Agric. Ecosyst. Environ.* 252, 74–82. doi: 10.1016/j.agee.2017.10.004

Ye, J., Wang, Y., Wang, Y., Hong, L., Jia, X., Kang, J., et al. (2022). Improvement of soil acidification in tea plantations by long-term use of organic fertilizers and its effect on tea yield and quality. *Front. Plant Sci.* 13:1055900. doi: 10.3389/fpls.2022.1055900

Zhang, Z., Ge, S. B., Fan, L. C., Guo, S., Hu, Q., Ahammed, G. J., et al. (2022). Diversity in rhizospheric microbial communities in tea varieties at different locations and tapping potential beneficial microorganisms. *Front. Microbiol.* 13:1027444. doi: 10.3389/fmicb.2022.1027444

Zhang, X., Long, H., Huo, D., Awan, M. I., Shao, J., Mahmood, A., et al. (2022). Insights into the functional role of tea microbes on tea growth, quality and resistance against pests and diseases. *Not. Bot. Horti. Agrobo.* 50:12915. doi: 10.15835/nbha50412915

Zhang, W., Ni, K., Long, L., and Ruan, J. (2023). Nitrogen transport and assimilation in tea plant (*Camellia sinensis*): a review. *Front. Plant Sci.* 14:1249202. doi: 10.3389/fpls.2023.1249202

Zhang, X. C., Wang, N. N., Hou, M. M., Wu, H. H., Jiang, H., Zhou, Z. W., et al. (2022). Contribution of K solubilizing bacteria (Burkholderia sp.) promotes tea plant growth (*Camellia sinensis*) and leaf polyphenols content by improving soil available K level. *Funct. Plant Biol.* 49, 283–294. doi: 10.1071/FP21193

Zhang, S., Wang, Y., Sun, L., Qiu, C., Ding, Y., Gu, H., et al. (2020). Organic mulching positively regulates the soil microbial communities and ecosystem functions in tea plantation. *BMC Microbiol.* 20:103. doi: 10.1186/s12866-020-01794-8

Zheng, X., Wu, Y., Xu, A., Lin, C., Wang, H., Yu, J., et al. (2023). Response of soil microbial communities and functions to long-term tea (*Camellia sinensis* L.) planting in a subtropical region. *Forests* 14:1288. doi: 10.3390/f14071288

Zheng, N., Yu, Y., Shi, W., and Yao, H. (2019). Biochar suppresses N_2O emmissions and alters microbial communities in acidic tea soil. *Environ. Sci. Pollut. Res.* 26, 35978–35987. doi: 10.1007/s11356-019-06704-8

Zi, H., Jiang, Y., Cheng, X., Li, W., and Huang, X. (2020). Change of rhizospheric bacterial community of the ancient wild tea along elevational gradients in Ailao Mountain, China. *Sci. Rep.* 10:9203. doi: 10.1038/s41598-020-66173-9

Zou, Z., Mi, W., Li, X., Hu, Q., Zhang, L., Zhang, L., et al. (2023). Biochar application method influences root growth of tea (*Camellia sinensis* L.) by altering soil biochemical properties. *Sci. Hortic.* 315, 111960–111969. doi: 10.1016/j.scienta.2023.111960

frontiers | Frontiers in Microbiology

TYPE Original Research
PUBLISHED 16 April 2024
DOI 10.3389/fmicb.2024.1359677

OPEN ACCESS

EDITED BY
Zhanfei He,
Zhejiang University of Technology, China

REVIEWED BY
Daniel Lipus,
GFZ German Research Centre for Geosciences, Germany
Thirumurugan Durairaj,
SRM Institute of Science and Technology, India

*CORRESPONDENCE
Rizlan Bernier-Latmani
✉ rizlan.bernier-latmani@epfl.ch

†PRESENT ADDRESS
Aislinn A. Boylan,
National Nuclear Laboratory, Stonehouse, United Kingdom

‡These authors have contributed equally to this work and share first authorship

RECEIVED 21 December 2023
ACCEPTED 19 March 2024
PUBLISHED 16 April 2024

CITATION
Rolland C, Burzan N, Leupin OX, Boylan AA, Frutschi M, Wang S, Jacquemin N and Bernier-Latmani R (2024) Microbial hydrogen sinks in the sand-bentonite backfill material for the deep geological disposal of radioactive waste.
Front. Microbiol. 15:1359677.
doi: 10.3389/fmicb.2024.1359677

Microbial hydrogen sinks in the sand-bentonite backfill material for the deep geological disposal of radioactive waste

Camille Rolland[1‡], Niels Burzan[1‡], Olivier X. Leupin[2], Aislinn A. Boylan[1†], Manon Frutschi[1], Simiao Wang[1], Nicolas Jacquemin[1] and Rizlan Bernier-Latmani[1*]

[1]Environmental Microbiology Laboratory, École Polytechnique Fédérale de Lausanne, Lausanne, Switzerland, [2]National Cooperative for the Disposal of Radioactive Waste, Wettingen, Switzerland

The activity of subsurface microorganisms can be harnessed for engineering projects. For instance, the Swiss radioactive waste repository design can take advantage of indigenous microorganisms to tackle the issue of a hydrogen gas (H_2) phase pressure build-up. After repository closure, it is expected that anoxic steel corrosion of waste canisters will lead to an H_2 accumulation. This occurrence should be avoided to preclude damage to the structural integrity of the host rock. In the Swiss design, the repository access galleries will be back-filled, and the choice of this material provides an opportunity to select conditions for the microbially-mediated removal of excess gas. Here, we investigate the microbial sinks for H_2. Four reactors containing an 80/20 (w/w) mixture of quartz sand and Wyoming bentonite were supplied with natural sulfate-rich Opalinus Clay rock porewater and with pure H_2 gas for up to 108 days. Within 14 days, a decrease in the sulfate concentration was observed, indicating the activity of the sulfate-reducing bacteria detected in the reactor, e.g., from *Desulfocurvibacter* genus. Additionally, starting at day 28, methane was detected in the gas phase, suggesting the activity of methanogens present in the solid phase, such as the *Methanosarcina* genus. This work evidences the development, under *in-situ* relevant conditions, of a backfill microbiome capable of consuming H_2 and demonstrates its potential to contribute positively to the long-term safety of a radioactive waste repository.

KEYWORDS

bentonite, hydrogen, methanogenesis, sulfate reduction, deep geological disposal, microcosm reactor, opalinus clay

1 Introduction

Confinement of radioactive waste must ensure that humans and environment are protected from radio toxicity. In case of high-level waste confinement period must last for several hundred thousand of years (Hedin, 1997). Switzerland will construct a deep geological repository (DGR) in Opalinus Clay at about 850 m below ground level (Nördlich Lägern). The planned repository consists of a series of blind-end tunnels (the disposal rooms), connected via access galleries. The safe confinement of the stainless-steel canisters containing the waste is ensured by the host rock (the clay rock) and engineered barriers (the backfill). Upon closure

of the repository and the establishment of low oxygen conditions, anoxic corrosion of low and intermediate level-waste steel containers is expected to produce up to 25 million m^3 of hydrogen gas (H_2), this is roughly 50 times the galleries volume (390,000 m^3 not including disposal waste chambers) (Diomidis et al., 2016; Leupin, 2016). This significant gas production potentially threatens the integrity of the host rock. A proposed strategy to address this issue is the choice of backfill and sealing materials enabling gas transport out of the disposal rooms in the backfilled access galleries, and colonization of this porous space by hydrogenotrophic microorganisms.

Evidence of microbial H_2 oxidation in Opalinus Clay porewater, in contact with the host rock, has been previously described *in-situ* (Bagnoud et al., 2016a), or in a cultivation experiment (Boylan et al., 2019), as involving primarily sulfate reduction, which results in the production of bisulfide by consumption of H_2 and sulfate (Eq. 1):

$$4\,H_2 + SO_4^{2-} + H^+ \rightarrow HS^- + 4\,H_2O \quad (1)$$

In this environment, sulfate is provided by the Opalinus Clay porewater, and the dissolution of sulfate-bearing minerals in the backfill material. In addition, inorganic carbon could fuel methanogenesis and homoacetogenesis serving as additional H_2 sinks. Homoacetogens have never been observed in Opalinus Clay rock and porewater, and methanogens were detected at very low relative abundance (Bagnoud et al., 2016b; Mitzscherling et al., 2023), although their activity was not established *in situ* (Stroes-Gascoyne et al., 2007; Vinsot et al., 2017).

Our work aimed at probing the growth of hydrogenotrophic microorganisms in backfill material under repository-relevant conditions and at estimating the *in-situ* H_2 consumption rate of the microbiome using sulfate as a proxy. We chose an 80% (w) quartz sand and 20% (w) Wyoming bentonite mixture as the porous backfill because of its consideration as a potential plug and backfill material for the Swiss low-level waste repository (Manca, 2016). To investigate the adequacy of the concept, flow-through reactors filled with sand-bentonite (80/20 (w/w)) received an influx of Opalinus Clay rock porewater and were amended with H_2 (100%). The results support the establishment of a microbiome consuming H_2 gas using sulfate from Opalinus Clay porewater and Wyoming bentonite. The hydrogenotrophic microbial community was composed of sulfate-reducing bacteria (SRB) and methanogens.

Together, these findings show that sulfate reduction and methanogenesis are the dominant drivers of H_2 consumption in the repository backfill material composed of sand and Wyoming bentonite.

2 Materials and methods

2.1 *In-situ* equipment

2.1.1 Reactors description

All experiments were carried out in the Underground Rock Laboratory (URL) "Mont Terri" (Switzerland). Four identical cylindrical reactors, with inner dimensions of 12 cm in height × 10 cm in diameter (Supplementary Figure S1), were used for the experiment. The porous matrix simulating the potential repository backfill material (sand-bentonite 80/20 (w/w)) was not in direct contact with the stainless-steel cylinder but held in place by an inner Plexiglas cylinder, including a top and a bottom plate, thus minimizing the interaction with stainless-steel surfaces. The matrix was placed between two layers of coarse sand (1.5 cm thick). These layers were introduced to distribute porewater at the top and bottom and favor the uniform advection of porewater through the sand-bentonite matrix. Sulfate-rich Opalinus Clay porewater was supplied by two titanium inlets at the bottom whereas H_2 was provided via a long titanium tube ending in the middle of the reactor (Supplementary Figure S1).

The sand-bentonite mix was produced with kiln-dried quartz sand with a 0.1–0.6 mm grain size. Wyoming bentonite MX-80 was provided by Nagra and is a well-characterized bentonite used in repository research and its mineral composition is given in Supplementary Table S1 (Karnland et al., 2006). Using a 70% ethanol-disinfected porcelain mortar and pestle, all large bentonite aggregates were ground manually to < 0.5 mm. Sand and bentonite were mixed using the four-fold method (Chen et al., 2019). All reactor parts were disinfected shortly before assembly under oxic conditions. No shaking or compacting method was applied. The modules were then transferred to the URL and placed within an anoxic chamber. The experimental setup is presented in Figure 1. Once set in the anoxic chamber and connected to a borehole drilled in Mont Terri URL ceiling, each reactor was saturated with porewater and left to equilibrate in batch mode. The start of the experiment was staggered by one week for each reactor. After 5 to 30 days the water dispensing system was opened and reactors received gravity-driven porewater flow for 73 to 108 days. The borehole (below the packer) and the outer steel tubing surrounding the water lines were flushed with argon to prevent oxygen diffusion into the porewater. H_2 was supplied to each reactor daily from a computer-controlled H_2-grade syringe pump (500D Syringe Pump, Teledyne ISCO Inc., Lincoln, Nebraska, United States). The outflow from reactors 2, 3 and 4 were measured by three complementary metal oxide semiconductor (CMOS)-based flow-recorders (SLI-0430, Sensirion AG, Staefa, Switzerland).

Two different set-ups for the reactor experiment were chosen:

Serial setup: Reactors 1 and 2 were connected such that 1 received borehole porewater as its inflow while 2 received the outflow of 1 as its inflow.

Parallel setup: Reactors 3 and 4 were both connected to the borehole water as their inflow.

A sterile sand-bentonite mix, saturated with sterile artificial porewater, and incubated for 30 days under a nitrogen gas phase was used as an abiotic control. More detail is available in the Supplementary material on the reactors (Supplementary Text S1.1), abiotic control (Supplementary Text S1.2), and Opalinus Clay borehole drilling (Supplementary Text S1.3), microbial characterization (Supplementary Text S2.1 and Supplementary Table S2), and chemical characterization (Supplementary Table S3).

2.2 Gas phase and porewater monitoring

2.2.1 Sampling

Reactors were sampled weekly for gas and water composition. All valves connecting the reactors to the porewater flow system were closed to avoid any potential backflow. Gas was sampled by attaching a sterile 50 mL serum bottle filled with filtered nitrogen gas (1 bar) to the gas trap

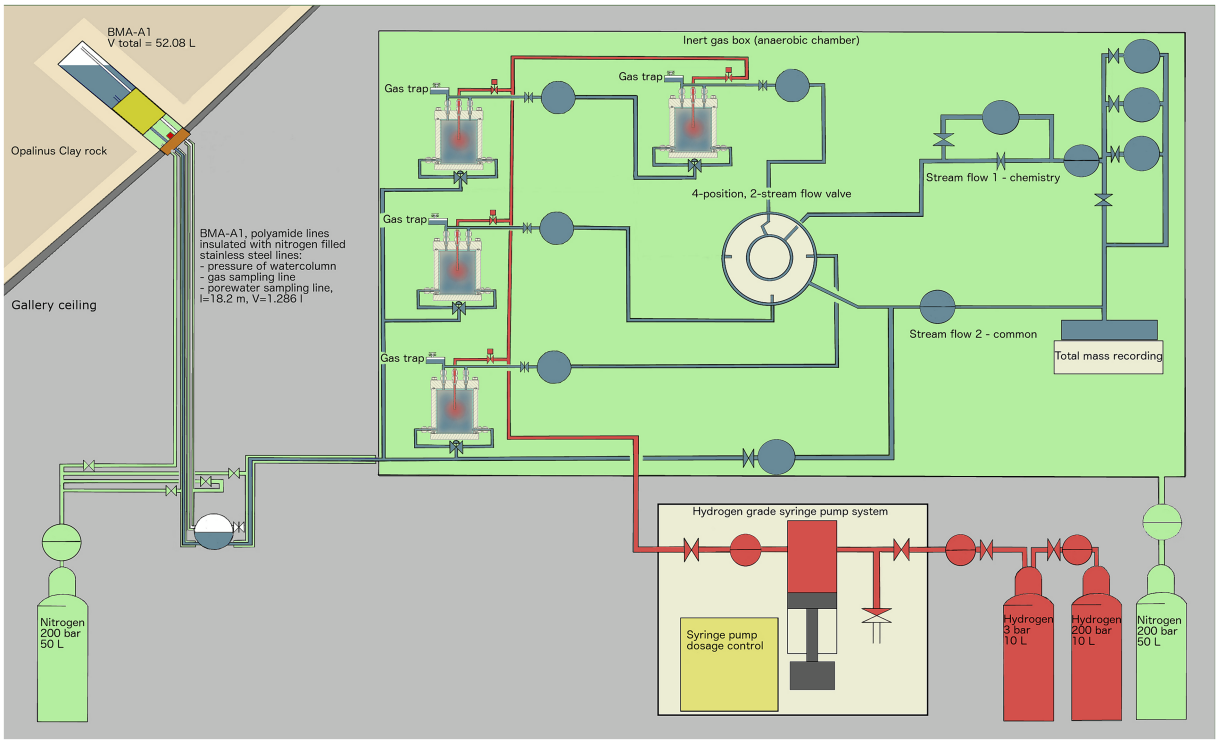

FIGURE 1
Experimental setup overview: Borehole BMA-A1 (upper left) provides water from the Opalinus Clay formation, which is transported in inert polyamide lines, isolated from the oxic gallery by stainless-steel tubes that are pressurized with 2.5–3.5 bar argon gas. Once within the glovebox, a controlled nitrogen atmosphere (green) is established and the porewater is continuously supplied to four reactors. The outflow is controlled by a pressure controller (PRC) and recorded by flowmeters (FR) and by a scale recording the total mass of porewater outflow. Gas pressure is controlled by pressure controllers (PRC). Once a day, H_2 (100%) gas was applied remotely using a syringe pump, delivering up to several milliliters of H_2 to each reactor to stimulate microbial activity. EDZ refers to the Excavation-Damaged Zone: the network of micro and macro fractures created during drilling of the tunnels.

and allowing it to equilibrate with the pressure inside the reactor. The bottle was removed when the first drop of water was observed in the bottle. Water was sampled by connecting a sterile syringe equipped with a 0.2 µm filter to the two outflow lines and extracting up to 7 mL. The outflow of gas and water was driven solely by the pressure difference between the interior of the reactor and the glovebox atmosphere. Additionally, borehole porewater was sampled for chemical analysis using the supply line in the glove box.

2.2.2 Gas phase analysis

The gas phase was analyzed qualitatively for the presence of methane using a gas chromatography system (GC-450, Varian, Middelburg, The Netherlands) equipped with a molecular sieve column (CP81071: 1.5 m*1/8″ ultimetal molsieve 13 9 80–100 mesh) and a flame ionization detector.

2.2.3 Porewater analysis

The filtered porewater was aliquoted in the glovebox and conditioned for subsequent chemical analysis of sulfide, ferrous iron, major cations and anions, and trace elements. Sulfide was analyzed using the Cline method (Cline, 1969) and ferrous iron using the ferrozine assay (Stookey, 1970) both with a UV-2501PC spectrometer (Shimadzu, Kyoto, Japan). Major anions and cations were detected and quantified by Ion Chromatography. An IonPac®CS13A-5 µm cation-exchange column (Thermo Fisher Scientific Inc., Waltham, Massachusetts, United States), with as gradient eluent 20 mM methane sulfonic acid, was used for major cations, whereas an IonPac® AS18-4 µm anion-exchange column (Thermo Fisher Scientific Inc., Waltham, Massachusetts, United States), with as gradient eluent KOH (from 0.0 to 30 mM), was used for major anions. Trace metals Al, Co, Cr, Cu, Fe, Mn, Mo, Ni, Si, Sr, Zn, were measured using inductively coupled plasma mass spectrometry (ICP-MS) on an Agilent 8,900 Triple Quadrupole (Agilent Technologies Inc., Santa Clara, United States), with all samples prepared in dilutions with 0.1 M HNO_3 (final concentration, ultra-pure grade, MilliporeSigma, Merck KGaA, Darmstadt, Germany).

2.3 Reactor characterization post-retrieval

2.3.1 Reactor disassembly and sampling

After between 73 to 108 days, the reactors were retrieved from the URL, packed in argon-filled Mylar® bags and transferred to EPFL. The reactors were disassembled within a nitrogen gas-filled MBraun anoxic chamber, and the sand-bentonite core contained within the Plexiglas cylinder was extracted. Sterile, DNA-free (autoclaved for 80 min) cleanroom grade wipes (Spec-Wipe® 7, VWR International LLC, Avantor Inc., Radnor, Pennsylvania, United States) were used to handle the Plexiglas core. A Dremel® 3,000 tool (DREMEL Europe Bosch Power Tools B.V., Breda, Netherlands) was used to cut open the

Plexiglas lengthwise. The left half was used for immediate DNA sampling within the glovebox. Five lines (outer left [OL], center left [CL], center [C], center right [CR] outer right [OR]), representing distinct radial locations, were sampled at seven heights, numbered from 1st row (top) to 7th row (bottom), resulting in 35 samples (Figure 2). Equipment was sampled as well (e.g., swab of the steel surface, and organza at the water inlet and outlet). For each sampling spot, a new scalpel blade was used, and the substrate was stored in DNA-free cryotubes at −20°C until DNA extraction. The right half was used for sample collection for subsequent synchrotron-based micro X-ray fluorescence (μXRF) imaging and micro X-ray absorption near edge spectroscopy (μXANES). The remaining part of the left half was embedded in resin for subsequent XRF mapping.

2.3.2 DNA extraction

DNA from the coarse sand and the sand-bentonite were extracted based on an established protocol (Engel et al., 2019a,b), which is a slightly modified protocol of the DNeasy® PowerSoil® Kit (QIAGEN NV, Venlo, Netherlands). The sample substrate (~ 0.2 g) was transferred to the kit-provided PowerBead® tubes in a sterile laminar flow hood with flame-sterilized spatulas. The mass was recorded and the sample briefly vortexed within the provided PowerBead® solution. After addition of the kit-provided solution C1 (containing SDS and disrupting agent for cell lysis), the samples were briefly vortexed and incubated for 10 min at 70°C. Homogenization was carried out with a Precellys 24 homogenizer (Bertin Technologies SAS, Montigny-le-Bretonneux, France), for 45 s at 6,000 rpm. The remaining steps were carried out as indicated by the kit manufacturer except for the elution of the extracted DNA, 65 μL of the kit-provided elution buffer C6 were applied to the center of the DNA binding membrane of a MB Spin Column. After centrifugation for 1 min at 8,000 g, the DNA was collected in a 2 mL Soreson™ Dolphin tube and stored at −20°C until DNA analysis. More details about the porewater DNA extraction method are available in Supplementary Text S2.1.

2.3.3 16S rRNA gene amplification, sequencing, and statistical data analysis

Briefly, all DNA was quantified using the Qubit® ds-DNA HS Assay Kit (Thermo Fisher Scientific Inc., Waltham, Massachusetts, United States). Amplification of the 16S rRNA gene was performed with a modified protocol of the *Quick*-16S™ NGS Library Prep Kit (Zymo Research Corp., Irvine, California, United States) with primers for the V3–V4 region of the 16S rRNA gene (covering both Bacteria and Archaea). Additionally, we took advantage of the fluorescence signal to perform a semi-quantitative assessment of the 16S rRNA gene copy number. qPCR provided insight into the relative quantities of 16S rRNA genes, and thus improved the robustness of the DNA sequencing interpretation (more detail available in Supplementary Text S2.2). The 16S rRNA gene-library was sequenced on an Illumina MiSeq platform (Illumina Inc., San Diego, California, United States) at the Lausanne Genomics Technologies Facility (University of Lausanne, Switzerland), applying 10 pM of the 16S rRNA library with a 15% Phi-X spike in a paired-end 300 bp mode. *t*-tests were achieved with Excel Analysis ToolPak, testing the equality of variance with an *F*-test beforehand, to assess statistical significance in spatial distribution of microbial biomass (Supplementary Figure S8), and to compare the growth in-between reactors (Supplementary Figure S9). More detail is available in the Supplementary material.

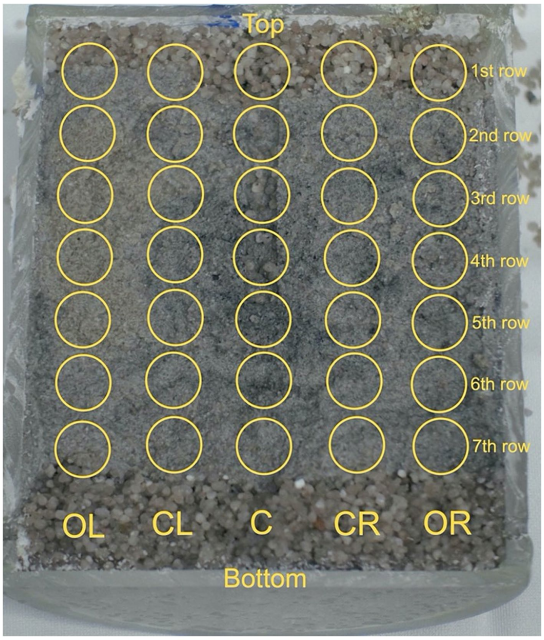

FIGURE 2
Sand-bentonite sampling grid. Samples were taken at 35 locations from one half of the reactors. Five lines (outer left [OL], center left [CL], center [C], center right [CR] outer right [OR]), representing various radial locations, were sampled at seven heights, numbered from 1st row (top) to 7th row (bottom). Sampling was done under anoxic conditions, using sterile scalpel blades. The collected samples were stored in DNA-free cryo-tubes at −20°C until DNA extraction.

2.3.4 16S rRNA gene analysis

Qualities of demultiplexed raw sequencing reads were assessed using FastQC, version 0.11.9 (Andrews, 2019). The processing of demultiplexed raw reads was carried out in R (version 4.1.2, November 2021), and as recommended in the dada2 pipeline documentation (version 1.2). Reads were first filtered and trimmed using the filterAndTrim function. The filtering and trimming parameters were established using Figaro, dockerized version 1.1.2 (Weinstein et al., 2019) with the forward and reverse primer length set to 16 and 24 bp, respectively, and the amplicon length set to 420 bp. With the highest expectation of read retention the following parameters were retained from Figaro output: truncLen = c(289, 191), maxN = 0, maxEE = c(2,1), truncQ = 2, and rm.phix = TRUE. Error rates were then learned using the learnErrors function to perform sample inference with the filtered and trimmed reads. The paired reads were then merged using mergePairs function. Chimeras were removed using the removeBimeraDenovo function with the method set to "consensus." Finally, the taxonomic assignment of Amplicon Sequence Variants (ASVs) was performed using SINTAX (Edgar, 2016) with the curated Ribosomal Database Project (RDP), trainset 18, release 11.5.

The high-quality reads were imported to ampvis2 (Andersen et al., 2018), which was used to analyze and visualize the sequence data of the sand-bentonite and equipment samples, using heatmaps (genus level), and Principal Component Analysis (PCA, using Hellinger transformation). Unknown taxonomic affiliations are indicated up to the taxonomic level identified. For bubble plots, and relative abundance calculation, the number of reads in the kitome for each Amplicon Sequence Variant (ASV) was removed from the samples, and the result was normalized to the total number of reads in the sample. Spatial maps of selected top ASVs and boxplots of 16S rRNA gene semi-quantification were generated using OriginPro, version 2022b (OriginLab Corporation, Northampton, Massachusetts, United States).

2.4 XRF and statistical data analysis

The core was dried in vacuum for 24 h within a MBraun antechamber and embedded using EPO-TEK 301-2 resin (JP Kummer Semiconductor Technology GmbH, Augsburg, Germany). 10 cycles of soft vacuum and ambient pressure were applied. After a low temperature curing for 48 h, a longitudinal cut was performed, approximately 1.5 cm below the plane used for DNA sampling, using a diamond wire saw (MURG 394, WELL Diamond Wire Saws SA, Le Locle, Switzerland). XRF maps of sodium, silicon, phosphorus, potassium, sulfur, calcium, titanium, vanadium, chromium, manganese, iron and nickel (all K-edge) were obtained at the Crystal Growth Facility (EPFL), with an EDAX Orbis PCMicro EDXRF analyzer system (AMETEK Inc., Berwyn, Pennsylvania, United States). Boxplots of counts of iron, sulfur, and calcium fluorescence signals (representing atom-percent values for each element, at scanning spots where the sulfur signal was above 10%) were generated using OriginPro, version 2022b (OriginLab Corporation, Northampton, Massachusetts, United States). *t*-tests were achieved (Excel Analysis ToolPak, previously testing equality of variance with *F*-test) to assess statistical significance of the minerals shifts between biotic reaction and abiotic control (Supplementary Figure S5). More details are available in Supplementary Text S2.3.

2.5 Synchrotron μXRF and Fe/S K-edge μXANES

Sand-bentonite samples of about 2.5 cm in length and 1.5 cm in width were obtained from the right half of each reactor in anoxic conditions. The samples were chosen based on visually observable features such as dark color and/or red/brownish halos (Supplementary Figure S2). These samples were placed into custom-built sample holders made of poly-(methyl methacrylate), dried in a high vacuum for 12 h, and stabilized in EPO-TEK 301-2 resin. A minimum of 6 soft-vacuum/ambient pressure cycles were applied to remove trapped gas bubbles. After 48 h of a low-temperature curing, the embedded sample surfaces were gradually exposed by rough removal of excess resin using a Dremel® 3,000 tool. Fine wet grinding using silicon carbide grinding paper of three grit grades (Struers Inc., Cleveland, Ohio, United States) and ethanol, analytical reagent grade (Thermo Fisher Scientific Inc., Waltham, Massachusetts, United States) was performed manually until an even and shiny sample plane was achieved. The prepared samples were sealed within a nitrogen atmosphere by packing in three layers of Mylar®. Synchrotron radiation μXRF maps and Fe K-edge XANES spectra were collected at beamline 2–3 of the Stanford Synchrotron Radiation Lightsource at the Stanford Linear Accelerator Laboratory (Menlo Park, California, United States). Fe-XANES data were collected in the energy range of 6,927 eV to 7,520 eV. μXRF imaging and S K-edge XANES was performed at beamline I-18 at the Diamond Light Source (Didcot, Oxfordshire, United Kingdom) using the Data Analysis WorkbeNch (DAWN) (Basham et al., 2015). The S K-edge XANES were collected in the energy range of 2,400 eV to 2,600 eV. Both Fe and S XANES spectra were analyzed using Linear Combination Fitting (Athena software) (Ravel and Newville, 2005).

3 Results

3.1 Water and H_2 availability

The experimental set-up aimed to establish a link between the evolving microbiome and the availability of H_2, the main electron donor, and sulfate, the major electron acceptor. Close to the H_2 inlet, the availability of H_2 is high and bioavailable sulfate is expected to be rapidly depleted due to the activity of SRB. As H_2 was applied daily, the total quantity provided to each reactor is proportional to the duration of the experiment (Table 1). Water flow was controlled by the sand-bentonite back-pressure, resulting in variable flow across time and reactors (Supplementary Figure S3). Reactors 1 and 2 received between 0 and 4 μL/min of porewater (Supplementary Figure S3C); in total, reactor 1 received 10.1 mmoles of sulfate from the porewater while reactor 2 received 8.1 mmoles (Table 1). Reactor 3 received a varying flow of water, on average 4 μL/min until day 57, which sharply increased after day 57 with an average of 20 μL/min until the end of the experiment (Supplementary Figure S3A); in total, reactor 3 received 16.1 mmoles of sulfate from the porewater (Table 1). Reactor 4 received on average 12 μL/min, with a sharp decrease towards the end of the experiment down to 0 μL/min on day 70 (Supplementary Figure S3B); in total, reactor 4 received 22.9 mmoles of sulfate from the porewater (Table 1).

$$SO_4^{2-}\ \text{rate} = \frac{Vin_{tot} \bullet \left[SO_4^{2-}\right]_{in} + n_{\text{gypsum dissolution}} - \Sigma_{\text{week}}\, V_w \bullet \left[SO_4^{2-}\right]_{out_w} - V_{voids} \bullet \left[SO_4^{2-}\right]_{out_{end}}}{\text{days} \bullet V_{voids}} \quad (2)$$

Vin_{tot} : total water volume injected in the reactor (L)

$\left[SO_4^{2-}\right]_{in}$: sulfate concentration in the inflow (mM)

$n_{\text{gypsum dissolution}}$: quantity of sulfate present in gypsum (10 mmol, Supplementary Text S3)

V_w and $\left[SO_4^{2-}\right]_{out_w}$ total outflow (L) and average concentration (mM) in the outflow during week w

V_{voids}: volume of voids in the reactor (L)

$\left[SO_4^{2-}\right]_{out_{end}}$: sulfate concentration in the outflow at the end of the experiment (mM)

3.2 Sulfate reduction rate

Sulfate is expected to serve as an electron acceptor. In the reactors, sulfate comes from the borehole porewater (approx. 15 mM, Figure 3 and Supplementary Table S3) and dissolution of gypsum from bentonite (Maanoja et al., 2020). Porewater was sampled and analyzed weekly during the H_2 injection phase, and the evolution of sulfate, sulfide, and ferrous iron is presented in Figure 3. Sulfate concentration followed a decreasing trend from the start of the experiment until the sacrifice of the reactors. Sulfate is reduced to sulfide, which abiotically precipitates with dissolved ferrous iron to form iron sulfide. The initial ferrous iron concentration in reactor 4 (80 µM) was lower than in the three other reactors (120 µM). Ferrous iron was depleted in the four reactors starting on day 10. During the entire experiment, any additional iron coming from the fresh porewater inflow was removed before reaching the outlet. Sulfide was not detected in the borehole porewater. In the reactors, the sulfide concentration remained one order of magnitude lower than the sulfate concentration. In reactors 3 and 4, the concentration of sulfide increased slightly to reach, respectively, 40 µM and 140 µM when sacrificed. In reactors 1 and 2, the sulfide concentration increase was greater, reaching, respectively, 360 µM and 240 µM. At the end of the experiment, the sulfide concentration has increased relative to the initial time point in all four reactors, but it showed temporal variations: a decrease from day 80 to 100 in reactor 1, and from day 80 until the end of the experiment in reactor 2.

Considering sulfate reduction as stoichiometrically linked to H_2 oxidation, we aimed at calculating the overall sulfate reduction rates in the four reactors during the whole experiment. To this end, we compared two calculations methods: a linear regression and a global mass balance. The sulfate rates calculated are summarized in Table 2. The linear regression model was applied to sulfate concentration curves (linear trend indicated in Figure 3A, detail in Supplementary Table S4). R-squared values obtained for reactors 1, 2, and 4 are above 0.95, which indicates that a zero-order model adequately captures the microbial activity in the reactors.

The above sulfate reduction rate was calculated assuming a batch system with the initial sulfate concentration corresponding to that after saturation with borehole porewater during 5 to 30 days (time 0 in Figure 3). This is clearly an assumption that results in an underestimated rate as it does not account for additional sulfate sources: (i) further dissolution of gypsum (dissolution during the initial equilibration released 1.71 to 2.96 mmol, while total gypsum available represents approximatively 8.2 mmol, Supplementary Table S1 and Supplementary Text S3); and (ii) inflow of fresh borehole water with a sulfate concentration of 15 mM. For reactors 1 and 2, the sulfate concentration increases during the 1st week (Figure 3) evidencing the limitations of the batch reasoning.

A global sulfate mass balance is considered as a second approximation of the sulfate reduction rate (Eq. 2) and the results summarized in Table 2. The rates are 2 to 5 times lower than the linear reduction rate, and there is a higher variability amongst the reactors.

3.3 Sulfur conversion from gypsum to iron sulfide

Due to microbial sulfate consumption, the reactor water is expected to become undersaturated with respect to gypsum, resulting in its dissolution. Furthermore, sulfide produced precipitates with ferrous iron to form iron–sulfur minerals (e.g., mackinawite FeS, greigite Fe_3S_4, or pyrite FeS_2) (Duverger et al., 2020). Patches of black color of the sand-bentonite matrix were observed after incubation with H_2 (Supplementary Figure S2).

We used XRF for elemental mapping of iron, sulfur, and calcium on one half of each reactor. Sulfur hotspots (i.e., with atomic percent above 10) expected to correspond to pre-existing gypsum (calcium sulfate) or to iron sulfide precipitation were selected to study the correlation between atomic percent of sulfur and calcium, or sulfur and iron. The mean iron to calcium ratio observed at sulfur spots for each reactor significantly shifted from approximatively 1.1 (abiotic control) to 1.5 (reactor 2, $p < 0.05$), up to 4.6 (reactor 1, $p < 0.05$) (Supplementary Figure S5C). Moreover, the decrease in calcium atomic percent at sulfur spots is statistically significant for the four biotic reactors compared to the abiotic control ($p < 0.00001$ for reactor 1, 2, and 4, $p < 0.005$ for reactor 3, Supplementary Figure S5A). In contrast, XRF data do not provide conclusive evidence of the change in iron concentration at sulfur

hotspots (Supplementary Figure S5B). In reactors 1, 3, 4 and in the abiotic control (reactor not exposed to H_2), the average iron to sulfur ratio is 0.45, close to 0.5, corresponding to pyrite, which is initially present in Wyoming bentonite MX-80 (0.60% by weight, Supplementary Table S1). In reactor 2, the iron to sulfur ratio is lower than in the abiotic control (0.17 compared to 0.45, $p < 0.05$). The number of sulfur hotspots in this reactor was greater than in any other reactors, including the abiotic control (225 compared to values ranging from 18 (reactor 4) to 40 (reactor 3)). *t*-test results are detailed in Supplementary Table S5.

We used μXANES to analyze sulfur speciation. For the abiotic control (no H_2), the best fit for the sulfur data was obtained with gypsum (Supplementary Table S7). For 14 out of the 18 samples exposed to H_2, the best fits were obtained with pyrite as the main sulfur phase and with mackinawite as the second most abundant phase. In one sample, mackinawite was identified as the main phase by fitting. Poor quality of the standard data impeded obtaining very good values for statistical indicators of the goodness-of-fit, but the values confirm qualitatively adequate fits. Iron XANES spectra analysis confirmed the presence of pyrite and mackinawite in the samples, with higher fit quality than the sulfur XANES spectra (Supplementary Table S8). XANES mapping of iron evidences the presence of a pyrite precipitate of 1 mm^2 in reactor 2 (Supplementary Figure S6). Unfortunately, the standards did not allow the identification of all the iron phases, with for instance the presence of an unknown iron phase in the middle of a ferrihydrite spot in reactor 3 (Supplementary Figure S7, sample 20 in Supplementary Table S8).

3.4 Hydrogenotrophic microbiome dominated by sulfate reducers and methanogens

The 35 sand-bentonite samples collected from the middle plane of each reactor and swabs from equipment parts of the reactors were analyzed to quantify biomass (16S rRNA gene copies number per gram of sand-bentonite) and phylogeny (16S rRNA gene amplicon sequencing). Here, we first discuss results obtained by averaging the relative abundance and biomass quantification results of the samples for each reactor (Figure 2 and Supplementary Tables S9–S11).

When comparing 16S rRNA gene copies number from the initial dry sand and dry bentonite, to the sand-bentonite samples post-incubation, it is clear that growth has taken place within all four reactors: the average 16S rRNA gene copies number per gram of material in reactors post incubation, dry bentonite, and dry sand are respectively: 8.2×10^8, 8.2×10^5, and 3.7×10^5 16S rRNA gene copies/gram substrate (Supplementary Figures S8, S9). The reactors were run for different durations and the flow rate was variable,

TABLE 1 Sulfate and H_2 supplied to each reactor, and H_2 to sulfate molar ratio.

Reactor	Setup	Experiment duration [days]	Sulfate from water [mmol]	Total H_2 [mmol]	Molar H_2 to sulfate ratio (water)	Molar H_2 to sulfate ratio (total)
1	Serial	108	10.1	49.1	4.9	2.7
2			8.1	49.0	6.1	3.0
3	Parallel	73	16.1	32.6	2.0	1.3
4		79	22.9	33.1	1.4	1.1

The molar H_2 to sulfate ratio (water) accounts only for sulfate from the borehole water, the molar H_2 to sulfate ratio (total) accounts for the complete dissolution of gypsum from bentonite, providing 8.2 mmol (calculation detailed in Supplementary Text S3).

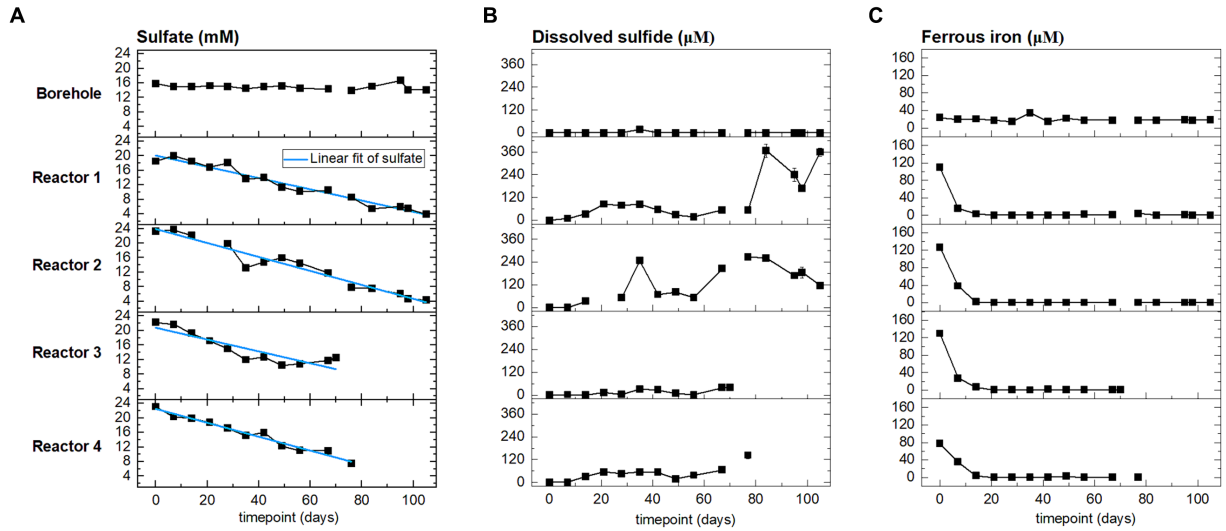

FIGURE 3
From left to right, time evolution of: **(A)** sulfate, **(B)** sulfide, and **(C)** ferrous iron concentrations at the outlet of the reactors (four bottom rows), and in the borehole porewater (top row). Points are the average of three sampling replicates, error bars represent one standard deviation.

TABLE 2 Sulfate consumption rate calculated through: (A) Linear regression (Figure 3) and (B) Mass balance (Eq. 2).

	(A) Linear regression			(B) Mass balance
	Rate $[\frac{\mu mol}{day\ cm^3}]$	Standard deviation $[\frac{\mu mol}{day\ cm^3}]$	Adjusted R-squared	Rate $[\frac{\mu mol}{day\ cm^3}]$
Reactor 1	1.548	0.090	0.958	0.35
Reactor 2	1.920	0.124	0.952	0.27
Reactor 3	1.630	0.277	0.794	0.62
Reactor 4	1.911	0.114	0.969	0.52
Average	1.752 ± 0.191			0.44 ± 0.14

For (A), the standard deviation and R-squared values are calculated wit the Linear Regression analysis tool or OriginPro (2022b).

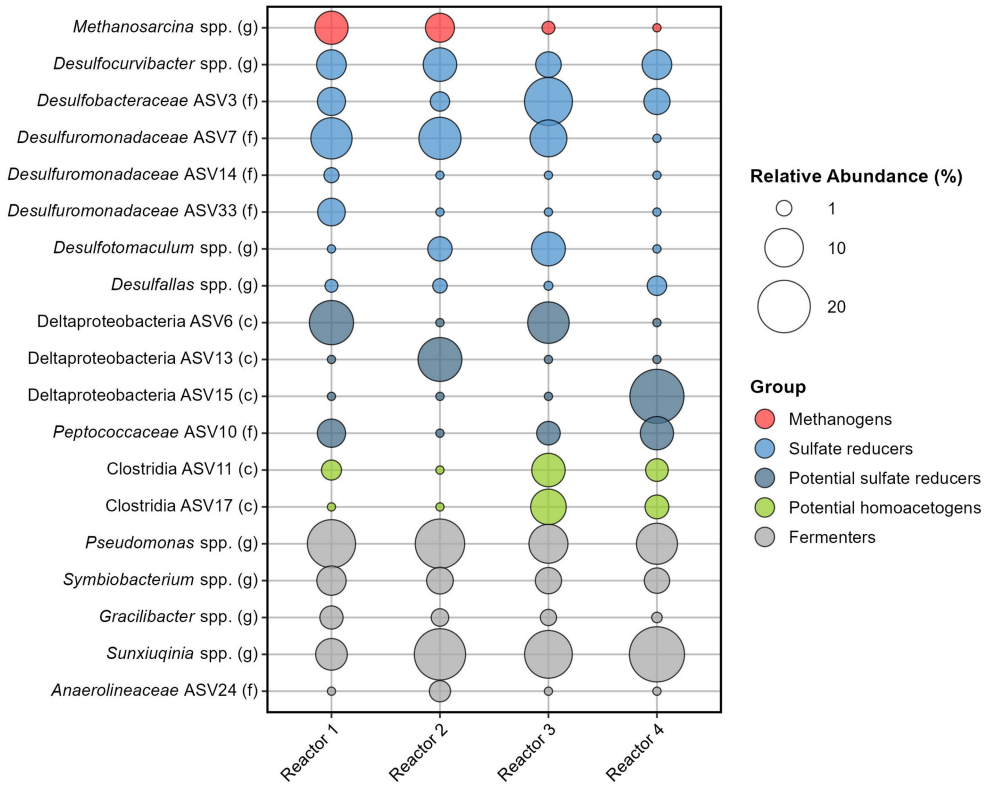

FIGURE 4
Relative abundance of the 19 most abundant ASVs among the four reactors. Number of reads were averaged for each reactor, and contributions from the Kitome were removed before calculating the relative abundance.

resulting in different amounts of total sulfate available (Section 3.1). We expected reactor 4, that received the most water and sulfate (Table 1) to host the highest biomass, but on average, reactor 3 has significantly higher biomass growth than the other reactors ($p < 0.01$ for reactor 1, $p < 0.05$ for reactor 2, and $p < 0.001$ for reactor 4, Supplementary Figure S9 and Supplementary Table S12). The flow in reactor 4 decreased sharply at the end of the experiment [from 20 µL/min at day 60 to 0 µL/min at day 70, with on average 3 µL/min during the last 10 days (Supplementary Figure S3)], meanwhile in reactor 3 it increased up to 32 µL/min, with on average 20 µL/min during the last 10 days (Supplementary Figure S3). Altogether, this suggests that biomass growth measured at the end of the experiment depends on the flow rate (and thus sulfate availability) in the reactors at the end of the experiment rather than during the whole experimental run.

The average relative abundance of the 35 sand-bentonite samples varies across reactors but all include sulfate reducers, methanogens, both known hydrogenotrophs, as well as fermenters (Figure 4 and Supplementary Tables S9, S10).

Among sulfate reducers, *Desulfocurvibacter* genus has a similar average relative abundance in the four reactors, ranging from 3.8% (reactor 3) to 7.3% (reactor 2). Sulfate reducers from the Proteobacteria phylum are well represented with four ASVs identified to be part of the *Desulfobacteraceae* or *Desulforomonadaceae* families (Figure 4). *Desulfuromonadaceae* (ASV7) has the highest overall relative abundance (6.8%,

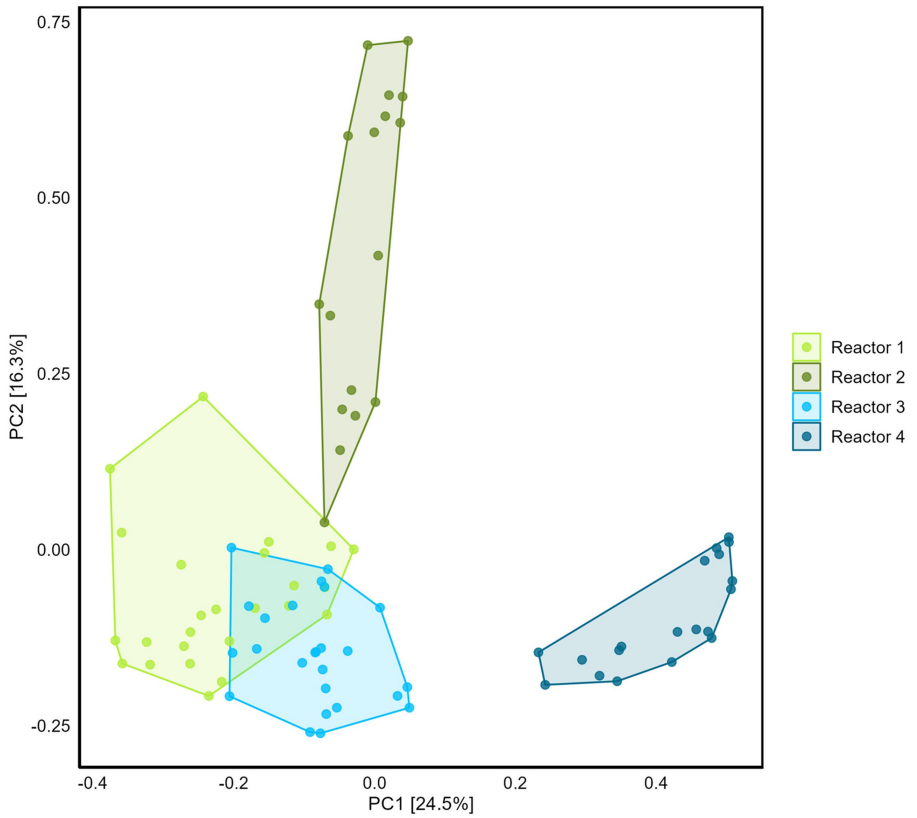

FIGURE 5
Comparison of the four reactors microbiome using Principal Component Analysis (with Hellinger transformation). Percentage of the variance corresponding to the principal components (PC) is indicated in the brackets for each axis.

Supplementary Tables S9, S10). Other sulfate reducers are Firmicutes, with *Desulfotomaculum* spp. identified in reactors 2 and 3 and *Desulfallas* spp. identified in all reactors. Three ASVs from the Deltaproteobacteria class could not be assigned down to the genus level, however, many families of this class are sulfate reducers. Data analysis using the RDPnaive algorithm (which is less restrictive) predicted the attribution of ASV6 to the order Desulfobacterales and of ASV10 from the family *Peptococcaceae* to genus *Desulfallas* (data not shown). If ASVs 6 and 10 are indeed sulfate reducers, the relative abundance of sulfate reducers is high in all reactors: 38.7% (reactor 2), 42.2% (reactor 4), 46.9% (reactor 1), and 50.2% (reactor 3) (Supplementary Tables S9, S10). Taking ASVs individually, we observe that only in reactor 3 does an ASV corresponding to a sulfate reducer have the highest relative abundance on average (ASV3 from *Desulfobacteraceae* family with 16.5%). In the other reactors, the most abundant ASV is from the genus *Pseudomonas* or *Sunxiuqinia*.

Methanosarcina genus is the only representative of methanogens. Averaging the 35 sand-bentonite samples in each reactor, the genus was detected as the 4th, the 7th, and the 13th most abundant ASV in reactors 1, 2, and 3, respectively. This genus was also detected in reactor 4, but the average number of reads was lower than the number of reads in the Kitome, and thus the presence of this genus in the sand-bentonite matrix could not be confirmed. Activity of this methanogen was confirmed via the detection of methane in all four reactors during the experiment (Supplementary Figure S4). Indeed, detection of methane in the gas phase of reactor 4 supports the presence of *Methanosarcina* spp. in this reactor, despite its low abundance based on reads count.

Fermenters do not participate in H_2 oxidation but foster availability of low molecular weight organic carbon substrates for the growth of H_2 oxidizers. Attribution of fermentative metabolism based on genus is an approximate endeavor as many bacteria capable of fermentation are also able to catalyze other reactions. For instance, members of the genus *Pseudomonas* can ferment many substrates but also carry out denitrification (Carlson and Ingraham, 1983) or iron reduction (Vasil, 2007). Therefore, while we classify *Pseudomonas* and *Sunxiuqinia* genera as fermenters here, they could also be involved in other metabolisms. These two genera are part of the top five most abundant ASVs, with relative abundance ranging from 10.3 to 17.6%, and 6.4 to 22.4%, respectively. Other putative fermenters are from *Symbiobacterium* genus., with a homogeneous relative abundance across the reactors, and from *Gracilibacter* genus.

Differences between reactor microbiomes were evidenced using PCA (Figure 5). Reactors 1, 2, and 3 present similarities with the overlapping of the clouds formed by the samples plotted on the two first principal component axes, while reactor 4 plots separately.

The PCA of the microbial community associated with equipment evidences similarity amongst the four reactors (Supplementary Figure S10). The top ASVs are from the genera *Pseudomonas, Desulfocurvibacter, Desulfobacteraceae (ASV3), Methanosarcina, Gracillibacter, Desulfallas, Sunxiuqinia*

(Supplementary Table S13). *Methanosarcina* genus was preferentially located at the water inlet of reactors 1 and 2 (data not shown). *Desulfocurvibacter* genus was observed at the water inlet, outlet (where it has the higher relative abundance), and on the H_2 tube, suggesting the dependence of this genus on H_2 (data not shown).

3.5 Microbiome spatial distribution

The spatial distribution of biomass and ASVs in each reactor also contains useful information that can be mined as a result of the spatially-resolved sampling. Biomass concentration was compared across vertical columns for each reactor and evidenced that growth had taken place mainly in the middle vertical column in each reactor, where the highest availability of H_2 is expected (Supplementary Figure S8). Indeed, for all reactors, at least one of the off-center columns showed significantly ($p < 0.05$) lower 16S rRNA gene copies number per gram of substrate than the central column (Supplementary Table S13). Notably, in reactor 3, the number of 16S rRNA copies is lower on either side of the central column ($p < 0.05$). For reactor 2, and reactor 4, three columns out of four have significantly lower number of 16S rRNA copies than the central one ($p < 0.05$). For reactor 1, only the outer left column presents significantly lower number of copies ($p < 0.05$). In this reactor, growth appears to have taken place homogeneously. *t*-test results for all reactors are detailed in Supplementary Table S13.

Maps of individual taxa within the microbiome (Figure 6) show that sulfate reducers, particularly member of *Desulfocurvibacter* genus, grow around the H_2 outlet. In reactor 3, *Desulfocurvibacter* spp. were outcompeted by other SRBs, and the middle column of the reactor is occupied by a member of *Desulfobacteraceae* family (which is the most abundant ASV in this reactor). In reactors 1, and 2, the most abundant sulfate reducer (from the *Desulfuromonadaceae* family) occupies mainly the outer left and bottom of the reactor (reactor 1) or is homogeneously distributed (reactor 2).

In reactor 2, *Methanosarcina* spp. grew near the H_2 outlet, with a similar growth pattern as that encountered for *Desulfocurvibacter* spp. However, in this reactor the highest relative abundance of *Methanosarcina* spp. is observed at the top right corner and corresponds to the highest number of 16S rRNA gene copies in this reactor. In reactor 1, members of *Methanosarcina* genus grew where there is no SRB growth; in reactor 3, they grew at the top left corner, overlapping with members of *Desulfocurvibacter* genus.

4 Discussion

4.1 Sulfate reduction and H_2 oxidation rates

The sulfate reduction rate was calculated using two approaches: a linear regression, and a global mass balance. The rates obtained by linear regression were two to five time higher (on average, $1.752 \pm 0.191 \frac{\mu mol}{day\ cm^3}$) than the global mass balance calculation (on average, $0.44 \pm 0.14 \frac{\mu mol}{day\ cm^3}$). The rates obtained by linear regression are similar for the four reactors (RSD of 11%, highest rate in reactors 2 and 4, and lowest in reactors 1 and 3, but no statistically significant differences), despite different running conditions (duration, water flow, parallel/serial setup). The global mass balance captures differences (RSD of 24%), especially related to water flow (highest rate in reactors in the parallel setup, lowest rate in reactors in the serial setup). The linear regression considered a batch system with no additional input of sulfate and gave an average value for the entire duration of the experiment. On the contrary, the global mass balance takes into consideration sulfate inputs (dissolution, fresh borehole water) and loss of sulfate in the outflow (Eq. 2). The mass balance is thus more complete and is considered to be a better model. The difference between the two rates highlights the limited quantitative information provided by the evolution of the concentration at the outflow, given the existence of preferential flow paths, and the heterogeneous sulfate dissolution and consumption in the porous matrix.

The range of the rates calculated is five to ten-fold higher than the sulfate reduction rate of 0.14 to 0.20 $\frac{\mu mol}{day\ cm^3}$ reported by Bagnoud et al. (2016c) for a similar Opalinus Clay rock derived microbial community but within a porewater-filled borehole. This suggests that the porous material (representing backfill in the future repository) provides more favorable growth and/or metabolic conditions. Considering a 1:4 stochiometric ratio, the H_2 oxidation rate was estimated to be 2–7 $\frac{\mu mol}{day\ cm^3}$ using the average of the results from the mass balance and the linear regression, respectively. Literature-reported rates of H_2 oxidation by sulfate reducers cover a wide range: 1.2 to 312 $\frac{\mu mol}{day\ cm^3}$ as reported by Thaysen et al. (2020). Dohrmann and Krüger (2023) measured H_2 oxidation in the formation fluid in a natural gas field and found the pressure-dependent rate to vary between 0.123–0.325 $\frac{\mu mol}{day\ cm^3}$ at ambient pressure and to increase up to 4 $\frac{\mu mol}{day\ cm^3}$ at 100 bar.

It is most useful for a DGR to compute the H_2 consumption rate as a function of the volume of backfill material. The rate is estimated to be 0.9–3.2 $\frac{mol}{day\ m^3_{backfill}}$ (calculation detailed in Supplementary material, Supplementary Text S4). Considering a production of 25 million m^3 (900×10^6 mol) of H_2 during a safety period of 1,000 years for the storage of radioactive waste, and constant H_2 oxidation rate, less than 1% of the backfill would be required for the microbial consumption of all the H_2 produced. There are clearly many approximations associated with these calculations: for instance, partial saturation of the backfill and limited water availability, sulfate depletion, or the dependence of microbial activity on temperature and pressure (Dohrmann and Krüger, 2023). In reality, one can expect variable H_2 production and consumption rates as a function of time.

In the work by Bagnoud et al. (2016c), the stoichiometry of sulfate reduction was observed to be close to 8.5 moles of H_2 per mole of sulfate reduced, which was attributed to other reduction reactions coupled with H_2 oxidation (i.e., reduction of intermediate valent state sulfur species, clay iron reduction) and H_2 losses. In our study, sequencing of the 16S rRNA gene did not provide conclusive

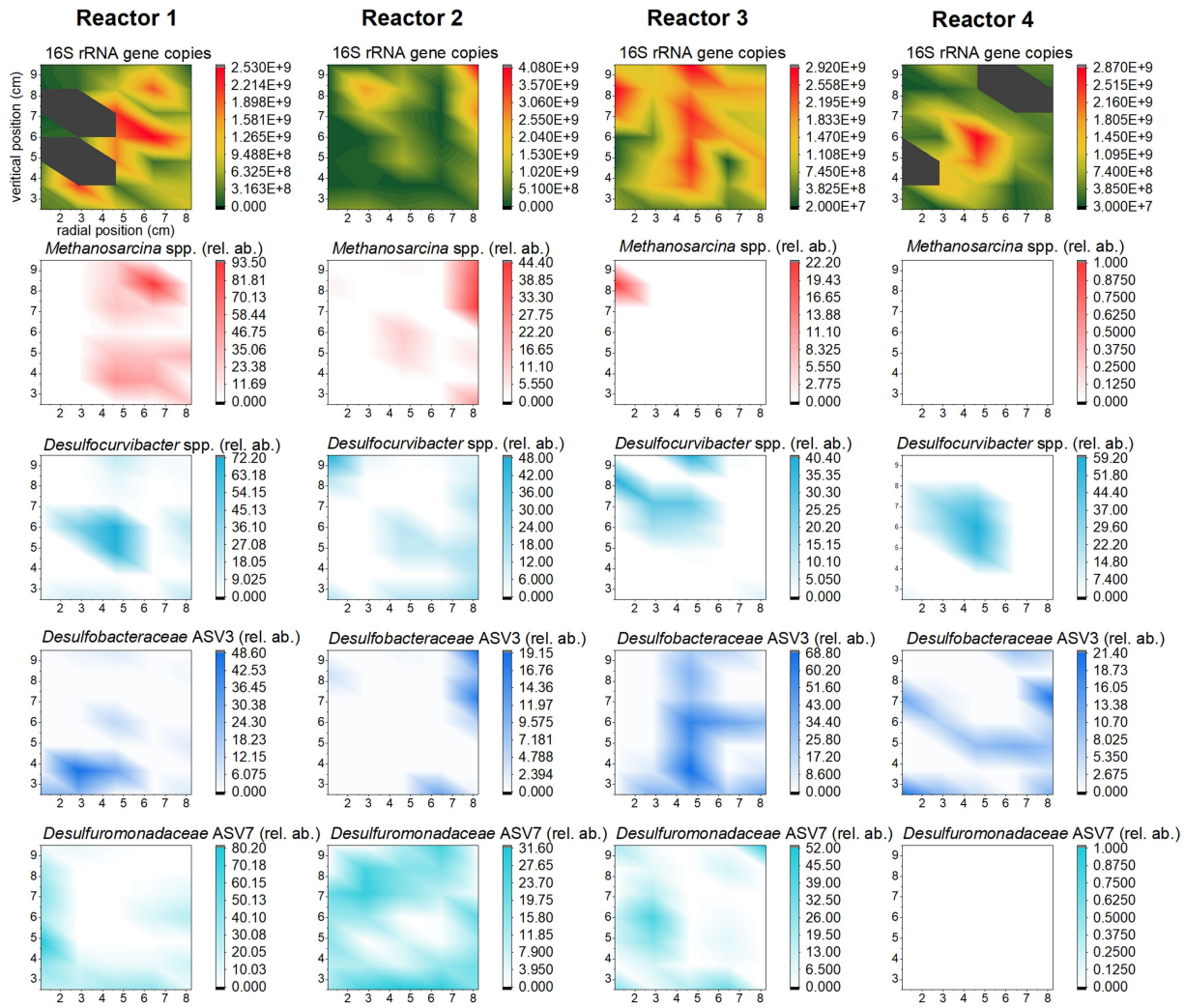

FIGURE 6
Distribution of biomass (top row) and selected ASVs (other rows) in the four reactors. The heat maps were achieved using OriginPro (2022b), with extrapolation of the data from the 35 sampling spots (Figure 2). The color scale corresponds to the number of 16S rRNA gene copy number per gram of substrate for biomass distribution, and to the distribution of the local abundance of the methanogen and sulfate reducers relative to total biomass, for each sampling spot.

information on the presence of homoacetogens and iron reducers. Nonetheless, given that ASVs from the class Clostridia, and the family *Desulfuromonadaceae* were detected, and are taxa that harbor homoacetogens and iron reducers, respectively, we cannot exclude a role for those metabolisms in H_2 consumption. Furthermore, the presence of hydrogenotrophic methanogens highlights the limitations of using sulfate reduction as a proxy for H_2 oxidation rate.

Mapping sulfate-reducing taxa indicates that, while some genera (e.g., *Desulfocurvibacter*) have grown close to the H_2 tube outlet, and, thus, their growth may be limited by H_2 availability, other ASVs capable of sulfate reduction were distributed homogeneously within all reactors. The homogeneous distribution suggests the use of other electron donors (e.g., low-molecular weight organic acids). Bentonite can release organic carbon (Maanoja et al., 2020) which could serve as an electron donor. So can the degradation of autotrophic biomass. If the contribution of organic carbon to sulfate reduction is substantial, the sulfate reduction rate could be an overestimation of the H_2 consumption rate. However, lactate and acetate were never detected in the outflow and total dissolved organic carbon was not measured, preventing meaningful assessment of the contribution of organic carbon to this metabolism. Rates measured by Bagnoud et al. (2016c) presented evidence that sulfate reduction did not account for all H_2 consumption as the amount of H_2 consumed was 8.5-fold greater than that calculated by the stoichiometric ratio with sulfate. However, in the same experiment, consumption of organic carbon supports the occurrence of heterotrophic growth, possibly of the sulfate reducers (Bagnoud, 2015). For the present study, this suggests that not all sulfate reduction is attributable to H_2 oxidation, but nonetheless we can expect that more H_2 is consumed than sulfate reduced, due to other metabolisms.

Overall, the reported rate of sulfate reduction can be viewed as a conservative range due to three important restrictions. First, the sulfate-reducing biofilm within the reactor was not fully developed as evidenced by the remaining sulfate within the outflow water after

more than 100 days of daily H_2 injections (Figure 3). Second, the H_2 oxidation rate calculated via sulfate reduction observed at the outflow does not account for sulfate consumption in the unconnected porosity. Third, the H_2-oxidizing community within the sand-bentonite matrix is not exclusively composed of SRB, but also of methanogens. Thus, the actual H_2 oxidation rate is likely to be higher.

4.2 Establishment of a hydrogenotrophic microbiome

To decipher whether the most abundant ASVs originated from the borehole water or the sand or bentonite solids, DNA from the dry sand and clay, and from borehole porewater, was extracted and sequenced (Supplementary Tables S2, S14). The microbiomes from the borehole porewater and the dry materials are clearly different from that of the reactors, except for *Pseudomonas* genus, that is present everywhere. This ASV is one of the most abundant in the borehole water and was detected in the coarse sand and in two out of three dry bentonite samples as well. None of the other 25 most abundant ASVs from reactors, dry sand, dry bentonite, or borehole water, overlap. The microbiome obtained from dry clay materials may not represent the full diversity of the community due to the inability to detect low-abundance species. This is evidenced when comparing the microbial diversity of dry clay and that of the same clay placed in water with an electron donor/acceptor (Vachon et al., 2021). Therefore, it is not a trivial exercise to pinpoint the origin of the microbial community identified in the 4 reactors. However, similarity in the microbial community amongst three of the four reactors (Figure 5), even though their preparation occurred up to a month apart, suggests that the origin of the microbiome is likely to be the dry materials or the borehole porewater, and not the equipment or preparation and handling conditions. Members of *Gracillibacter*, and *Peptococacceae* genera could originate from the borehole water (number of reads >500). ASVs from *Paenibacillaceae*, which was among the most abundant families in the borehole water, did not grow in the reactors. ASVs from the order Clostridiales represent some of the most abundant genera in the borehole porewater, but do not correspond to the ASVs from the class Clostridia detected in the reactors. Finally, surprisingly, few reads (88 reads on average, with 45 reads in the Kitome considered to be contamination) were detected in the reactor for the most abundant borehole porewater sulfate reducer, *Desulfosporosinus* genus, suggesting that it did not thrive in the sand-bentonite porous medium amended with H_2. Altogether, comparing the microbiomes of the dry materials, the borehole porewater, and the reactors did not allow to conclusively disentangle the origin of the most abundant genera in the reactors.

Sampling the internal surfaces of the equipment (water inlet/outlet, gas trap, gas inlet, steel and Plexiglas surfaces) provided the opportunity (i) to decipher the potential contribution of the microbiome associated with the equipment to sulfate consumption and methane production, (ii) to identify whether conditions in the sand-bentonite support growth of a matrix-specific community, distinct from the one on the equipment surfaces. PCA highlighted a marked difference of the community in the sand-bentonite in reactor 4 compared to that in the three other reactors, which was not reflected in the sulfate reduction rate. Contrary to the sand-bentonite matrix, samples obtained from the equipment were similar in the four reactors (overlapping of clouds on equipment PCA, Supplementary Figure S11) and *Desulfocurvibacter*, *Pseudomonas*, and *Methanosarcina* genera were detected with the highest relative abundance (Supplementary Table S13). This observation suggests that the equipment community might contribute non-negligibly to sulfate reduction rates, and would explain why the rates from the linear-regression are similar across reactors despite differences in the sand-bentonite matrix microbial community. Additionally, it suggests the development of distinct communities within the sand-bentonite porous medium in each reactor that differ from that on the equipment. Thus, the sand-bentonite microbial community in each reactor may have been shaped by the specific flow rate, that impacts the availability of solutes as well as the ratio of H_2 to sulfate (Table 1).

Monitoring the outflow sulfate concentration associated with the linear-regression analysis has the advantage of giving information on temporal variations in sulfate consumption, and thus, the activity of sulfate reducers. The linear-regression fitted the sulfate consumption data for reactors 1, 2, and 4 adequately (R-squared superior to 0.95) indicating a steady-state activity during the experiment, but less so for reactor 3 (R-squared of 0.79). The low R-squared value for the reactor 3 linear model is explained by an increase in sulfate concentration after 57 days, which is likely due to a steep increase in the water inflow rate (Supplementary Figure S3). Sulfate may not have been consumed by the microbial community rapidly enough to overcome this abrupt increase. Another possibility is the creation of preferential water flow paths not yet colonized by sulfate-reducing communities. If only the low water flow regime is considered (first 50 days) for reactor 3, a linear sulfate reduction rate of 2.569 $\frac{\mu mol}{day\ cm^3}$ is observed, with a R-squared of 0.96. This is the highest rate measured in the four reactors, and matches sequencing results which indicated that, on average, SRB were present with a higher relative abundance in this reactor (Results 3.4). However, the underlying reasons for greater growth and activity of SRB in this specific reactor are not understood.

4.3 Evidence for H_2 consumption via methanogenesis

Methane was detected in the gas phase of all reactors. *Methanosarcina* spp. are versatile methanogens capable of all three methanogenic pathways (Madigan et al., 2018), thus no direct conclusion of its role in H_2 consumption can be extracted from this system. However, its growth and the detection of methane strongly support methanogenesis as an important metabolism stimulated by H_2 (directly or indirectly). Methanogenesis consumes 5 moles of gas, for 1 mole of CH_4 produced, thus participating to pressure decrease despite gas production ($4H_2 + CO_2 \rightarrow CH_4 + 2H_2O$). The average relative abundance of *Methanosarcina* spp. was higher in reactors 1 and 2, which received the least water, and thus the least sulfate. Detection of this genus in reactor 3, which received variable water flow rate (very low for the first 2/3 of the experiment and high in the last third), suggests growth during the first period when the reactor received little sulfate. The number of reads associated to *Methanosarcina* spp. was below that of the kitome in all samples from reactor 4, which received by far the highest total porewater volume (Table 1). Not taking into consideration gypsum dissolution as a source of sulfate, total H_2 to sulfate ratio in reactors 1 and 2 is above the expected stoichiometry (respectively 6.2:1 and 4.9:1 vs. 4:1, Table 1), meaning that

the sulfate provided could not have oxidized all H_2, pointing to CO_2 as a potential additional electron acceptor. Indeed, there is circumstantial evidence for hydrogenotrophic metabolism by members of *Methanosarcina* genus by the fact that its growth is localized at the point at which H_2 is delivered into reactor 2. In addition, the relative abundance of *Desulfocurvibacter* genus is lower than in reactors 1 and 4 at the same spot. Therefore, *Methanosarcina* genus is hypothesized to be outcompeted by SRB when sulfate is not limited but grow actively in case of sulfate depletion.

Representatives of Archaea have been detected in Opalinus Clay rock at very low abundances (Stroes-Gascoyne et al., 2011; Mitzscherling et al., 2023), and there is no direct evidence of their activity to date (Poulain, 2006; Stroes-Gascoyne et al., 2007; Vinsot et al., 2017). They are also found at extremely low abundance in borehole water (only the genus *Methanolobus* was detected) (Vinsot et al., 2014; Bagnoud et al., 2016a). This is likely due to the absence of an abundant electron donor and the abundance of sulfate, both of which favor SRB over methanogens. The higher substrate affinity of SRB to H_2 as compared to that of methanogens and homoacetogens accounts for SRB's competitive advantage (Kristjansson et al., 1982; Muyzer and Stams, 2008). When methanogens and SRB are present, the latter can maintain H_2 at a low steady-state concentration, at which methanogenesis is endergonic (Hoehler et al., 2001). In the subsurface, methanogen-, or methanogen/homoacetogen-dominated communities were detected in water with sulfate concentration around 1 mM (i.e., 15-fold lower than in Opalinus Clay porewater) (Kotelnikova and Pedersen, 1997, 1998; Chapelle et al., 2002). In the sand/bentonite backfill, methanogens could be indigenous to bentonite, as evidenced by the detection of methane during bentonite incubation (Maanoja et al., 2020). Unfortunately, phylogeny was not investigated in that work.

This result highlights that metabolisms other than sulfate reduction should be considered as microbial H_2 sinks in a DGR backfill.

5 Conclusion

This work demonstrates the natural occurrence of a hydrogenotrophic microbiome in a backfill-like porous material mimicking the one planned for the deep geological repository of radioactive waste in the Swiss concept. The origin of the microbiome, whether porewater, sand-bentonite or equipment, was not ascertained. The microbiome was dominated by sulfate reducers as sulfate was the main electron acceptor. In addition to the dissolved sulfate in the borehole porewater, the dissolution of gypsum from the backfill material provided substantial sulfate and was promoted by microbial activity. The sulfide formed was scavenged by iron. The rate of sulfate consumption was higher than in previous studies in a Opalinus Clay borehole, indicating that the backfill material provides a propitious environment for microbial growth and activity. The microbiome composition varied with the amount of water provided to the reactors. In the case of a low flow rate, methanogens were detected in the porous medium, and their activity was validated by the detection of methane. Hydrogenotrophy by methanogens was supported by their spatial localization, and increased abundance when fresh porewater was less available, creating zones of local sulfate depletion. This suggests that methanogens can outcompete sulfate reducers when sulfate is depleted.

Using sulfate consumption as a stoichiometric proxy for H_2 oxidation represents an underestimate of the H_2 oxidation rate: first, because the amount of sulfate present is underestimated due to gypsum dissolution; and second, because of the presence of other electron acceptors (e.g., ferric iron, inorganic carbon), and microorganism able of carrying out these other metabolisms. Direct quantification of H_2 oxidation will be required to build predictive models of the evolution of the gas phase in a DGR.

Data availability statement

The datasets generated and analyzed for this study can be found in the Zenodo repository using the following URL: https://zenodo.org/records/10352904.

Author contributions

CR: Methodology, Validation, Visualization, Writing – original draft, Writing – review & editing. NB: Conceptualization, Investigation, Methodology, Visualization, Writing – original draft, Writing – review & editing. OL: Conceptualization, Writing – review & editing. AB: Investigation, Writing – review & editing. MF: Investigation, Writing – review & editing. SW: Investigation, Writing – review & editing. NJ: Investigation, Writing – review & editing. RB-L: Conceptualization, Supervision, Writing – original draft, Writing – review & editing.

Funding

The author(s) declare financial support was received for the research, authorship, and/or publication of this article. The National Cooperative for the Disposal of Radioactive Waste (NAGRA), Wettingen, Switzerland, provided funding for this research.

Acknowledgments

We are thankful for the insightful discussion with Dr. Paul Wersin, University of Bern, about the fate of sulfide in bentonite. Furthermore, we would like to express our gratitude to the Mont Terri URL project partners and the helpful technical team at the site. Thanks also to the Crystal Growth Facility at EPFL for access to their X-ray fluorescence spectrometer and to the Blokesch Lab at EPFL for access to their quantitative PCR system. Finally, thanks to the Stanford Synchrotron Radiation Light source, and the Diamond Light Source, for their flexibility to enable the measurement of X-ray Absorption maps and spectra for respectively, iron, and sulfur, during the challenging times of a global pandemic crisis.

Conflict of interest

The authors declare that the research was conducted in the absence of any commercial or financial relationships that could be construed as a potential conflict of interest.

The author(s) declared that they were an editorial board member of Frontiers, at the time of submission. This had no impact on the peer review process and the final decision.

Publisher's note

All claims expressed in this article are solely those of the authors and do not necessarily represent those of their affiliated organizations, or those of the publisher, the editors and the reviewers. Any product that may be evaluated in this article, or claim that may be made by its manufacturer, is not guaranteed or endorsed by the publisher.

Supplementary material

The Supplementary material for this article can be found online at: https://www.frontiersin.org/articles/10.3389/fmicb.2024.1359677/full#supplementary-material

References

Andersen, K. S., Kirkegaard, R. H., Karst, S. M., and Albertsen, M. (2018). ampvis2: an R package to analyse and visualise 16S rRNA amplicon data. *bioRxiv*:299537. doi: 10.1101/299537

Andrews, S. (2019). *FastQC: A quality control tool for high throughput sequence data*. Available at: http://www.bioinformatics.babraham.ac.uk/projects/fastqc/

Bagnoud, A. (2015). *Microbial metabolism in the deep subsurface: Case study of Opalinus clay*, 189.

Bagnoud, A., Chourey, K., Hettich, R. L., de Bruijn, I., Andersson, A. F., Leupin, O. X., et al. (2016a). Reconstructing a hydrogen-driven microbial metabolic network in Opalinus clay rock. *Nat. Commun.* 7:12770. doi: 10.1038/ncomms12770

Bagnoud, A., de Bruijn, I., Andersson, A. F., Diomidis, N., Leupin, O. X., Schwyn, B., et al. (2016b). A minimalistic microbial food web in an excavated deep subsurface clay rock. *FEMS Microbiol. Ecol.* 92:fiv138. doi: 10.1093/femsec/fiv138

Bagnoud, A., Leupin, O., Schwyn, B., and Bernier-Latmani, R. (2016c). Rates of microbial hydrogen oxidation and sulfate reduction in Opalinus clay rock. *Appl. Geochem.* 72, 42–50. doi: 10.1016/j.apgeochem.2016.06.011

Basham, M., Filik, J., Wharmby, M. T., Chang, P. C. Y., El Kassaby, B., Gerring, M., et al. (2015). Data analysis Workbe Nch (DAWN). *J Synchrotron Rad* 22, 853–858. doi: 10.1107/S1600577515002283

Boylan, A. A., Perez-Mon, C., Guillard, L., Burzan, N., Loreggian, L., Maisch, M., et al. (2019). H2-fuelled microbial metabolism in Opalinus clay. *Appl. Clay Sci.* 174, 69–76. doi: 10.1016/j.clay.2019.03.020

Carlson, C. A., and Ingraham, J. L. (1983). Comparison of denitrification by Pseudomonas stutzeri, Pseudomonas aeruginosa, and Paracoccus denitrificans. *Appl. Environ. Microbiol.* 45, 1247–1253. doi: 10.1128/aem.45.4.1247-1253.1983

Chapelle, F. H., O'Neill, K., Bradley, P. M., Methé, B. A., Ciufo, S. A., Knobel, L. L., et al. (2002). A hydrogen-based subsurface microbial community dominated by methanogens. *Nature* 415, 312–315. doi: 10.1038/415312a

Chen, L., Larson, S. L., Ballard, J. H., Ma, Y., Zhang, Q., Li, J., et al. (2019). Laboratory spiking process of soil with various uranium and other heavy metals. *Methods X* 6, 734–739. doi: 10.1016/j.mex.2019.03.026

Cline, J. D. (1969). Spectrophotometric determination of hydrogen sulfide in natural waters. *Limnol. Oceanogr.* 14, 454–458. doi: 10.4319/lo.1969.14.3.0454

Diomidis, N., Cloet, V., Leupin, O. X., Marschall, P., Poller, A., and Stein, M. (2016). Production, consumption and transport of gases in deep geological repositories according to the Swiss disposal concept. *Radioactive Waste* 148:35.

Dohrmann, A. B., and Krüger, M. (2023). Microbial hydrogen consumption by a formation fluid from a natural gas field at high-pressure conditions relevant for underground hydrogen storage. *Environ. Sci. Technol.* 57, 1092–1102. doi: 10.1021/acs.est.2c07303

Duverger, A., Berg, J. S., Busigny, V., Guyot, F., Bernard, S., and Miot, J. (2020). Mechanisms of pyrite formation promoted by sulfate-reducing bacteria in pure culture. *Front. Earth Sci.* 8:588310. doi: 10.3389/feart.2020.588310

Edgar, R. C. (2016). SINTAX: a simple non-Bayesian taxonomy classifier for 16S and ITS sequences. *bioRxiv*. 074161. doi: 10.1101/074161

Engel, K., Coyotzi, S., Vachon, M. A., McKelvie, J. R., and Neufeld, J. D. (2019a). Validating DNA extraction protocols for bentonite clay. *mSphere* 4:4. doi: 10.1128/mSphere.00334-19

Engel, K., Ford, S. E., Coyotzi, S., McKelvie, J., Diomidis, N., Slater, G., et al. (2019b). Stability of microbial community profiles associated with compacted bentonite from the Grimsel underground research laboratory. *mSphere* 4:4. doi: 10.1128/mSphere.00601-19

Hedin, A. (1997). *Spent nuclear fuel – how dangerous is it?*

Hoehler, T. M., Alperin, M. J., Albert, D. B., and Martens, C. S. (2001). Apparent minimum free energy requirements for methanogenic Archaea and sulfate-reducing bacteria in an anoxic marine sediment. *FEMS Microbiol. Ecol.* 38, 33–41. doi: 10.1111/j.1574-6941.2001.tb00879.x

Karnland, O., Olsson, S., and Nilsson, U. (2006). *Mineralogy and sealing properties of various bentonites and smectite-rich clay materials*. TR-06-30.

Kotelnikova, S., and Pedersen, K. (1997). Evidence for methanogenic Archaea and homoacetogenic bacteria in deep granitic rock aquifers. *FEMS Microbiol. Rev.* 20, 339–349. doi: 10.1111/j.1574-6976.1997.tb00319.x

Kotelnikova, S., and Pedersen, K. (1998). Distribution and activity of methanogens and homoacetogens in deep granitic aquifers at Äspö hard rock laboratory, Sweden. *FEMS Microbiol. Ecol.* 26, 121–134. doi: 10.1111/j.1574-6941.1998.tb00498.x

Kristjansson, J. K., Schönheit, P., and Thauer, R. K. (1982). Different Ks values for hydrogen of methanogenic bacteria and sulfate reducing bacteria: an explanation for the apparent inhibition of methanogenesis by sulfate. *Arch. Microbiol.* 131, 278–282. doi: 10.1007/BF00405893

Leupin, O. (2016). *An assesment of the possible fate of gas generated in a repository for low- and intermediate-level waste*

Maanoja, S., Lakaniemi, A.-M., Lehtinen, L., Salminen, L., Auvinen, H., Kokko, M., et al. (2020). Compacted bentonite as a source of substrates for sulfate-reducing microorganisms in a simulated excavation-damaged zone of a spent nuclear fuel repository. *Appl. Clay Sci.* 196:105746. doi: 10.1016/j.clay.2020.105746

Madigan, M. T. S., Bender, K., Buckley, D. H., Sattlew, W. M., and Stahl, D. A. (2018). *Brock biology of microorganisms*. New York, Pearson: Global Edition.

Manca, D. (2016). *Gas transport and related chemo-hydro-mechanical response of sand bentonite mixture*

Mitzscherling, J., Genderjahn, S., Schleicher, A. M., Bartholomäus, A., Kallmeyer, J., and Wagner, D. (2023). Clay-associated microbial communities and their relevance for a nuclear waste repository in the Opalinus clay rock formation. *Microbiology Open* 12:e1370. doi: 10.1002/mbo3.1370

Muyzer, G., and Stams, A. J. M. (2008). The ecology and biotechnology of sulphate-reducing bacteria. *Nat. Rev. Microbiol.* 6, 441–454. doi: 10.1038/nrmicro1892

Poulain, S. (2006). *Caractérisation microbiologique de l'argile à Opalinus du Mont Terri et de l'argilite du Callovo-Oxfordien de Meuse/Haute-Marne*

Ravel, B., and Newville, M. (2005). ATHENA, ARTEMIS, HEPHAESTUS: data analysis for X-ray absorption spectroscopy using IFEFFIT. *J Synchrotron Rad* 12, 537–541. doi: 10.1107/S0909049505012719

Stookey, L. L. (1970). Ferrozine, a new spectrophotometric reagent for iron. *Anal. Chem.* 42, 779–781. doi: 10.1021/ac60289a016

Stroes-Gascoyne, S., Schippers, A., Schwyn, B., Poulain, S., Sergeant, C., Simonoff, M., et al. (2007). Microbial community analysis of Opalinus clay drill core samples from the Mont Terri underground research laboratory, Switzerland. *Geomicrobiol J.* 24, 1–17. doi: 10.1080/01490450601134275

Stroes-Gascoyne, S., Sergeant, C., Schippers, A., Hamon, C. J., Nèble, S., Vesvres, M.-H., et al. (2011). Biogeochemical processes in a clay formation in situ experiment: part D-microbial analyses – synthesis of results. *Appl. Geochem.* 26, 980–989. doi: 10.1016/j.apgeochem.2011.03.007

Thaysen, E., McMahon, S., Strobel, G., Butler, I., Ngwenya, B., Heinemann, N., et al. (2020). Estimating microbial hydrogen consumption in hydrogen storage in porous media as a basis for site selection. *Life Sci.* 23:e5hc7h. doi: 10.31223/X5HC7H

Vachon, M. A., Engel, K., Beaver, R. C., Slater, G. F., Binns, W. J., and Neufeld, J. D. (2021). Fifteen shades of clay: distinct microbial community profiles obtained from bentonite samples by cultivation and direct nucleic acid extraction. *Sci. Rep.* 11:22349. doi: 10.1038/s41598-021-01072-1

Vasil, M. L. (2007). How we learnt about iron acquisition in Pseudomonas aeruginosa: a series of very fortunate events. *Biometals* 20, 587–601. doi: 10.1007/s10534-006-9067-2

Vinsot, A., Appelo, C. A. J., Lundy, M., Wechner, S., Cailteau-Fischbach, C., De Donato, P., et al. (2017). Natural gas extraction and artificial gas injection experiments in Opalinus clay, Mont Terri rock laboratory (Switzerland). *Swiss J. Geosci.* 110, 375–390. doi: 10.1007/s00015-016-0244-1

Vinsot, A., Appelo, C. A. J., Lundy, M., Wechner, S., Lettry, Y., Lerouge, C., et al. (2014). In situ diffusion test of hydrogen gas in the Opalinus clay. *Geol. Soc. Lond., Spec. Publ.* 400, 563–578. doi: 10.1144/SP400.12

Weinstein, M. M., Prem, A., Jin, M., Tang, S., and Bhasin, J. M. (2019). FIGARO: An efficient and objective tool for optimizing microbiome rRNA gene trimming parameters. *BioRxiv*. 610394.

frontiers | Frontiers in Microbiology

TYPE Original Research
PUBLISHED 01 May 2024
DOI 10.3389/fmicb.2024.1384367

OPEN ACCESS

EDITED BY
Jeanette M. Norton,
Utah State University, United States

REVIEWED BY
Weidong Kong,
Chinese Academy of Sciences (CAS), China
Shuyidan Zhou,
Chinese Academy of Sciences (CAS), China

*CORRESPONDENCE
Xiawei Peng
✉ xiaweipeng@163.com

†These authors share first authorship

RECEIVED 09 February 2024
ACCEPTED 08 April 2024
PUBLISHED 01 May 2024

CITATION
Dong X, Chen M, Chen Q, Liu K, Long J, Li Y, Ren Y, Yang T, Zhou J, Herath S and Peng X (2024) Rare microbial taxa as the major drivers of nutrient acquisition under moss biocrusts in karst area.
Front. Microbiol. 15:1384367.
doi: 10.3389/fmicb.2024.1384367

Rare microbial taxa as the major drivers of nutrient acquisition under moss biocrusts in karst area

Xintong Dong[1†], Man Chen[1†], Qi Chen[1], Kangfei Liu[1], Jie Long[1], Yunzhou Li[1], Yinuo Ren[1], Tao Yang[1], Jinxing Zhou[2], Saman Herath[3] and Xiawei Peng[1,4,5*]

[1]College of Biological Sciences and Technology, Beijing Forestry University, Beijing, China, [2]Jianshui Research Station, School of Soil and Water Conservation, Beijing Forestry University, Beijing, China, [3]Department of Export Agriculture, Faculty of Animal Science and Export Agriculture, Uva Wellassa University, Badulla, Sri Lanka, [4]Beijing Key Laboratory of Food Processing and Safety in Forestry, Beijing Forestry University, Beijing, China, [5]National Engineering Laboratory for Tree Breeding, Beijing Forestry University, Beijing, China

Karst rocky desertification refers to the process of land degradation caused by various factors such as climate change and human activities including deforestation and agriculture on a fragile karst substrate. Nutrient limitation is common in karst areas. Moss crust grows widely in karst areas. The microorganisms associated with bryophytes are vital to maintaining ecological functions, including climate regulation and nutrient circulation. The synergistic effect of moss crusts and microorganisms may hold great potential for restoring degraded karst ecosystems. However, our understanding of the responses of microbial communities, especially abundant and rare taxa, to nutrient limitations and acquisition in the presence of moss crusts is limited. Different moss habitats exhibit varying patterns of nutrient availability, which also affect microbial diversity and composition. Therefore, in this study, we investigated three habitats of mosses: autochthonal bryophytes under forest, lithophytic bryophytes under forest and on cliff rock. We measured soil physicochemical properties and enzymatic activities. We conducted high-throughput sequencing and analysis of soil microorganisms. Our finding revealed that autochthonal moss crusts under forest had higher nutrient availability and a higher proportion of copiotrophic microbial communities compared to lithophytic moss crusts under forest or on cliff rock. However, enzyme activities were lower in autochthonal moss crusts under forest. Additionally, rare taxa exhibited distinct structures in all three habitats. Analysis of co-occurrence network showed that rare taxa had a relatively high proportion in the main modules. Furthermore, we found that both abundant and rare taxa were primarily assembled by stochastic processes. Soil properties significantly affected the community assembly of the rare taxa, indirectly affecting microbial diversity and complexity and finally nutrient acquisition. These findings highlight the importance of rare taxa under moss

crusts for nutrient acquisition. Addressing this knowledge gap is essential for guiding ongoing ecological restoration projects in karst rocky desertification regions.

KEYWORDS

land degradation, bryophytes, extracellular enzyme stoichiometry, assembly processes, co-occurrence networks

1 Introduction

Land degradation associated with karst rocky desertification is caused by both natural processes and human activities on a fragile karst background (Meng et al., 2021). Rocky desertification has become a challenge for the sustainable ecological development of Southwest China (Yang et al., 2022a). Moss biocrusts are crucial for reducing and preventing soil erosion on rock surfaces and for supporting the long-term viability of the vegetation restoration process (Kidron and Drahorad, 2022). On the other hand, the microbial community in these moss biocrusts plays a significant ecological role (Cheng et al., 2022). Therefore, it is essential to comprehend the functions and mechanisms of these microorganisms in ecological functions.

Moss biocrusts in the karst areas contain a large number of highly diverse microorganisms. Microbial diversity is a fundamental aspect of supporting the services provided by the soil ecosystem (Fanin et al., 2018). These communities are influential in processes such as the turnover of soil organic matter (SOM), soil carbon (C) sequestration, and water acquisition (Xiao and Veste, 2017). Essentially, the presence of abundant and diverse soil microorganisms, particularly in biocrusts, can greatly benefit various soil processes, especially those related to C and nitrogen (N) acquisition (Bhattacharyya and Furtak, 2022). During nutrient deficiencies, microorganisms obtain nutrients by increasing secretion of extracellular enzymes that decompose SOM (Cui et al., 2018). For example, in N-limited regions, it has been shown that soil organic N mineralization is related to soil extracellular N-acquisition enzymes (Xiao et al., 2021). These interactions between soil microbes and soil enzymes are essential for understanding nutrient limitations in land restoration in degraded areas (Liu et al., 2023).

Assembly processes of microbial communities play crucial roles in determining the rate and efficiency of microbial growth (Anthony et al., 2020). Community assembly arises from the interaction of deterministic factors such as heterogeneous selection, homogenous selection, and stochastic processes such as dispersion limitations and homogeneous dispersal (Xue et al., 2018). Assembly processes drive ecosystem functions (Knelman and Nemergut, 2014); they are mainly reflected in aspects such as climate regulation, nutrient cycle, and plant growth (Gao et al., 2020; Hartmann and Six, 2022). Stochastic processes could bring new species from the regional pool which carry traits affecting ecosystem functioning but are not present in the initial community. In this way, stochastic processes could enhance the effect of biodiversity on functions through sampling effects (Knelman and Nemergut, 2014). Meanwhile, microbial communities commonly display an inclined distribution of species abundance with a large proportion of rare taxa coexisting with a small number of abundant taxa (Lynch and Neufeld, 2015; Jia et al., 2018). Under low-salt-stress environments, the abundant taxa play an important role in stabilizing ecological networks. However, the role of rare taxa becomes more and more important when salt stress increases (Li et al., 2023). Furthermore, although rare taxa have a low abundance, they are highly diverse and have functional redundancy, such as nitrogen fixation, sulfur oxidation, and accelerating organic matter breakdown (Peter et al., 2011; Sauret et al., 2014; Hua et al., 2015). The community composition of rare taxa is more stable under the influence of climate change and other disturbances, such as copper stress, freeze-thaw, and mechanical disturbances (Pedrós-Alió, 2011). The role of abundant and rare microorganisms under moss crusts in karst areas remains poorly understood. The problem of nutrient limitation is more prominent in karst areas (Zhou et al., 2020). Researchers have highlighted the important role of abundant and rare taxa on nutrient acquisition. In the karst area, microbes under moss crusts show inconsistent assembly processes. Based on this background, understanding the contribution of abundant and rare taxa and to nutrient acquisition is essential concerning the restoration of karst areas. This knowledge can offer novel insights into the microorganisms under bryophytes in karst areas.

In the present study, we focused on three different moss habitats: (i) lithophytic moss crust of forest, (ii) autochthonal moss crusts of forest, and (iii) lithophytic moss crust of cliff. We used high-throughput amplicon sequencing based on 16S rRNA genes to evaluate the community structure and network stability of bacteria under moss crust. Enzyme stoichiometric analysis (EEA) was performed. We also studied the abundant and rare taxa assembly process and analyzed the links with soil physicochemical properties and nutrient acquisition. We hypothesized that (i) different bryophyte habitats lead to different soil properties and soil enzyme activities; (ii) the microbial response to nutrient restriction differs in the three habitats; and (iii) the assembly processes of abundant and rare microorganisms are inconsistent in different habitats. Bryophytes and microorganisms are closely linked, and this study also aimed to provide recommendations for the restoration of karst areas in Southwest China using bryophytes combined with associated microbes.

2 Materials and methods

2.1 Study sites and soil sampling

Soil samples were collected from Guiyang and Anshun, Guizhou Province, China (94°37′9″–103°31′9″ E, 36°56′9″–40°34′9″ N). In total, 36 soil samples under bryophytes were

collected from three different sites (site A, 11 samples from lithophytic moss crust under the forest; site B, 17 samples from autochthonal moss crusts under the forest; site C, 8 samples from lithophytic moss crust of cliff). The study area is situated in a warm and subtropical region characterized by a humid temperate landscape with a continental monsoon pattern. The annual average rainfall is 1,100 mm and the mean air temperature ranges from 15.3 to 19.8°C. There is very little soil under the lithophytic moss crust. We collected the soil using the five-point sampling method to be mixed together as a sample; samples from the same type of moss habitat were replications. There were 11 replications in site A, 17 replications in site B, and 8 replications in site C. The specific sampling method is as follows: for lithophytic moss crust, we used a sterile blade to shovel the moss crust tightly against the rock wall; then, we used a sterile brush to sweep the roots of the moss crust and collect the soil. For autochthonal moss crust, we randomly selected some 1 m × 1 m plots in the study area. The nearest distance between sampling points in the sample field was approximately 10 m, and the sampling depth of soil samples under the crust was 0–2 cm. The soil samples were sieved to a particle size of 2 mm eliminating any discernible roots or rock fragments. The soil samples were separated into three portions: the first portion was kept at a temperature of −80°C to extract microbial DNA from the soil; we put the second portion at a temperature of 4°C to measure the activity of soil enzymes within a week; and the third portion was dried in air for analysis physical and chemical properties of the soil.

2.2 Determination of soil physical and chemical properties

Soil pH and electrical conductivity (EC) were measured using a pH-EC meter in the soil: water (1:5) extraction solution. Soil moisture content was determined gravimetrically. Soil samples were extracted with 2 M KCl and ammonium and nitrate nitrogen (NH_4^+-N and NO_3^--N) were determined using an automatic flow injection analyzer (AutoAnalyzer-AA3, Sea Analytics, Norderstedt, Germany). Soil organic carbon (SOC) content was determined by the external heating method of $K_2Cr_2O_7$ (Rayment and Lyons, 2011). Additionally, a Hanon Kjeltec 9840 analyzer (K9840, Hanon, CHN) was used to identify soil total nitrogen (TN) while a microplate reader (Infinite M200PRO, Tecan, CH) was used to measure the total phosphorus (TP) in the soil. We used a 0.5 M $NaHCO_3$ solution and a microplate analyzer (Infinite M200PRO, Tecan, CH) to assess the available phosphorus (AP) for plants. Neutral ammonium acetate (1 M) was used to extract the soil available potassium (AK), and a flame spectrophotometer (FP6450, INESA, CHN) was used to measure the amount of AK.

2.3 Analysis of soil extracellular enzyme activity and the stoichiometry of extracellular enzymes

Quantification was made for the soil enzymes that are involved in carbon acquisition including α-1,4-glucosidase (AG), β-1,4-glucosidase (BG), xylosidase (XS), and β-D-cellobiohydrolase (CB); nitrogen acquisition enzymes including leucine aminopeptidase (LAP), and β-N-acetylglucosaminidase (NAG); phosphorus acquisition enzymes such as alkaline phosphatase (AP). The enzyme activities were evaluated using the microplate method described by Ai et al. (2012). All enzyme activities were standardized using *Z*-score to visually evaluate the differences between the three sites. We used **Eq. 1** to calculate the *Z*-score:

$$Z{-}score = x{-}\mu/\sigma \quad (1)$$

where x, μ, and σ represent individual activity, average activity, and standard deviation of activity, respectively.

Two methods were used to investigate the microbial limitations. The first method was generating a scatter plot of the eco-enzymatic stoichiometry. The *x*-axis was determined by (LAP + NAG) / AP while the *y*-axis was determined by BG / (LAP + NAG). This strategy was based on the guidelines provided by Sinsabaugh et al. (2009). In this plot, four distinct categories of resource limitations were observed, as determined by deviations from the expected enzyme ratio of C:N (1:1) or N:P (1:1) as presented by Sinsabaugh et al. (2009). The soil enzyme activity ratio were calculated using **Eqs 2–4**.

$$Soil\ enzyme\ C{:}N\ ratio = Ln(BG)/Ln\,(LAP + NAG) \quad (2)$$

$$Soil\ enzyme\ C{:}P\ ratio = Ln(BG)/Ln\,(AP) \quad (3)$$

$$Soil\ enzyme\ N{:}P\ ratio = Ln(LAP{+}NAG)/Ln\,(AP) \quad (4)$$

The second method was calculating the lengths and angles of the vectors for enzymatic activity to quantify the microbial nutrient limitation. The vector length indicates the relative microbial C limitation; the larger the vector length greater the relative microbial C limitation degree (Ma et al., 2021). The vector angle represents the soil relative microbial N (or P) limitation degree. Vector angles $<45°$ indicate microbial N limitation, while vector angles $>45°$ indicate microbial P limitation. The vector length and angle were calculated using **Eqs 5–8**.

$$X = (BG + CBH)/\,(BG + CB + AP) \quad (5)$$

$$Y = (BG + CBH)/(BG + CB + NAG + LAP) \quad (6)$$

$$Vector\ length = \sqrt{X^2 + Y^2} \quad (7)$$

$$Vector\ angle = Degree\,(ATAN2\,(X, Y)) \quad (8)$$

2.4 DNA extraction and sequencing data processing

DNA Isolation Kit, which is produced by MP Biomedicals in Switzerland, was used to extract DNA from 0.5 g of fresh soil samples. The extraction process followed the manufacturer's recommendations. The extracted DNA was assessed for its quality and quantity using a Nanodrop ND-2000 UV-vis spectrophotometer produced by Nanodrop Technologies in Wilmington, DE, USA. Primers 515F

(5′-GTGCCAGCMGCCGCGGTAA-3′) and 806R (5′-GGACTACHVGGGTWTCTAAT-3′) were used to enhance the bacterial 16S rRNA gene V4 hypervariable region (Dong et al., 2022). PCR reactions were performed in triplicate (S1000 apparatus, Bio-Rad Laboratory, Hercules, CA, USA). The PCR conditions were 5 min at 94°C followed by 30 cycles of 94°C for 45 s, annealing at 54°C for 45 s, 72°C for 1 min followed by a final extension step of 10 min at 72°C (Katiraei et al., 2022). PCR products were purified using the Qiagen Gel Extraction Kit produced by Qiagen in Germany, following the instructions provided by the manufacturer. In the end, the library was sequenced using an Illumina Nova6000 platform, which produced paired end reads of 250 base pairs. The sequencing procedure was conducted by Guangdong Magigene Biotechnology Co., Ltd., situated in Guangzhou, China.

2.5 Sequencing data processing

A series of standard processing steps, including demultiplexing, sample inference, read merging, quality filtering, and chimeric elimination, were applied to the raw FASTQ data. The DADA2 pipeline (version 1.20.0) was used to carry out these procedures. After that, an amplicon sequence variant (ASV) microbiological profile was generated (Deissová et al., 2023), ASVs with 100% sequence identity, which are more dependable and can be replicated, were employed to represent microbial taxonomic units. The Ribosomal Database Project (RDP) Classifier was utilized to determine the taxonomic details of every ASV,[1] with an 80% level of confidence (Matheri et al., 2023).

2.6 Statistics analysis

Depending on their relative abundance and/or frequency, the microbial ASVs were divided into two groups: abundant and rare taxa. Rare taxa were defined as those with an average relative abundance of <0.1%, whereas an average relative abundance of >1% was classified as abundant taxa (Galand et al., 2009). Based on the copiotrophic-oligotrophic framework and additional documentation, those annotated identified phyla into copiotrophic and oligotrophic taxa (Fierer et al., 2007; Li H. et al., 2021; Li J. et al., 2021). To calculate the microbial copiotroph:oligotroph ratios, the relative abundance of known copiotrophic and oligotrophic members were summed, respectively (Ma et al., 2023).

Also, we evaluated the α-diversity of the microbial community using the vegan package in R version 4.1.2. We employed canonical principal coordinates analysis (PCoA) to investigate the bacterial community's pattern (Cui et al., 2019). All networks were constructed based on Pearson correlations of log-transformed ASV abundances, followed by an RMT-based approach that determines the correlation cut-off threshold automatically (Yuan et al., 2021). The random forest tests in "RandomForest" package were used to forecast the significant factors (Chen et al., 2021). Additionally, the "rfPermute" package in R was used to analyze each predictor's significance (Jiao et al., 2018). To assess the ecological processes taking place in microbial communities, we calculated β Nearest Taxon Index (βNTI) (Stegen et al., 2012). Through the integration of |βNTI| (2) and |RCbray| (0.95), we successfully elucidated underlying mechanisms governing community assembly processes. These mechanisms encompass heterogeneous selection, homogeneous selection, dispersal limitation, homogenous dispersal, and undominated processes (Zhou and Ning, 2017). Mantel tests comparing βNTI values with the Euclidean distance matrixes of physicochemical parameters were then performed in the "vegan" R package to explore the major factors influencing the assembly of abundant and rare taxa, and the relationship among soil enzyme activity ratio and network complexity standardized by *Z*-scores. The direct and indirect effects between soil physical and chemical properties, assembly processes of abundant and rare microbial communities, microbial diversity, microbial complexity, and nutrient acquisition were identified using structural equation models (SEMs) created with the "lavaan" package in R software.

TABLE 1 The physicochemical properties of soil under bryophytes in different sites.

Physico-chemical properties	Site A	Site B	Site C
pH	7.74 ± 0.3a	7 ± 1.04b	7.98 ± 0.05a
EC (μS/cm)	153.71 ± 42.69b	133.91 ± 67.84b	271.63 ± 27.92a
SWC (%)	8.54 ± 3.22b	21.28 ± 6.06a	5.85 ± 1.24b
SOC (g/kg)	41.36 ± 17.08b	44.19 ± 27.23b	64.94 ± 13.87a
TN (g/kg)	4.16 ± 1.72a	3.59 ± 2.14a	5.09 ± 1.17a
NH_4^+-N (mg/kg)	38.43 ± 13.12a	47.08 ± 20.35a	40.38 ± 14.18a
NO_3^--N (mg/kg)	13.64 ± 10.06a	17.35 ± 9.89a	18.47 ± 9.97a
TP (g/kg)	0.99 ± 0.28a	0.58 ± 0.38b	0.66 ± 0.17b
A-P (mg/kg)	28.19 ± 16.33a	67.72 ± 103.04a	49.88 ± 19.6a
AK (mg/kg)	253.56 ± 51.49b	197.18 ± 61.61c	332.91 ± 47.44a

All values are reported as "mean @ standard deviation" based on measurement results for samples. The statistical differences in physicochemical properties within a row are indicated by different letters (one-way ANOVA, α = 0.05). pH, potential of hydrogen; EC, electric conductivity; SWC, soil water content; SOC, soil organic carbon; TN, soil total nitrogen; NH_4^+-N, soil ammonium; NO_3^--N, soil nitrate; TP, soil total phosphorus; A-P, soil available phosphorus; AK, soil available potassium.

3 Results

3.1 Enzyme activity and soil nutrient limitation in different habitats

The availability of SOC, NH_4^+-N, NO_3^--N, and A-P in site B was higher, but the enzyme activities were lower compared with sites A and C (**Table 1** and **Figure 1A**). The activity of BG, XS, NAG, and LAP showed significant differences in sites A and C ($P < 0.05$) (**Figure 1A**). The scatter plot of eco-enzymatic stoichiometry reveals that most microorganisms were limited by C&N and C&P (**Figure 1B**). Most microorganisms

1 https://sourceforge.net/projects/rdp-classifier/

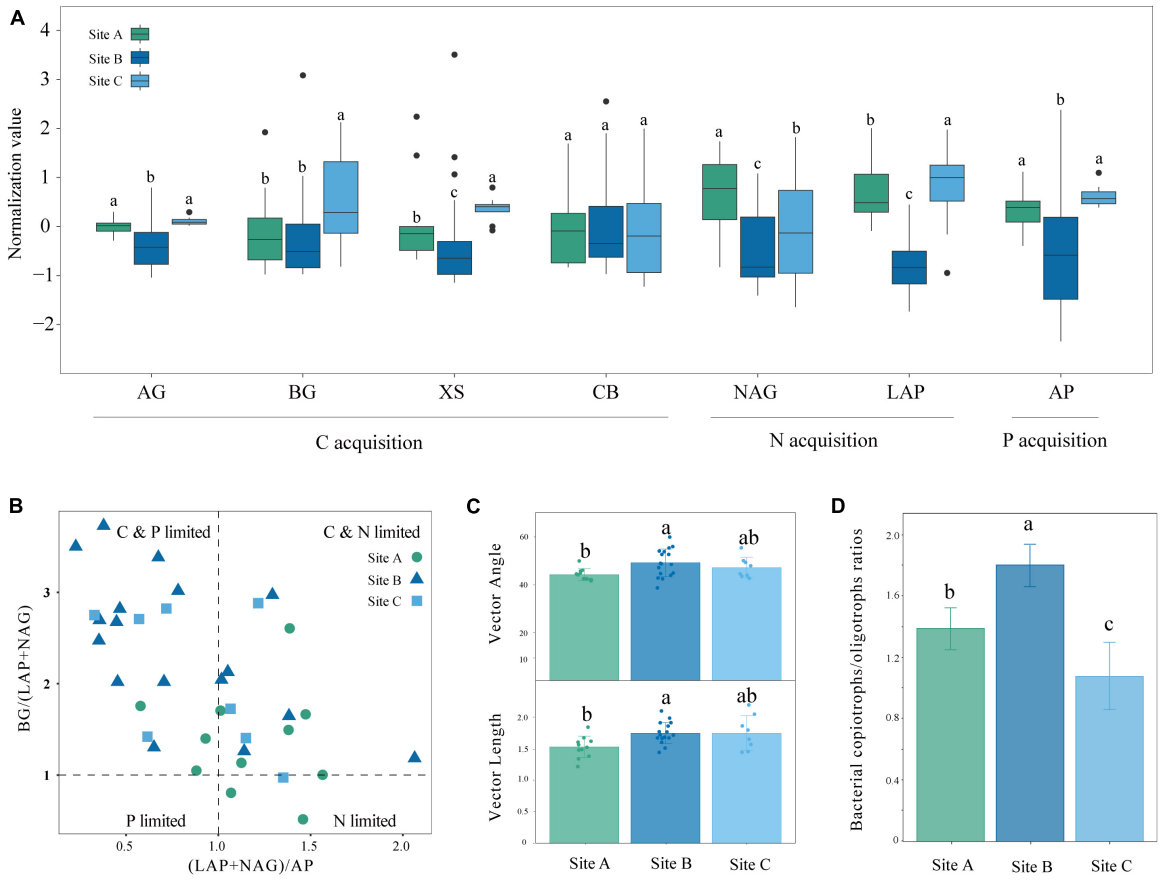

FIGURE 1
Enzyme activity and soil nutrient limitation in different moss biocrusts habitats: **(A)** soil enzyme activity of carbon, nitrogen, and phosphorus at three sites, **(B)** scatter plots of soil enzymatic stoichiometry for studied sites, **(C)** the vector length and vector angle of the studied sites, and **(D)** microbial copiotrophs and oligotrophic ratios at different sites. Different lowercase letters indicate significant differences among the three sites ($P < 0.05$). Different letters indicate statistically significant differences (one-way ANOVA, $\alpha = 0.05$). AG, α-glucosidase; BG, β-glucosidase; XS, xylosidase; CB, β-D-cellobiohydrolase; NAG, N-acetyl-β-D-glucosidase; LAP, leucine aminopeptidase; AP, alkaline phosphatase.

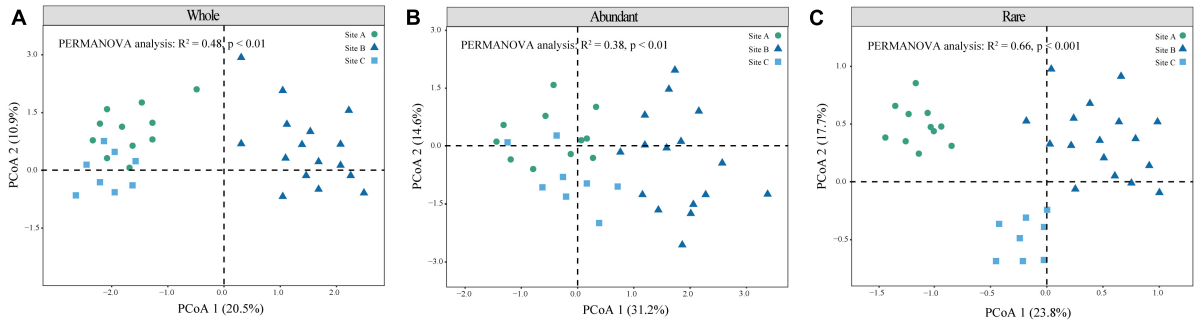

FIGURE 2
Microbial community structure of different moss crust habitats. Principal coordinate analysis (PCoA) of the whole **(A)**, abundant **(B)**, and rare **(C)** bacteria communities is given based on Bray–Curtis distances.

of the site A were limited by C&N, the microorganisms of sites B and C were susceptible to be limited by C&P (Figure 1B). Vector analysis showed that the site A had the lowest vector length among the three sites representing microbial C limitation. The vector angle at site A was below 45° whereas the vector angles at the other sites were above 45° (Figure 1C). Angles <45° are perceived as more constrained by N rather than P while the converse interpretation applies to angles >45°. This is consistent with the low content of SOC, NH_4^+-N, and NO_3^--N in site A (Table 1). The soil microorganisms at site B were predominantly characterized by the r-strategy species, as indicated by the largest copiotroph/oligotroph ratio (Figure 1D). The high ratio reflected a more nutrient-rich environment.

TABLE 2 The α-diversity (Shannon-index) in three sites.

Bacterial community	Site A	Site B	Site C
Whole	4.23 ± 0.39b	4.56 ± 0.62a	4.42 ± 0.59b
Abundant	3.13 ± 0.23b	3.56 ± 0.48a	3.42 ± 0.19ab
Rare	3.89 ± 0.46b	4.26 ± 0.72a	3.42 ± 0.38c

All values are reported as "mean ± standard deviation" based on measurement results for samples. The statistical differences in Shannon-index within a row are indicated by different letters (one-way ANOVA, α = 0.05).

3.2 Diversity and co-occurrence network of soil microbial communities

β-Diversity reflects differences in species composition between the three sites. The microbial community structures can be observed according to the principal coordinates analysis (PCoA), and permutational analysis of variance by Adonis. The results showed significance for the whole (R^2 = 0.48, P < 0.01), abundant (R^2 = 0.48, P < 0.01), and rare (R^2 = 0.66, P < 0.001) communities (Figures 2A–C). While the structure of the rare community was obviously differentiated in all three sites (Figure 2C). The Shannon index of site B was significantly higher than that of the other two sites (Table 2) (P < 0.05). The α-diversity of rare communities was significantly different in the three sites (P < 0.05); however, there was no significant difference between the site C and the other two sites in abundant communities (Table 2). We further analyzed the correlation between the Shannon index of abundant and rare taxa and soil C, N, and P and their stoichiometry (Supplementary Figures 1, 2) and observed a significant correlation between rare taxa diversity and soil C, N, and P nutrients (Supplementary Figures 1, 2). For example, the diversity of rare taxa was negatively correlated with SOC (R^2 = −0.38, P = 0.021), TN (R^2 = −0.52, P = 0.0012), and TP (R^2 = −0.4, P = 0.016). However, the diversity of abundant taxa

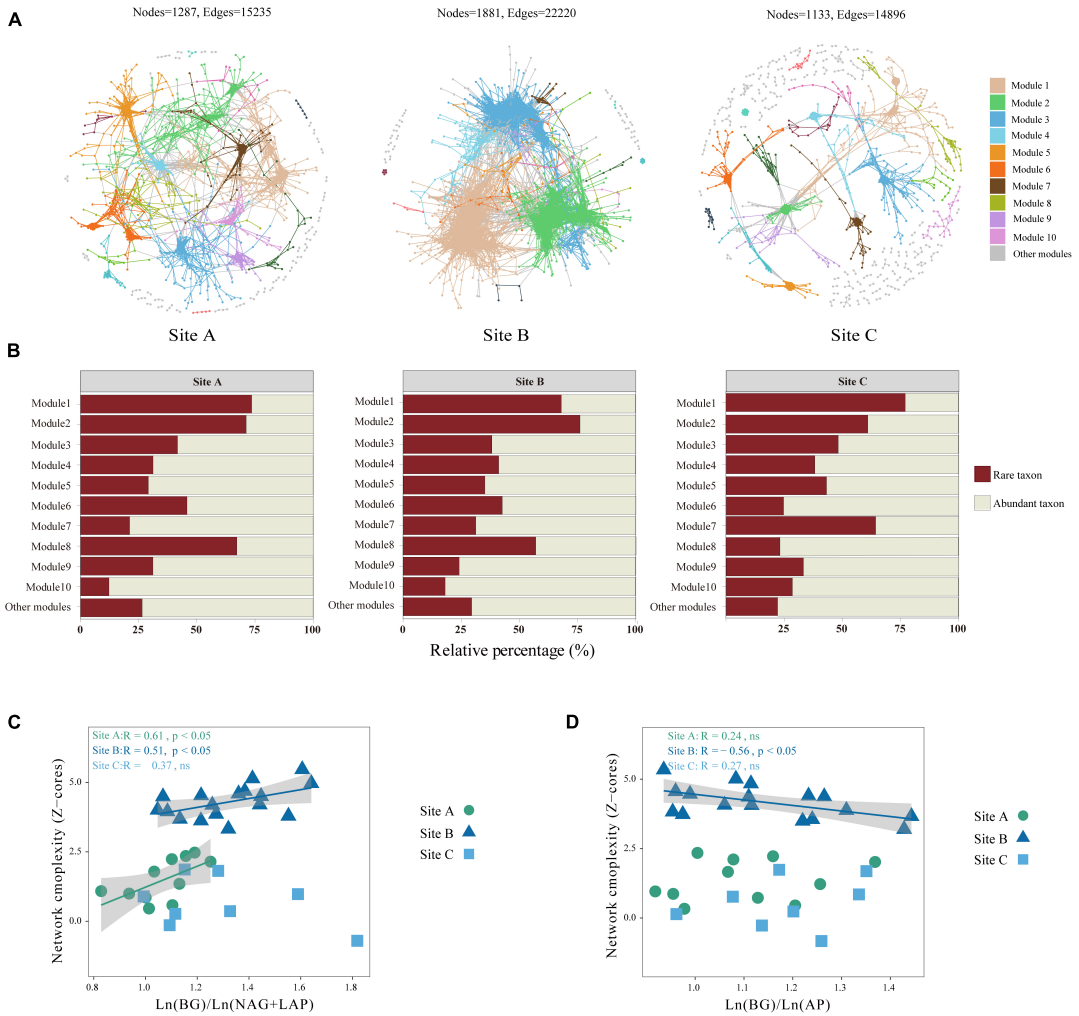

FIGURE 3
Co-occurrence pattern of bacteria in three sites: **(A)** the co-occurrence patterns among ASVs were revealed by network analysis. Large modules with ≥5 nodes are shown in different colors, and smaller modules are shown in gray. Details of network topological attributes are listed in Table 3: **(B)** ASVs abundance ratios of abundant and rare microorganisms in different modules; **(C)** relationships between network complexity standardized by Z-scores and Ln (BG)/Ln (NAG + LAP); and **(D)** relationships between network complexity standardized by Z-scores and Ln (BG)/Ln (AP). Different lowercase letters indicate significant differences among the three sites (P < 0.05). ns, not significant.

had no significant correlations with soil C, N, and P nutrients. Further, we analyzed the relationship between the dominant phyla of rare microorganisms and soil nutrients (Supplementary Figure 3), most of which showed negative correlation. There were significant negatively correlations between TN and *Acidobacteriota*, *Actinobacteriota*, *Bacteroidota*, and *Desulfobacterota* ($P < 0.05$), and significant positively correlations were observed between C:N ratio and *Bacteroidota* and *Chloroflexi* ($P < 0.05$). These bacterial groups play an important role in soil C, N, and P nutrient cycling.

Most network nodes and edges were available in site B, resulting in highly clustered microbial network modules. Site C has the simplest network structure (Figure 3A). We used the network topological parameters of node and edge numbers, average degree, diameter, average clustering coefficient, and relative modularity to assess soil microbial network complexity, with higher topological properties representing greater network complexity. In the three sites, the network topology parameters of the site B were higher than those of the other two sites (Table 3). The key modules of

TABLE 3 Topological properties of bacterial networks of three sites.

Topological properties	Site A	Site B	Site C
Node	1,287	1,881	1,133
Edges	15,235	22,220	14,896
Average degree	1.64	1.95	1.14
Diameter	10.46	13.54	9.57
Average clustering coefficient	0.38	0.45	0.26
Relative modularity	0.23	0.37	0.08

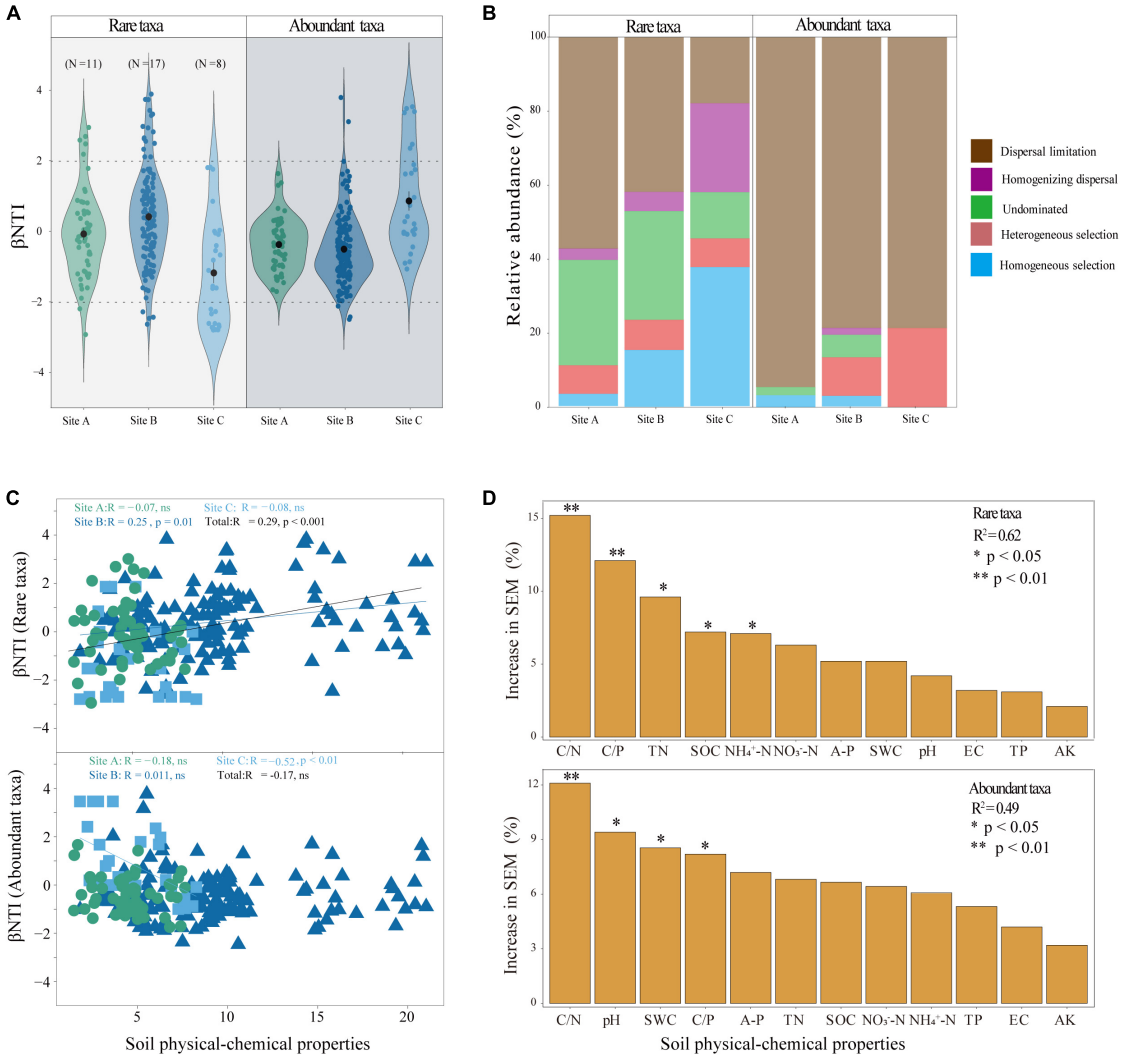

FIGURE 4
Assembly process and driving factors of abundant and rare taxa: **(A)** beta nearest taxon index (βNTI) value under different habitats. The horizontal dashed lines indicate the βNTI values of −2 and 2; **(B)** relative contribution of each ecological process to community assembly; **(C)** relationships between βNTI of the rare and abundant bacterial taxa and divergences of physical-chemical properties standardized; and **(D)** the random forest model identifies the major contributors to assembly processes of the abundant and rare taxa. ns, not significant. Asterisks denote significance levels. SWC, soil water content; EC, soil electric conductivity; TN, total nitrogen; AK, available potassium; A-P, available phosphorus; TP, total phosphorus; pH, potential of hydrogen; NO_3^--N, nitrate nitrogen; NH_4^+-N, ammonium nitrogen; SOC, soil organic carbon; C/N, the ratio of soil organic carbon and total nitrogen; C/P, the ratio of soil organic carbon and total phosphorus.

the microbial co-occurrence network (major microbial clusters, modules 1 and 2) in the three habitats were dominated by rare taxa (Figure 3B). Our results showed that there was a significant positive correlation between Ln (BG)/Ln (NAG + LAP) and network complexity in sites A and B ($P < 0.05$) (Figure 3C). This indicates that the microbial network complexity increased as N limitation decreased in sites A and B. Further, there was a significant negative correlation between Ln (BG)/Ln (AP) and network complexity in site B ($P < 0.05$) (Figure 3D). This indicated that the complexity of microbial network was positively related to the level of P limitation in the site B. There was no significant relationship between network complexity and enzyme activity ratio in site C (Figures 3C, D).

3.3 Assembly process and driving factors of abundant and rare taxa

In the three different habitats, most of the beta-nearest taxon index (βNTI) values of abundant taxa and rare taxa were between −2 and 2 indicating that the assembly process of abundant and rare taxa was dominated by stochastic processes (Figure 4A). However, the dispersal limitation of stochastic processes dominated the assembly of abundant taxa (Figure 4B). We observed that the assembly process of rare taxa was significantly ($P < 0.001$) correlated with the changes in soil physical and chemical properties (Figure 4C). To identify the potential main contributors to the assembly processes of abundant and rare taxa, we applied random forest analysis which demonstrated that C/N, C/P, TN, SOC, and NH_4^+-N were the significant impact factors in determining the rare taxa assembly process. C/N and C/P were significant factors ($P < 0.01$) (Figure 4D). Overall, C/N, pH, SWC, and C/P were the significantly impacting factors in determining the abundant taxa assembly process, and among them, C/N was significant ($P < 0.01$) (Figure 4D).

3.4 Microbial nutrient acquisition potential and driving factors

To explore the microbial factors that affect nutrient acquisition, we applied a random forest model. The random forest analysis revealed that network complexity, network modules α-diversity, and the ratio of copiotrophs and oligotrophs significantly affected nutrient acquisition in the whole microbial community. βNTI, β-diversity, and α-diversity significantly affected the nutrient acquisition of the rare microbial community. In the abundant microbial community, α-diversity significantly affected nutrient acquisition (Figure 5A). We further employed SEMs to explore the interaction influence between microbial factors by combining the physical and chemical properties of soil. The findings demonstrated that soil physicochemical properties had a significant effect on the assembly process of rare taxa leading to an increase in the complexity of the microbial network and diversity of community composition, and further stimulated nutrient acquisition (Figure 5B).

4 Discussion

4.1 Nutrient limitation on different bryophyte habitats

The availability of SOC, NH_4^+-N, NO_3^--N, and A-P in sites A and C were lower but the enzyme activities were higher than those of site B (Tables 1, 4 and Figure 1A). This confirms that when the nutrient availability of the soil is low, microbes secrete more enzymes to meet the demand for nutrients (Sinsabaugh et al., 2002; Fierer et al., 2009; Wallenius et al., 2011; Xu et al., 2017). Significant differences were observed between site A and site C in the activity of BG, XS, NAG, and LAP ($P < 0.05$) (Table 4 and Figure 1A). Although sites A and C were both lithophytic moss crust habitats, site A was situated under forests, while site C was on the cliff. The difference made site A susceptible to shade from forests and site C susceptible to direct sunlight, resulting in varying soil moisture and nutrient conditions at the two sites. Soil nutrients have a significant influence on enzyme activities (Meier et al., 2020; Li et al., 2022). The scatter plot with eco-enzymatic stoichiometry reveals that microbial limitations in C&P, and C&N were prevalent across all locations (Figure 1B). It has been suggested that microbial C limitation is widespread (Schimel, 2003). N and P are mainly released from the decomposition of SOM (Pan et al., 2016; Alewell et al., 2020). Therefore, P or N limitation often coexists with C limitation in the three sites. Compared with site C, site A was not susceptible to C&P limitation (Figures 1B, C). This may be due to the higher diversity of rare taxa in site A (Table 2). Rare taxa exhibit diverse functions (Sauret et al., 2014), including microorganisms that can solubilize phosphorus and accelerate the breakdown of organic matter.

Site B had the higher nutrient availability and highest microbial diversity (Tables 1, 2), yet was still susceptible to significant nutrient limitations (Figures 1B, C). This can be explained by the nutritional strategies of microorganisms. Nutritional strategies involve a basic trade-off between the rate of growth and the efficiency of resource utilization (Fierer et al., 2007; Ho et al., 2017), enabling us to establish a direct correlation between microbial performance and environmental conditions. The soil microorganisms at site B were predominantly characterized as r-strategists, as indicated by the largest copiotroph/oligotroph ratio (Figure 1D). The r-strategy species (copiotrophic species) have a fast growth rate and a rapid response to available C and nutrient inputs, typically flourishing in environments enriched in nutrients (Yang et al., 2022c). In contrast, k-strategy species (oligotrophic species) are slow-growing and more common in oligotrophic environments (Yang et al., 2022c). The high ratio of copiotrophs results in significant nutrient demand, contributing to higher levels of nutrient limitations (Giovannoni et al., 2014). This further explains nutrient limitations of C, N, and P in site B (Figures 1B, C).

4.2 Diversity and complexity of soil bacterial under bryophytes

Microbial diversity depends on the availability of resources (Zhu L. et al., 2023). Varying ecosystems exhibit distinct soil temperatures, moisture levels, pH levels, and nutrient content

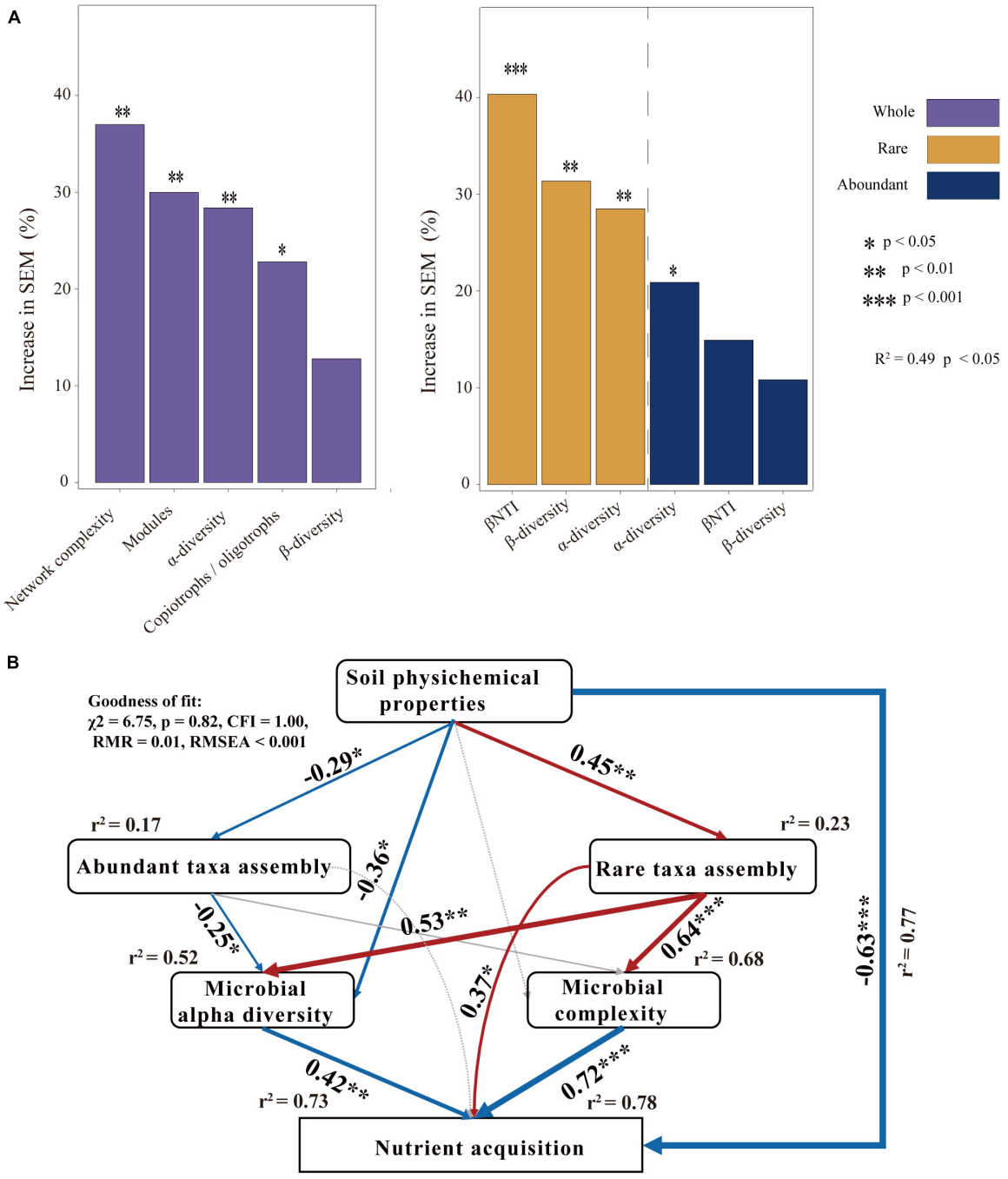

FIGURE 5
Analysis of factors affecting nutrient acquisition: **(A)** the random-forest model predicts the main factors for nutrient acquisition of bacterial communities and **(B)** structural equation model (SEM) revealing the direct and indirect effects of abundant taxon and rare taxon on nutrient acquisition. The numbers on the arrows are the path coefficients and are indicative of the standardized effect size of the relationship. Arrows in red and blue indicate positive and negative effects, respectively. R^2 means the proportion of variance explained.

which can influence the diversity and composition of soil microorganisms (Bahram et al., 2018). Site B had higher available nutrient content, such as NH_4^+-N, NO_3^--N, and A-P than the other two sites (**Table 1**). However, sites A and C were characterized by lithophytic moss environments that exhibited low nutrient levels and supported oligotrophic microorganisms. The copiotroph/oligotroph ratio also showed the nutrient availability in the three sites (**Figure 1D**). This further explains the effect of different bryophyte habitats on microbial diversity. In addition, the abundant and rare microbial diversity of the three sites also showed distinct differences, rare microbes show a higher diversity (**Table 2**). Qin et al. (2022) indicated that rare biosphere possesses higher taxonomic diversity. This depended on multiple ecological principles behind the assembly of microbial communities (Lynch and Neufeld, 2015). The tremendous diversity of the rare biosphere is subjected to more complicated ecological processes such as

speciation, drift, and extinction (Mo et al., 2018). Abundant communities have higher niche breadth and hence show strong resistance and adaptability to different environments, and spread in different ecosystems (Yang et al., 2022b). This explains the lack of clear structure of abundant communities in the three sites (**Figure 2B**). This study analyzed the relationship between abundant and rare microbial α-diversity and soil C, N, and P nutrients. There is usually a positive correlation between microbial diversity and soil nutrients (Chen et al., 2020); however, we found a negative relationship between diversity and soil nutrients in rare taxa (**Supplementary Figure 1**), inconsistent with previous findings. This can be explained by the competition for scarce nutrients occurs between bacteria and dominant plants, in nutrient-limited karst ecosystems (Wang et al., 2020). Furthermore, lower microbial metabolic activity may lead to the negative relationship between microbial diversity and soil nutrients (Hu et al., 2021). The karst rocky desertification ecosystem may have more dormant or inactive microorganisms, which explains that the metabolic activities of microorganisms are not strong, resulting in a slow turnover of resources. In addition, the soil C:N ratio in this study was much lower than the normal value, hindering the metabolic activities of soil microorganisms (Liu et al., 2018; Hu et al., 2021). Therefore, the dominant phyla of rare taxa were positively correlated with C/N, but negatively correlated with TN (**Supplementary Figure 3**). According to a previous study, there was a difference in structure and co-occurrence networks of the soil bacteria between different habitats (Zhong et al., 2022). Site B exhibited the highest complexity and community stability of the microbial network (**Figure 3A**). The complexity and stability of microbial networks are related to the network structure. As listed in **Table 3**, the network topology parameter of site B was the highest among the three sites. A previous study has reported a positive relationship between network complexity and microbial diversity (Ma et al., 2020). The microbial diversity at site B was also the highest (**Table 2**). We further found that rare taxa were the main component of microbial network modules 1 and 2 in the three sites (**Figure 3B**). The results indicated that rare taxa may play crucial roles in maintaining the structure of the co-occurrence network. Rare taxa form complex interactions and relationships with other taxa to maintain the network structure (Zhu M. et al., 2023; He et al., 2024). Reduced N limitation or enhanced P limitation increased microbial network complexity in site B (**Figures 3C, D**). Microorganisms in site B were more susceptible to P limitation than N limitation (**Figure 1B**). In this condition, soil microbial communities of site B can adapt their strategies in response to resource availability. Microbial strategies enhance their complexity to maintain a steady state (Yang et al., 2022c).

4.3 Factors of affecting nutrient acquisition

Community assembly describes how different ecological processes shape the composition and structure of microbial communities (Ning et al., 2024). Studying the effects of environmental factors on the assembly of microbial communities is critical to understanding microbial biodiversity and ecological function (Kang et al., 2023). The present study found that the community assembly of both abundant and rare microbes was mostly influenced by stochastic processes. Further, it was noted that the assembly process of abundant taxa was dominated by dispersal limitations of stochastic processes (**Figure 4B**). More individuals of abundant taxa are likely to be involved in dispersal events but vulnerable to physical barriers, distance and other factors (Liu et al., 2015). Diverse assembly processes contribute to the rare taxa (**Figure 4B**). Rare taxa occupy narrower niches, are closer in phylogenetic clustering, and are more likely to be filtered and dispersed by diverse assembly processes (He J. et al., 2022). Diverse assembly processes can drive high diversity and versatility of rare taxa (Zhou and Ning, 2017). From this perspective, the rare taxa may be the main driving force for maintaining ecosystem functional stability and diversity of the soil microbial communities (Gobet et al., 2012; Hugoni et al., 2013; Alonso-Sáez et al., 2015). Determining the elements that lead to the occurrence of different processes in the formation of microbial communities is essential in the study of community ecology. Prior studies have demonstrated a correlation between assembly processes and soil attributes such as pH and NH_4^+-N (Jiang et al., 2019; Wan et al., 2021). We found that soil C/N and C/P together significantly affected the community assembly of both abundant and rare taxa ($P < 0.05$) (**Figure 4D**). Especially, our findings indicated that TN, SOC and NH_4^+-N significantly influenced the assembly processes of the rare taxon. The assembly processes of the abundant taxa were significantly influenced by soil pH and SWC ($P < 0.05$) (**Figure 4D**). Soil C, N, and P are essential nutrients in soil ecosystems, and the stoichiometric ratio of soil C, N, and P affected the assembly process of microorganisms by affecting microbial investment in nutrient acquisition (Li J. et al., 2021; Xu et al., 2022; Duan et al., 2023). Therefore, both abundant and rare microbes were affected by soil C/N and C/P. It was worth distinguishing that abundant taxa were more susceptible to the non-nutrient properties of soil, such as pH and SWC. Soil pH and SWC can affect the cellular homeostasis of microorganisms and thus affect the exchange with external substances. The versatility of rare microbes allows for their ability to withstand substantial variances and be less affected by changes in environmental pH and SWC (He Z. et al., 2022). In total, the SEM demonstrated that the physical and chemical properties of soil mainly significantly affected the community assembly of the

TABLE 4 The soil enzyme activities in three sites.

Soil enzymes	Site A	Site B	Site C
AG (μmol/L)	14.47 ± 5.38a	12.41 ± 7.47b	18.14 ± 4.57a
BG (μmol/L)	49.18 ± 25.4ab	44.52 ± 27.55b	73.48 ± 32.85a
XS (U/g)	20.98 ± 11.57b	16.39 ± 13.8c	26.75 ± 3.76a
CB (U/g)	19.84 ± 13.5a	14.94 ± 9.12a	17.78 ± 13.51a
NAG (U/g)	27.75 ± 9.92a	16.76 ± 9.74c	21.43 ± 13.97b
LAP (U/g)	7.67 ± 2.44b	3.23 ± 1.84c	8.69 ± 2.97a
AP (g/kg)	40.19 ± 14.94a	34.48 ± 11.31b	47.72 ± 10.45a

All values are reported as "mean ± standard deviation" based on measurement results for samples. The statistical differences in soil enzyme activities within a row are indicated by different letters (one-way ANOVA, α = 0.05). AG, α-glucosidase; BG, β-glucosidase; XS, xylosidase; CB, β-D-cellobiohydrolase; NAG, N-acetyl-β-D-glucosidase; LAP, leucine aminopeptidase; AP, alkaline phosphatase.

rare taxa, indirectly affecting microbial diversity and complexity and finally nutrient acquisition (Figure 5B). This suggested that rare microbial taxa were major drivers of nutrient.

5 Conclusion

This study aimed to determine the response of microorganisms under moss crust to nutrient acquisition in karst area. There were nutrient limitations in the three habitats. Our study demonstrated that nutrient acquisition was mainly driven by microbial assembly, diversity, and complexity. The microbial diversity and complexity were higher in the autochthonal moss crust of forest compared to the lithophytic moss crust. The microbial responses were influenced by the specific habitats of bryophytes, especially differences in soil nutrients. To enhance the efficiency of ecological restoration initiatives in karst rocky desertification areas, it is imperative to understand the influence of soil microbial communities on ecosystem processes. Further, with a full understanding of local nutrient limitations, the practice of cultivating bryophytes alongside rare microorganisms serves as a significant approach to managing and mitigating the process of rocky desertification. By addressing these technological limitations, it is possible to enhance the effectiveness and precision of the restoration activities aimed at mitigating karst rocky desertification and land degradation.

Data availability statement

The datasets presented in this study can be found in online repositories. The names of the repository/repositories and accession number(s) can be found in the article/ Supplementary material.

Author contributions

XD: Conceptualization, Investigation, Methodology, Writing – original draft. MC: Conceptualization, Formal analysis, Investigation, Methodology, Writing – original draft. QC: Formal analysis, Software, Writing – review & editing. KL: Data curation, Methodology, Writing – review & editing. JL: Formal analysis, Software, Writing – review & editing. YL: Investigation, Methodology, Writing – review & editing. YR: Data curation, Investigation, Writing – review & editing. TY: Software, Writing – review & editing. JZ: Funding acquisition, Writing – review & editing. SH: Supervision, Writing – review & editing. XP: Funding acquisition, Supervision, Visualization, Writing – review & editing.

Funding

The author(s) declare financial support was received for the research, authorship, and/or publication of this article. This study was supported by the National Natural Science Foundation of China (31971729 and 31870707) and the Innovation and Entrepreneurship Training Program for College Students of Beijing Forestry University (S202310022059).

Conflict of interest

The authors declare that the research was conducted in the absence of any commercial or financial relationships that could be construed as a potential conflict of interest.

Publisher's note

All claims expressed in this article are solely those of the authors and do not necessarily represent those of their affiliated organizations, or those of the publisher, the editors and the reviewers. Any product that may be evaluated in this article, or claim that may be made by its manufacturer, is not guaranteed or endorsed by the publisher.

Supplementary material

The Supplementary Material for this article can be found online at: https://www.frontiersin.org/articles/10.3389/fmicb.2024.1384367/full#supplementary-material

References

Ai, C., Liang, G., Sun, J., Wang, X., and Zhou, W. (2012). Responses of extracellular enzyme activities and microbial community in both the rhizosphere and bulk soil to long-term fertilization practices in a fluvo-aquic soil. *Geoderma* 173, 330–338. doi: 10.1016/j.geoderma.2011.07.020

Alewell, C., Ringeval, B., Ballabio, C., Robinson, D. A., Panagos, P., and Borrelli, P. (2020). Global phosphorus shortage will be aggravated by soil erosion. *Nat. Commun.* 11:4546. doi: 10.1038/s41467-020-18326-7

Alonso-Sáez, L., Díaz-Pérez, L., and Morán, X. G. (2015). The hidden seasonality of the rare biosphere in coastal marine bacterioplankton. *Environ. Microbiol.* 17, 3766–3780. doi: 10.1111/1462-2920.12801

Anthony, M. A., Crowther, T. W., Maynard, D. S., Van Den Hoogen, J., and Averill, C. (2020). Distinct assembly processes and microbial communities constrain soil organic carbon formation. *One Earth* 2, 349–360. doi: 10.1016/j.oneear.2020.03.006

Bahram, M., Hildebrand, F., Forslund, S. K., Anderson, J. L., Soudzilovskaia, N. A., Bodegom, P. M., et al. (2018). Structure and function of the global topsoil microbiome. *Nature* 560, 233–237. doi: 10.1038/s41586-018-0386-6

Bhattacharyya, S. S., and Furtak, K. (2022). Soil–plant–microbe interactions determine soil biological fertility by altering rhizospheric nutrient cycling and biocrust formation. *Sustainability* 15:625. doi: 10.3390/su15010625

Chen, Q.-L., Ding, J., Zhu, D., Hu, H.-W., Delgado-Baquerizo, M., Ma, Y.-B., et al. (2020). Rare microbial taxa as the major drivers of ecosystem multifunctionality in long-term fertilized soils. *Soil Biol. Biochem.* 141:107686. doi: 10.1016/j.soilbio.2019.107686

Chen, Q.-L., Hu, H.-W., Yan, Z.-Z., Li, C.-Y., Nguyen, B. T., Sun, A.-Q., et al. (2021). Deterministic selection dominates microbial community assembly in termite mounds. *Soil Biol. Biochem.* 152:108073. doi: 10.1016/j.soilbio.2020.108073

Cheng, C., Li, Y., Long, M., Gao, M., Zhang, Y., Lin, J., et al. (2022). Moss biocrusts buffer the negative effects of karst rocky desertification on soil properties and soil microbial richness. *Plant Soil* 475, 163–168. doi: 10.1007/s11104-020-04602-4

Cui, Y., Bing, H., Fang, L., Wu, Y., Yu, J., Shen, G., et al. (2019). Diversity patterns of the rhizosphere and bulk soil microbial communities along an altitudinal gradient in an alpine ecosystem of the eastern Tibetan Plateau. *Geoderma* 338, 118–127. doi: 10.1016/j.geoderma.2018.11.047

Cui, Y., Fang, L., Guo, X., Wang, X., Zhang, Y., Li, P., et al. (2018). Ecoenzymatic stoichiometry and microbial nutrient limitation in rhizosphere soil in the arid area of the northern Loess Plateau, China. *Soil Biol. Biochem.* 116, 11–21. doi: 10.1016/j.soilbio.2017.09.025

Deissová, T., Zapletalová, M., Kunovský, L., Kroupa, R., Grolich, T., Kala, Z., et al. (2023). 16S rRNA gene primer choice impacts off-target amplification in human gastrointestinal tract biopsies and microbiome profiling. *Sci. Rep.* 13:12577. doi: 10.1038/s41598-023-39575-8

Dong, W., Yang, Q., George, T. S., Yin, H., Wang, S., Bi, J., et al. (2022). Investigating bacterial coupled assimilation of fertilizer-nitrogen and crop residue-carbon in upland soils by DNA-qSIP. *Sci. Total Environ.* 845:157279. doi: 10.1016/j.scitotenv.2022.157279

Duan, P., Fu, R., Nottingham, A. T., Domeignoz-Horta, L. A., Yang, X., Du, H., et al. (2023). Tree species diversity increases soil microbial carbon use efficiency in a subtropical forest. *Glob. Change Biol.* 29, 7131–7144. doi: 10.1111/gcb.16971

Fanin, N., Gundale, M. J., Farrell, M., Ciobanu, M., Baldock, J. A., Nilsson, M. C., et al. (2018). Consistent effects of biodiversity loss on multifunctionality across contrasting ecosystems. *Nat. Ecol. Evol.* 2, 269–278. doi: 10.1038/s41559-017-0415-0

Fierer, N., Bradford, M. A., and Jackson, R. B. (2007). Toward an ecological classification of soil bacteria. *Ecology* 88, 1354–1364. doi: 10.1890/05-1839

Fierer, N., Strickland, M. S., Liptzin, D., Bradford, M. A., and Cleveland, C. C. (2009). Global patterns in belowground communities. *Ecol. Lett.* 12, 1238–1249. doi: 10.1111/j.1461-0248.2009.01360.x

Galand, P. E., Casamayor, E. O., Kirchman, D. L., and Lovejoy, C. (2009). Ecology of the rare microbial biosphere of the Arctic Ocean. *Proc. Am. Natl. Sci. U. S.A.* 106, 22427–22432. doi: 10.1073/pnas.0908284106

Gao, G.-F., Peng, D., Tripathi, B., Zhang, Y., and Chu, H. (2020). Distinct community assembly processes of abundant and rare soil bacteria in coastal wetlands along an inundation gradient. *mSystems* 5:e01150-20. doi: 10.1128/mSystems.01150-20

Giovannoni, S. J., Cameron Thrash, J., and Temperton, B. (2014). Implications of streamlining theory for microbial ecology. *ISME J.* 8, 1553–1565. doi: 10.1038/ismej.2014.60

Gobet, A., Böer, S. I., Huse, S. M., Van Beusekom, J. E., Quince, C., Sogin, M. L., et al. (2012). Diversity and dynamics of rare and of resident bacterial populations in coastal sands. *ISME J.* 6, 542–553. doi: 10.1038/ismej.2011.132

Hartmann, M., and Six, J. (2022). Soil structure and microbiome functions in agroecosystems. *Nat. Rev. Earth Environ.* 4, 4–18. doi: 10.1038/s43017-022-00366-w

He, J., Zhang, N., Muhammad, A., Shen, X., Sun, C., Li, Q., et al. (2022). From surviving to thriving, the assembly processes of microbial communities in stone biodeterioration: A case study of the West Lake UNESCO World heritage area in China. *Sci. Total Environ.* 805:150395. doi: 10.1016/j.scitotenv.2021.150395

He, X., Xiao, X., Wei, W., Li, L., Zhao, Y., Zhang, N., et al. (2024). Soil rare microorganisms mediated the plant cadmium uptake: The central role of protists. *Sci. Total Environ.* 908:168505. doi: 10.1016/j.scitotenv.2023.168505

He, Z., Liu, D., Shi, Y., Wu, X., Dai, Y., Shang, Y., et al. (2022). Broader environmental adaptation of rare rather than abundant bacteria in reforestation succession soil. *Sci. Total Environ.* 828:154364. doi: 10.1016/j.scitotenv.2022.154364

Ho, A., Di Lonardo, D. P., and Bodelier, P. L. (2017). Revisiting life strategy concepts in environmental microbial ecology. *FEMS Microbiol. Ecol.* 93:fix006. doi: 10.1093/femsec/fix006

Hu, W., Ran, J., Dong, L., Du, Q., Ji, M., Yao, S., et al. (2021). Aridity-driven shift in biodiversity–soil multifunctionality relationships. *Nat. Commun.* 12:5350. doi: 10.1038/s41467-021-25641-0

Hua, Z.-S., Han, Y.-J., Chen, L.-X., Liu, J., Hu, M., Li, S.-J., et al. (2015). Ecological roles of dominant and rare prokaryotes in acid mine drainage revealed by metagenomics and metatranscriptomics. *ISME J.* 9, 1280–1294. doi: 10.1038/ismej.2014.212

Hugoni, M., Taib, N., Debroas, D., Domaizon, I., Jouan Dufournel, I., Bronner, G., et al. (2013). Structure of the rare archaeal biosphere and seasonal dynamics of active ecotypes in surface coastal waters. *Proc. Am. Natl. Sci. U.S.A.* 110, 6004–6009. doi: 10.1073/pnas.1216863110

Jia, X., Dini-Andreote, F., and Salles, J. F. (2018). Community assembly processes of the microbial rare biosphere. *Trends Microbiol.* 26, 738–747. doi: 10.1016/j.tim.2018.02.011

Jiang, Y., Song, H., Lei, Y., Korpelainen, H., and Li, C. (2019). Distinct co-occurrence patterns and driving forces of rare and abundant bacterial subcommunities following a glacial retreat in the eastern Tibetan Plateau. *Biol. Fertil.* 55, 351–364. doi: 10.1007/s00374-019-01355-w

Jiao, S., Chen, W., Wang, J., Du, N., Li, Q., and Wei, G. (2018). Soil microbiomes with distinct assemblies through vertical soil profiles drive the cycling of multiple nutrients in reforested ecosystems. *Microbiome* 6, 1–13. doi: 10.1186/s40168-018-0526-0

Kang, Y., Wu, H., Zhang, Y., Wu, Q., Guan, Q., Lu, K., et al. (2023). Differential distribution patterns and assembly processes of soil microbial communities under contrasting vegetation types at distinctive altitudes in the Changbai Mountain. *Front. Microbiol.* 14:1152818. doi: 10.3389/fmicb.2023.1152818

Katiraei, S., Anvar, Y., Hoving, L., Berbée, J. F., Van Harmelen, V., and Willems Van Dijk, K. (2022). Evaluation of full-length versus V4-region 16S rRNA sequencing for phylogenetic analysis of mouse intestinal microbiota after a dietary intervention. *Curr. Microbiol.* 79:276. doi: 10.1007/s00284-022-02956-9

Kidron, G. J., and Drahorad, S. L. (2022). Biocrust-induced extracellular polymeric substances are responsible for dune stabilization in the Negev. *Land. Degrad. Dev.* 33, 425–438. doi: 10.1002/ldr.4146

Knelman, J. E., and Nemergut, D. R. (2014). Changes in community assembly may shift the relationship between biodiversity and ecosystem function. *Front. Microbiol.* 5:424. doi: 10.3389/fmicb.2014.00424

Li, C., Jin, L., Zhang, C., Li, S., Zhou, T., Hua, Z., et al. (2023). Destabilized microbial networks with distinct performances of abundant and rare biospheres in maintaining networks under increasing salinity stress. *iMeta* 2:e79. doi: 10.1002/imt2.79

Li, H., Yang, S., Semenov, M. V., Yao, F., Ye, J., Bu, R., et al. (2021). Temperature sensitivity of SOM decomposition is linked with a K-selected microbial community. *Glob. Change Biol.* 27, 2763–2779. doi: 10.1111/gcb.15593

Li, J., Pei, J., Dijkstra, F. A., Nie, M., and Pendall, E. (2021). Microbial carbon use efficiency, biomass residence time and temperature sensitivity across ecosystems and soil depths. *Soil Biol. Biochem.* 154:108117. doi: 10.1016/j.soilbio.2020.108117

Li, M., You, Y., Tan, X., Wen, Y., Yu, S., Xiao, N., et al. (2022). Mixture of N2-fixing tree species promotes organic phosphorus accumulation and transformation in topsoil aggregates in a degraded karst region of subtropical China. *Geoderma* 413:115752. doi: 10.1016/j.geoderma.2022.115752

Liu, G., Wang, H., Yan, G., Wang, M., Jiang, S., Wang, X., et al. (2023). Soil enzyme activities and microbial nutrient limitation during the secondary succession of boreal forests. *Catena* 230:107268. doi: 10.1016/j.catena.2023.107268

Liu, L., Yang, J., Yu, Z., and Wilkinson, D. M. (2015). The biogeography of abundant and rare bacterioplankton in the lakes and reservoirs of China. *ISME J.* 9, 2068–2077. doi: 10.1038/ismej.2015.29

Liu, X., Zhang, W., Wu, M., Ye, Y., Wang, K., and Li, D. (2018). Changes in soil nitrogen stocks following vegetation restoration in a typical karst catchment. *Land. Degrad. Dev.* 30, 60–72. doi: 10.1002/ldr.3204

Lynch, M. D., and Neufeld, J. D. (2015). Ecology and exploration of the rare biosphere. *Nat. Rev. Microbiol.* 13, 217–229. doi: 10.1038/nrmicro3400

Ma, L., Zhang, J., Li, Z., Xin, X., Guo, Z., Wang, D., et al. (2020). Long-term phosphorus deficiency decreased bacterial-fungal network complexity and efficiency across three soil types in China as revealed by network analysis. *Appl. Soil Ecol.* 148:103506. doi: 10.1016/j.apsoil.2020.103506

Ma, S., Zhu, W., Wang, W., Li, X., and Sheng, Z. (2023). Microbial assemblies with distinct trophic strategies drive changes in soil microbial carbon use efficiency along vegetation primary succession in a glacier retreat area of the southeastern Tibetan Plateau. *Sci. Total Environ.* 867:161587. doi: 10.1016/j.scitotenv.2023.161587

Ma, Z., Zhang, X., Zheng, B., Yue, S., Zhang, X., Zhai, B., et al. (2021). Effects of plastic and straw mulching on soil microbial P limitations in maize fields: Dependency on soil organic carbon demonstrated by ecoenzymatic stoichiometry. *Geoderma* 388:114928. doi: 10.1016/j.geoderma.2021.114928

Matheri, F., Kambura, A. K., Mwangi, M., Ongeso, N., Karanja, E., Adamtey, N., et al. (2023). Composition, structure, and functional shifts of prokaryotic communities in response to co-composting of various nitrogenous green feedstocks. *BMC Microbiol.* 23:50. doi: 10.1186/s12866-023-02798-w

Meier, I. C., Tuckmantel, T., Heitkotter, J., Muller, K., Preusser, S., Wrobel, T. J., et al. (2020). Root exudation of mature beech forests across a nutrient availability gradient: The role of root morphology and fungal activity. *New Phytol.* 226, 583–594. doi: 10.1111/nph.16389

Meng, W., Dai, Q., Ren, Q., Tu, N., and Leng, T. (2021). Ecological stoichiometric characteristics of soil-moss C, N, and P in restoration stages of karst rocky desertification. *PLoS One* 16:e0252838. doi: 10.1371/journal.pone.0252838

Mo, Y., Zhang, W., Yang, J., Lin, Y., Yu, Z., and Lin, S. (2018). Biogeographic patterns of abundant and rare bacterioplankton in three subtropical bays resulting from selective and neutral processes. *ISME J.* 12, 2198–2210. doi: 10.1038/s41396-018-0153-6

Ning, D., Wang, Y., Fan, Y., Wang, J., Van Nostrand, J. D., Wu, L., et al. (2024). Environmental stress mediates groundwater microbial community assembly. *Nat. Microbiol.* 9, 490–501. doi: 10.1038/s41564-023-01573-x

Pan, F., Liang, Y., Zhang, W., Zhao, J., and Wang, K. (2016). Enhanced nitrogen availability in karst ecosystems by oxalic acid release in the rhizosphere. *Front. Plant Sci.* 7:687. doi: 10.3389/fpls.2016.00687

Pedrós-Alió, C. (2011). The rare bacterial biosphere. *Annu. Rev. Mar. Sci.* 4, 449–466. doi: 10.1146/annurev-marine-120710-100948

Peter, H., Beier, S., Bertilsson, S., Lindström, E. S., Langenheder, S., and Tranvik, L. J. (2011). Function-specific response to depletion of microbial diversity. *ISME J.* 5, 351–361. doi: 10.1038/ismej.2010.119

Qin, Z., Zhao, Z., Xia, L., Wang, S., Yu, G., and Miao, A. (2022). Responses of abundant and rare prokaryotic taxa in a controlled organic contaminated site subjected to vertical pollution-induced disturbances. *Sci. Total Environ.* 853:158625. doi: 10.1016/j.scitotenv.2022.158625

Rayment, G. E., and Lyons, D. J. (2011). *Soil chemical methods: Australasia*. Clayton, VIC: CSIRO publishing.

Sauret, C., Séverin, T., Vétion, G., Guigue, C., Goutx, M., Pujo-Pay, M., et al. (2014). Rare biosphere' bacteria as key phenanthrene degraders in coastal seawaters. *Environ. Pollut.* 194, 246–253.

Schimel, J. (2003). The implications of exoenzyme activity on microbial carbon and nitrogen limitation in soil: A theoretical model. *Soil Biol. Biochem.* 35, 549–563. doi: 10.1016/s0038-0717(03)00015-4

Sinsabaugh, R., Carreiro, M., and Repert, D. (2002). Allocation of extracellular enzymatic activity in relation to litter composition, N deposition, and mass loss. *Biogeochemistry* 60, 1–24. doi: 10.1023/A:1016541114786

Sinsabaugh, R. L., Hill, B. H., and Follstad Shah, J. J. (2009). Ecoenzymatic stoichiometry of microbial organic nutrient acquisition in soil and sediment. *Nature* 462, 795–798. doi: 10.1038/nature08632

Stegen, J. C., Lin, X., Konopka, A. E., and Fredrickson, J. K. (2012). Stochastic and deterministic assembly processes in subsurface microbial communities. *ISME J.* 6, 1653–1664. doi: 10.1038/ismej.2012.22

Wallenius, K., Rita, H., Mikkonen, A., Lappi, K., Lindström, K., Hartikainen, H., et al. (2011). Effects of land use on the level, variation and spatial structure of soil enzyme activities and bacterial communities. *Soil Biol. Biochem.* 43, 1464–1473. doi: 10.1016/j.soilbio.2011.03.018

Wan, W., Gadd, G. M., Yang, Y., Yuan, W., Gu, J., Ye, L., et al. (2021). Environmental adaptation is stronger for abundant rather than rare microorganisms in wetland soils from the Qinghai-Tibet Plateau. *Mol. Ecol.* 30, 2390–2403. doi: 10.1111/mec.15882

Wang, X., Li, F. Y., Wang, Y., Liu, X., Cheng, J., Zhang, J., et al. (2020). High ecosystem multifunctionality under moderate grazing is associated with high plant but low bacterial diversity in a semi-arid steppe grassland. *Plant Soil* 448, 265–276. doi: 10.1007/s11104-020-04430-6

Xiao, B., and Veste, M. (2017). Moss-dominated biocrusts increase soil microbial abundance and community diversity and improve soil fertility in semi-arid climates on the Loess Plateau of China. *Appl. Soil Ecol.* 117-118, 165–177. doi: 10.1016/j.apsoil.2017.05.005

Xiao, L., Liu, G., Li, P., and Xue, S. (2021). Ecological stoichiometry of plant-soil-enzyme interactions drives secondary plant succession in the abandoned grasslands of Loess Plateau, China. *Catena* 202:105302. doi: 10.1016/j.catena.2021.105302

Xu, Z., Wang, Y., Sun, D., Li, H., Dong, Y., Wang, Z., et al. (2022). Soil nutrients and nutrient ratios influence the ratios of soil microbial biomass and metabolic nutrient limitations in mountain peatlands. *Catena* 218:106528. doi: 10.1016/j.catena.2022.106528

Xu, Z., Yu, G., Zhang, X., He, N., Wang, Q., Wang, S., et al. (2017). Soil enzyme activity and stoichiometry in forest ecosystems along the North-South Transect in eastern China (NSTEC). *Soil Biol. Biochem.* 104, 152–163. doi: 10.1016/j.soilbio.2016.10.020

Xue, Y., Chen, H., Yang, J. R., Liu, M., Huang, B., and Yang, J. (2018). Distinct patterns and processes of abundant and rare eukaryotic plankton communities following a reservoir cyanobacterial bloom. *ISME J.* 12, 2263–2277. doi: 10.1038/s41396-018-0159-0

Yang, T., Chen, Q., Yang, M., Wang, G., Zheng, C., Zhou, J., et al. (2022a). Soil microbial community under bryophytes in different substrates and its potential to degraded karst ecosystem restoration. *Int. Biodeter. Biodegr.* 175:105493. doi: 10.1016/j.ibiod.2022.105493

Yang, Y., Dou, Y., Wang, B., Xue, Z., Wang, Y., An, S., et al. (2022c). Deciphering factors driving soil microbial life-history strategies in restored grasslands. *iMeta* 2:e66. doi: 10.1002/imt2.66

Yang, Y., Cheng, K., Li, K., Jin, Y., and He, X. (2022b). Deciphering the diversity patterns and community assembly of rare and abundant bacterial communities in a wetland system. *Sci. Total Environ.* 838:156334. doi: 10.1016/j.scitotenv.2022.156334

Yuan, M. M., Guo, X., Wu, L., Zhang, Y., Xiao, N., Ning, D., et al. (2021). Climate warming enhances microbial network complexity and stability. *Nat. Clim. Change* 11, 343–348. doi: 10.1038/s41558-021-00989-9

Zhong, Y., Sorensen, P. O., Zhu, G., Jia, X., Liu, J., Shangguan, Z., et al. (2022). Differential microbial assembly processes and co-occurrence networks in the soil-root continuum along an environmental gradient. *iMeta* 1:e18. doi: 10.1002/imt2.18

Zhou, J., and Ning, D. (2017). Stochastic community assembly: Does it matter in microbial ecology? *Microbiol. Mol. Biol. Rev.* 81, e00002–e00017. doi: 10.1128/mmbr.00002-17

Zhou, L., Wang, X., Wang, Z., Zhang, X., Chen, C., and Liu, H. (2020). The challenge of soil loss control and vegetation restoration in the karst area of southwestern China. *Int. Soil Water Conserv.* 8, 26–34. doi: 10.1016/j.iswcr.2019.12.001

Zhu, L., Chen, Y., Sun, R., Zhang, J., Hale, L., Dumack, K., et al. (2023). Resource-dependent biodiversity and potential multi-trophic interactions determine belowground functional trait stability. *Microbiome* 11:95. doi: 10.1186/s40168-023-01539-5

Zhu, M., Qi, X., Yuan, Y., Zhou, H., Rong, X., Dang, Z., et al. (2023). Deciphering the distinct successional patterns and potential roles of abundant and rare microbial taxa of urban riverine plastisphere. *J. Hazard.* 450:131080. doi: 10.1016/j.jhazmat.2023.131080

frontiers | Frontiers in Microbiology

TYPE Original Research
PUBLISHED 11 December 2024
DOI 10.3389/fmicb.2024.1428517

OPEN ACCESS

EDITED BY
Jeanette M. Norton,
Utah State University, United States

REVIEWED BY
Carl-Eric Wegner,
Heinrich Heine University of Düsseldorf, Germany
András Táncsics,
Hungarian University of Agricultural and Life Sciences, Hungary

*CORRESPONDENCE
Marcus A. Horn
✉ horn@ifmb.uni-hannover.de

†These authors have contributed equally to this work and share first authorship

RECEIVED 06 May 2024
ACCEPTED 29 November 2024
PUBLISHED 11 December 2024

CITATION
Kujala K, Schmidt O and Horn MA (2024) Synergy and competition during the anaerobic degradation of N-acetylglucosamine in a methane-emitting, subarctic, pH-neutral fen.
Front. Microbiol. 15:1428517.
doi: 10.3389/fmicb.2024.1428517

Synergy and competition during the anaerobic degradation of N-acetylglucosamine in a methane-emitting, subarctic, pH-neutral fen

Katharina Kujala[1†], Oliver Schmidt[2†] and Marcus A. Horn[3*]

[1]Water, Energy and Environmental Engineering Research Unit, University of Oulu, Oulu, Finland, [2]Department of Arctic and Marine Biology, UiT The Arctic University of Norway, Tromsø, Norway, [3]Institute of Microbiology, Leibniz University Hannover, Hannover, Germany

Peatlands are invaluable but threatened ecosystems that store huge amounts of organic carbon globally and emit the greenhouse gasses carbon dioxide (CO_2) and methane (CH_4). Trophic interactions of microbial groups essential for methanogenesis are poorly understood in such systems, despite their importance. Thus, the present study aimed at unraveling trophic interactions between fermenters and methanogens in a nitrogen-limited, subarctic, pH-neutral fen. *In situ* CH_4 emission measurements indicated that the fen is a source of CH_4, and that CH_4 emissions were higher in plots supplemented with ammonium compared to unsupplemented plots. The amino sugar N-acetylglucosamine was chosen as model substrate for peat fermenters since it can serve as organic carbon and nitrogen source and is a monomer of chitin and peptidoglycan, two abundant biopolymers in the fen. Supplemental N-acetylglucosamine was fermented to acetate, ethanol, formate, and CO_2 during the initial incubation of anoxic peat soil microcosms without preincubation. Subsequently, ethanol and formate were converted to acetate and CH_4. When methanogenesis was inhibited by bromoethanesulfonate, acetate and propionate accumulated. Long-term preincubation considerably increased CH_4 production in unsupplemented microcosms and microcosms supplemented with methanogenic substrates. Supplemental H_2-CO_2 and formate stimulated methanogenesis the most, whereas acetate had an intermediary and methanol a minor stimulatory effect on methane production in preincubated microcosms. Activity of acetogens was suggested by net acetate production in microcosms supplemented with H_2-CO_2, formate, and methanol. Microbial community analysis of field fresh soil indicated the presence of many physiologically unresolved bacterial taxa, but also known primary and secondary fermenters, acetogens, iron reducers, sulfate reducers, and hydrogenotrophic methanogens (predominately *Methanocellaceae* and *Methanoregulaceae*). Aceticlastic methanogens were either not abundant (*Methanosarcinaceae*) or could not be detected due to limited coverage of the used primers (*Methanotrichaceae*). The collective results indicate a complex interplay of synergy and competition between fermenters, methanogens, acetogens, and potentially iron as well as sulfate reducers. While acetate derived from fermentation or acetogenesis in this pH-neutral fen likely plays a crucial role as carbon source for the predominant hydrogenotrophic methanogens, it remains to be resolved whether acetate is also converted to CH_4 via aceticlastic methanogenesis and/or syntrophic acetate oxidation coupled to hydrogenotrophic methanogenesis.

KEYWORDS

N-acetylglucosamine, intermediary ecosystem metabolisms, anaerobic feed chain, intermediates, methyl-CoM-reductase genes, hydrogenase genes, microbial community

Introduction

Arctic and boreal peatlands are long-term carbon stores which have sequestered carbon dioxide (CO_2) over millennia, and as a consequence have accumulated thick organic layers that can span several meters (Tarnocai et al., 2009). Northern peatlands are considered especially affected by climate warming and may switch from net C sinks to net C sources if greenhouse gas (methane (CH_4) and CO_2) emissions exceed sequestration with climate warming and changes in precipitation (Gallego-Sala et al., 2018). Moreover, peatland carbon may be lost by leaching of organic matter into streams, lakes, and nearshore ocean systems that may substantially affect water quality and nutrient regimes of typically nutrient-limited aquatic systems in the Arctic (Limpens et al., 2008).

Microorganisms are drivers of greenhouse gas production and consumption in peatland ecosystems (Conrad, 1996; Kolb and Horn, 2012), and microbial activity thus determines whether peatlands are net sources or sinks for greenhouse gasses. In water-saturated anoxic peat with low availability of alternative electron acceptors such as nitrate or sulfate, mineralization of organic matter will be driven primarily by fermentations and methanogenesis (Limpens et al., 2008; Drake et al., 2009). Carbohydrate monomers like glucose, xylose, and N-acetylglucosamine (NAG), which are derived from complex polymers such as cellulose, hemicellulose, and chitin, respectively, are degraded via primary and secondary fermentations to alcohols, short chain fatty acids like acetate, formate or propionate as well as CO_2 and molecular hydrogen (H_2) (Drake et al., 2009). These fermentation products are eventually consumed by methanogens, which form CH_4 and CO_2 (Drake et al., 2009).

Chitin (a component of fungal cell walls and the exoskeleton of many invertebrates) is the second most abundant biopolymer on earth, and together with ligno-cellulose, the two refractory compounds constitute the main source of organic matter in wetlands (Mann, 1988; Mitsch, 1994). NAG is the single monomer of chitin, and it has been shown for anoxic river sediments that chitin-derived NAG is typically consumed by chitinolytic fermenters although many non-chitinolytic fermenters have the ability to degrade NAG as well under the premise that it becomes bioavailable (Gooday, 1994; Wörner and Pester, 2019). NAG is also a major monomer in peptidoglycan, a component of bacterial cell walls, and since dead microbial cells constitute an abundant and readily degradable source of organic carbon in peatlands, peptidoglycan-derived NAG can be assumed to be an important substrate for non-chitinolytic fermenters in these ecosystems (Pazos and Peters, 2019; Tveit et al., 2015).

Since NAG is an amino sugar, the decomposition of NAG-containing polymers from organic matter could be important for both carbon and nitrogen cycling in peatlands (Kang et al., 2005; Beier and Bertilsson, 2013). However, information on how NAG is fermented and what trophic links between NAG-consuming fermenters and methanogens exist in peatlands is scarce (Wüst et al., 2009).

Communities of methanogens in peatlands are typically dominated by hydrogenotrophic methanogens that use H_2 (and often also formate) as electron donor to reduce CO_2 to CH_4 and/or aceticlastic methanogens that split acetate into CH_4 and CO_2 (Kotsyurbenko et al., 2019; Bräuer et al., 2020). Methanol disproportionation to CH_4 and CO_2 or complete reduction to CH_4 with H_2 as electron donor are well known. Some peat methanogens utilize methanol, but it is considered to be less important for the overall CH_4 production in peatlands (Conrad, 2020). The methanogenic potentials and the contribution of hydrogenotrophic versus aceticlastic methanogenesis in peatlands are variable and depend on various factors such as temperature, pH, hydrology, and vegetation (Kotsyurbenko et al., 2007; Rooney-Varga et al., 2007; Hines et al., 2008; Conrad, 2020). As an example, the deposition of easily degradable organic carbon compounds from *Carex* roots especially during the growing season has been conceptualized to stimulate methanogenesis and favor aceticlastic methanogens in fens whereas hydrogenotrophic methanogenesis is often more important in acidic bogs covered predominately by *Sphagnum* mosses that generally produce less methane (Kelly et al., 1992; Kotsyurbenko et al., 2019). Furthermore, CH_4 production and the methanogenic communities in one peatland often change seasonally, with depth (i.e., the recalcitrance of the peat organic matter), and based on the microtopography of the sampling site (Galand et al., 2003; Reiche et al., 2008; Hodgkins et al., 2014; Zalman et al., 2018).

In the present study, NAG was chosen as an easily degradable model amino sugar substrate providing both organic carbon and nitrogen to stimulate primary fermentation processes and subsequent processes that are trophically linked to methanogenesis in Puukkosuo fen (Northern Finland), a nitrogen-limited, subarctic, meso-eutrophic and pH-neutral peatland dominated by *Carex* sedges and *Sphagnum* mosses (Palmer and Horn, 2015). The stimulatory effect of methanogenic substrates was evaluated to investigate potential bottle necks for the methanogens inhabiting the fen soil. In addition to soil incubation experiments, *in situ* measurements of CO_2 and CH_4 emissions as well as microbial community analysis of field fresh soil were performed to unravel bacterial taxa, methanogens and H_2-metabolizers present at Puukkosuo fen (Supplementary Figure S1).

Materials and methods

Sampling site and soil parameters

The study site, Puukkosuo fen, is located in northeastern Finland (66°22′38″N, 29°18′28″E; elevation 200 m NN). The mean annual air temperature and mean annual precipitation at the site are −0.43 ± 0.09°C and 772 ± 12 mm, respectively (average of years 1966–2011, measured at Oulanka research station). Puukkosuo fen is pH-neutral (pH ~ 6.9), meso-eutrophic and water saturated with a vegetation consisting mainly of mosses (*Sphagnum* spp.) and graminoids (e.g., *Carex* spp.). Four replicate soil cores from layers 0 to

20 cm were taken on July 28th, 2010. These four cores were pooled on site and mixed thoroughly. The mixed sample was divided into subsamples for incubation studies and molecular analyses, and the subsamples were transported on ice to the laboratory where they were stored at 4°C for up to 11 months for microcosm analyses or at −80°C for approximately 3 weeks for nucleic acid extractions. The sampled surface soil had a soil moisture content of 90%, soil carbon, soil nitrogen and the carbon-to-nitrogen ratio were 434 g kg_{DW}^{-1}, 29 g/kg_{DW}^{-1} and 15, respectively (Palmer and Horn, 2015).

Assessment of *in situ* gas emissions

In situ gas emissions of fen soil were determined by the closed-chamber technique as described previously (Palmer and Horn, 2015). Briefly, closed poly(methyl methacrylate) (PMMA) chambers were placed onto the soil surface and gas samples (5 mL per sampling timepoint) were taken from the chambers via gas outlets at 4 timepoints (0–3 h). Prior to installation of the chambers, plots were watered with 2 L fen porewater without supplements (control) and with 20 mM supplemented ammonium (4 replicate plots per treatment). Gas samples were injected into gas tight evacuated containers (Exetainers, Labco Limited, High Wycombe, UK), and CO_2 and CH_4 concentrations were determined using Hewlett-Packard 5980 series II gas chromatographs equipped with thermal conductivity and flame ionization detectors, respectively, as described in Küsel and Drake (1995).

Assessment of fermentation and methanogenesis potentials in soil microcosms

Two separate sets of anoxic microcosms experiments were conducted to assess fermentative and methanogenic potentials of the sampled surface soil (0–20 cm depth), respectively. All incubations were set up in triplicates of 1:10 dilutions of fen soil (20 g soil +180 mL anoxic water or 10 g of soil +90 mL of anoxic water) in gas-tight 0.5 L infusion flasks (Müller & Krempel, Bülach, Switzerland) that were sealed with screw caps and rubber stoppers (Glasgerätebau Ochs, Bovenden, Germany). Headspaces were flushed with sterile argon. For the fermentation potential experiments, the following treatments were set up in May 2011 and incubated at 20°C in the dark for 10 days: (i) unsupplemented control microcosms, (ii) microcosms supplemented with 500 µM N-acetylglucosamine (NAG), (iii) microcosms with 500 µM NAG and bromoethanesulfonate (BES; 20 mM), and (iv) unsupplemented control microcosms with BES. In the latter two microcosms, BES was used as an inhibitor for methanogenesis (Oremland and Capone, 1988), thus allowing for the detection of fermentation products that might be used by methanogens in microcosms without BES. Fermentation potentials were tested without preincubation of the microcosms. Net turnover of carbon and reductant for the time frames day 0–4, 4–10, and 0–10 was calculated as follows: The initial concentrations of compounds measured at the beginning of a time frame were subtracted from final concentrations measured at the end of a time frame in both, NAG treatments and unsupplemented controls. Then, the resulting concentrations in unsupplemented controls with and without BES were subtracted from those in NAG supplemented microcosms with and without BES, respectively, to get net turnover concentrations for each compound. Finally, net turnover concentrations of compounds were multiplied with 8/32 for NAG, 1/2 for formate, 2/12 for ethanol, 2/8 for acetate, 3/14 for propionate, 1/8 for methane, and 1/0 for CO_2 to get net turnovers of carbon/reductant for each compound. Positive and negative values indicate net production and consumption of a compound in a given time frame, respectively.

For the methanogenic potential experiments, one subset of microcosms was set up in May 2011 and preincubated for 120 days at 20°C in the dark, and a second subset of microcosms was set up in July 2011 without preincubation. The preincubation served to reduce potentially existing alternative electron acceptors in the soil and thus stimulate peat methanogens. 1 mM formate, 1 mM acetate, 1 mM methanol or 8 vol % H_2 (i.e., 8.4 mmol L^{-1} microcosm slurry) and 2 vol % CO_2 (i.e., 2.1 mmol L^{-1} microcosm slurry) were supplemented at the beginning of the main incubation, which was 11 days at 20°C in the dark. Methanogenic substrates were resupplemented after 8 days of incubation (note that formate was not resupplemented in preincubated microcosms initially supplemented with formate). In addition to microcosms supplemented with potential methanogenic substrates, unsupplemented control microcosms with or without 20 mM BES were set up (note that BES was added at the beginning of the preincubation for the respective control of the preincubated microcosms).

Microcosms' headspaces and liquid phases were sampled in 1–2 day intervals. Concentrations of CH_4 and CO_2 in gas samples were analyzed with a gas chromatograph (Hewlett Packard 5890 series II equipped with FID or TCD detector); reliable concentrations of H_2 could not be quantified due to technical problems; concentrations of sugars, organic acids, and alcohols in liquid samples were analyzed via high pressure liquid chromatography equipped with an Aminex HPX-87H ion exclusion column and refractive index and UV detectors (Küsel and Drake, 1995). Amounts of gaseous and dissolved compounds in microcosms are given as µM concentrations and can be converted to µmol per g dry weight of soil by dividing with a conversion factor of 10.5.

Molecular characterization of fen bacteria, hydrogen metabolizers, and methanogens

Nucleic acids were extracted from a single replicate of fresh homogenized pooled surface layer fen soil as previously described using a bead-beating protocol (Peršoh et al., 2008; Palmer and Horn, 2015). Bacterial 16S rRNA genes as well as the functional gene markers *mcrA*, [FeFe]-hydrogenase and group 4 [NiFe]-hydrogenase genes were amplified using the primer pairs 341F (5′-CCT ACG GGA GGC AGC AG-3′)/907RM (5′-CCG TCA ATT CMT TTG AGT TT-3′) (Muyzer et al., 1993), ME1 (5′-GCM ATG CAR ATH GGW ATG TC-3′)/ME2 (5′-TCA TKG CRT AGT TDG GRT AGT-3′) (Hales et al., 1996), NiFe-gF (5′-GAY CGI RTI TGY GGI ATY TGY GG-3′)/NiFe-gR (5′-GTR CAI GAR TAR CAI GGR TC-3′), and HydH1f (5′-TIA CIT SIT GYW SYC CIG SHT GG-3′)/HydH3r (5′-CAI CCI YMI GGR CAI SNC AT-3′) (Schmidt et al., 2010, 2011), respectively. Each primer was preceded by a 6-bp-long barcode (5′-ACTATC - gene specific primer-3′), to allow for separation of target sequences after batch sequencing as the sequencing run also

included samples that were not part of the present study. Barcoded amplicon pyrosequencing of PCR products was conducted in 2011 as previously described at the Göttingen Genomics Laboratory using the Roche GS-FLX 454/Titanium technology (Palmer et al., 2012; Palmer and Horn, 2015). Sequence analysis of forward reads was done at a later date in QIIME 2 version 2022.2.0 (Bolyen et al., 2019). Imported sequences were demultiplexed using the q2-cutadapt plugin version 2022.2.0 by searching for the barcode + primer with a maximum error rate of 0.1 and removing them as a well as any preceding bases (Martin, 2011).

Quality controlled amplicon sequence variants (ASVs) were generated using the q-dada2 plugin for 454 sequencing ("denoise-pyro"; Callahan et al., 2016) with the following parameters: Sequences were trimmed to a length of 300 bp ("—p-trunc-len" 300), excluding any shorter sequences, and the "consensus" method was used for chimera detection and removal. Taxonomic assignment of ASVs was conducted by subjecting ASVs representative sequences of 16S rRNA gene and functional gene amplicons to a BLAST search of nucleotide (BlastN) and *in silico* translated protein sequences (BlastX), respectively, to identify the most closely related cultured relatives for each sequence (Altschul et al., 1990). Alpha diversity metrics [observed ASVs, Faith phylogenetic diversity (Faith, 1992), Shannon diversity (Shannon, 1948)] were calculated for reads subsampled at different sequencing depths using the "alpha-rarefaction" command of the q2-diversity plugin version 2022.2.0 in QIIME 2. Amplicon sequence reads have been deposited in the European Nucleotide Archive (ENA) under accession number PRJEB58427.

Results

In situ CO_2 and CH_4 emissions

In Puukkosuo fen, CO_2 and CH_4 emissions of plots irrigated with unamended porewater were approx. 400 µmol m^{-2} h^{-1} and 35 µmol m^{-2} h^{-1}, respectively (Figures 1A,B). Amendment with ammonium affected CO_2 and CH_4 emissions: Both CO_2 and CH_4 emissions were higher from plots with ammonium amendment, indicating that ammonium might stimulate methanogenesis as well as general microbial activity via alleviation of nitrogen limitation. The resulting CO_2:CH_4 ratios were approx. 12.5 and 18 for unamended and ammonium amended plots, respectively (Figure 1C).

Phylogenetic and functional diversity of microorganisms in field-fresh fen soil

Amplicon pyrosequencing of bacterial 16S rRNA genes yielded a total of 3,459 quality filtered reads forming 239 ASVs. Alpha diversity parameters indicated that the sequencing depth was sufficient to cover most of the bacterial diversity present in the fen (Supplementary Figure S2). Blast search revealed low (<90%) identity of some ASV representatives to sequences of cultured representatives (Supplementary Table S1), indicating that there is a high degree of uncultured bacterial diversity in Puukkosuo fen. The bacterial community was dominated by *Proteobacteria*, *Actinobacteriota, Acidobacteria* and *Firmicutes* (Figure 2A), microbial taxa that are commonly found to be abundant in peatlands (Pankratov et al., 2005; Dedysh, 2011; Tveit et al., 2013). Some of the detected ASVs were affiliated to genera known to comprise fermenters (e.g., *Clostridium*, *Pelosinus*, *Opitutus,* and *Spirochaeta*), acetogens (*Clostridium*), iron reducers (e.g., *Acidithermonas*, *Anaeromyxobacter*, and *Geobacter*), and sulfate reducers (e.g., *Desulfosporosinus* and *Desulfomonile*) (Supplementary Table S1).

Nine hundred and eighty-one quality-filtered [FeFe]-hydrogenase reads were obtained which grouped into 58 ASVs (see Supplementary Figure S3 for alpha diversity plots). Identities of ASV representative sequences to sequences of the next cultured representatives ranged between 56 and 89% (Supplementary Table S1). Based on a previously established family-level hydrogenase amino acid sequence similarity cut-off of 80% (Schmidt et al., 2011), 82% of the [FeFe]-hydrogenase reads could be affiliated to the *Dysgonomonadaceae*, a family harboring propionate fermenters that can degrade carbohydrates and/or proteins (Hahnke et al., 2016) (Figure 2A). Other [FeFe]-hydrogenase ASVs with low relative abundance had identities above or next to 80% to known syntrophic fermenters (*Syntrophus* and *Smithella*), sulfate reducers (*Desulfovirgula*), and iron reducers (*Mesoterricola*) (de Bok et al., 2001; Kaksonen et al., 2007; James et al., 2016; Itoh et al., 2023) (Supplementary Table S1). Several ASVs were only distantly related (<70% identity) to hydrogenases of cultured bacteria (Supplementary Table S1), and an adequate phylogenetic or functional affiliation of such essentially novel [FeFe]-hydrogenases is not possible.

Two hundred and sixty quality-filtered reads were obtained for group 4 [NiFe]-hydrogenase genes, and it is likely that such low sequencing depth was insufficient to capture the full diversity of group 4 [NiFe]-hydrogenase genes. However, flattening out rarefaction curves indicated that the 20 ASVs that were detected largely represent the hydrogenase diversity that could be amplified with the used primer pair, which was originally designed to detect group 4 [NiFe]-hydrogenases of *Gammaproteobacteria* (Schmidt et al., 2011) (Supplementary Figure S4). Identities of ASV representative sequences to sequences of the next cultured representatives ranged from 68 to 86% (Supplementary Table S1). About one half of the group 4 [NiFe]-hydrogenase reads were affiliated to the *Enterobacterales*-families *Budviciaceae* and *Enterobacteriaceae* that harbor facultative aerobes performing mixed acid fermentation under anoxic conditions (Brenner and Farmer, 2005; Adeolu et al., 2016) (Figure 2A). Most of the remaining group 4 [NiFe]-hydrogenase reads formed three ASVs with 71% identity to the H_2-oxidizing sulfate reducer *Thermodesulfovibrio thiophilus* (Supplementary Table S1); however, due to the relatively low identity, a closer phylogenetic and functional affiliation of the detected hydrogenases remains elusive.

For *mcrA*, 1,661 quality-filtered reads were obtained, which grouped into 37 ASVs (see Supplementary Figure S5 for alpha diversity plots). Most of the *mcrA* reads were affiliated either to the *Methanoregulaceae* (44% relative abundance) or the *Methanocellaceae* (52% relative abundance; Figure 2B). Both families comprise hydrogenotrophic methanogens that can be commonly found in peatlands or other wetlands (Oren, 2014a; Sakai et al., 2014). Notably, only one ASV (mcrA-fw-33; 1% relative abundance) was affiliated with the *Methanosarcinaceae*, a family that comprise many aceticlastic methanogens (note that the closest cultured relative, *Methanosarcina lacustris* (81% identity), does not utilize acetate as a growth substrate) (Oren, 2014b). None of the ASVs was affiliated with *Methanothrix* (formerly *Methanosaeta*), a genus comprising exclusively aceticlastic methanogens that have been

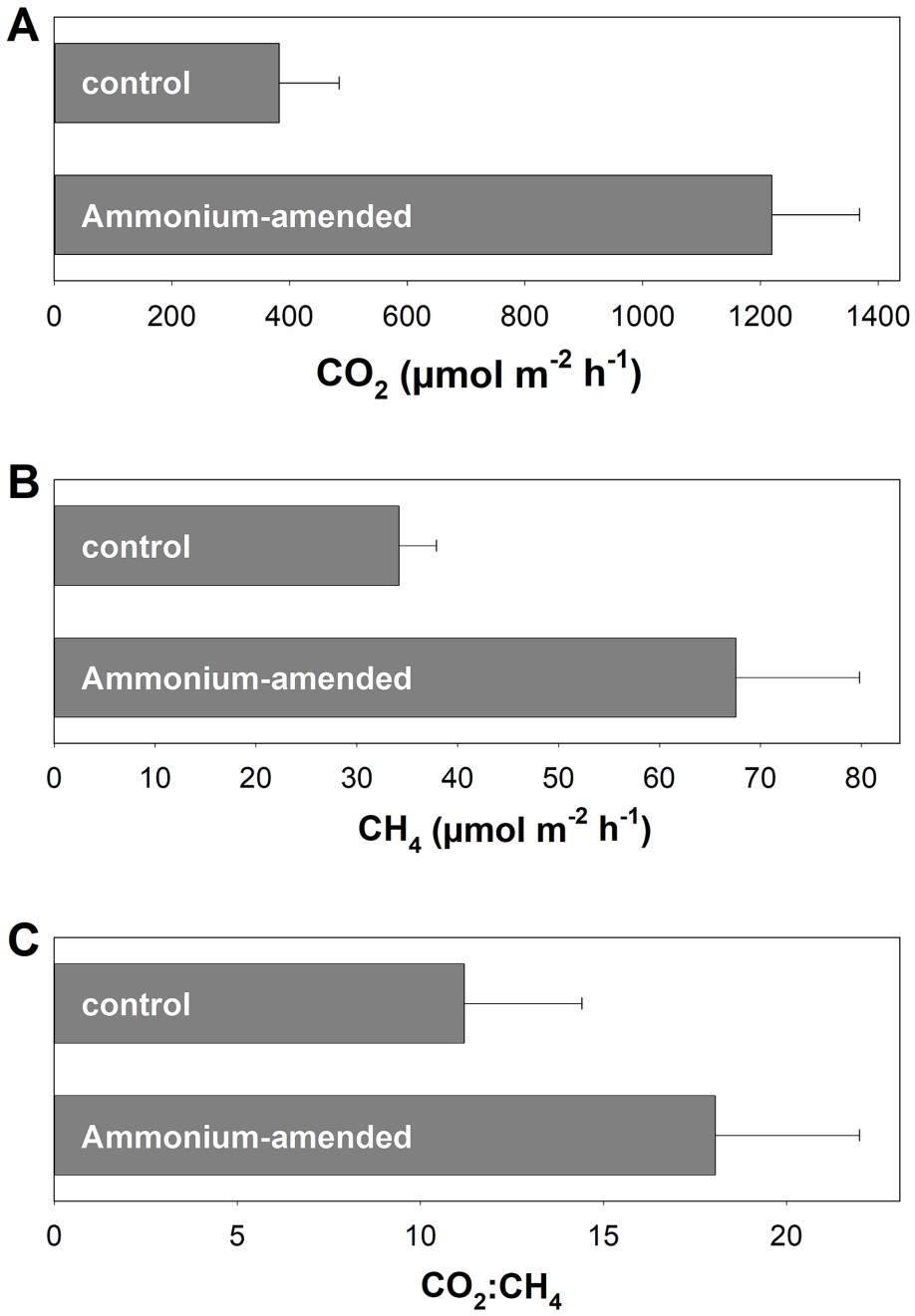

FIGURE 1
In situ emission of CO_2 **(A)** and CH_4 **(B)** as well as CO_2:CH_4 ratios **(C)** in control plots and plots amended with 2 L of fen porewater containing 20 mM ammonium. Measurements were conducted in August 2010. Mean values and standard errors of 4 replicates per treatment are displayed.

repeatedly detected in peatlands (Kotsyurbenko et al., 2019; Bräuer et al., 2020). However, the used primer pair ME1/2 has been reported to be unsuitable for the amplification of *Methanothrix* (e.g., Lueders et al., 2001; Shigematsu et al., 2004), which needs to be taken into consideration.

Product profiles in unsupplemented fen microcosms with and without BES addition

In unsupplemented microcosms without BES, CO_2 steadily accumulated, and it was by far the most prominent of the detected products (Figure 3). CH_4 concentrations increased steadily as well, but comparatively low amounts of the gas accumulated during the 10 days of anoxic incubation (Insert in Figure 3G). The relatively low accumulation of CH_4 compared to that of CO_2 is reflected by generally high CO_2:CH_4 ratios that were highest at day 2 (1,600) and subsequently decreased to ~300 toward the end of the incubation (Supplementary Figure S6). Thus, while methanogenesis became relatively more important over time, alternative (and unresolved) respiratory processes dominated the mineralization of endogenous peat organic carbon. Other fermentation products frequently detected in anoxic peat microcosms like acetate, formate, ethanol, and

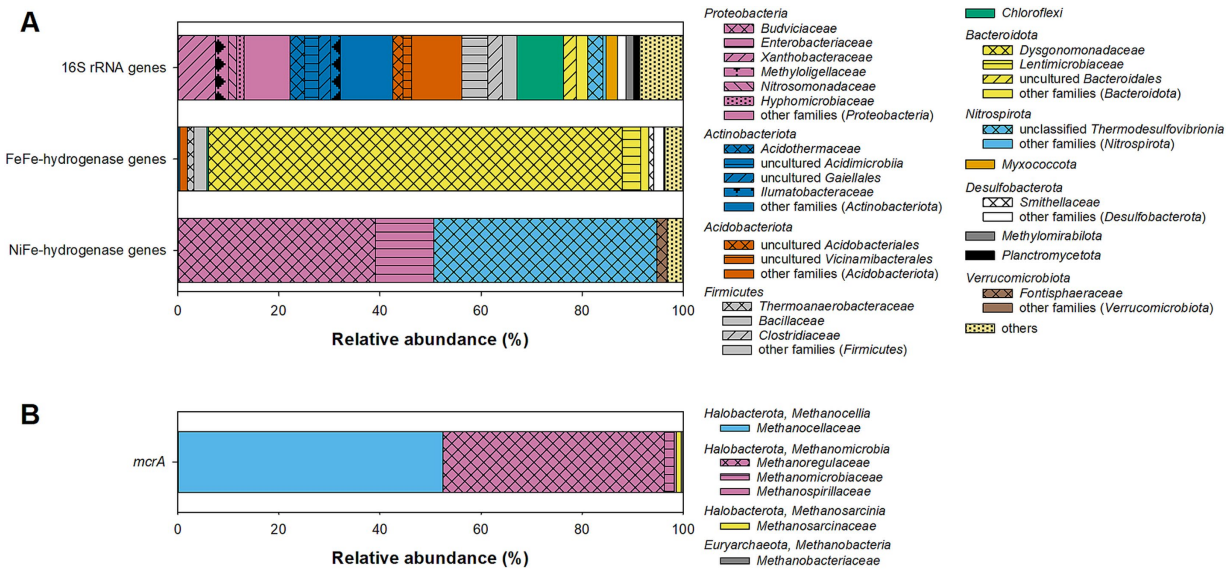

FIGURE 2
Relative abundance of bacterial **(A)** and archaeal **(B)** taxa in forward reads of **(A)** 16S rRNA genes, [FeFe]-hydrogenase genes, and group 4 [NiFe]-hydrogenase genes and **(B)** *mcrA* genes in field-fresh pH-neutral fen soil. Taxonomic classification was done on family-level based on the classifications in Supplementary Table S1. Families with relative abundances <1.5% were grouped as "other families (phylum)." Phyla with a relative abundance <1% and unclassified sequences were grouped as "others" in **(A)**.

propionate did not accumulate (Figures 3B–E). In unsupplemented microcosms with added BES, CH_4 accumulation was suppressed while the residual product profile was overall similar to that in unsupplemented microcosms without BES.

Effect of supplemental NAG on the product profiles in fen microcosms with or without BES

In NAG-supplemented microcosms without BES, NAG was consumed completely within 4 days without appreciable delay, with most rapid consumption from day 2 to 4 (Figure 3A). NAG consumption was accompanied by the accumulation of acetate, formate, ethanol, and CO_2, suggesting ongoing primary fermentation (Figure 3). In the second stage of the incubation (Day 4–10), formate, ethanol, and partially CO_2 were consumed while mainly CH_4, some acetate, and traces of propionate accumulated. In NAG-supplemented microcosms with BES, the same fermentation products were observed as in NAG-supplemented microcosms without BES during the initial stage (Day 0–4), however, transient accumulation of formate and ethanol were more prominent with BES (Figure 3). In the subsequent stage (Day 4–10), concentrations of formate, ethanol, and CO_2 decreased, whereas acetate and some propionate accumulated in NAG-supplemented microcosms with BES, in which methanogenesis was largely blocked.

Net carbon and reductant turnover analysis was performed to determine which of the observed products could be directly linked to NAG consumption and which products were formed during the degradation of primary NAG-fermentation products. In NAG-supplemented microcosms without BES, only about 50% of the carbon and reductant theoretically derived from the amount of NAG consumed could be recovered in the detected products during the initial stage (Day 0–4, Figures 4A,C). Acetate accounted for ~75% of recovered carbon and reductant and was therefore the dominant detected fermentation product followed by ethanol, CO_2, and formate. During the second stage (Day 4–10, Figures 4A,C), net consumption of ethanol, formate, and CO_2 could account for the net production of acetate and CH_4. Carbon and reductant recovered in acetate, ethanol, formate, and CO_2 accounted for most of the NAG that was degraded during the initial incubation in NAG-supplemented microcosms with BES (Day 0–4, Figures 4B,D). In the subsequent stage (Day 4–10, Figures 4B,D), only a part of the acetate and propionate that were formed could be explained by the observed consumption of ethanol, formate, and CO_2, indicating that other undetected sources of carbon and reductant were converted as well. Furthermore, when comparing the net carbon and reductant turnover in NAG-supplemented microcosms without BES to that in NAG-supplemented microcosms with BES over the whole 10 day incubation period, it was remarkable that less than half the consumed carbon and reductant could be recovered in the absence of BES (Day 0–10) whereas more carbon and reductant were recovered in the products than what was theoretically available from the substrates in the presence of BES (Figure 4). The reasons for this discrepancy were unknown.

Effect of methanogenic substrates on CH_4 production in fen soil microcosms with and without preincubation

CH_4 accumulation in unsupplemented microcosms without preincubation was slow (Figure 5). An equally slow CH_4 accumulation was observed in unsupplemented microcosms of the fermentation experiment that were also not preincubated (Figure 3). In contrast, CH_4 accumulated readily and without delay in unsupplemented microcosms preincubated for 120 d in which the final CH_4

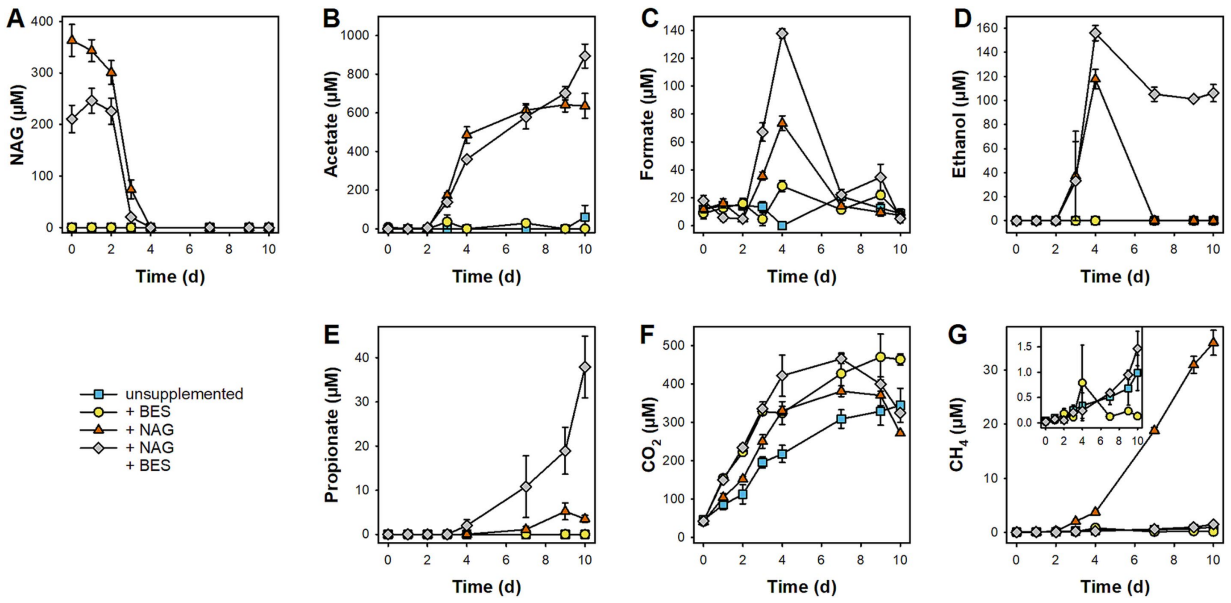

FIGURE 3
Effect of N-Acetylglucosamine (NAG) on production and consumption of fermentation products and methane in pH-neutral fen soil during 10 days of anoxic incubation. Microcosms were incubated in absence and presence of 20 mM BES (+ BES) as well as without and with supplemented NAG (+ NAG). Mean values of three replicates and standard errors are displayed for concentrations of NAG **(A)**, acetate **(B)**, formate **(C)**, ethanol **(D)**, propionate **(E)**, CO_2 **(F)**, and CH_4 **(G)**. The insert in panel **(G)** is an enlargement of the low concentration range to better show low levels of CH_4.

concentrations were more than 30 times higher than in unsupplemented microcosms without preincubation (Figure 5). All tested supplemented substrates (H_2/CO_2, formate, acetate, and methanol) stimulated CH_4 production in microcosms with and without preincubation; however, the stimulatory effect was more pronounced in preincubated microcosms (Figure 5). In fact, the fast initial consumption of supplemental formate and supplemental acetate in microcosms without preincubation was largely uncoupled from CH_4 accumulation, indicating that these substrates were predominately consumed by microbial oxidation processes others than methanogenesis at least at the start of the incubation (Figure 5; Supplementary Figure S7). In preincubated microcosms, the stimulatory effect on CH_4 accumulation was highest for H_2/CO_2 and formate and lowest for methanol (Figure 5). Note that, in contrast to the other substrates, formate was not resupplemented in preincubated microcosms (Supplementary Figure S7), and therefore CH_4 accumulation slowed down once the initially supplemented formate was consumed (Figure 5). Supplemental H_2/CO_2 did not only stimulate methane accumulation but also the accumulation of acetate, especially in microcosms without preincubation (Supplementary Figure S7), indicating that hydrogenotrophic methanogenesis and hydrogenotrophic acetogenesis were going on in parallel. Acetate also accumulated in BES-supplemented microcosms without preincubation and during the preincubation in BES-supplemented microcosms with preincubation in which methanogenesis was largely blocked (Figure 5; Supplementary Figure S7). Whether acetate accumulation in BES-supplemented microcosms was due to ongoing acetogenesis or fermentation could not be resolved. However, the accumulation of propionate, either during the incubation or during the preincubation, indicates that fermentation processes were going on in BES-supplemented microcosms (Supplementary Figure S7).

In summary, the stimulatory effect of methanogenic substrates could be better evaluated in microcosms with 120 d preincubation in which electron acceptors other than CO_2 were presumably largely depleted. The potential for hydrogenotrophic methanogenesis was higher than for aceticlastic methanogenesis, while the potential for methylotrophic methanogenesis was low during the 11 d incubation.

Discussion

Puukkosuo fen, a pH-neutral peatland as source for atmospheric CH_4

To date, peatlands are well recognized for their complex importance for the global climate since they can function as sinks or sources for the greenhouse gasses CO_2, CH_4, and N_2O (Frolking and Roulet, 2007; Strack et al., 2008; Harris et al., 2022). Previously, the potential to function as N_2O sink has been reported for the pH-neutral Puukkosuo fen (Palmer and Horn, 2015). In the present study, *in situ* gas measurements at Puukkosuo fen showed that CH_4 was emitted alongside CO_2, indicating that at the time point of the measurements methanogenesis was ongoing and exceeded or bypassed methane oxidation (Figure 1B). The 35 µmol CH_4 m^{-2} h^{-1} that have been emitted on average were in the lower range of what has been observed in other peatlands (Horn et al., 2003; Hamberger et al., 2008; Salmon et al., 2022). However, the values given in the aforementioned references are maximum emissions for the respective sites measured over a much longer period than in the present study, and prolonged measurement campaigns would be needed to determine the temporal changes and the range in CH_4 emissions at Puukkosuo fen over different seasons and years. The finding that *in situ* CH_4 emissions were higher when ammonium was amended indicated that

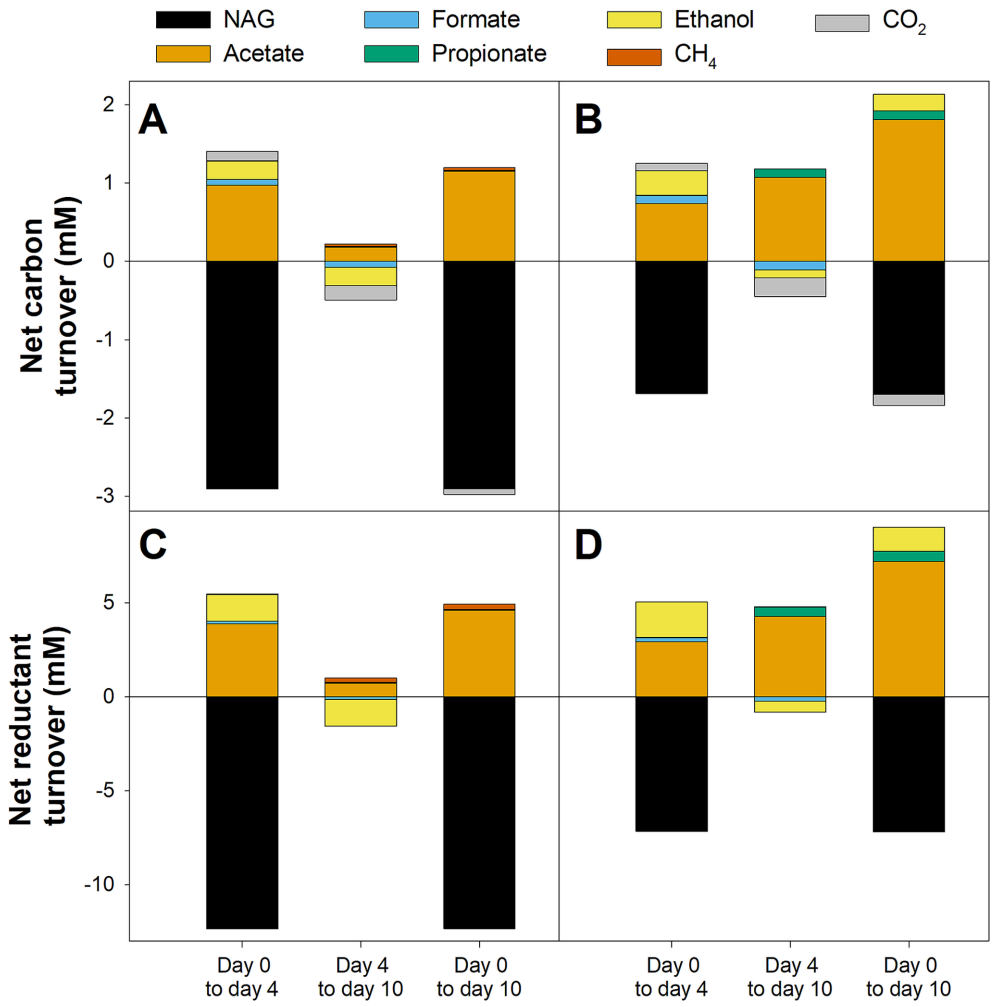

FIGURE 4
Net turnover of carbon **(A,B)** and reductant **(C,D)** for different stages in N-Acetylglucosamine (NAG) supplemented anoxic fen soil microcosms. Microcosms were supplemented with NAG and incubated in absence **(A,C)** or presence of 20 mM BES **(B,D)**. See the materials and methods section for a detailed description of the calculation. Mean values of three replicates are displayed.

methanogenesis was limited by N-availability (Figure 1B), which is in line with the low concentrations of inorganic nitrogen reported for the fen (Palmer and Horn, 2015). Puukkosuo fen is a pristine peatland and anthropogenic N-influx or -deposition is likely limited. Thus, methanogens and other microbes rely on natural reactive nitrogen input like precipitation and groundwater flow, energy intensive nitrogen fixation, and/or the release of nitrogen from the decomposition of peat organic matter.

Primary fermentation activities

As discussed above, the overall microbial activity and methanogenesis in particular are limited by the availability of nitrogen in Puukkosuo fen. Therefore, NAG as an easily degradable carbon and nitrogen source was chosen as model substrate to study primary fermentation and subsequent degradation processes in peat soil microcosms. The immediate fermentation of NAG indicates that fen microbes are poised to consume NAG (Figure 3). Acetate, ethanol and formate were the primary fermentation products that were observed during NAG consumption in the presence and absence of BES (Figures 3, 4). The fermentation profile is indicative of mixed acid fermentation as performed by facultative aerobic enterobacteria (Müller, 2008) which were abundant in group 4 [NiFe]-hydrogenase gene libraries of fresh peat soil (families *Budviciaceae* and *Enterobacteriaceae* in Figure 2). However, the detected fermentation products can be also produced by other fermentative taxa like many members of the *Clostridiaceae* (Wiegel, 2015), a family that accounted for 3% of the 16S rRNA gene sequences retrieved from fresh peat soil (Figure 2). A time-resolved community analysis on transcript or protein level would be necessary to better identify active fermenters in NAG-supplemented peat soil microcosms.

Acetate and ethanol were also observed in NAG-supplemented microcosms with peat soil from a temperate, moderately acidic fen (Wüst et al., 2009). While acetate is also commonly observed as major fermentation product in peat soil microcosms supplemented with glucose or xylose, ethanol was not detected so frequently when these sugar monomers were fermented (Kotsyurbenko et al., 1996; Hamberger et al., 2008; Wüst et al., 2009; Hunger et al., 2015). Nevertheless, ethanol was detected in fresh and incubated peat soil

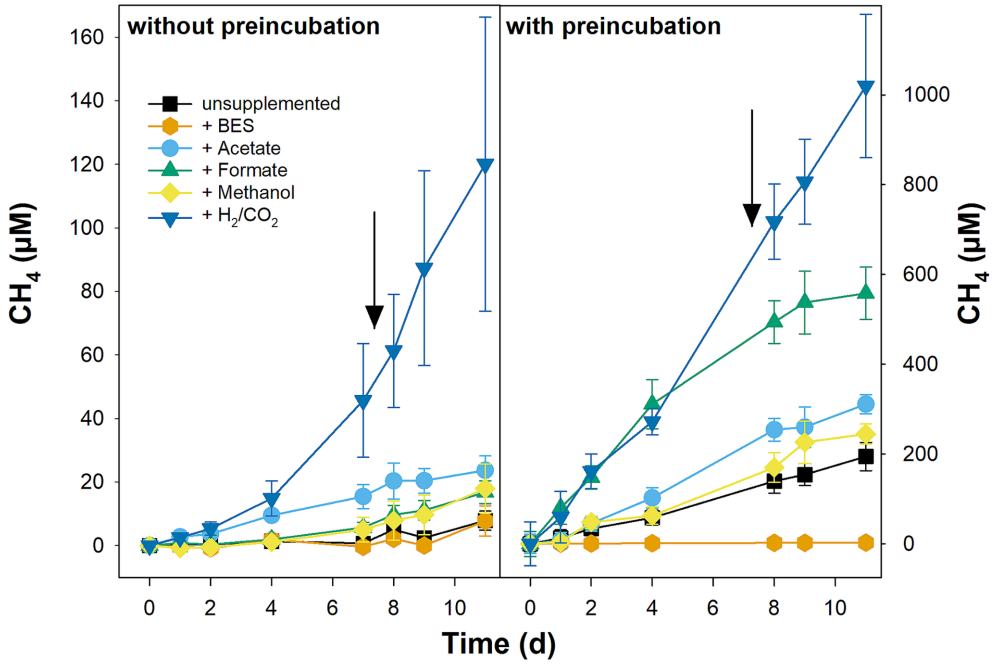

FIGURE 5
Effect of methanogenic substrates on the production of CH_4 in pH-neutral fen soil. Microcosms were set-up without (left) and with (right) preincubation of 120 days to reduce alternative electron acceptors. Microcosm were left unsupplemented or supplemented with 20 mM BES, 1,000 µM acetate, formate, or methanol, or with 8% vol. H_2 and 2% vol. CO_2. Substrates were resupplemented after sampling on day 7 (indicated by arrows; formate was not resupplemented in the preincubated microcosms). Mean values of three replicates and standard errors are displayed. Methane present at t_0 was subtracted to allow for better comparison of net CH_4 production in microcosms without and with preincubations.

and was a potential product of the fermentation of root-derived organic carbon (Metje and Frenzel, 2005, 2007; Tveit et al., 2015; Meier et al., 2021). Butyrate and propionate are other fermentation products that can transiently or permanently accumulate in sugar-supplemented peat soil microcosms (Kotsyurbenko et al., 1996; Hamberger et al., 2008; Wüst et al., 2009; Hunger et al., 2015). However, propionate accumulation was largely uncoupled from NAG consumption and butyrate was not detected in the present study (Figure 3). Interestingly, butyrate was observed during NAG fermentation when the initial concentrations of the substrate were increased to 0.9 mM or higher (i.e., at least twice as high as in the present study), suggesting a tight coupling of butyrate production and consumption in the fen (Wüst et al., 2009).

While propionate accumulation was not observed in unsupplemented microcosms with BES (without preincubation) in the NAG experiment (Figure 3E), propionate accumulated after day 7 in the respective treatment of the methanogenic substrates experiment (Supplementary Figure S7). In addition, propionate accumulated during the preincubation of microcosms with BES (Supplementary Figure S7). These findings indicated that propionate was produced during the fermentation of endogenous organic matter derived from Puukkosuo fen soil. In this regard, (transient) propionate accumulation was observed in microcosms with unsupplemented peat soil before (Schmidt et al., 2015; Tveit et al., 2015), suggesting that propionate is a common product of the fermentation of peat-derived organic carbon. Taxa known to comprise propionate fermenters dominated in [FeFe]-hydrogenase gene libraries (*Dysgonomonadaceae* and *Lentimicrobiaceae* (Chen and Dong, 2005; Hahnke et al., 2016; Sun et al., 2016), Figure 2) and were also present in 16S rRNA gene libraries (ASV r85, 97.3% identity to *Psychrosinus fermentans* (Sattley et al., 2008), and ASV r238, 98.3% identity to *Opitutus* sp. VeSm13 (Janssen et al., 1997); Supplementary Table S1) of fresh Puukkosuo fen soil.

Secondary fermentation activities

The term secondary fermenter is mostly used when describing a syntrophic association in which an alcohol- or organic acid-oxidizing bacterium (i.e., the secondary fermenter) depends on H_2 (or formate) removal by a methanogenic partner (Schink, 1997). However, ethanol can be converted to propionate and acetate independent of interspecies hydrogen transfer between a fermenter and a methanogen (Schink et al., 1987), and such a conversion of ethanol was proposed to occur in anoxic incubations with arctic, pH-neutral peat soil (Tveit et al., 2015). In the current study, ethanol consumption in parallel to propionate accumulation was observed especially in the second stage (between day 4 and day 10) of NAG treatments with BES in which methanogenesis was inhibited (Figure 3). Propionate accumulation was less pronounced in NAG treatments without BES in which the transiently accumulated ethanol was completely consumed between day 4 and day 7 (Figure 3). This suggested that ethanol oxidation was largely performed in syntrophic association without the formation of propionate [as known for *Pelobacter carbinolicus* (Schmidt et al., 2014)] when methanogenesis was not inhibited. Alternatively, syntrophic oxidation of propionate might have prevented the accumulation of propionate derived from ethanol oxidation in NAG treatments without BES. In this respect, [FeFe]-hydrogenase genes

affiliated with the family *Smithellaceae* were detected in fresh peat soil (Figure 2) and the type species of this family, *Smithella propionica,* is capable of syntrophic propionate oxidation (de Bok et al., 2001). Syntrophic propionate oxidation likely also prevented the accumulation of propionate derived from the fermentation of endogenous organic carbon in unsupplemented microcosms with or without preincubation (Supplementary Figure S7). Syntrophic propionate oxidation was studied in a moderately acidic fen in Germany in which *Smithella* and *Syntrophobacter*, two genera with contrasting metabolic pathways of propionate oxidation, were identified as active propionate oxidizers (Schmidt et al., 2016). However, the responsible propionate oxidizers in the neutral Puukkosuo fen still need to be identified.

Methanogenesis

Hydrogenotrophic methanogens are well known partners of syntrophic fermenters. *mcrA*-gene libraries of fresh peat soil were largely dominated by ASVs that were affiliated to either *Methanoregulaceae* or *Methanocellaceae* (Figure 2), both of which comprise hydrogenotrophic methanogens (Oren, 2014a; Sakai et al., 2014). Both families together represent the dominant groups of hydrogenotrophic methanogens in various peatlands (Galand et al., 2002, 2005; Hunger et al., 2011, 2015; Yavitt et al., 2012; Blake et al., 2015; Schmidt et al., 2016; Bräuer et al., 2020). In line with the high abundance of hydrogenotrophic methanogens in fresh Puukkosuo fen soil, CH_4 production was highest in H_2/CO_2-supplemented microcosms with or without preincubation (Figure 5). Except for *Methanoregula boonei*, all other cultured members of the *Methanoregulaceae* and *Methanocellaceae* can utilize formate in addition to H_2 as electron donor during methanogenesis (Oren, 2014a; Sakai et al., 2014). Thus, it was not surprising that supplemental formate stimulated CH_4 production equally well as supplemental H_2/CO_2 until formate got depleted in microcosms with preincubation (Figure 5). Interestingly, the stimulatory effect of formate was much weaker compared to that of H_2/CO_2 in microcosms without preincubation although formate was available throughout the incubation (Figure 5; Supplementary Figure S7). The lower availability of acetate might have caused weaker methane production in formate-supplemented microcosms without preincubation compared to those supplemented with H_2/CO_2 (Supplementary Figure S7), since all cultured members of the *Methanoregulacea* and *Methanocellaceae* require acetate for growth (Oren, 2014a; Sakai et al., 2014).

While supplemental H_2/CO_2 and formate commonly stimulate methanogenesis in peat microcosms, supplemental acetate can have a positive, neutral or negative effect (Williams and Crawford, 1984; Kotsyurbenko et al., 1996; Horn et al., 2003; Bräuer et al., 2004; Wüst et al., 2009; Hunger et al., 2011, 2015; Blake et al., 2015). The inhibitory effect of acetate on methanogens is observed exclusively in acidic peatlands in which undissociated acetic acid permeating into the cell can be toxic to methanogens at elevated concentrations (Russell, 1991; Horn et al., 2003; Bräuer et al., 2004). A stimulatory effect of supplemental acetate on CH_4 production, as observed in the present study (Figure 5) and in other peatlands (Bräuer et al., 2004; Hunger et al., 2015), indicates that the potential of acetate consumption by the complex microbial community involved in methanogenic degradation exceeds the acetate production from endogenous organic carbon. As discussed above, the stimulatory effect of acetate in the present study could be explained by the acetate requirements for growth of *Methanoregulaceae* and *Methanocellaceae*, the two dominant methanogenic taxa observed in fresh peat soil (Figure 2) (Oren, 2014a; Sakai et al., 2014). In addition, acetate might have been converted to CH_4 either in syntrophic cooperation between acetate oxidizers and hydrogenotrophic methanogens (Nusslein et al., 2001; Hattori, 2008) or by aceticlastic methanogens. It must be pointed out that aceticlastic methanogens of the family *Methanosarcinaceae* were largely absent in the *mcrA*-gene libraries of field fresh fen soil (Figure 2). However, in a slightly alkaline fen in Germany *Methanosarcinaceae* were not detected in field fresh soil, but represented 4–27% of the *mcrA*-gene sequences after 3 weeks of incubation in microcosms with contrasting substrate supply (see Mire 1 in Hunger et al., 2015), underlining that rare aceticlastic methanogens can considerably increase in relative abundance within comparatively short incubation times. Furthermore, the relative abundance of aceticlastic *Methanotrichaceae* in field fresh soil could not be evaluated due to the insufficient coverage of their *mcrA* genes by the primer set ME1/2 (Lueders et al., 2001; Shigematsu et al., 2004).

Methanol, which is released by living plants and the degradation of plant material (Galbally and Kirstine, 2002), is conceptualized to be only of minor importance as a substrate for methanogens in peatlands (Drake et al., 2009; Kotsyurbenko et al., 2019). Nevertheless, methanol can have a stimulatory effect on methanogenesis in peat soil microcosms (Bräuer et al., 2004; Wüst et al., 2009; Jiang et al., 2010). In the present study, a relatively weak stimulation of methanogenesis was observed in Methanol-supplemented microcosms with and without preincubation (Figure 5), suggesting that methanol is probably not a major substrate for methanogenesis in Puukkosuo fen.

Acetogenesis

The ecological significance of acetogens in peatlands is still uncertain despite recent findings that indicated the contribution of acetogens to acetate production in some peatlands (Drake et al., 2009; Hunger et al., 2011, 2015; Hädrich et al., 2012; Ye et al., 2014; Kotsyurbenko et al., 2019; Meier et al., 2022). In the 16S rRNA gene library of field fresh peat soil, ASV r72 (0.8% relative abundance) and ASV r73 (0.3% relative abundance) were affiliated with the two acetogens *Clostridium magnum* (98.3% identity) and *Clostridium muellerianum* (94.3% identity), respectively (Supplementary Table S1) (Bomar et al., 1991; Doyle et al., 2022). In this respect, distinct acetate accumulation in H_2/CO_2-supplemented microcosms without preincubation and to a lesser extent in H_2/CO_2-supplemented microcosms with preincubation as well as in formate-supplemented microcosms with and without preincubation suggested that acetogens successfully competed with methanogens for both substrates under the experimental conditions (Supplementary Figure S7). Similarly, acetate accumulation was observed in H_2/CO_2 or formate supplemented microcosms in various peatlands, suggesting that acetogens successfully compete with methanogens at elevated concentrations of these substrates (Kotsyurbenko et al., 1996; Horn et al., 2003; Bräuer et al., 2004; Wüst et al., 2009; Hunger et al., 2011, 2015, 2016; Hädrich et al., 2012; Meier et al., 2022). Some acetate accumulated in methanol-supplemented microcosms with or without preincubation (Supplementary Figure S7), and it is possible that the

weak stimulatory effect of methanol on methanogenesis was due to trophic links between acetogens and methanogens rather than direct consumption of methanol by methanogens (Jiang et al., 2010). Furthermore, ethanol can be a substrate for acetogens (Bertsch et al., 2016), and the finding that ethanol was consumed parallel to acetate accumulation during the second stage of the NAG-supplemented microcosms with or without BES might indicate that acetogens were involved in the degradation of NAG-derived ethanol (Figures 3, 4). In this regard, it has been hypothesized that acetogens could be involved in the degradation of ethanol released during the fermentation of root organic carbon in peatlands (Meier et al., 2021, 2022).

As discussed above, syntrophic acetate oxidation to CH_4 might play a role in Puukkosuo fen. In such a trophic cooperation acetate conversion to H_2/CO_2 or formate by the acetate oxidizer can be conducted via the oxidative citric acid cycle or the oxidative acetyl-CoA cycle (Müller et al., 2015; Manzoor et al., 2016). The latter resembles the reversal of H_2/CO_2- or formate-dependent acetogenesis (Zinder, 1994), and some acetogens can indeed reverse their metabolism according to the thermodynamic conditions and substrate availability (Lee and Zinder, 1988; Oehler et al., 2012). However, if acetogens function as acetate oxidizers when H_2 concentrations are low and acetogenesis becomes thermodynamically unfavorable in Puukkosuo fen remains to be elucidated.

Alternative respiratory processes

In theory, CO_2 and CH_4 are produced in a 1:1 ratio during the complete anaerobic degradation of organic carbon at the redox level of glucose if methanogenesis is the sole terminal electron accepting process ($C_6H_{12}O_6 \rightarrow 3CO_2 + 3CH_4$) (Zinder, 1993), whereas ratios >1 are usually attributed to the use of other inorganic electron acceptors like O_2, nitrate, ferric iron, or sulfate in addition to CO_2 (McCarty, 1972). Humic substances that are abundant in peat can be used as organic electron acceptors, and thus also contribute to high CO_2:CH_4 ratios in peat soil *in situ* or *in vitro* (Heitmann et al., 2007; Roden et al., 2010; Gao et al., 2019). In this study, average CO_2:CH_4 ratios measured *in situ* were 12.4 ± 3.1 (Figure 1C), suggesting that methanogenesis was not the sole terminal electron accepting process in Puukkosuo fen at the time point of sampling. In this respect, a high denitrification potential has been observed in Puukkosuo fen although the availability of nitrate is low (Palmer and Horn, 2015). Notable sulfate concentrations were detected in the soil (53 and 23 μg/gDW in 0–20 cm and 20–40 cm soil, respectively), and such a relatively small pool of sulfate can sustain comparatively high rates of sulfate reduction when reduced sulfur compounds are continuously reoxidized (Pester et al., 2012). 16S rRNA gene and [FeFe]-hydrogenase gene ASVs related to sulfate reducers of the genera *Desulfosporosinus*, *Desulfomonile*, and *Desulfovirgula* of fresh peat soil underlined the possibility of sulfate reducers contributing to the anaerobic degradation of organic matter in Puukkosuo fen (Supplementary Table S1). Furthermore, some 16S rRNA gene ASVs were related to iron reducers from the genera *Acidithermonas*, *Anaeromyxobacter*, and *Geobacter* (Supplementary Table S1), indicating that iron reduction, which can be important in peatlands (Reiche et al., 2008), might play a role in anaerobic degradation of organic carbon in Puukkosuo fen. Moreover, aerobic or anaerobic methane oxidation might have contributed to CO_2:CH_4 ratios greater than 1 as well (Smemo and Yavitt, 2011; Zalman et al., 2018). In this respect, ASV r154 and ASV r229 of the 16S rRNA gene library were affiliated to the methanotrophic genera *Methylocystis* and *Methylobacter* (Supplementary Table S1).

CO_2:CH_4 ratios in unsupplemented fresh peat soil microcosms were much higher than those observed *in situ* (Figure 1C; Supplementary Figure S6), supporting the assumption that sample handling, storage, and incubation procedures can obscure methanogenic conditions when peat soil is incubated *in vitro*, supporting the need for a pre-incubation to better mimic *in situ* near conditions (Yavitt and Seidman-Zager, 2006).

Conclusions and future perspectives

The accumulation of fermentation products in NAG supplemented microcosms indicated a high fermentation potential of the microbial community in the fen, and formate as well as ethanol as important intermediates (Figure 3). Such fermentations were performed by a fen community harboring phylogenetically novel hydrogenases and organisms, thus the fen represents a reservoir of hitherto unknown microbial diversity.

In the present study, NAG, a monomer of the second most abundant biopolymer chitin, was used as a model compound. Since polymer hydrolysis often is the rate-limiting step resulting in low concentrations of NAG, chitin supplementation, and treatments with NAG in the lower μM range with refeeding coupled to time-resolved mRNA analysis of peat soil microcosms is recommended to identify key organisms of chitin and NAG degradation. Future research should likewise address the fate of acetate at Puukkosuo fen as a model system for pH neutral subarctic fens.

In conclusion, the microbial community of the CH_4-emitting Puukkosuo fen showed a pronounced response to supplemental substrates for fermentation and hydrogenotrophic methanogenesis, indicating a high potential activity of both processes. Elucidating active primary and secondary fermenters, the role of acetogens, as well as the pathways of anaerobic acetate conversion to methane and involved taxa are key challenges for future research. Our current study provides a good starting point for conducting such subsequent studies.

Data availability statement

The datasets presented in this study can be found in online repositories. The names of the repository/repositories and accession number(s) can be found below: https://www.ebi.ac.uk/ena, PRJEB58427.

Author contributions

KK: Conceptualization, Formal analysis, Funding acquisition, Investigation, Project administration, Visualization, Writing – original draft, Writing – review & editing. OS: Formal analysis, Visualization, Writing – original draft, Writing – review & editing. MH: Conceptualization, Supervision, Writing – review & editing, Funding acquisition, Resources.

Funding

The author(s) declare that financial support was received for the research, authorship, and/or publication of this article. Financial support for this study was provided by LAPBIAT (part of the Sixth EU Framework Programme Infrastructures), the German Academic Exchange Service (DAAD), the German Research Foundation (DFG Research Unit 562 "Dynamics of soil processes under extreme meteorological boundary conditions," FOR562, HO4020/2-2), the University of Bayreuth, and the Research Council of Finland (project 322753 awarded to KK).

Acknowledgments

The authors would like to thank Harold L. Drake for continuous support, Jyrki Manninen for organizational help, the team at Oulanka research station for excellent on-site support, Sonja Perras Mertens for help with laboratory experiments, the Central Analytics Department of BayCEER for analyses of nitrate, nitrite, ammonium, TC, TN, and TOC, as well as Rolf Daniel and Andrea Thürmer for pyrosequencing.

Conflict of interest

The authors declare that the research was conducted in the absence of any commercial or financial relationships that could be construed as a potential conflict of interest.

The author(s) declared that they were an editorial board member of Frontiers, at the time of submission. This had no impact on the peer review process and the final decision.

Publisher's note

Supplementary material

The Supplementary material for this article can be found online at: https://www.frontiersin.org/articles/10.3389/fmicb.2024.1428517/full#supplementary-material

References

Adeolu, M., Alnajar, S., Naushad, S., and Gupta, R. S. (2016). Genome-based phylogeny and taxonomy of the '*Enterobacteriales*': proposal for *Enterobacterales* Ord. Nov. divided into the families *Enterobacteriaceae*, *Erwiniaceae* fam. Nov., *Pectobacteriaceae* fam. Nov., *Yersiniaceae* fam. Nov., *Hafniaceae* fam. Nov., *Morganellaceae* fam. Nov., and *Budviciaceae* fam. Nov. *Int. J. Syst. Evol. Microbiol.* 66, 5575–5599. doi: 10.1099/ijsem.0.001485

Altschul, S. F., Gish, W., Miller, W., Myers, E. W., and Lipman, D. J. (1990). Basic local alignment search tool. *J. Mol. Biol.* 215, 403–410. doi: 10.1016/S0022-2836(05)80360-2

Beier, S., and Bertilsson, S. (2013). Bacterial chitin degradation—mechanisms and ecophysiological strategies. *Front. Microbiol.* 4:149. doi: 10.3389/fmicb.2013.00149

Bertsch, J., Siemund, A. L., Kremp, F., and Müller, V. (2016). A novel route for ethanol oxidation in the acetogenic bacterium *Acetobacterium woodii*: the acetaldehyde/ethanol dehydrogenase pathway. *Environ. Microbiol.* 18, 2913–2922. doi: 10.1111/1462-2920.13082

Blake, L. I., Tveit, A., Øvreås, L., Head, I. M., and Gray, N. D. (2015). Response of methanogens in Arctic sediments to temperature and methanogenic substrate availability. *PLoS One* 10:e0129733. doi: 10.1371/journal.pone.0129733

Bolyen, E., Rideout, J. R., Dillon, M. R., Bokulich, N. A., Abnet, C. C., Al-Ghalith, G. A., et al. (2019). Reproducible, interactive, scalable and extensible microbiome data science using QIIME 2. *Nat. Biotechnol.* 37, 852–857. doi: 10.1038/s41587-019-0209-9

Bomar, M., Hippe, H., and Schink, B. (1991). Lithotrophic growth and hydrogen metabolism by *Clostridium magnum*. *FEMS Microbiol. Lett.* 83, 347–350. doi: 10.1111/j.1574-6968.1991.tb04488.x

Bräuer, S. L., Basiliko, N., Siljanen, H. M. P., and Zinder, S. H. (2020). Methanogenic archaea in peatlands. *FEMS Microbiol. Lett.* 367:fnaa172. doi: 10.1093/femsle/fnaa172

Bräuer, S. L., Yavitt, J. B., and Zinder, S. H. (2004). Methanogenesis in McLean bog, an acidic peat bog in upstate New York: stimulation by H_2/CO_2 in the presence of rifampicin, or by low concentrations of acetate. *Geomicrobiol J.* 21, 433–443. doi: 10.1080/01490450490505400

Brenner, D. J., and Farmer, J. J. (2005). "Family I. *Enterobacteriaceae*" in Bergey's manual of systematics of Archaea and Bacteria. eds. G. M. Garrity, D. J. Brenner, N. R. Krieg and J. T. Staley (New York: Springer), 587–850.

Callahan, B. J., McMurdie, P. J., Rosen, M. J., Han, A. W., Johnson, A. J. A., and Holmes, S. P. (2016). DADA2: high-resolution sample inference from Illumina amplicon data. *Nat. Methods* 13, 581–583. doi: 10.1038/nmeth.3869

Chen, S., and Dong, X. (2005). *Proteiniphilum acetatigenes* gen. Nov., sp. nov., from a UASB reactor treating brewery wastewater. *Int. J. Syst. Evol. Microbiol.* 55, 2257–2261. doi: 10.1099/ijs.0.63807-0

Conrad, R. (1996). Soil microorganisms as controllers of atmospheric trace gases (H_2, CO, CH_4, OCS, N_2O, and NO). *Microbiol. Rev.* 60, 609–640. doi: 10.1128/mr.60.4.609-640.1996

Conrad, R. (2020). Importance of hydrogenotrophic, aceticlastic and methylotrophic methanogenesis for methane production in terrestrial, aquatic and other anoxic environments: a mini review. *Pedosphere* 30, 25–39. doi: 10.1016/S1002-0160(18)60052-9

de Bok, F. A. M., Stams, A. J. M., Dijkema, C., and Boone, D. R. (2001). Pathway of propionate oxidation by a syntrophic culture of *Smithella propionica* and *Methanospirillum hungatei*. *Appl. Environ. Microbiol.* 67, 1800–1804. doi: 10.1128/AEM.67.4.1800-1804.2001

Dedysh, S. N. (2011). Cultivating uncultured bacteria from northern wetlands: knowledge gained and remaining gaps. *Front. Microbiol.* 2:184. doi: 10.3389/fmicb.2011.00184

Doyle, D. A., Smith, P. R., Lawson, P. A., and Tanner, R. S. (2022). *Clostridium muellerianum* sp. nov., a carbon monoxide-oxidizing acetogen isolated from old hay. *Int. J. Syst. Evol. Microbiol.* 72:005297. doi: 10.1099/ijsem.0.005297

Drake, H. L., Horn, M. A., and Wüst, P. K. (2009). Intermediary ecosystem metabolism as a main driver of methanogenesis in acidic wetland soil. *Environ. Microbiol.* 1, 307–318. doi: 10.1111/j.1758-2229.2009.00050.x

Faith, D. P. (1992). Conservative evaluation and phylogenetic diversity. *Biol. Conserv.* 61, 1–10. doi: 10.1016/0006-3207(92)91201-3

Frolking, S., and Roulet, N. T. (2007). Holocene radiative forcing impact of northern peatland carbon accumulation and methane emissions. *Glob. Change Biol.* 13, 1079–1088. doi: 10.1111/j.1365-2486.2007.01339.x

Galand, P. E., Fritze, H., and Yrjälä, K. (2003). Microsite-dependent changes in methanogenic populations in a boreal oligotrophic fen. *Environ. Microbiol.* 5, 1133–1143. doi: 10.1046/j.1462-2920.2003.00520.x

Galand, P. E., Juottonen, H., Fritze, H., and Yrjälä, K. (2005). Methanogen communities in a drained bog: effect of ash fertilization. *Microb. Ecol.* 49, 209–217. doi: 10.1007/s00248-003-0229-2

Galand, P. E., Saarnio, S., Fritze, H., and Yrjälä, K. (2002). Depth related diversity of methanogen Archaea in Finnish oligotrophic fen. *FEMS Microbiol. Ecol.* 42, 441–449. doi: 10.1111/j.1574-6941.2002.tb01033.x

Galbally, I. E., and Kirstine, W. V. (2002). The production of methanol by flowering plants and the global cycle of methanol. *J. Atmos. Chem.* 43, 195–229. doi: 10.1023/A:1020684815474

Gallego-Sala, A. V., Charman, D. J., Brewer, S., Page, S. E., Prentice, I. C., Friedlingstein, P., et al. (2018). Latitudinal limits to the predicted increase of the peatland carbon sink with warming. *Nat. Clim. Chang.* 8, 907–913. doi: 10.1038/s41558-018-0271-1

Gao, C., Sander, M., Agethen, S., and Knorr, K.-H. (2019). Electron accepting capacity of dissolved and particulate organic matter control CO_2 and CH_4 formation in peat soils. *Geochim. Cosmochim. Acta* 245, 266–277. doi: 10.1016/j.gca.2018.11.004

Gooday, G. W. (1994). "Physiology of microbial degradation of chitin and chitosan" in Biochemistry of microbial degradation. ed. C. Ratledge (Dordrecht: Springer Netherlands), 279–312.

Hädrich, A., Heuer, V. B., Herrmann, M., Hinrichs, K.-U., and Küsel, K. (2012). Origin and fate of acetate in an acidic fen. *FEMS Microbiol. Ecol.* 81, 339–354. doi: 10.1111/j.1574-6941.2012.01352.x

Hahnke, S., Langer, T., Koeck, D. E., and Klocke, M. (2016). Description of *Proteiniphilum saccharofermentans* sp. nov., *Petrimonas mucosa* sp. nov. and *Fermentimonas caenicola* gen. Nov., sp. nov., isolated from mesophilic laboratory-scale biogas reactors, and amended description of the genus *Proteiniphilum*. *Int. J. Syst. Evol. Microbiol.* 66, 1466–1475. doi: 10.1099/ijsem.0.000902

Hales, B. A., Edwards, C., Ritchie, D. A., Hall, G., Pickup, R. W., and Saunders, J. R. (1996). Isolation and identification of methanogen-specific DNA from blanket bog peat by PCR amplification and sequence analysis. *Appl. Environ. Microbiol.* 62, 668–675. doi: 10.1128/aem.62.2.668-675.1996

Hamberger, A., Horn, M. A., Dumont, M. G., Murrell, J. C., and Drake, H. L. (2008). Anaerobic consumers of monosaccharides in a moderately acidic fen. *Appl. Environ. Microbiol.* 74, 3112–3120. doi: 10.1128/AEM.00193-08

Harris, L. I., Richardson, K., Bona, K. A., Davidson, S. J., Finkelstein, S. A., Garneau, M., et al. (2022). The essential carbon service provided by northern peatlands. *Front. Ecol. Environ.* 20, 222–230. doi: 10.1002/fee.2437

Hattori, S. (2008). Syntrophic acetate-oxidizing microbes in methanogenic environments. *Microb. Environ.* 23, 118–127. doi: 10.1264/jsme2.23.118

Heitmann, T., Goldhammer, T., Beer, J., and Blodau, C. (2007). Electron transfer of dissolved organic matter and its potential significance for anaerobic respiration in a northern bog. *Glob. Change Biol.* 13, 1771–1785. doi: 10.1111/j.1365-2486.2007.01382.x

Hines, M. E., Duddleston, K. N., Rooney-Varga, J. N., Fields, D., and Chanton, J. P. (2008). Uncoupling of acetate degradation from methane formation in Alaskan wetlands: connections to vegetation distribution. *Glob. Biogeochem. Cycles* 22:GB2017. doi: 10.1029/2006GB002903

Hodgkins, S. B., Tfaily, M. M., McCalley, C. K., Logan, T. A., Crill, P. M., Saleska, S. R., et al. (2014). Changes in peat chemistry associated with permafrost thaw increase greenhouse gas production. *Proc. Natl. Acad. Sci.* 111, 5819–5824. doi: 10.1073/pnas.1314641111

Horn, M. A., Matthies, C., Küsel, K., Schramm, A., and Drake, H. L. (2003). Hydrogenotrophic methanogenesis by moderately acid-tolerant methanogens of a methane-emitting acidic peat. *Appl. Environ. Microbiol.* 69, 74–83. doi: 10.1128/AEM.69.1.74-83.2003

Hunger, S., Gößner, A. S., and Drake, H. L. (2015). Anaerobic trophic interactions of contrasting methane-emitting mire soils: processes versus taxa. *FEMS Microbiol. Ecol.* 91:fiv045. doi: 10.1093/femsec/fiv045

Hunger, S., Schmidt, O., Gößner, A. S., and Drake, H. L. (2016). Formate-derived H_2, a driver of hydrogenotrophic processes in the root-zone of a methane-emitting fen. *Environ. Microbiol.* 18, 3106–3119. doi: 10.1111/1462-2920.13301

Hunger, S., Schmidt, O., Hilgarth, M., Horn, M. A., Kolb, S., Conrad, R., et al. (2011). Competing formate- and carbon dioxide-utilizing prokaryotes in an anoxic methane-emitting fen soil. *Appl. Environ. Microbiol.* 77, 3773–3785. doi: 10.1128/AEM.00282-11

Itoh, H., Sugisawa, Y., Mise, K., Xu, Z., Kuniyasu, M., Ushijima, N., et al. (2023). *Mesoterricola silvestris* gen. Nov., sp. nov., *Mesoterricola sediminis* sp. nov., *Geothrix oryzae* sp. nov., *Geothrix edaphica* sp. nov., *Geothrix rubra* sp. nov., and *Geothrix limicola* sp. nov., six novel members of *Acidobacteriota* isolated from soils. *Int. J. Syst. Evol. Microbiol.* 73:006073. doi: 10.1099/ijsem.0.006073

James, K. L., Ríos-Hernández, L. A., Wofford, N. Q., Mouttaki, H., Sieber, J. R., Sheik, C. S., et al. (2016). Pyrophosphate-dependent ATP formation from acetyl coenzyme a in *Syntrophus aciditrophicus*, a new twist on ATP formation. *MBio* 7, e01208–e01216. doi: 10.1128/mBio.01208-16

Janssen, P. H., Schuhmann, A., Mörschel, E., and Rainey, F. A. (1997). Novel anaerobic ultramicrobacteria belonging to the *Verrucomicrobiales* lineage of bacterial descent isolated by dilution culture from anoxic rice paddy soil. *Appl. Environ. Microbiol.* 63, 1382–1388. doi: 10.1128/aem.63.4.1382-1388.1997

Jiang, N., Wang, Y., and Dong, X. (2010). Methanol as the primary methanogenic and acetogenic precursor in the cold Zoige wetland at Tibetan plateau. *Microb. Ecol.* 60, 206–213. doi: 10.1007/s00248-009-9602-0

Kaksonen, A. H., Spring, S., Schumann, P., Kroppenstedt, R. M., and Puhakka, J. A. (2007). *Desulfovirgula thermocuniculi* gen. Nov., sp. nov., a thermophilic sulfate-reducer isolated from a geothermal underground mine in Japan. *Int. J. Syst. Evol. Microbiol.* 57, 98–102. doi: 10.1099/ijs.0.64655-0

Kang, H., Freeman, C., Soon Park, S., and Chun, J. (2005). N-Acetylglucosaminidase activities in wetlands: a global survey. *Hydrobiologia* 532, 103–110. doi: 10.1007/s10750-004-9450-3

Kelly, C. A., Dise, N. B., and Martens, C. S. (1992). Temporal variations in the stable carbon isotopic composition of methane emitted from Minnesota peatlands. *Glob. Biogeochem. Cycles* 6, 263–269. doi: 10.1029/92GB01478

Kolb, S., and Horn, M. A. (2012). Microbial CH_4 and N_2O consumption in acidic wetlands. *Front. Microbiol.* 3:78. doi: 10.3389/fmicb.2012.00078

Kotsyurbenko, O. R., Friedrich, M. W., Simankova, M. V., Nozhevnikova, A. N., Golyshin, P. N., Timmis, K. N., et al. (2007). Shift from acetoclastic to H_2-dependent methanogenesis in a west Siberian peat bog at low pH values and isolation of an acidophilic *Methanobacterium* strain. *Appl. Environ. Microbiol.* 73, 2344–2348. doi: 10.1128/AEM.02413-06

Kotsyurbenko, O. R., Glagolev, M. V., Merkel, A. Y., Sabrekov, A. F., and Terentieva, I. E. (2019). "Methanogenesis in soils, wetlands, and peat" in Biogenesis of hydrocarbons. eds. A. J. M. Stams and D. Z. Sousa (Cham: Springer), 211–228.

Kotsyurbenko, O. R., Nozhevnikova, A. N., Soloviova, T. I., and Zavarzin, G. A. (1996). Methanogenesis at low temperatures by microflora of tundra wetland soil. *A. Van Leeuw. J. Microb.* 69, 75–86. doi: 10.1007/BF00641614

Küsel, K., and Drake, H. L. (1995). Effects of environmental parameters on the formation and turnover of acetate by forest soils. *Appl. Environ. Microbiol.* 61, 3667–3675. doi: 10.1128/aem.61.10.3667-3675.1995

Lee, M. J., and Zinder, S. H. (1988). Isolation and characterization of a thermophilic bacterium which oxidizes acetate in syntrophic association with a methanogen and which grows acetogenically on H_2-CO_2. *Appl. Environ. Microbiol.* 54, 124–129. doi: 10.1128/aem.54.1.124-129.1988

Limpens, J., Berendse, F., Blodau, C., Canadell, J. G., Freeman, C., Holden, J., et al. (2008). Peatlands and the carbon cycle: from local processes to global implications – a synthesis. *Biogeosciences* 5, 1475–1491. doi: 10.5194/bg-5-1475-2008

Lueders, T., Chin, K. J., Conrad, R., and Friedrich, M. (2001). Molecular analyses of methyl-coenzyme M reductase α-subunit (mcrA) genes in rice field soil and enrichment cultures reveal the methanogenic phenotype of a novel archaeal lineage. *Environ. Microbiol.* 3, 194–204. doi: 10.1046/j.1462-2920.2001.00179.x

Mann, K. H. (1988). Production and use of detritus in various freshwater, estuarine, and coastal ecosystems. *Limnol. Oceanogr.* 33, 910–930. doi: 10.4319/lo.1988.33.4_part_2.0910

Manzoor, S., Bongcam-Rudloff, E., Schnürer, A., and Müller, B. (2016). Genome-guided analysis and whole transcriptome profiling of the mesophilic syntrophic acetate oxidising bacterium *Syntrophaceticus schinkii*. *PLoS One* 11:e0166520. doi: 10.1371/journal.pone.0166520

Martin, M. (2011). Cutadapt removes adapter sequences from high-throughput sequencing reads. *EMBnet.journal* 17, 10–12. doi: 10.14806/ej.17.1.200

McCarty, P. L. (1972). "Energetics of organic matter degradation" in Water pollution microbiology. ed. R. Mitchell (New York: John Wiley), 91–118.

Meier, A. B., Oppermann, S., Drake, H. L., and Schmidt, O. (2021). Organic carbon from graminoid roots as a driver of fermentation in a fen. *FEMS Microbiol. Ecol.* 97:fiab143. doi: 10.1093/femsec/fiab143

Meier, A. B., Oppermann, S., Drake, H. L., and Schmidt, O. (2022). The root zone of graminoids: a niche for H2-consuming acetogens in a minerotrophic peatland. *Front. Microbiol.* 13:978296. doi: 10.3389/fmicb.2022.978296

Metje, M., and Frenzel, P. (2005). Effect of temperature on anaerobic ethanol oxidation and methanogenesis in acidic peat from a northern wetland. *Appl. Environ. Microbiol.* 71, 8191–8200. doi: 10.1128/AEM.71.12.8191-8200.2005

Metje, M., and Frenzel, P. (2007). Methanogenesis and methanogenic pathways in a peat from subarctic permafrost. *Environ. Microbiol.* 9, 954–964. doi: 10.1111/j.1462-2920.2006.01217.x

Mitsch, W. J. (1994). Global wetlands: Old world and new. New York: Elsevier.

Müller, V. (2008). "Bacterial fermentation" in Encyclopedia of life sciences (Chichester: John Wiley).

Müller, B., Manzoor, S., Niazi, A., Bongcam-Rudloff, E., and Schnürer, A. (2015). Genome-guided analysis of physiological capacities of *Tepidanaerobacter acetatoxydans* provides insights into environmental adaptations and syntrophic acetate oxidation. *PLoS One* 10:e0121237. doi: 10.1371/journal.pone.0121237

Muyzer, G., de Waal, E. C., and Uitterlinden, A. G. (1993). Profiling of complex microbial populations by denaturing gradient gel electrophoresis analysis of polymerase chain reaction-amplified genes coding for 16S rRNA. *Appl. Environ. Microbiol.* 59, 695–700. doi: 10.1128/aem.59.3.695-700.1993

Nusslein, B., Chin, K.-J., Eckert, W., and Conrad, R. (2001). Evidence for anaerobic syntrophic acetate oxidation during methane production in the profundal sediment of subtropical Lake Kinneret (Israel). *Environ. Microbiol.* 3, 460–470. doi: 10.1046/j.1462-2920.2001.00215.x

Oehler, D., Poehlein, A., Leimbach, A., Müller, N., Daniel, R., Gottschalk, G., et al. (2012). Genome-guided analysis of physiological and morphological traits of the fermentative acetate oxidizer *Thermacetogenium phaeum*. *BMC Genomics* 13:723. doi: 10.1186/1471-2164-13-723

Oremland, R. S., and Capone, D. G. (1988). "Use of 'specific' inhibitors in biogeochemistry and microbial ecology" in *Advances in microbial ecology* advances in microbial ecology. ed. K. C. Marshall (Boston, MA: Springer US), 285–383.

Oren, A. (2014a). "The family Methanoregulaceae" in The prokaryotes. eds. E. Rosenberg, E. F. DeLong, S. Lory, E. Stackebrandt and F. Thompson (Berlin, Heidelberg: Springer Berlin Heidelberg), 253–258.

Oren, A. (2014b). "The family Methanosarcinaceae" in The prokaryotes. eds. E. Rosenberg, E. F. Delong, S. Lory, E. Stackebrandt and F. Thompson (Berlin, Heidelberg: Springer Berlin Heidelberg), 259–281.

Palmer, K., Biasi, C., and Horn, M. A. (2012). Contrasting denitrifier communities relate to contrasting N_2O emission patterns from acidic peat soils in arctic tundra. *ISME J.* 6, 1058–1077. doi: 10.1038/ismej.2011.172

Palmer, K., and Horn, M. A. (2015). Denitrification activity of a remarkably diverse fen denitrifier community in Finnish Lapland is N-oxide limited. *PLoS One* 10:e0123123. doi: 10.1371/journal.pone.0123123

Pankratov, T. A., Belova, S. E., and Dedysh, S. N. (2005). Evaluation of the phylogenetic diversity of prokaryotic microorganisms in *Sphagnum* peat bogs by means of fluorescence in situ hybridization (FISH). *Microbiology* 74, 722–728. doi: 10.1007/s11021-005-0130-8

Pazos, M., and Peters, K. (2019). "Peptidoglycan" in *Bacterial cell walls and membranes* subcellular biochemistry. ed. A. Kuhn (Cham: Springer International Publishing), 127–168.

Peršoh, D., Theuerl, S., Buscot, F., and Rambold, G. (2008). Towards a universally adaptable method for quantitative extraction of high-purity nucleic acids from soil. *J. Microbiol. Methods* 75, 19–24. doi: 10.1016/j.mimet.2008.04.009

Pester, M., Knorr, K.-H., Friedrich, M. W., Wagner, M., and Loy, A. (2012). Sulfate-reducing microorganisms in wetlands – fameless actors in carbon cycling and climate change. *Front. Microbiol.* 3:72. doi: 10.3389/fmicb.2012.00072

Reiche, M., Torburg, G., and Küsel, K. (2008). Competition of Fe(III) reduction and methanogenesis in an acidic fen. *FEMS Microbiol. Ecol.* 65, 88–101. doi: 10.1111/j.1574-6941.2008.00523.x

Roden, E. E., Kappler, A., Bauer, I., Jiang, J., Paul, A., Stoesser, R., et al. (2010). Extracellular electron transfer through microbial reduction of solid-phase humic substances. *Nat. Geosci.* 3, 417–421. doi: 10.1038/ngeo870

Rooney-Varga, J. N., Giewat, M. W., Duddleston, K. N., Chanton, J. P., and Hines, M. E. (2007). Links between archaeal community structure, vegetation type and methanogenic pathway in Alaskan peatlands. *FEMS Microbiol. Ecol.* 60, 240–251. doi: 10.1111/j.1574-6941.2007.00278.x

Russell, J. B. (1991). Intracellular pH of acid-tolerant ruminal bacteria. *Appl. Environ. Microbiol.* 57, 3383–3384. doi: 10.1128/aem.57.11.3383-3384.1991

Sakai, S., Conrad, R., and Imachi, H. (2014). "The family Methanocellaceae" in The prokaryotes. eds. E. Rosenberg, E. F. Delong, S. Lory, E. Stackebrandt and F. Thompson (Berlin, Heidelberg: Springer Berlin Heidelberg), 209–214.

Salmon, E., Jégou, F., Guenet, B., Jourdain, L., Qiu, C., Bastrikov, V., et al. (2022). Assessing methane emissions for northern peatlands in ORCHIDEE-PEAT revision 7020. *Geosci. Model Dev.* 15, 2813–2838. doi: 10.5194/gmd-15-2813-2022

Sattley, W. M., Jung, D. O., and Madigan, M. T. (2008). *Psychrosinus fermentans* gen. Nov., sp. nov., a lactate-fermenting bacterium from near-freezing oxycline waters of a meromictic Antarctic lake. *FEMS Microbiol. Lett.* 287, 121–127. doi: 10.1111/j.1574-6968.2008.01300.x

Schink, B. (1997). Energetics of syntrophic cooperation in methanogenic degradation. *Microbiol. Mol. Biol. Rev.* 61, 262–280. doi: 10.1128/mmbr.61.2.262-280.1997

Schink, B., Kremer, D. R., and Hansen, T. A. (1987). Pathway of propionate formation from ethanol in *Pelobacter propionicus*. *Arch. Microbiol.* 147, 321–327. doi: 10.1007/BF00406127

Schmidt, O., Drake, H. L., and Horn, M. A. (2010). Hitherto unknown [Fe-Fe]-hydrogenase gene diversity in anaerobes and anoxic enrichments from a moderately acidic fen. *Appl. Environ. Microbiol.* 76, 2027–2031. doi: 10.1128/AEM.02895-09

Schmidt, A., Frensch, M., Schleheck, D., Schink, B., and Müller, N. (2014). Degradation of acetaldehyde and its precursors by *Pelobacter carbinolicus* and *P. acetylenicus*. *PLoS One* 9:e115902. doi: 10.1371/journal.pone.0115902

Schmidt, O., Hink, L., Horn, M. A., and Drake, H. L. (2016). Peat: home to novel syntrophic species that feed acetate- and hydrogen-scavenging methanogens. *ISME J.* 10, 1954–1966. doi: 10.1038/ismej.2015.256

Schmidt, O., Horn, M. A., Kolb, S., and Drake, H. L. (2015). Temperature impacts differentially on the methanogenic food web of cellulose-supplemented peatland soil. *Environ. Microbiol.* 17, 720–734. doi: 10.1111/1462-2920.12507

Schmidt, O., Wüst, P. K., Hellmuth, S., Borst, K., Horn, M. A., and Drake, H. L. (2011). Novel [NiFe]- and [FeFe]-hydrogenase gene transcripts indicative of active facultative aerobes and obligate anaerobes in earthworm gut contents. *Appl. Environ. Microbiol.* 77, 5842–5850. doi: 10.1128/AEM.05432-11

Shannon, C. E. (1948). A mathematical theory of communication. *Bell Syst. Tech. J.* 27, 379–423. doi: 10.1002/j.1538-7305.1948.tb01338.x

Shigematsu, T., Tang, Y., Kobayashi, T., Kawaguchi, H., Morimura, S., and Kida, K. (2004). Effect of dilution rate on metabolic pathway shift between aceticlastic and nonaceticlastic methanogens in chemostat cultivation. *Appl. Environ. Microbiol.* 70, 4048–4052. doi: 10.1128/AEM.70.7.4048-4052.2004

Smemo, K. A., and Yavitt, J. B. (2011). Anaerobic oxidation of methane: an underappreciated aspect of methane cycling in peatland ecosystems? *Biogeosciences* 8, 779–793. doi: 10.5194/bg-8-779-2011

Strack, M., Waddington, J., Turetsky, M., Roulet, N., and Byrne, K. (2008). "Northern peatlands, greenhouse gas exchange and climate change" in Peatlands and climate change. ed. M. Strack (Jyväskylä, Finland: International Peat Society), 44–69.

Sun, L., Toyonaga, M., Ohashi, A., Tourlousse, D. M., Matsuura, N., Meng, X.-Y., et al. (2016). *Lentimicrobium saccharophilum* gen. Nov., sp. nov., a strictly anaerobic bacterium representing a new family in the phylum *Bacteroidetes*, and proposal of *Lentimicrobiaceae* fam. Nov. *Int. J. Syst. Evol. Microbiol.* 66, 2635–2642. doi: 10.1099/ijsem.0.001103

Tarnocai, C., Canadell, J. G., Schuur, E., Kuhry, P., Mazhitova, G., and Zimov, S. (2009). Soil organic carbon pools in the northern circumpolar permafrost region. *Global Biogeochem. Cycles* 23:GB2023. doi: 10.1029/2008GB003327

Tveit, A., Schwacke, R., Svenning, M. M., and Urich, T. (2013). Organic carbon transformations in high-Arctic peat soils: key functions and microorganisms. *ISME J.* 7, 299–311. doi: 10.1038/ismej.2012.99

Tveit, A. T., Urich, T., Frenzel, P., and Svenning, M. M. (2015). Metabolic and trophic interactions modulate methane production by Arctic peat microbiota in response to warming. *Proc. Natl. Acad. Sci.* 112, E2507–E2516. doi: 10.1073/pnas.1420797112

Wiegel, J. (2015). "Clostridiaceae," in *Bergey's manual of systematics of Archaea and Bacteria. Bergey's Manual of Systematics of Archaea and Bacteria*. eds. M. E. Trujillo, S. Dedysh, P. DeVos, B. Hedlund, P. Kämpfer, F. A. Rainey, et al. (Hoboken, New Jersey: John Wiley & Sons, Inc.).

Williams, R. T., and Crawford, R. L. (1984). Methane production in Minnesota peatlands. *Appl. Environ. Microbiol.* 47, 1266–1271. doi: 10.1128/aem.47.6.1266-1271.1984

Wörner, S., and Pester, M. (2019). Microbial succession of anaerobic chitin degradation in freshwater sediments. *Appl. Environ. Microbiol.* 85, e00963–e00919. doi: 10.1128/AEM.00963-19

Wüst, P. K., Horn, M. A., and Drake, H. L. (2009). Trophic links between fermenters and methanogens in a moderately acidic fen soil. *Environ. Microbiol.* 11, 1395–1409. doi: 10.1111/j.1462-2920.2009.01867.x

Yavitt, J. B., and Seidman-Zager, M. (2006). Methanogenic conditions in northern peat soils. *Geomicrobiol J.* 23, 119–127. doi: 10.1080/01490450500533957

Yavitt, J. B., Yashiro, E., Cadillo-Quiroz, H., and Zinder, S. H. (2012). Methanogen diversity and community composition in peatlands of the central to northern Appalachian Mountain region, North America. *Biogeochemistry* 109, 117–131. doi: 10.1007/s10533-011-9644-5

Ye, R., Jin, Q., Bohannan, B., Keller, J. K., and Bridgham, S. D. (2014). Homoacetogenesis: a potentially underappreciated carbon pathway in peatlands. *Soil Biol. Biochem.* 68, 385–391. doi: 10.1016/j.soilbio.2013.10.020

Zalman, C., Keller, J. K., Tfaily, M., Kolton, M., Pfeifer-Meister, L., Wilson, R. M., et al. (2018). Small differences in ombrotrophy control regional-scale variation in methane cycling among *Sphagnum*-dominated peatlands. *Biogeochemistry* 139, 155–177. doi: 10.1007/s10533-018-0460-z

Zinder, S. H. (1993). "Physiological ecology of methanogens" in Methanogenesis: Ecology, physiology, Biochemistry & Genetics. ed. J. G. Ferry, Chapman & Hall microbiology series (Boston, MA: Springer US), 128–206.

Zinder, S. H. (1994). "Syntrophic acetate oxidation and 'reversible Acetogenesis" in Acetogenesis. ed. H. L. Drake, Chapman & Hall Microbiology Series (Boston, MA: Springer US), 386–415.

Frontiers in Microbiology

Explores the habitable world and the potential of microbial life

The largest and most cited microbiology journal which advances our understanding of the role microbes play in addressing global challenges such as healthcare, food security, and climate change.

Discover the latest Research Topics

See more →

Frontiers

Avenue du Tribunal-Fédéral 34
1005 Lausanne, Switzerland
frontiersin.org

Contact us

+41 (0)21 510 17 00
frontiersin.org/about/contact